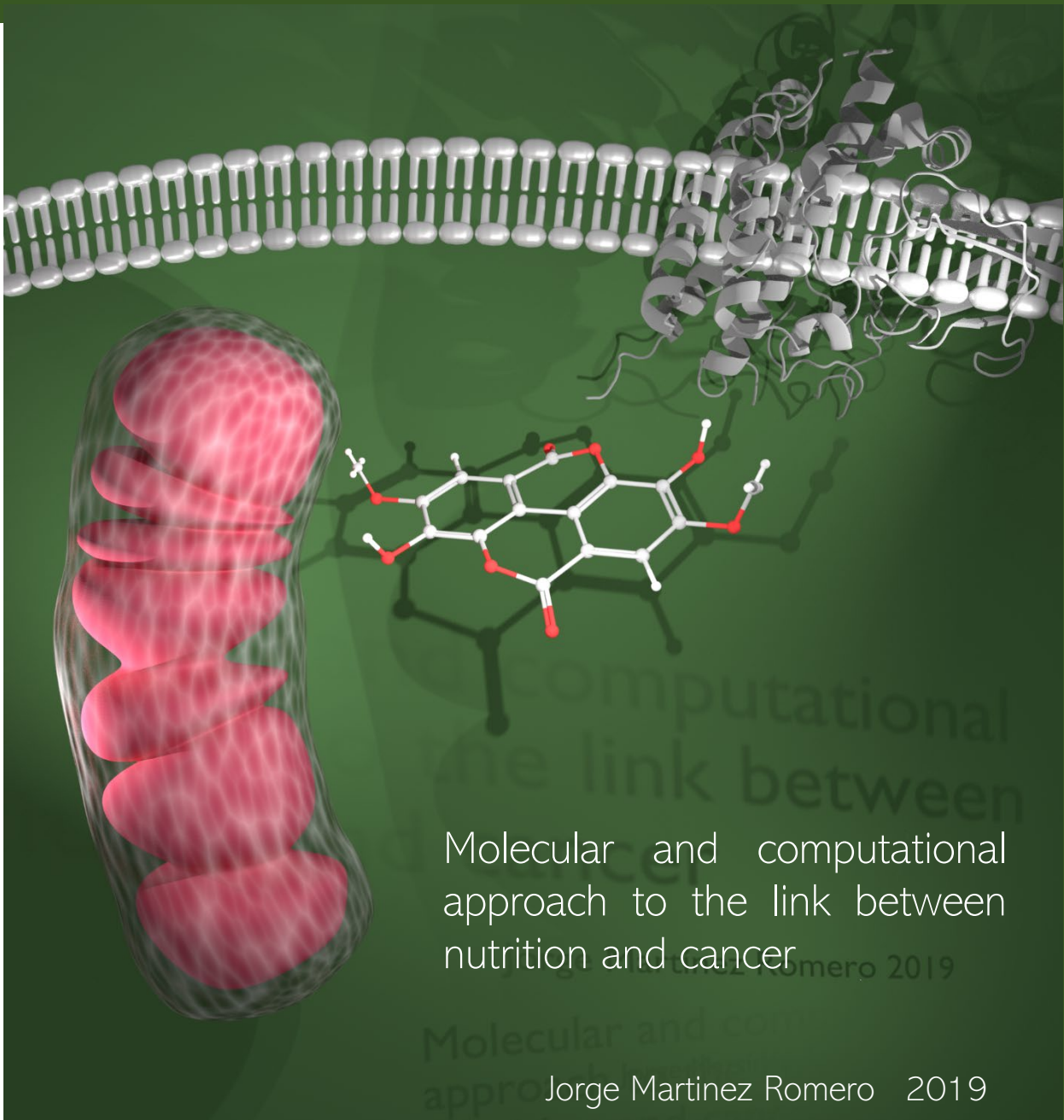


UNIVERSIDAD AUTÓNOMA DE MADRID
SCHOOL OF SCIENCES. DEPARTAMENT OF BIOLOGY



Doctoral Thesis

UNIVERSIDAD AUTÓNOMA DE MADRID
SCHOOL OF SCIENCES
DEPARTAMENT OF BIOLOGY
CELLULAR BIOLOGY



Imdea Food Research Institute
Molecular Oncology Group

TITLE:

Molecular and computational approach to the
link between nutrition and cancer

Jorge Martínez Romero
Doctoral THESIS

Madrid, 2019

UNIVERSIDAD AUTÓNOMA DE MADRID
FACULTAD DE CIENCIAS
DEPARTAMENTO DE BIOLOGIA
BIOLOGIA CELULAR



Instituto Imdea Alimentación
Grupo de Oncología Molecular

TITULO:

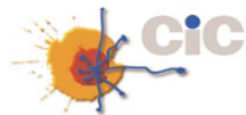
Molecular and computational approach to the
link between nutrition and cancer

Memoria presentada por:
Jorge Martínez Romero

Para optar al grado de
DOCTOR EN BIOLOGÍA

Directora: Dra. Ana Ramírez de Molina
Codirector: Prof. Dr. Guillermo Reglero Rada
Tutor: Prof. María José Hazen de San Juan

Madrid, 2019



Drs. Ana Ramírez de Molina, PhD in Biochemistry and Molecular Biology at the University Autónoma de Madrid, and currently Deputy Director of the IMDEA Food Research Institute, Director of the Precision Nutrition and Cancer Program and Principal Investigator of the Molecular Oncology Group. As Director of this Thesis,

Prof. Guillermo Reglero Rada, PhD in Chemistry, Full Professor of Food Sciences at the University Autónoma de Madrid and Senior Researcher of the Spanish National Research Council (CSIC). Currently he is the Director of the IMDEA Food Research Institute and Principal Investigator of the Food Products for Precision Nutrition Program. As co-director of this Thesis,

INFORM:

That the present work entitled “Molecular and computational approach to the link between nutrition and cancer” and that constitutes the Thesis presented by Mr. Jorge Martínez Romero to apply for the degree of Doctor in Biology, has been carried out at the Madrid Institute for Advanced Studies in Food (IMDEA Food), Spain; the Biomedical Research Center, National Institutes of Health (NIH), Baltimore, MD, USA; and the Cancer Research Center, Salamanca, Spain, under their direction. They consider that the experimental study is original, and the results have sufficient scientific quality for presentation as a Doctoral Thesis in the School of Science, Department of Biology, of the University Autónoma de Madrid.



Thesis Director: PhD Ana Ramírez de Molina



Thesis Codirector: Professor Guillermo Reglero Rada

Index

INDEX

ACKNOWLEDGEMENTS.....	15
INDEX OF FIGURES AND TABLES.....	21
LIST OF ABBREVIATIONS.....	27
SUMMARY	33
1. INTRODUCTION	39
1.1. CANCER	41
1.1.1. Cancer overview	41
1.1.2. Colorectal cancer (CRC).....	48
1.1.3. Breast Cancer (BC)	57
1.2. BIOINFORMATICS APPLIED TO GENOME-WIDE EXPRESSION TO ANALYZE THE CANCER GENOME ALTERATIONS.	62
1.2.1. Functional genomics in cancer	62
1.3. NUTRITIONAL STRATEGIES IN CANCER BASED ON MOLECULAR EFFECTS:	69
1.3.1. Bioactive compounds: Phitochemicals, Phenolic compound Ellagic acid and derivatives in CRC.	72
1.3.2. Caloric restriction and fasting in breast cancer.	78
2. HYPOTHESIS.....	89
3. OBJECTIVES	91
3.1. IDENTIFICATION OF GENES INVOLVED IN NUTRIENT SENSING OR CELL METABOLISM ASSOCIATED WITH CRC PROGNOSIS AND PATIENT SURVIVAL.	91
3.2. IDENTIFICATION OF POTENTIAL PRECISION STRATEGIES IN CANCER FOCUSED ON MOLECULAR NUTRITION.	91
3.2.1. Nutritional strategies based on the inclusion of bioactive compounds: Analysis of bioactive compounds with potential beneficial effect in CRC	91
3.2.2. Nutritional strategies based on the inhibition of tumor nutrient requirements: Analysis of the inhibition of tumor progression and metastatic burden in BC through fasting strategies.....	91
4. MATERIALS AND METHODS.....	93
4.1. IN SILICO ANALYSIS: IDENTIFICATION OF GENES INVOLVED IN NUTRIENT SENSING OR CELL METABOLISM ASSOCIATED WITH CRC PROGNOSIS AND PATIENT SURVIVAL.	95
4.1.1. Dataset Integration and batch effect removal.	101
4.1.2. Batch effect removal evaluation	102
4.1.3. Differential expression analysis.....	103
4.1.4. Survival analysis.....	103
4.1.5. Gene expression profiles of epithelial CRC samples vs CRC tumor samples	104
4.1.6. Geneset enrichment analysis (GSEA)	105
4.2. IN VITRO ANALYSIS: ANALYSIS OF BIOACTIVE COMPOUNDS WITH POTENTIAL BENEFICIAL EFFECT IN CRC.....	106
4.2.1. Phenolic Compounds and Derived Metabolites	106
4.2.2. Cell Culture	106
4.2.3. Cell Viability Assays.....	107
4.2.4. RNA Extraction and Quantification.....	107
4.2.5. Gene Expression Assays	108
4.2.6. Real time qPCR	108
4.2.7. Top-Fop tranfection assay	109
4.2.8. miRNAs Expression Assay.....	111
4.2.9. Cell Culture, Protein Extraction and Quantification	111

4.2.10.	Western Blot analysis.....	111
4.2.11.	Cell Migration Assay.....	113
4.2.12.	Mitochondrial respiration and glycolytic function monitoring.....	113
4.3.	IN VIVO ANALYSIS: ANALYSIS OF THE INHIBITION OF TUMOR PROGRESSION AND METASTATIC BURDEN IN BC THROUGH FASTING STRATEGIES.....	115
4.3.1.	Animals.....	116
4.3.2.	Diets.....	117
4.3.3.	Establishing and monitoring BC tumor.....	118
4.3.4.	Sacrifice, collection of tissues, lysates and protein extraction, metastasis analysis.....	118
5.	RESULTS.....	121
5.1.	IDENTIFICATION OF GENES INVOLVED IN NUTRIENT SENSING OR CELL METABOLISM ASSOCIATED WITH CRC PROGNOSIS AND PATIENT SURVIVAL.....	123
5.1.1.	Identification of 765 genes associated with differential survival among CRC patients.....	123
5.1.2.	Identification of one major pathway (IGFBP signalling), deeply involved in cell nutrition and highly modulated by caloric restriction.....	133
5.1.3.	SLC2A3, NPR3 and LCA5 involvement in patient survival.....	134
5.2.	IDENTIFICATION OF POTENTIAL PRECISION STRATEGIES IN CANCER FOCUSED ON MOLECULAR NUTRITION.....	141
5.2.1.	Nutritional strategies based on the inclusion of bioactive compounds: Screening of bioactive compounds with potential beneficial effect in CRC.....	141
5.2.2.	Nutritional strategies based on the inhibition of tumor nutrient requirements: Intermittent Fasting as a potential precision nutrition strategy in BC.....	162
5.3.	COMPARATIVE ANALYSIS OF DIFFERENT NUTRITIONAL STRATEGIES THROUGHOUT IN VIVO, IN VITRO AND IN SILICO RESULTS	171
6.	DISCUSSION.....	173
6.1.	IDENTIFICATION OF GENES INVOLVED IN NUTRIENT SENSING OR CELL METABOLISM ASSOCIATED WITH CRC PROGNOSIS AND PATIENT SURVIVAL.....	175
6.2.	IDENTIFICATION OF POTENTIAL PRECISION STRATEGIES IN CANCER FOCUSED ON MOLECULAR NUTRITION.....	184
6.2.1.	Nutritional strategies based on the inclusion of bioactive compounds: Screening of bioactive compounds with potential beneficial effect in CRC.....	184
6.2.2.	Nutritional strategies based on the inhibition of tumor nutrient requirements: Intermittent Fasting as a potential precision nutrition strategy in BC.....	190
6.3.	COMPARATIVE ANALYSIS OF DIFFERENT NUTRITIONAL STRATEGIES THROUGHOUT IN VIVO, IN VITRO AND IN SILICO RESULTS	198
6.3.1.	Modulation of SLC2A3 in BC tumor by IF.....	198
6.3.2.	Modulation of Wnt16 in BC tumor by IF.....	199
7.	CONCLUSIONS.....	201
8.	PERSPECTIVES.....	207
9.	BIBLIOGRAPHY.....	213
10.	PUBLICATIONS AND POSTERS.....	249
10.1.	PAPER 1: BMC GENOMICS: “GENE MARKERS OF COLORECTAL CANCER SURVIVAL DERIVED FROM CONSISTENT TRANSCRIPTOMIC PROFILING”.....	251
10.2.	PAPER 2: JOURNAL OF PHARMACOLOGY: “THE ELLAGIC ACID DERIVATIVE 4,4’-DI-O-METHYLELLAGIC ACID EFFICIENTLY INHIBITS COLON CANCER CELL GROWTH THROUGH A MECHANISM INVOLVING WNT16”.....	252
10.3.	POSTER AT NIA-NIH: “CANCER PROTECTION BY THE FASTING MIMICKING DIET; COMPOSITION, CALORIES OR FASTING TIME?”.....	253
11.	ANNEXES.....	255

11.1.	NIH LIVE ANIMAL HANDLING COURSE	257
11.2.	SUPPLEMENTAL FIGURES AND TABLES.....	257

Acknowledgements

AGRADECIMIENTOS

La idea de volver a estudiar décadas después me resultaba seductora por sí sola, no necesitaba otros estímulos aparte de la mera curiosidad y las ganas de aprender y conocer la ciencia desde dentro.

Y lo hice, me acerqué a las oficinas de la UAM a matricularme en la facultad de ciencias, en algo que no tuviera que ver con la economía, que no me resultara demasiado absorbente, que me posibilitara atender mi medio de vida y no alterara ni el confort ni la armonía familiar de la que disfrutaba. Y ahí empezasteis a aparecer, un compañero, luego otro, un profesor, luego otro, el primer científico, otro más...como si de un collar se tratara, se empezaron a unir cuentas hasta llegar a dar varias vueltas alrededor de mi cuello, pero cuentas que no pesan. La diplomatura se convirtió en grado, el grado en máster y el máster en doctorado. Tres, cuatro, cinco, diez años. Y cada vez erais más, mejores. Pocos son tres folios, para agradecer lo que me habéis hecho disfrutar, aprender, mejorar, reír, vivir. No me quiero dejar ni una sola cuenta de esta preciosa alhaja que me ha acompañado durante el hermoso paseo que he tenido el privilegio de recorrer.

Gracias Guillermo, gracias, Ana, por creer en mí, por aceptarme en este nicho de gente estupenda que es IMDEA, por dirigirme, por vuestro consejo, por vuestra ayuda.

Gracias Ana y Silvita, mi mujer y mi hija, por no odiar la bioquímica o por odiarla profundamente y seguir queriéndome. Es recíproco, os quiero, y ahora mismo creo que también la odio yo. Vuestro aliento me hace perseverar, llegar más lejos. Sin vosotras simplemente no habría Tesis.

Gracias a mi familia, grande, toda, con la que comparto sangre y la que no, tan cercana, tan cálida, tan especial. Le dais sentido a lo que hago y hacéis de mi mejor persona.

Gracias, padre, por dirigir desde arriba. Te marchaste joven, de cáncer. Con los años que casi tengo ahora, tras unos meses de intenso dolor. Dejándome una horrible sensación de alivio. Como me gustaría volver a verte y ponerte en la mano una copia de este texto, y pedirte algo con que escribir, y garabatearte una dedicatoria, y charlar, sin dolor, sin angustia, de lo mal que va el país, de que no tenemos remedio, del mejor país del mundo...No te imaginas como te echo de menos. Se que estas disfrutando este momento. Esta Tesis va por ti.

A mis imdeanos. A todos. Gracias por vuestra ayuda, por vuestro cariño, por vuestra amistad, por vuestros ánimos, por vuestras sonrisas. A mis Omygenes, me habéis hecho mejor investigador. Gracias Silvita (Serás mejor madre que científica y ya eres una gran científica), Marta (mil gracias), Cris, Ruth, Lara, Sonia y Elenita, por vuestro consejo y cariño. Esos lab-meeting que odio han sido mucho más llevaderos con vosotras cerca. Gracias Juanito, científico a pie de hospital, un placer contarte entre los amigos. Su, gracias por esos ánimos incondicionales, por tu increíble generosidad, y por ver el medio μL que yo no veo en la pipeta. Sin tu ayuda y amistad esto no habría salido bien.

Pablo, Marta, engancháis. Colarme en vuestros despachos a consultaros dudas moleculares (y de las otras), ha sido uno de los grandes placeres de la tesis, aunque no estemos de acuerdo en lo que es ayuno. Por fin os voy a dejar en paz. Luis, mi querido amigo Luis, tú vas en el pack también. Todo un privilegio compartir doctorado contigo. Las Cristinas, Adrian...Vuestro grupo es estupendo y va mi recuerdo y cariño para todos sus miembros.

La sonrisa de Esther, de Julia, de Rubén, de Carmen, de Carlos, de Gema, de Jowita, de Carolina, de Lorena, de Javi durante los cafés arriba, todos estos años y su "¿Que, como va esa tesis?". Me habéis aportado combustible inagotable con vuestro aliento. Verdadera "nutrición de precisión". Mil gracias.

Al grupo de la plataforma. Vivi, recuerdo cuando entré aquí y me pusiste a medir y pesar pacientes, no paraba de sudar, mi color de cara no perdía el tono escarlata hasta que llegaba a casa después de las sesiones maratonianas. Gracias por enseñarme y por tu amabilidad todos estos años. Isabel, siempre sonriendo, siempre alegre, siempre activa, siempre muy Isabel. Gracias Kalesi, por ser simplemente tu. Y por supuesto, las Elenas, con h y sin ella, y Roberto (co-doctor), mi agradecimiento.

Al grupo de Ordovás, de Alberto y de Enrique. Gracias, chicos, por momentos geniales abajo, en especial a Lidia, Alberto (me ha bajado el colesterol gracias a tu ciencia), Joao, Emma, Judit (animo no queda nada), Maika, Víctor, Carmen, Paloma, las Lauras, Teresa y mi queridísima Ruth, la de los apellidos de colores que marchó al mundo de los probióticos sin que casi me enterara. Gracias científicos.

Sara, Mónica. ¿Podría yo haber llegado hasta aquí sin vosotras? Impensable. Mil gracias por vuestra simpatía y afecto, todos los minutos, desde el primer día.

Moisés, gracias por tantos buenos momentos, ciencia y no ciencia.

Jesús, Enrique, Manuel, se mas de todo esto gracias a vosotros. Vuestros consejos, vuestras explicaciones, me han enriquecido profundamente. Va mi cálido y afectuoso agradecimiento por momentos científicos inolvidables.

Rodrigo, a ti te agradezco todo, buenos momentos, consejos, generosidad infinita dentro y fuera de Imdea... Que placer tenerte ahí.

Fran y su ayuda informática, muchísimas gracias, Fran.

Queridas Josune y Tabernero. ¿Qué os puedo decir? El privilegio de conoceros y trabajar cerca vuestro no lo cambio. Y además de conocimiento, ese humor fantástico que transmitís a los que se os acercan. Tenemos que buscar la forma de patentarlo. Es simplemente genial. Dar solo gracias es menos de lo que os merecéis.

Y gracias a mis vecinos de Box, y a alguno que ha migrado hasta un despacho, esa chavalería que me contagia juventud y me insufla energía por la mañana. Arancha, Andrés, Pepe, los dos Adrianes, Adriana, Mario y Marina. Yaiza, a ti también, aunque estés más lejos. La ciencia es grande en buena parte por gente como vosotros, "keep going", que nadie se rinda, seguir peleando. Sois formidables y estoy seguro de que haréis tesis dignas que os llevaran a sitios interesantes. Mi agradecimiento y profundo reconocimiento.

Agria, amarga la idea de dejar de veros todos los días. Un pedazo grande del corazón se queda ahí, en IMDEA, con vosotros.

A la gente del NIH. A De Cabo. Gracias por aceptarme, por ser un magnifico mentor, por tu ciencia, por ayudarme con la intendencia, por presentarme, por facilitar todo, por considerarme un chaval más del "Labo". A Annette, Margaux, Nelson, Tyler, Laura, Isabel, Ioana, Andrea, Clara, Yingchun, Hagai, Kato (espero que sigas teniendo todos los dedos) , Kelsey, Sam, Jackie, Erin, Fatemeh... a los compatriotas Alberto, Nacho (conseguir que un ratón desmonte el carrusel y se haga una cama cuando quieres monitorizar ejercicio físico nocturno requiere un sólido conocimiento del modelo murino. ¿Qué fue del ratón?, ¿le matriculasteis en Harvard?) y Marta, por vuestra amistad y cariño, por facilitarme la vida entre la comunidad roedora de Baltimore. También a ti Dawn Boyer, vecina de box y extraordinaria profesional con los animales. A Michel Bernier, entrañable y brillante bioquímico, profundamente canadiense, aunque no te guste el hockey. A Louis Rezanka, siempre atento, cordial, conozco algo más de Baltimore gracias a tus consejos. A Miguel Aon, Sonia Cortassa y Steven Sollott, (Mr. Heart) por sus charlas científicas, pero

sobre todo por las no científicas. Me hicisteis disfrutar de vuestro inmenso conocimiento y sentir un cariñoso afecto.

A la gente del CiC. Gracias Javier, por acogerme en el seno de tu Laboratorio. Por ser tan cordial conmigo, por transmitirme algo de tu conocimiento y por hacerme la vida más feliz en Salamanca. Curro, hablas varios idiomas, pero, sobre todo, hablas en R. Gracias por meterlo en mi cabeza. Santiago, Jose, Manuel, Oscar, Conrad o mejor Kurt. Gracias por hacerme la vida entre computadoras tan agradable. Me siento un microchip más del grupo.

A mis amigos del otro mundo, el que no es de ciencia. Tanto ánimo, tanto interés por mis avances, tanto cariño, abrume.

Un último párrafo y acabo. Quiero expresaros una reflexión: Primero tiraba de mi la curiosidad, luego esa curiosidad se convirtió en pasión, y la pasión un poco en insana obsesión. Ahora que he terminado de escribir me doy cuenta de que lo que más me importa de este precioso y extraordinario paseo a lo largo de la tesis no son los resultados, ni mucho menos; es poder llegar algún día a ser acreedor de algo del profundo respeto que siento por todos vosotros.

No es poco.

Sería un enorme privilegio.

Y a seguir sumando cuentas al collar...

“El éxito consiste en ir de fracaso en fracaso sin desanimarse”

Sir Winston Churchill

Index of figures and tables

Figure	Description	Page #
1.1	Cancer Hallmarks	43
1.2	MicroRNA Pathway	47
1.3	Colorectal cancer: Oncogenesis	51
1.4	Cartoon representative of a section of a human colon with five tumors in different stages.	53
1.5	Plot of mutation frequency from 2,497 human CRC samples	56
1.6	Plot of mutation frequency from 4,437 human BC samples	61
1.7	High-density oligonucleotide expression arrays. Detail of technology.	65
1.8	Major pathways implicated in cancer altered by caloric restriction in mammals.	81
4.1	Example of NUSE boxplot for quality control of microarrays	100
4.2	Representative examples of graphical exploratory data analysis.	101
4.3	Plasmids used to transfect SW620 CRC cells for monitoring β -catenin/TCF/LEF activity after 24 hr. treatment with 20 μ M 4,4'DiOMEA	110
4.4	Flowchart representing the experimental design to test fasting cycles with different diets in breast cancer murine model	115
5.1	Hierarchical clustering correlation heatmap in gene expression integrated dataset preprocessed with 5 different algorithms.	125
5.2	Score plot of the first two principal components (PCA) of 1,273 CRC samples corresponding to 7 independent studies integrated with 5 different preprocessing methods.	126
5.3	Plots of survival analysis using 1273 samples from human colorectal cancer (CRC) patients. Only top two genes shown, <i>DCBLD2</i> and <i>EPHB2</i> .	131
5.4	Validation of previous KM analysis corresponding to top hit gene <i>EPHB2</i> .	132
5.5	Forest plot representing the hazard ratio of the 3-gene signature <i>SLC2A3</i> , <i>NPR3</i> , <i>LCA5</i> in each independent dataset.	136
5.6	Distribution comparison of expression signal corresponding to twenty top-ranked genes in 25 human samples from normal colorectal epithelium.	138
5.7	Hierarchical clustering correlation heatmap of 1273 microarrays to identify cluster corresponding to any specific CRC subtype (C1 to C6).	140
5.8	Dose-response curves after treating SW620 CRC cell line with EA and derivatives.	143

Figure	Description	Page #
5.9	Antioxidant activity of EA and derivatives 3,3'DiOMEA and 4,4'DiOMEA	144
5.10	WNT16 expression in human SW-620 CRC cells treated with different concentrations of 4,4'-DiOMEA.	147
5.11	Results of the TOP/FOP assay performed on SW-620 CRC cells treated with 4,4'DIOMEA.as a reporter of Wnt/ β -catenine activity.	149
5.12	RT-qPCR analysis showing the SW-620 cells mRNA levels of several epithelial and mesenchymal markers to analyze EMT upon 72 hours of treatment with 4,4'DIOMEA (5 μ M and 20 μ M) vs control.	151
5.13	Wound Healing Assay	153
5.14	Level of expression of miRNA 203 and miRNA 96 after performing a Taqman Low Density Array (TLDA) analysis on SW-620 CRC cells treated with 4,4' DiOMEA at different concentrations	154
5.15	TLDA analysis results showing the expression levels of 33 miRNA from SW620 CRC cells that responded to 4,4'DIOMEA treatment in a dose dependent way	155
5.16	Representation of the Warburg effect.	158
5.17	Energy Phenotype analysis on CRC SW-620 cells that after ,4'DIOMEA treatment at two concentrations	160
5.18	Spare respiratory capacity of CRC SW620 cells after treatment with concentrations of 4,4'DiOMEA equivalent to the IC50 and 2xIC50	161
5.19	Body weight trajectories of mice fed SD, FSD and FMD.	163
5.20	Breast tumor size measurements of mice fed SD, FSD and FMD.	164
5.21	Lung metastatic nodules of mice fed SD, FSD and FMD.	165
5.22	Western blot analysis in tumoral tissue from mice fed SD, FSD and FMD including mTOR and AKT proteins	168
5.23	Western blot analysis of protein p70S6K in tumoral tissue from mice fed SD, FSD and FMD.	169
5.24	Western blot analysis in tumoral tissue from mice fed SD, FSD and FMD including rpS6 and p-rpS6 proteins.	170
5.25	Western blot analysis of protein SLC2A3 in tumoral tissue from mice fed SD, FSD and FMD.	171
5.26	Western blot analysis of protein WNT16 performed in tumoral tissue from mice fed SD, FSD and FMD.	172
6.1	Venn diagram showing different hits after performing LIMMA analysis using same gene expression microarrays preprocessed with 3 different methods (fRMA, fRMA+Combat, fRMA+Mean centering).	176
6.2	Canonical Wnt signaling in vertebrates.	186
6.3	Non-Canonical Wnt signaling in mammals	187
6.4	Control of Translation Reprogramming by eIF2a Phosphorylation according to nutrient availability.	195
6.5	Cartoon representing the hypothesis of CR-mediated increment in BC cancer metastasis in the lung due to lack of protection against own immune system	197

Table	Description	Page #
1.1	The TNM staging system	53
1.2	Consensus CRC molecular subtype classification	55
1.3	Breast cancer molecular classification.	61
1.4	Phenolic compounds and in vivo derivatives included in the study and the main reported properties related to antitumor potential	76
1.5	Clinical trials involving different types of dietary restriction in patients undergoing breast cancer. Major pathways implicated in cancer altered by caloric restriction	87
4.1	Integrative meta dataset (IMD) used in this study	97
4.2	Phenotypical data of patients used in this study	98
4.3	Primary antibodies used in Western Blot analysis	112
5.1	Coefficients obtained from regressing gene expression on array batch per preprocessing method.	128
5.2	Genes selected as top-50 best survival markers of colorectal cancer (CRC).	129
5.3	Pathway enrichment analysis	133
5.4	Multivariate survival analysis.	135
5.5	β Coefficients after performing the multivariate Cox regression considering the gene signature SLC2A3, NPR3, LCA5 as explanatory variable and using samples of stage I and II only..	136
5.6	Association between level of expression in tumor and normal colon epithelium	138
5.7	Anti-proliferative activity [IC50 (μ M)] of different polyphenols in several CRC cell lines	142
5.8	Differentially expressed genes identified in microarray analysis	146
5.9	Bioinformatic analysis of biological processes, pathways and transcription factors significantly altered by 4,4'-DiOMEA in SW-620 colon cancer cells according to microarray data.	146
5.10	Genes selected for EMT analysis and related phenotype	150
5.11	TLDA analysis showing modulation of the expression level of top miRNAs by 4,4'-DiOMEA at different concentrations.	156

List of abbreviations

3,3'-DIOMEA 3,3'-Di-O-methylelagic acid
 4,4'-DIOMEA 4,4'-di-O-methylelagic acid
 4E-BP 4E binding protein
 5-FU 5-fluorouracil
 AAT alpha1-Antitrypsin
 AJCC The American Joint Cancer Committee
 AKT Protein Kinase B
 ALDOA Fructose-1,6-Bisphosphate Aldolase A
 AMPK AMP-Dependent Kinase
 BC Breast Cancer
 BER Batch Effect Removal
 BRCA Breast Cancer Gene
 CDF Chip Definition File
 CI Confidence Interval
 CIMP CpG Island Methylator Phenotype
 CIN Chromosomal Instability
 CISD3 CDGSH Iron Sulfur Domain 3
 CMS Consensus Molecular Subtypes
 COMBAT Combating Batch Effect Method
 COPD Chronic Obstructive Pulmonary Disease
 CR Caloric Restriction
 CRC Colorectal Cancer
 CT Chemotherapy
 DCA Dichloroacetate
 DCBLD2 Discoidin CUB And LCCL Domain Containing 2
 DEG Differentially Expressed Genes
 DPPH 2,2-Diphenyl-1-Picrylhydrazyl
 DR Dietary Restriction
 DSR Differential Stress Resistance
 DSS Disease Specific Survival
 EA Ellagic Acid
 ECAR Extracellular Acidification Rate
 EDA Exploratory Data Analysis
 eIF2 Eukaryotic Translation Initiation Factor 2
 eIF-4E Eukaryotic Initiation Factor 4E
 EIO European Institute Of Oncology
 EMT Epithelium-Mesenchymal Transition
 ER Estrogen Receptor
 PR Progesterone Receptor
 ET Ellagitannins
 FFA Free Fatty Acids
 FG Functional Genomics
 FMD Fasting Mimicking Diet

FRAP Ferric Reducing Antioxidant Power
fRMA Frozen Robust Multiarray Average,
FSD Fasting Standard Diet
GADD45B Growth Arrest And DNA-Damage-Inducible 45 Beta
GAV Group Assignment Vector
GEO Gene Expression Omnibus
GEP Gene Expression Profiling
GFs Growth Factors
GH Growth Hormone
GI Gastrointestinal
GSEA Gene Set Enrichment Analysis
HER2 Human Epidermal Growth Factor Receptor 2
HMW High Molecular Weight
HR Hazard Ratio
IA Integrative Analysis
IF Intermittent Fasting
IGF-1 Insulin-Like Growth Factor 1
IGFBP Insulin-Like Growth Factor Binding Protein
IMD Integrative Meta Dataset
KD Ketogenic Diet
LCA5 Leber Congenital Amaurosis 5
LIMMA Linear Model For Microarrays Analysis
LMW Low Molecular Weight
LS Location-Scale
MAPK Mitogen-Activated Protein Kinase
MAS Monoclonal Antibodies
MF Matrix-Factorization
miRNA MicroRNA
MLH1/2 Mutl Homologue 1/2
MM Mismatch Probe
MMR Mismatch Repair
MRD Methionine Restricted Diet
MS Metabolic Syndrome
MSI Microsatellite Instability
MTORC1 Mammalian Target Of Rapamycin Complex 1
NCI National Cancer Institute
NIA National Institute On Aging
NIH National Institutes Of Health
NPR3 Natriuretic Peptide Receptor 3
NRF2 Factor NF-E2-Related Factor
NUSE Normalized Unscaled Standard Error
OCR Oxygen Consumption Rate
OS Overall Survival

P:C:F Proportions of Protein, Carbohydrate, Fat
PCA Personal Component Analysis
PDK1 3-Phosphoinositide-Dependent Kinase 1
PDQ Nutrition In Cancer Care
PF Periodic Fasting
PI Prognostic Index
PI3K Phosphatidylinositol 3-Kinase
PIP2 Phosphatidylinositol-4,5-P2
PLM Probe-Level Model
PM Perfect Match Probe
PPAR Peroxisome Proliferator-Activated Receptor
PR Progesterone Receptor
PREMIO Prevalence Of Malnutrition In Oncology
PTEN Phosphatase And Tensin homolog protein
QC Quality Control
QOL Quality Of Life Scale
RB Retinoblastoma
RFS Relapse Free Survival
RISC RNA-Induced Silencing Complex
RMA Robust Multiarray Average
RNAi RNA Interference
ROS Reactive Oxygen Species
RPS6 Ribosomal Protein S6
S6K S6 Kinase
SCNA Somatic Copy Number Alterations
SD Standard Diet
SERPINA1 Alpha 1-Antitrypsin
siRNA Short Interference RNA
SIRTS Sirtuins
SLC2A3 Solute Carrier Family 2 Member 3 (GLUT:3)
TGF Transforming Growth Factor
TLDA Taqman Low Density Array (cards)
TLDU Terminal Duct Lobular Units
TNM Tumor Nodule Metastasis Staging System
TPN Triple Negative
VEGF Vascular Endothelial Growth Factor
YAP1 Yes-Associated Protein 1

Summary

Abstract

Several studies indicate that cancer is strongly associated with diet, in fact, diet constitutes an important risk factor in some types of cancer such as those related to the digestive system. Precision nutrition based on adapting nutrients or incorporating bioactive compounds to the specific individual circumstances, can contribute to a better comprehensive treatment of the disease, either by helping to inhibit its progression or by improving the effects associated with the use of chemotherapy.

This thesis analyzes the transcriptome of 1273 colorectal cancer patients to identify genes related to cellular sensing or metabolism of nutrients that are also associated with patient prognosis or survival. An integrative analysis identified two groups of genes whose differential expression (overexpression or repression) correlates with low survival in late stages of the disease (III and IV). The ten differentially expressed genes that show best association with poor prognosis in colorectal cancer are: *DCBLD2*, *PTPN14*, *LAMP5*, *TM4SF1*, *NPR3*, *LEMD1*, *LCA5*, *CSGALNACT2*, *SLC2A3* and *GADD45B*. In addition, the 3-gene signature *SLC2A3*, *NPR3* and *LCA5* seems to be a strong survival marker related to nutrition, especially relevant in early stages I and II (HR: 3.60; CI: 3.43-3.77; p-val.:0.00187]).

This thesis also investigates two strategies based on precision nutrition with the intention of identifying its implication in the inhibition of cell viability, tumor growth and metastases development. At the molecular level, a strategy based on the inclusion of bioactive compounds in the diet is analyzed in colorectal cancer, a type of cancer that frequently correlates with malnutrition of patients. By means of a screening of several phenolic compounds and derivatives, 4,4'-Di-O-methyl ellagic acid is identified as a potent agent inhibiting cell proliferation in various colorectal cancer cell lines including a line resistant to 5-Fluorouracil. It is found that the inhibition of cell viability is mediated by the down regulation of *Wnt16*, a gene that signals various pathways involved in normal cell growth and proliferation during embryogenesis, carcinogenesis and chemotherapy resistance. Additionally, this work analyzes a second precision nutrition strategy centered in the restriction of nutrients in breast cancer, a type of cancer that frequently correlates with patient overweight and metabolic syndrome. More specifically, this Thesis explores the implication of an intervention with intermittent fasting cycles and two different diets (standard diet and plant-based diet) in tumor progression and metastasis development.

It is identified that the intermittent fasting in young Balb/c female mice with induced breast cancer, decreases the size of the tumors regardless of the type of diet tested. In addition, it is found that mice subjected to intermittent fasting under the conditions analyzed here, show higher metastatic burden in the lung. This event occurs irrespective of the composition of the diet applied in the experiment.

Resumen

Diversos estudios indican que el cáncer está fuertemente asociado a la dieta, de hecho, constituye un factor de riesgo importante en algunos tipos de cáncer como los relacionados con el aparato digestivo. La nutrición de precisión basada en adaptar nutrientes o incorporar compuestos bioactivos a las circunstancias específicas del individuo, puede contribuir a un mejor tratamiento integral de la enfermedad, ya sea ayudando a inhibir su progresión o mejorando los efectos asociados al uso de quimioterapia.

Inicialmente, esta tesis analiza el transcriptoma de 1273 pacientes de cáncer colorrectal para identificar genes relacionados con detección o metabolismo celular de nutrientes que, además, estén asociados a pronóstico o supervivencia del paciente. Por medio de un análisis integrativo, se identifican dos grupos de genes cuya expresión diferencial (sobrexpresión o represión) correlaciona con baja supervivencia en estadios tardíos de la enfermedad (III y IV). Los diez genes cuya sobre expresión diferencial mejor se asocia a mal pronóstico en cáncer colorrectal son: *DCBLD2*, *PTPN14*, *LAMP5*, *TM4SF1*, *NPR3*, *LEMD1*, *LCA5*, *CSGALNACT2*, *SLC2A3* y *GADD45B*. Además, se identifica la huella de 3 genes *SLC2A3*, *NPR3* y *LCA5* como biomarcador de supervivencia relacionado con nutrición, especialmente relevante en estadios tempranos I y II (HR: 3.60; CI: 3.43-3.77; p-val.:0.00187]).

Por otra parte, esta tesis investiga dos estrategias basadas en la nutrición de precisión, con la intención de identificar su implicación en la inhibición de la viabilidad celular, el crecimiento tumoral y el desarrollo de metástasis. A nivel molecular, se analiza una estrategia basada en la inclusión de compuestos bioactivos de la dieta en un tipo de cáncer que correlaciona frecuentemente con malnutrición de los pacientes, el cáncer colorrectal. Por medio de un screening de varios compuestos fenólicos y derivados, se identifica el 4,4' Di-O-metil ácido elágico como potente agente inhibidor de la

proliferación celular, en diversas líneas de cáncer colorrectal, incluyendo una línea resistente al 5 Fluorouracilo. Se identifica que la inhibición de la viabilidad celular esta mediada por una disminución de la expresión del gen *Wnt16*, que señala diversas rutas implicadas en procesos de crecimiento y proliferación celular durante la embriogénesis, carcinogénesis y resistencia a quimioterapia. Finalmente, se analiza una estrategia basada en la restricción de nutrientes en cáncer de mama, un tipo de cáncer que correlaciona frecuentemente con sobrepeso y síndrome metabólico del paciente. Se estudia la implicación de una intervención que incluye ciclos de ayuno intermitentes con dos tipos de dieta diferente (dieta estándar y dieta rica en alimentos de origen vegetal), en la progresión tumoral y el desarrollo de metástasis. Se identifica que el ayuno intermitente en ratones jóvenes Balb/c con cáncer de mama inducido, disminuye el tamaño de los tumores independientemente del tipo de dieta asociada. Además, se constata que los ratones sometidos a ayuno intermitente, en las condiciones analizadas, presentan mayor número de metástasis en el pulmón. Este hecho ocurre independientemente de la composición de la dieta utilizada.

1. Introduction

1.1. Cancer.

1.1.1. Cancer overview

According to the World Health Organization, cancer is the second leading cause of death globally, and it is responsible for an estimated 9.6 million deaths in 2018 (WHO, 2019).

Cancer is extraordinarily heterogeneous. Variability in patient response to treatment, different mutation map of each individual or tumor, high diversity in cell types and clones inside the tumors, wide variety of biomarkers and subtypes; a significant number of singularities that make the approach particularly difficult to address.

Cancer is not a unique disease. The U.S. National Cancer Institute (NCI) describes cancer as “a collection of related diseases” and identify more than 100 different cancer types according to the organ or tissue (“Cancer Types,” 1980).

The challenge is to understand the molecular basis of this heterogeneity to determine factors implicated in disease initiation, progression, and responsiveness or resistance to antitumoral therapies.

Multifactorial disease

Cancer is constitutively a multifactorial disease that develops when cells stop submitting to the fine-tuned control patterns. Environmental factors and genetic alterations switch on the mechanisms causing cancer. In the absence of normal regulation, shifts in the genetic map lead to an aberrant transformation of the cell. Cancer cells acquire comparative advantages in relation to their predecessors enough to persist, grow, proliferate, migrate and colonize new tissues (Hanahan, Weinberg, 2000) (Hanahan and Weinberg, 2011). The advantages or new capabilities of these transformed cells comprise:

- ✓ Sustaining Proliferative Signaling
- ✓ Evading growth suppressors
- ✓ Avoiding immune destruction
- ✓ Enabling replicative immortality
- ✓ Tumor-promoting inflammation
- ✓ Activating invasion & metastasis
- ✓ Inducing angiogenesis
- ✓ Genome instability & mutation
- ✓ Resisting cell to death
- ✓ Deregulating cellular energetics



Figure 1.1. Cancer Hallmarks. Hanahan and Weinberg, 2011.

Since these frequently cited ten-hallmarks of cancer (figure 1.1), new observations in cancer research raise other abilities that contribute to increase the evidence of complexity. Emerging hallmarks include the termed axonogenesis or the infiltration of tumors by growing nerves (Magnon et al., 2013), (Pundavela et al., 2015) and the referred to as lymphangiogenesis that includes the formation of new lymphatic vasculature inside the tumor and its active implication in the metastatic burden (Stacker et al., 2014).

Hallmarks are related to each other, mostly in a cause-effect way and it is difficult for researcher to discern whether these changes are the cause or an effect of cancer itself.

A disease of the genome

Probably the most characteristic trait associated to cancer encompasses the alteration of genes. Cancer is a disease of the genome (Getty, 2008) (MacConaill and Garraway, 2010). Multiple modifications in DNA performance at different levels occurs, from nucleotide to chromosome, leading to further changes in transcripts and proteins and the consequent dysregulation of multiple biochemical pathways. Although a wide variety of these different processes contribute to gene alteration, DNA mutations seems to achieve special relevance in the inter and intratumoral individuality.

The genome of cancer cells accumulates somatic mutations (a term that is coined to distinguish them from the germinal ones) throughout the life of the individual, some are acquired when the lineages of the cell are biologically normal and do not show phenotypical characteristics of cancer. In a comprehensive review of the cancer genome Michael Stratton firstly used the terms "passenger" and "driver" to refer to the two major groups of somatic mutations depending on their involvement in oncogenesis. The "driver" mutations provide comparative advantages to the cell that contribute to higher proliferation of these transformed clones leading to oncogenesis and tumor progression. The "passenger" mutations do not grant advantage to the cell compared to the rest of the clones (Stratton et al., 2009).

Cancer mutations have their origin in three defined causes (Tomasetti et al., 2017): genetic inheritance, errors during DNA replication and mutations due to exogenous or environmental factors. Most driver mutations are caused by errors in DNA replication. Recent studies from "The UK cancer database, cancer genome sequencing efforts"(Ledford, 2017), carried out in 32 different types of cancer and more than 25,000

tumors indicate that around 66% of the mutations are caused by errors in DNA replication, more than 29% have their origin in environmental factors and confirm that just 5% are due to hereditary mutations. Surprisingly, although cancer is a genetic disease, few cases appear to be due to genetic inheritance.

Although the burden of mutation varies depending on the age of cancer onset, the exposure to carcinogenic agents and the DNA-repairing ability, it seems to be directly associated to the type of cancer. For instance, Ewing's sarcoma and thyroid cancer have relatively lower mutation rates with frequencies ranging 0.1 to 1 mutation per Mb, whereas lung cancer or melanoma show the highest mutation frequencies with rates above 100 mutations per Mb. (Lawrence et al., 2013)

All these modification prompts subsequent alterations in gene expression, altered allele-specific expression or differential alternative splicing (MacConaill and Garraway, 2010).

The specific alterations in the expression of oncogenes and tumor suppressor genes have special importance in the appearance of the tumoral phenotype (Hall, 1984) (Knudson, 2002).

Oncogenes encompass the mutated form of genes that in normal cells (referred to as proto-oncogenes), drive proliferation and differentiation processes. They code for transduction signaling proteins rendering cell cycle or apoptosis. Overexpression of these genes due to different causes, e.g. gain of function, amplification, alteration in the numbers of copies (Somatic Copy Number alterations [SCNA]) or when a gene is under the influence of a very active promotor, prone cell transformation and uncontrolled proliferation, previous step for cancer development. (Koolman J Rohm K, 2012). Some examples of oncogenes or products of them comprise i) ligands like insulin like growing factor 1 (IGF-1) or Wnt; ii) membrane receptors that binds growth factors and hormones such as the estrogen or progesterone receptors (ER, PR); iii) GTP binding proteins and adaptative proteins such as the RAS family; iv) DNA-specific binding proteins or transcription factors such as myc, fos or Jun; v) protein kinases involved in signal transduction like AKT, PI3K or ERK, among others.

Tumor suppressors or *Anti-oncogenes* comprise a group of genes controlling normal cell development and proliferation. They are mainly implicated in the inhibition of differentiated cells returning to the cell division cycle, DNA repairing and genome

instability avoidance. Downregulation or absence of these genes leads to the accelerated uncontrolled cell division encompassing cancer. *TP53* or *RB*, the genes that code for the protein p53 or retinoblastoma protein, are good examples of tumor suppressor genes.

A broad variety of genes reveals to have oncogenic or tumor suppressing abilities, therefore, the same gene may exert alternatively oncogene or tumor suppressor activity depending on the cancer type or the biological background surrounding (Vogelstein and Kinzler, 2004).

Regulatory genes such as those coding for microRNAs are another class of altered genes with major implication in cancer progression (Abdelrahim et al., 2006)(Iorio and Croce, 2012)(Gambari et al., 2016). MicroRNAs are short non-coding RNA molecules that silence specific genes by blocking or degrading target mRNA, inhibiting further translation (Tabara et al., 1999) (Zamore, 2006). Figure 1.2 briefly captures the process of microRNA maturation and the different steps until final hybridization with the target mRNA which results in translation inhibition or mRNA degradation. miRNA has incomplete base-pairing and targets multiple mRNA (Pillai et al., 2007). miRNAs are excised from genome-encoded RNA precursors (Großhans and Filipowicz, 2008). Alteration of genes expressing miRNAs can post transcriptionally enhance cancer progression, for instance, negatively regulating the translation of tumor suppressor mRNAs (Reddy, 2015) (Volinia et al., 2006).

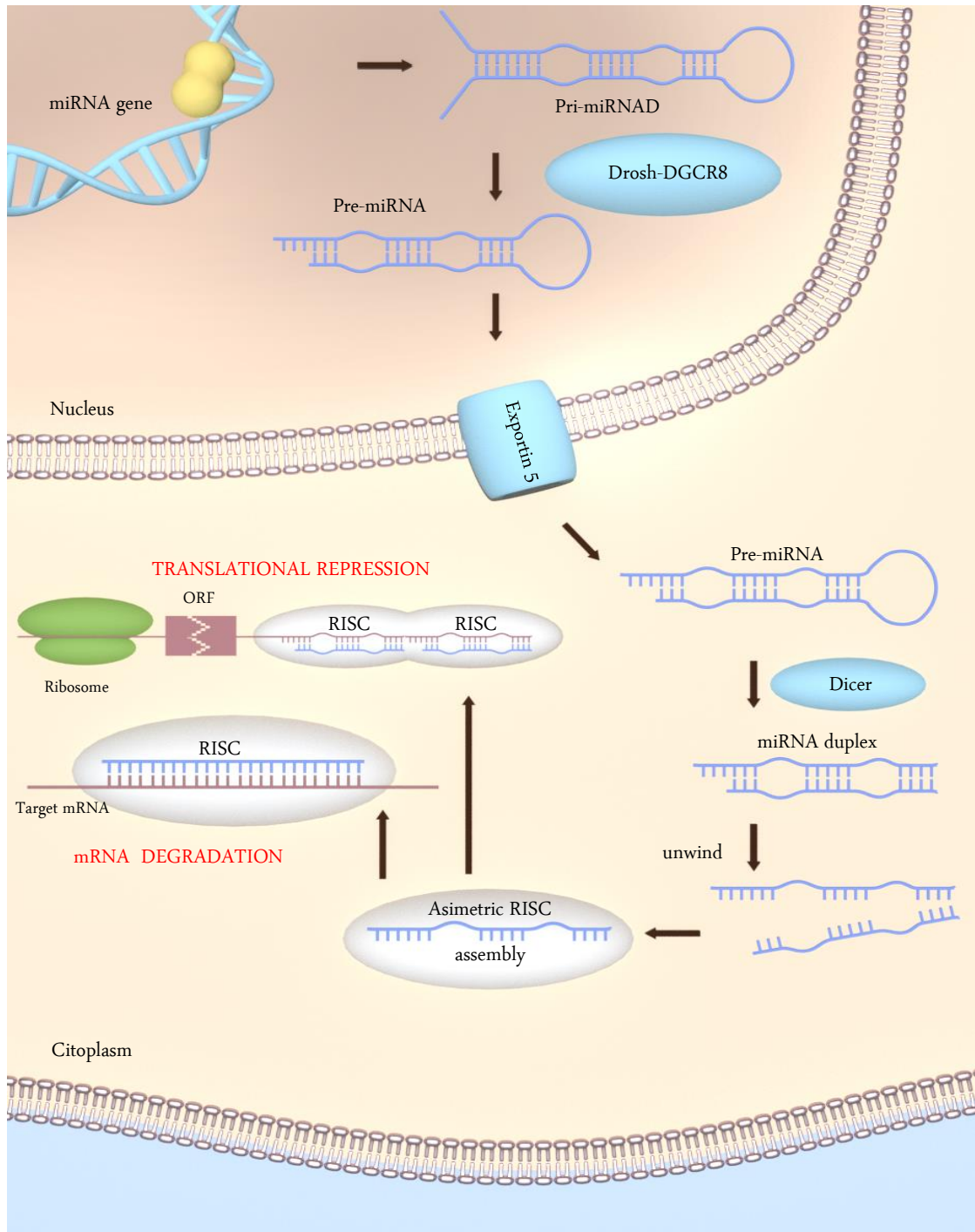


Figure 1.2. MicroRNA Pathway. Summarizing a much complex process, MicroRNAs are transcribed as large RNA precursors (pri-miRNAs) and then processed in the nucleus by the microprocessor complex, Drosha/DGCR8. The resulting pre-miRNAs (70-nucleotides approx. in length) are then exported to the cytoplasm by the protein Exportin 5. Once in the cytoplasm, the enzyme Dicer generates the miRNA, a double-stranded RNA (22-nucleotide approx. in length). Dicer also originates the formation of the RNA-induced silencing complex (RISC). RISC is responsible for the two different outcomes of miRNA-based gene silencing: mRNA degradation and translational repression. Figure adapted from sigmaaldrich.com, Functional genomics and RNAi. miRNA.

1.1.2. Colorectal cancer (CRC)

Epidemiology

CRC is the third more diagnosed cancer overall with 1,8 million new cases and 862,000 deaths previewed for 2018. (WHO, 2019). CRC affects more to men than women. Population over 65 years old and non-Hispanic black race show higher prevalence. It is noteworthy the increasing trend of CRC onset in younger individuals (≤ 50 years old), in contrast to the favorable trend in the older strata. (Siegel et al., 2017).

Survival, explained as percentage of individuals with CRC that live five years or longer free of disease from diagnostic date, exceeds 65% between years 2006 and 2012 (Siegel et al., 2017) .

Europe CRC statistics are similar (Malvezzi et al., 2018) and specifically in Spain, "The Global Cancer Observatory Project" places CRC as the most prevalent cancer of all with 34,331 new cases previewed for 2017 in the Spanish territory (SEOM, 2018). This study identifies CRC behind lung as those cancers with higher mortality in 2016.

Etio pathology

Risk and prevention factors

CRC is highly related to diet. Among substantiated risk factors, age, physical inactivity, excess of body weight, central deposition of adiposity in the body, alcohol consumption and smoking, seems to be the most relevant ones. Nutritional habits such as low fiber intake and the frequent consumption of red or processed meat seems to increase the risk of suffering CRC. (CRU, 2015) (Giovannucci, 2001) .

Early screening is the key preventive factor of CRC. Good nutritional habits with frequent consumption of legumes, fruit and vegetables, rich in fiber, can contribute to decrease risk of CRC as well. Epidemiological studies have also revealed that the recurrent use of non-steroidal anti-inflammatory drugs, especially in elder population, contribute to lower the risk of this type of cancer. (Bastiaannet et al., 2012) (Markowitz, 2007) (Schreinemachers and Everson, 1994)

Oncogenesis of CRC

The adenoma-carcinoma sequence of events has been proposed throughout the years as the classical pathway leading to CRC. It describes CRC genesis as an sprouting process that begins with an early adenoma which evolves into an advanced adenoma with

high-grade dysplasia and then progresses to an invasive cancer (Fearon and Vogelstein, 1990). This process is orchestrated by a number of sequential driver mutations leading to the tumor formation and the spreading to other tissues by a process of metastasis (Markowitz and Bertagnolli, 2009) (figure 1.3.A).

Latter studies showed that a minority of CRC tumors develops according to the Fearon and Vogelstein model and new oncogenesis pathways were suggested but unable to entirely capture the strong complexity of CRC. The chromosomal instability pathway; the microsatellite instability (MSI) pathway; and the CpG island methylator pathway, also referred to as the serrated neoplasia pathway, are among those majorly accepted by experts. (IJspeert et al., 2015). The most relevant molecular characteristics of these pathways include a sequence of genetic alterations captured in figure 1.3.B.

The chromosomal instability (CIN) pathway. It is suggested that more than 70% of total CRCs arise due to CIN pathway (Jass, 2007a). CIN occurs due to chromosomal alterations, in numbers (gain or loss of entire chromosomes, aneuploidy), structure (e.g., duplications, inversions, translocations, or deletions), or a combination of both (Pino and Chung, 2010).

The microsatellite instability (MSI) pathway. Comprises more than 15 % of CRC and one out of five tumors includes a germline mutation associated with Lynch syndrome (Jass, 2007b). The main feature of this route encompasses deficiencies in the mechanism to repair DNA caused by alterations in mismatch repair (MMR) genes such as the human *MutL* homologue *MLH1* and *MLH2*. The name of microsatellite is attributed to small segments of DNA between 4 and 6 bp located generally in non-coding zones along the genome. It is the variations in the number of repetitions and not the sequence that determines each allele in particular. This MSI gives rise to extraordinarily high mutation rates, mainly indels and substitution. This, alters the DNA sequence and modifies the reading frame at the time of processing each codon, originating the synthesis of erroneous proteins (Boland and Goel, 2010) (IJspeert et al., 2015).

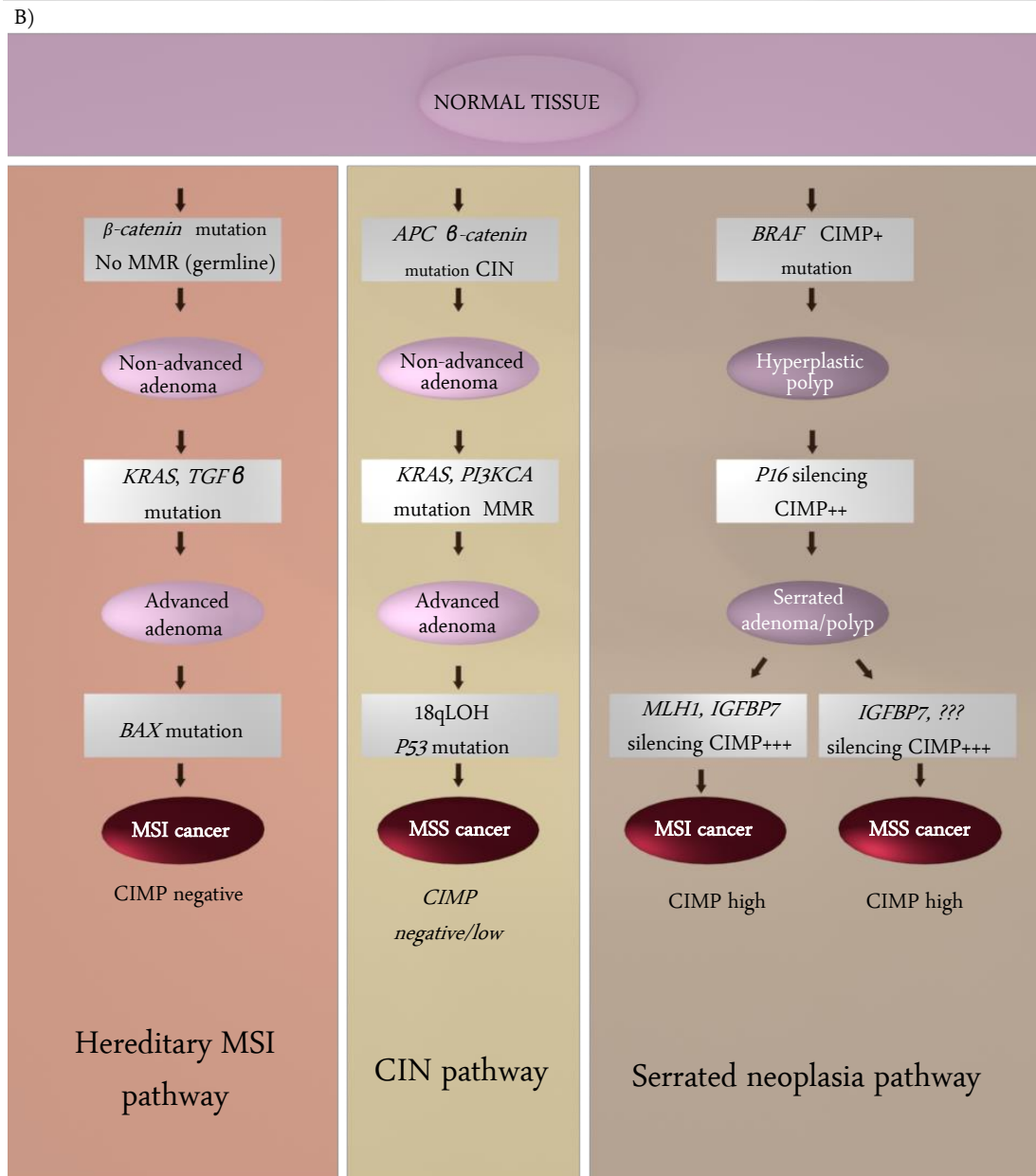
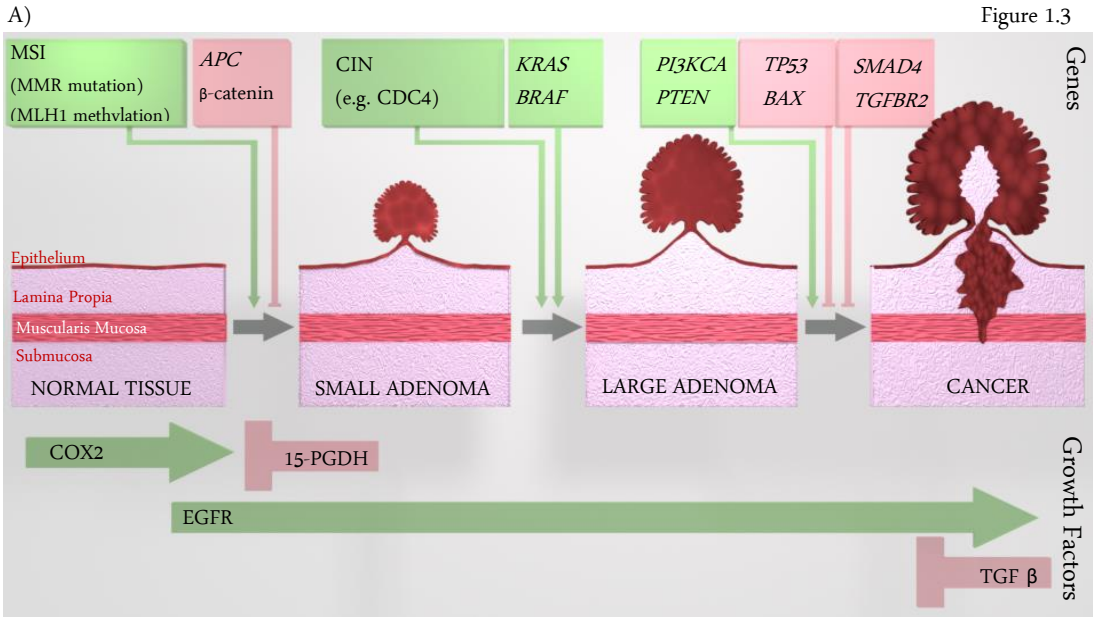
The serrated neoplasia pathway. The precursor lesion of these tumors consists in the formation of polyps and serrated adenomas with specific saw-toothed structures as representative trait of its morphology (Hawkins et al., 2002). Higher metastasis burden and worse survival seem to be highly associated with serrated CRC, in comparison with conventional CRC (Laiho et al., 2007). A special phenomenon occurring in cancer and

highly frequent within tumors arisen through this pathway encompasses the CpG island methylator phenotype (CIMP). Methylation is used as epigenetic mechanism by which methylases add a methyl group to the carbon 5 of a cytosine located before a guanine (CpG). CpG islands are not randomly distributed in the human genome. One high density CpG area appears next to the promoter of more than a half of all genes (CpG islands). This CpG islands are hardly methylated in normal tissue but frequently methylated in cancer cells, silencing tumor-suppressor, mismatch-repair or apoptosis genes, among others. CIM achieves unusual relevance in CRC due to the frequent *MLH1* silencing by an aberrant CpG methylation. This singularity is referred to as "CpG island methylator phenotype" (CIMP or CIMP high) (Snover, 2011).

Figure 1.3 shows three heavily studied pathways found in the literature and some of the most relevant molecular singularities of each one. Nevertheless, authors claim to be cautious when approaching CRC oncogenesis, since these pathways are unable to fully explain CRC heterogeneity, their sequence of events would likely not follow the proposed order and overlapping and crosslinking with each other should be expected (IJspeert et al., 2015).



Figure 1.3. Colorectal cancer: Oncogenesis. Cartoon representative of the extreme complexity of CRC oncogenesis. A) In the upper part of the figure, a representation of "Genes and Growth Factor Pathways That Drive the Progression of Colorectal Cancer" (Markowitz and Bertagnolli, 2009). Green color indicates oncogenic mediators activated in CRC and red color denotes tumor-suppressor de-activated. B) The figure shows main CRC independent genetic alterations in 3 heavily studied pathways. Adapted from the review (IJspeert et al., 2015) and previous works (Fearon and Vogelstein, 1990) (Walther y col., 2009) (Esteve, 2010). Authors claim to be cautious when approaching CRC oncogenesis, since these pathways are unable to fully explain CRC heterogeneity, their sequence of events would likely not follow the proposed order and overlapping and crosslinking with each other should be expected



Clinical Classification of CRC. Staging

The American Cancer Society classification of CRC differentiates between hereditary and sporadic CRC. Hereditary CRCs are associated with a specific inherited genetic abnormality and the most frequent are the Non-Polyposis Colon Cancer, Lynch Syndrome with less than 5% of total CRCs and the Familial Adenomatous Polyposis with 1% of total CRC. Some other relevant hereditary CRC are: Attenuated Familial Adenomatous Polyposis, Peutz-Jehger's Syndrome, MYH Associated Polyposis, Juvenile Polyposis, Hereditary Polyposis and APC1307K. (ACS, 2018). The other group, sporadic colorectal cancer, comprises the most common type of CRC, with 90% of people diagnosed at the age of 50 or older. (CRU, 2015)

In the clinic, patients are classified into different stages based in the histopathological characteristics of their tumors (severity of dysplasia and the proportion of villous component) (Stanley H, Lauri A, 2000). The American Joint Cancer Committee, (AJCC) and European Institute of Oncology (EIO) recommend TNM Staging System (where T stands for tumor, N for lymph node, and M for metastasis) (Denoix PF, 1952); is the most frequently used, but also Full Dukes and Astler-Coller modified classifications are common in clinic (Akkoca et al., 2014). All methods categorize CRC by considering the degree of bowel wall invasion, the lymph node spreading and the distant metastases appearance. TNM also allows grouping the patients in progressive cancer stages, indicated by 0 and roman numerals I, II, III, and IV (Table 1. 1. Figure 1.4). In this way, stages 0, I and II correspond to cases which had not shown cancer cells beyond the tumor, lymph nodes or blood. By contrast, stages III and IV correspond to individuals in where the cancer has disseminated to the lymph system or other organs in the body. This five-stage categorization determines the treatment and represents significantly distinctive patient groups in terms of risk and prognosis (ACS, 2018).

Stage	Tumor	Nodes	Metastasis
Stage 0	T0	N0	M0
Stage I	T1	N0	M0
	T2	N0	M0
Stage II	T3	N0	M0
	T4	N0	M0
Stage III	Any of T	N1	M0
	Any of T	N2	M0
Stage IV	Any of T	Any of N	M1

Table 1.1. The TNM staging system according to primary tumor characteristics, lymph nodes invaded and presence of metastases. (Denoix PF, 1952)

Legend:

T = primary tumor.

TX- Primary tumor of unknown.

T0- No primary tumor.

Tis- Carcinoma in situ.

T1- Tumor invades submucosa.

T2- Tumor invades muscularis propria.

T3- Tumor invasion to subserosa or to pericolic/perirectal tissue.

T4- Tumor invasion to neighboring organs or structures and/or visceral peritoneum is perforated.

N = Regional lymph nodes.

NX- Regional lymph nodes cannot be assessed.

N0- No lymph node metastases.

N1- 1 to 3 lymph node involvement.

N2- 4 or more lymph node involvement.

M = Distant metastasis.

MX- Distant metastasis cannot be assessed.

M0- No distant metastases.

M1- Distant metastases

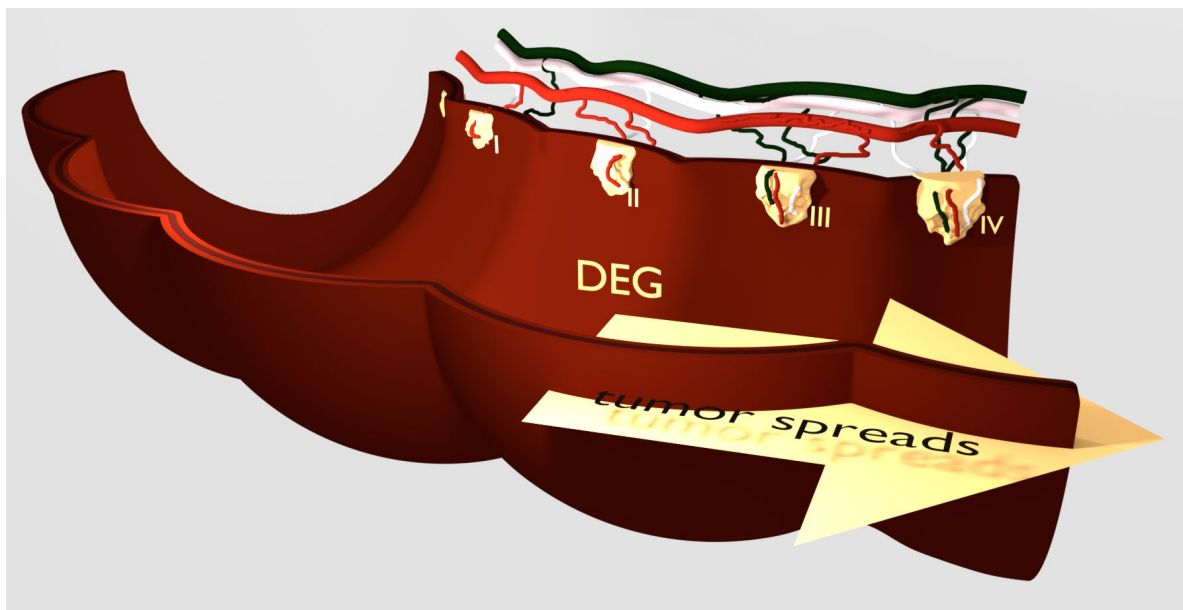


Figure 1.4. Cartoon representative of a section of a human colon with five tumors in different stages (Stage 0 to V). Stages 0, I and II correspond to cases in which cancer cells has not been detected beyond the tumor, or the lymph nodes. By contrast, stages III and IV correspond to tumors in where the cancer has spread outside the tumor to the lymph system or other organs in the body. This event has been considered in this Thesis to identify Differentially Expressed Genes (DEG) and explore their implication in prognosis and survival.

Molecular classification of CRC

Because of its heterogeneity, the molecular classification of CRC is difficult, as occurred when defining oncogenesis. By using gene expression profiling (GEP) and further bioinformatics analysis in large cohorts of samples, a wide number of CRC molecular classifications have been identified by researchers in recent years (Calon et al., 2015) (De Sousa E Melo et al., 2013) (Sadanandam et al., 2013) (Marisa et al., 2013). GEP is an omics-level technology that measures expression of thousands of genes at a time to identify global cell functionality and it has been used in this Thesis for the identification of genes associated with CRC prognosis and patient survival (See next chapter 1.2). Special mention deserves the works of Justin Guiney in an international consortium data sharing. To study the association among six highly recognized CRC classification systems, each containing three to six subtypes and collectively numbering 27 unique subtypes, a network-based approach was performed generating a remarkable CRC categorization that achieved strong consensus among professionals. (Guinney et al., 2015). This classification identifies 4 consensus molecular subtypes (CMS) with dissimilar prognosis and different response to treatment: CMS1 shows activation of immune system; CMS2 displays epithelial phenotype features, CMS3 has a denoted metabolic reprogramming and CMS4 includes mesenchymal characteristics. Table 1.2 summarizes the main features of each subtype. The CMS classification has been used in the first part of this Thesis to analyze whether any of the geneset identified and proposed as CRC biomarkers, is able to recognize or discriminate CRC samples of a particular consensus molecular subtype.

CMS1	CMS2	CMS3	CMS4
MSI Immune	Canonical	Metabolic	Mesenchymal
14%	37%	13%	23%
MSI, CIMP high, hypermutation	SCNA high	Mixed MSI status, SCNA low, CIMP low	SCNA high
BRAF mutations		KRAS mutations	
Immune infiltration and activation	WNT and MYC activation	Metabolic deregulation	Stromal infiltration, TGF-beta activation, angiogenesis
Worse survival after relapse			Worse relapse-free and overall survival

Table 1.2. Consensus CRC molecular subtype classification (adapted from Guinney et al., 2015a). It differentiates four molecular subtypes with dissimilar prognosis and different response to treatment: CMS1 shows activation of immune system, includes 14% of CRCs; CMS2 encompass epithelial phenotype features, is the most frequent, CMS3 has a denoted metabolic reprogramming phenotype and CMS4 includes mesenchymal characteristics. Abbreviations: CIMP, CpG Island Methylator Phenotype; MSI, microsatellite instability; SCNA, somatic copy number alterations; TGF, transforming growth factor.

Although this integrative classification seems to be consistent and well accepted, it still leaves an important number of CRC tumors (above 13%) molecularly uncategorized, highlighting the extraordinary complexity of the disease (Guinney et al., 2015).

An approach that could help covering this gap focuses in the sharp singularities found in the mutation map inter and intra tumors. It postulates that the great number of low frequency mutations in each individual, becomes an authentic fingerprint of the tumor itself and explains, to some extent, why similar patients in constitution and

conditions, with similar background and same diagnostic, react contradictory to an identical treatment in the clinic. (Chang et al., 2018)

Following this line of investigation, researchers of the Sloan Kettering Cancer Center have recently analyzed, in more than 24,000 tumors, those low frequency mutations trying to unravel new molecular patterns, referred to as "meaning in long tails" (Chang et al., 2018). Figure 1.5 shows an example of CRC long tail of mutations. Most frequently mutated genes from 2,497 CRC samples with a long tail of 18,952 low frequency mutations (cBioportal, 2019). The left side of the plot depicts 15 recurrent mutated genes (orange colored) with a rate from 20 to 70 % of total samples. The right side of the plot displays a blue colored long tail of top 35 mutated genes out of 18,952 (not shown) with a much lower frequency.

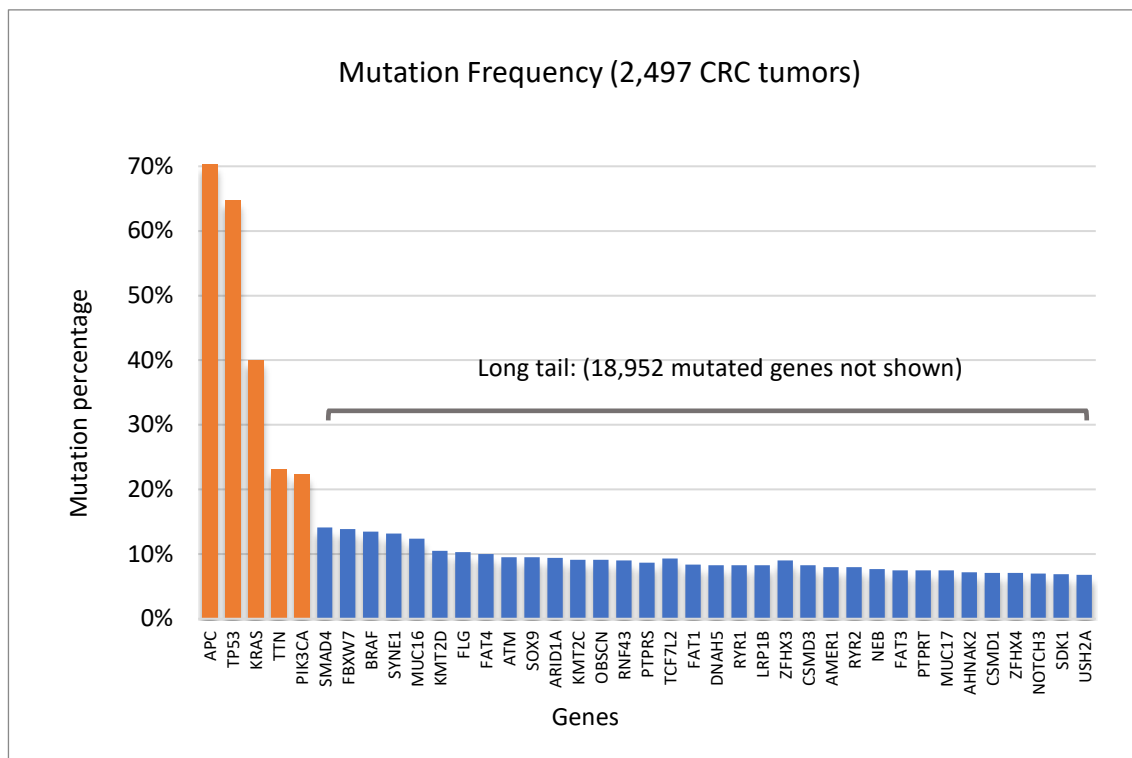


Figure 1.5. Plot of mutation frequency from 2,497 CRC samples with a long tail of 18,952 low frequency mutations (cBioportal, 2019). The left side of the plot depicts 15 recurrent mutated genes arbitrary orange colored with a rate from 20 to 70.30 %. The right side of the plot displays a blue colored long tail of top 35 genes with low mutation frequency out of 18,952 (not shown).

Treatment of CRC.

CRC treatment mainly encompass surgery and a broad variety of different drug-based therapies and targets. CRC chemotherapy (CT) is based in a sort of recurrently used drugs, including taxanes, antibiotics, antimetabolites (5-fluorouracil [5-FU] is one the most commonly used chemotherapeutic agent in CRC), alkylating agents and platin-based agents as the most widely selected by oncologists. The targeted therapies based in the use of monoclonal antibodies (MAs) are habitually considered in cancer therapeutics, as well (WCRF, 2018).

Overall, there seems to be strong evidence to indicate that surgery encompasses benefits in terms of survival, even in late stage IV (Lee et al., 2016), but results of current drug-based therapies show lack of efficacy in many cases and the vast majority of therapeutic treatments produce adverse side effects that habitually persist after a long-term period. Furthermore, cancer cells frequently develop resistance to these type of treatments (WCRF, 2018). All this suggest the need for further molecular-based alternatives able to properly identify the biochemical differences between normal and cancer cells. The nutritional approach could be particularly helpful in this scenario.

1.1.3. Breast Cancer (BC)

Epidemiology

According to the World Cancer Research Fund, breast cancer is the most frequent cancer in women and the second most common cancer of all with 2 million new cases previewed in 2018. (WCRF, 2018)

Spain is one of the few exceptions in where breast cancer incidence rates are decreasing 0.8%–1.6% per year (DeSantis et al., 2015). The estimated incidence of the most frequent tumors in Spain in 2017 previously mentioned for CRC places BC as the first cancer in women and the fourth major incidence cancer overall with 26,370 new cases previewed for 2017 (SEOM, 2018).

Etiopathology

Risk and preventive factors

Age, alcohol consumption, obesity and physical inactivity seems to be associated with higher risk of BC. Besides these behavioral aspects, reproductive factors such as not having children, not breastfeeding, use of oral contraceptives, birth control implants, intrauterine devices, skin patches and vaginal rings while including the use of hormones increase the risk of suffering sporadic BC. Post-menopausal hormone therapy appears to be associated as well. Furthermore, it has been reported that having a first-degree relative with BC increases the risk of having cancer more than 2-fold. (Arriaga et al., 2019) (ACS, 2015) (Dinger et al., 2011) (Kelsey et al., 1993) (Brinton et al., 1983). Early screening is the key factor in BC prevention.

Mutations in tumor suppressor Breast Cancer Gene 1/2 (*BRCA1/2*) are associated with increased risk for non-sporadic BC (Narod, 1994). They are considered high penetrance mutations responsible of 90 to 95% of hereditary BC (5-10% of all BC). Due to this high penetrance, monitoring and breast screening achieves special importance in women harboring *BRCA* mutations. Its appearance shows a 5-fold risk of suffering the disease (Marcus et al., 1996) (Nkondjock and Ghadirian, 2004).

Clinical classification of BC

BC is formerly grouped as non-specific ductal carcinoma with 60-75% of total BC and specific subtypes comprising 20-25% of all being lobular, tubular, papillary, and mucinous tumors, the most frequent of this last group (Ellis IO, 2003).

It has been substantially reported that the vast majority of human BC have their origin in the luminal cells of the terminal duct lobular units (TLDU) and not in the ductal system. (Gusterson et al., 2005) (Wellings, 1980). Each human mammary gland contains lobes and each lobe is comprised of TLDU. The TDLU is the functional unit of the breast and each TLDU drains the ductal system (Cardiff et al., 2018).

Although some other structures can be found, two cell layers constitute the main architecture in the human breast, the inner layer with a luminal cell population and the outer basal cell layer located next to the basement membrane. The difference between luminal and basal cells expression of high molecular cytokeratin is used to histologically categorize BC tumors (Anbazhagan et al., 1998).

To classify tumor in order to address treatment decisions, histopathologist primarily make an evaluation of tumor differentiation (tubule formation), nuclear pleomorphism (nucleus shape) and the mitotic rate of biopsied samples. This leads to the microscopic grading of the BC carcinoma. Bloom-Richardson and Nottingham systems are the classical three-grade scoring methods used to classify BC tumors according to these standards (Galea et al., 1992) (Eliyatkın et al., 2015).

BC tumors are mainly categorized by immuno-histochemistry detection of estrogen receptor (ER), human epidermal growth factor receptor 2 (HER2) and progesterone receptor (PR). Hormone receptors ER and PR drives the carcinogenic cell to proliferate in presence of estrogen or progesterone. HER2 is a member of the tyrosine Kinase receptor family overexpressed in certain types of BC due to an amplification of *ERBB2*, the gene encoding HER2. This pathway also induce BC cell hyper proliferation besides hormonal cell response (Torregrosa et al., 1997).

The presence or absence of these biomarkers determine therapy and prognosis and therefore are routinely used to subtype BC in the classical ER+, HER2+ and Triple-negative (TPN) groups, this last based on the lack of those biomarkers.

As in CRC, TNM system is also applied in BC to stratify patients and to normalize data. It makes use of previously mentioned criteria comprising tumor size, number of lymph nodes invaded and presence of metastasis to establish risk but adds a molecular subclassification according the expression of ER, PR and HER2 (Veronesi et al., 2006).

After the 9th St Gallen (Switzerland) BC experts meeting in 2005 onwards, the St. Gallen criteria considers response to hormonal treatment (endocrine response) as the first step in the decision algorithm to categorize tumors (Goldhirsch et al., 2005).

The ER, PR, HER2 classification is effective in guiding clinical treatment of BC patients, especially those enclosed in the ER+ group but reveals significant differences among patients within the same subtypes in response to treatment and recurrence, supporting the need of finding a more precise categorization for diagnosis and risk stratification (Eliyatkın et al., 2015)

There have been multiple molecular classifications based on GEP. The first intrinsic molecular classification by Perou and the works following by Weigelt and coworkers revealed 5 different categories with different prognosis and survival data. These analyses exposed proliferation divergences among subtypes, specifically in the expression of

MKI67 and *PCNA* biomarkers (Perou et al., 2000) (Weigelt et al., 2010). The subtyping identified 2 ER positive groups, Luminal A and a more aggressive phenotype with higher proliferation Luminal B and 3 ER negative, HER2 enriched, Basal like and the normal breast cancer subtype. Normal breast is a rare and poorly characterized TPN tumor with adipose tissue like gene expression profile and low proliferation features (Weigelt et al., 2010).

A rare epithelium-mesenchymal-transition (EMT) like phenotype cluster with specially bad prognosis was identified in 2007, the claudin low subtype, characterized by low expression of genes involved in tight junctions and some intercellular adhesion proteins (Herschkowitz et al., 2007).

Table 1. 3 shows relevant characteristics of the 6 main tumor subtypes (Eliyatkın et al., 2015) (Eroles et al., 2012).

Some other GEP works have been used to molecularly categorize BC tumors leading to a number of different gene signatures with therapeutic application. Oncotype (Paik et al., 2004) and MammaPrint (Veer et al., 2002) are two good examples of molecular profiling approved by the health authorities and incorporated in many decision algorithms employed by oncologist to sage patients (Moo et al., 2018).

As CRC, breast cancer displays an extreme diversification in the mutation burden. Figure 1.6 shows the top ranked recurrent mutated genes of a list over 17,000 mutations in nearly 4,500 BC tumor samples, capturing the extraordinary diversity and the high difficulty of defining groups of tumors in order to address therapy (cBioportal, 2019) (Kalimutho et al., 2019)

	Luminal A	Luminal B	HER2	Basal like	Normal breast	Claudin Low
Cytokeratin:	HMW	HMW	HMW/LMW	LMW	HMW	HMW/LMW
Frequency:	50-60%	10-20%	10-15%	10-20%	5-10%	12-14%
ER/PR:	+	+/-	-	-	-	-
HER2:	-	+/-	+	-	-	-
Ki67:	Low	High	High	High	Low	High
St. Gallen criteria:	Endocrine +	Endocrine +/-	Endocrine -	Endocrine -	Endocrine +/-	Endocrine-
TP53 mutation:	Low	High	High	High	High	Low
Characteristic genes altered:	<i>ESR1, GATA3, KRT8, KRT18, XBP1, FOXA1, TFF3, CCND1, LIV1</i>	<i>ESR1, GATA3, KRT8, KRT18, XBP1, FOXA1, TFF3, SQLE, LAPTM4B</i>	<i>ERBB2, GRB7</i>	<i>KRT5, CDH3, ID4, FABP7, KRT17, TRIM29, LAMC2</i>	<i>PTN, CD36, FABP4, AQP7, ITGA7</i>	<i>CD44, SNAIL3</i>
Prognosis:	Good	Intermediate Bad	Bad (Exceptions)	Bad (Exceptions)	Intermediate Bad	Bad (Exceptions)

Table 1.3. Breast cancer molecular classification. Adaptation of tables (Eliyatkın et al., 2015) (Eroles et al., 2012). Six subtypes are included, two ER positive groups, Luminal A and a more aggressive phenotype with higher proliferation Luminal B and four ER negative, HER2 enriched, Basal like and the normal breast cancer subtype. Normal breast is a rare and poorly characterized triple negative tumor with adipose tissue like gene expression profile and low proliferation features. HMW, High molecular weight; LMW, Low molecular weight. St Gallen criteria, endocrine response.

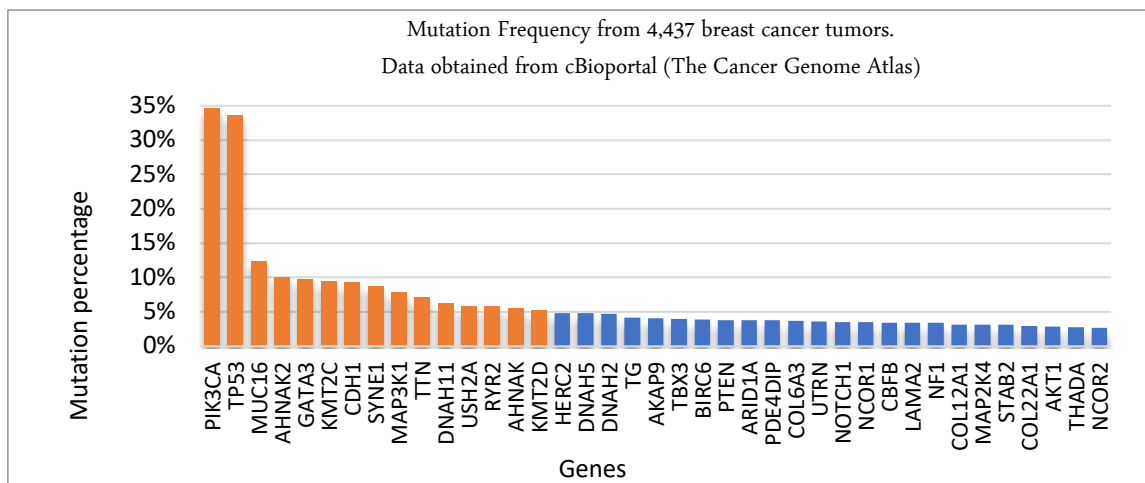


Figure 1.6. Plot of mutation frequency from 4,437 BC samples with a long tail of low frequency mutations (cBioportal, 2019). The left side of the plot depicts recurrent mutated genes (orange) with a rate over 5%. The right side of the plot (blue) displays long tail of top 35 genes low frequency mutated out of more than 17,000 (not shown) capturing the extraordinary diversity and the high heterogeneity inter and intratumor.

1.2. Bioinformatics applied to genome-wide expression to analyze the cancer genome alterations.

One of the main problems in biomedicine is the molecular identification among subtypes of complex disease such as cancer. Despite clinical evolution of the patient and response to treatment are known to be different, there are no molecular biomarkers capable to identify discrepancies among some patient subclasses. Finding new molecular markers to recognize subtypes is fundamental to help clinicians addressing therapeutics in a more precise and effective way.

By using bioinformatics approaches and more specific functional genomics analysis, researcher can make use of huge amount of genetic data to detect major swifts in gene expression and their eventual association to a specific class or condition.

1.2.1. Functional genomics in cancer

Omics technologies

In biology the neologism "omics" informally refers to large-scale use of pools of similar biological molecules such as DNA, (genomics), RNA (transcriptomics), proteins (proteomics), etc. (Lederberg, J, 2001).

Functional genomics (FG) is the field of molecular biology that accomplish the use of a vast amount of genomic data meant to identify the biological operative between genes and their products. FG mainly focuses on the dynamics characteristics of the genes such as transcription, translation, regulation or functional interactions between them or their products (Holtorf et al., 2002) (EMBL-EBI, 2010) (Kellis et al., 2014).

There are two main families of omics technologies that FG uses: the one based in hybridization, using complementarity with nucleotides sequences of reference (probes) and the one based in sequencing the nucleotides on nucleic acid fragments. It is worth to say that sequencing technology use hybridization to identify fragments as well.

Since cost has considerable decreased in the last years, sequencing-based technologies are the leading edge for omics-level data generating in biomedicine. They are open platforms, do not require previous genome knowledge and can implement the

new information about genome in an easy and fluent way. The use of these platforms permits finding of alterations in sequences like mutations, isoforms, new transcripts, etc. They are also used for gene expression quantification by generating absolute-value estimations based in frequency annotation of fragment readings. One of the drawbacks of sequencing data relies in the computational power associated with its handling. Sequencing generates large files, difficult to manage and heavy to process, which requires high computational capacity and tedious methods to finally interpret the data.

A main representative of the hybridization-based family encloses chips and microarrays, initially used for quantification of mRNA or DNA among different biological conditions. Today microarrays are employed in a wide variety of biomedical analysis such as Single Nucleotide Polymorphism, Methylation, Alternative Splicing, etc.

Microarray technologies like Illumina or Affymetrix do not require much computational power when processing the information. Since they have been persistently used for many years, a wide variety of statistical tools and algorithms have been developed to integrate and compare arrays, identify biological-specific signal and correct background noise.

They are very reproducible as well but contrary to sequencing, these technologies are closed platforms which does not allow to quantify unknown sequences or sequences that are not included in the microarray. Since knowledge about genome is constantly evolving, probe measures in the array can be mismatched or inaccurate unless probe set mapping is adequately updated. To overcome this issue, a file referred to as Chip Definition File (CDF) is used when processing the data to indicate which probe sets correspond to a particular gene, in a process known as gene mapping. The CDF needs to be updated to include genomics recent discoveries and adapt probe set mapping according to the latest biological information available.

Human Genome microarrays

This thesis focuses on high-density oligonucleotide one-channel expression arrays. Figure 1.7 shows an example of this technology.

High-density oligonucleotide expression arrays are composed by micro cells distributed in rows and columns. Each cell includes small fraction of nucleic acids that will hybridize with a specific complimentary sequence of targeted nucleic acid marked with fluorescent molecules. By using short oligonucleotides (25 bases aprox.) this type of

microarrays probes for genes in an RNA sample. Since probes may not hybridize due to its shortness, multiple probes are used to improve specificity. Each of these microarrays contains between 40 and 60000 probe sets with sequences of the entire transcriptome of the studied specie. Each probe set comprises 11 to 16 different oligonucleotide probes corresponding to different coding regions of the gene they represent. Each specific sequence-probe includes two oligos (probe pair) called perfect match (PM) that corresponds exactly to a section of the mRNA molecule of interest, next to an oligo called mismatch (MM). MM has the same sequence excluding one nucleotide and is used for detecting nonspecific hybridizations (www.affymetrix.com) (www.agilent.com) (Fontanillo, 2013).

Microarrays can be classified according to the number of channels or fluorescent colors used. Two channels microarrays are used for contrasting relative quantities between two samples, usual in control-vs-disease assessment. The data resulting is a relative value indicating which sample has larger amount of each gene with a specific color (E.g. Red fluorescent Cy5 for higher amount and green fluorescent Cy3 for lower amount of gene related RNA in a sample). One channel arrays measure absolute quantity of transcript in a given sample by out putting a variety of one-color intensities (Aibar Santos, 2015).

Despite sequencing based technology is the forefront in large scale data analysis, microarrays are still considered by scientist to perform GEP or analyzing multiple genes in several samples, which allows to shape normalized expression profiles, i.e. groups of genes showing differential expression levels, associated to a particular condition or phenotype, identify classes and detect patterns. GEP has been used in cancer to identify gene signatures associated to prognosis and survival or to classify molecular subtypes of diverse cancer types (Guinney et al., 2015) (Perou et al., 2000) (Weigelt et al., 2010).

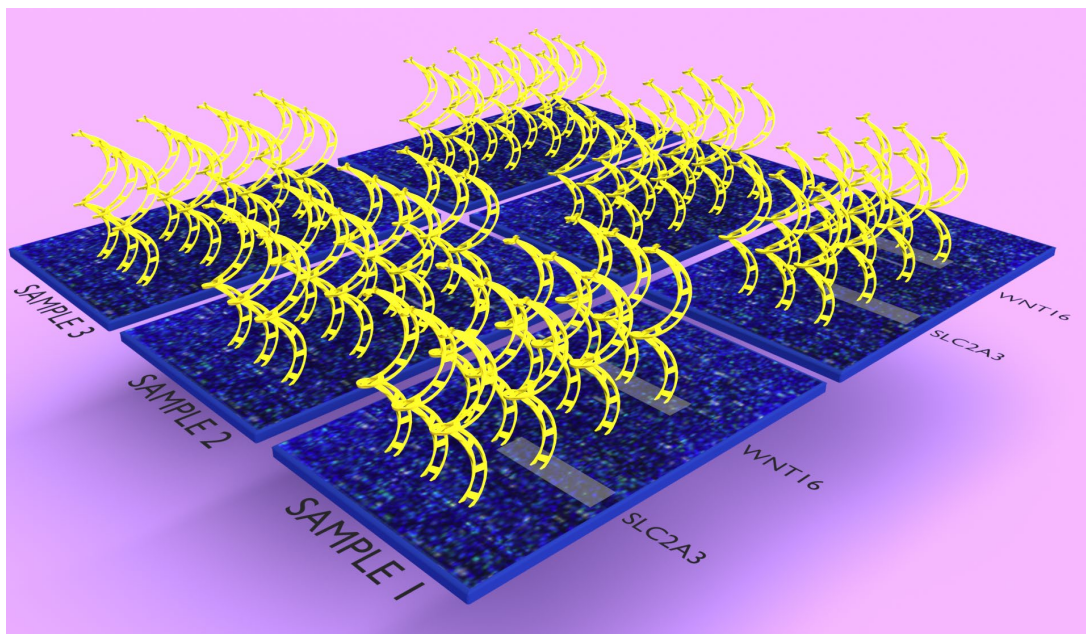
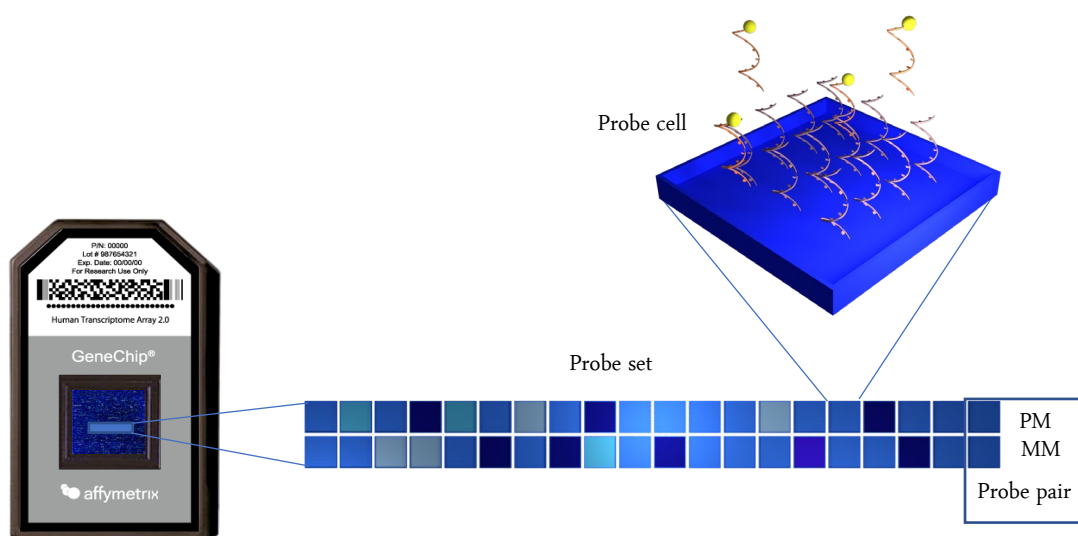


Figure 1.7 High-density oligonucleotide expression arrays. Detail of technology. Microarrays are composed by micro cells distributed in rows and columns. Each cell includes small fraction of nucleic acids that will hybridize with a specific complimentary sequence of targeted nucleic acid marked with fluorescent molecules. By using short oligonucleotides (25 bases aprox.) this type of microarrays probes for genes in an RNA sample. Since probes may not hybridize due to its shortness, multiple probes are used to improve specificity. Each of these microarrays contains between 40 and 60,000 probesets with sequences of the entire transcriptome of the studied species. Each probe set comprises 11 to 16 different oligonucleotide probes corresponding to different coding regions of the gene they represent. Each specific sequence-probe includes two oligos (probe pair) called perfect match (PM) that corresponds exactly to a section of the mRNA molecule of interest next to an oligo called mismatch (MM). MM has the same sequence excluding one nucleotide and is used for detecting nonspecific hybridizations. The chip definition file (CDF) maps probe sets to genes. The use of updated CDFs permits new probe-gene assignment according to latest biological knowledge. By analyzing multiple genes in several samples, this technique allows to shape normalized expression profiles, i.e. groups of genes showing differential expression levels, associated to a particular condition or phenotype.

Preprocessing algorithms

The integrative analysis (IA) of multiple microarray gene expression datasets has been recognized to be a very useful approach for obtaining relevant biological information from genomic datasets (Rhodes and Chinnaiyan, 2005).

Two main strategies are commonly followed when performing integrative analysis of gene expression datasets: "meta-analysis" and "integrative analysis via data merging or pooling" (Ma, 2009). In meta-analysis, each study is independently analyzed, and results are combined to assume (or not) that significant results for a big number of studies will be significant for a particular study with similar background.

In merged IA, individual results are not considered in the process. This approach is based in combining single datasets to build a new integrated large dataset in where further analysis can be achieved obtaining results with more statistical relevance and leading to more robust inferences. The main drawback of this type of IA is that pooled data inevitably suffers of batch effect(Lazar et al., 2013a).

Batch effect is a common issue that occurs when multiples arrays from different sources are integrated in one assay. An appropriate definition says that batch effect represents the "systematic technical differences" when samples are processed and measured in different batches and which are unrelated to any biological variation recorded during the experiment (Chen et al., 2011). The term batch denotes a collection of microarrays (or samples) processed at the same site over a short period of time using the same platform and under approximatively equal conditions. (Chen et al., 2011)

The choice of one preprocessing method to avoid batch effect entails substantial impact on the ultimate result in a genomic analysis. It always encompasses a tradeoff between homogenizing information to make data comparable and maintain signal as raw as possible to preserve maximal biological meaning.

In regular one channel microarrays, the scanner yields raw values that comprise the intensity signal of each cell given by the hybridation of probes plus the undesired signals due to noise in the optical detection system or unspecific hybridation. This data is not used directly in subsequent analysis. The background must be removed in a process call background correction. Other factors such as the RNA degradation, the physical location of probesets in the array, proportion of GC, etc. can interfere the signal and make impossible a proper comparison among arrays. By using a similar scale, these systematic

interferences in the arrays and among them can be minimized in a process referred to as normalization. In platforms where transcripts are represented by many probes, intensities need one third step. A summarization process by which adjusted and normalized intensities are transformed into a unique value proportional to the quantity of transcript per gene (Gentleman et al., 2006).

These three steps are known as "preprocessing method" and are present in most of the algorithms used in microarrays for transforming the intensity signal into useful information. The selection of an appropriate method is extremely important (Gentleman et al., 2006). Result validation highly depends on the adequate choice

Robust Multiarray Average (RMA) (Irizarry et al., 2003) is one of the most frequently used preprocessing methods for one channel Affymetrix microarrays. It uses three particular steps: convolution background correction, quantile normalization, and summarization based on a multi-array model, fitted robustly using the median polish algorithm.

Most of the background correction methods calculate probe specific signal by subtracting MM from PM. The problem is that more than 30% of MM show signal of larger magnitude than related PM, resulting in a significant number of negative values. This attenuates the average signal. (Irizarry et al., 2003). The convolution background correction of RMA computes a specific background for each probe set, using MM only when it is physically possible, and quantities smaller than PM in the remaining cases. This leads to avoid negative values and signal attenuation. RMA's quantile normalization method transforms the distribution of probe intensities for each array in a set of arrays into the same value. (Bolstad et al., 2003). RMA is widely used in bioinformatics but has important limitations when preprocessing a substantial number of samples, since RMA needs to analyze all the arrays simultaneously.

Frozen RMA, (fRMA) (McCall et al., 2010) is another frequently used preprocessing algorithm that solves the limitation in computational resources of dealing with large number of arrays at a time. The basic idea sustaining fRMA consist in using precomputed parameters estimates (probe-specific effects and variances) from a large database of microarrays in order to grasp the variability in probe behavior, and then "freeze" it. This frozen parameter vector can be later employed to preprocess new-added arrays.

There is a wide variety of techniques to address batch effect removal (BER) contained in two main groups of methods: location-scale (LS) methods and matrix-factorization (MF) methods. LS methods assume a model for the mean and/or variance of the data within the batches and adjust the batches to these models. MF techniques assume that the variation in the data corresponding to batch effects is independent on the variation corresponding to the biological variable of interest and it can be captured in a small set of factors which can be estimated through some matrix factorization methods (Lazar et al., 2013a). Batch mean centering, gene standardization, scaling relative to a dataset of reference or an Empirical Bayes method known as Extended Johnson-Li-Rabinovitch or Combat (Johnson et al., 2007) are some of the most broadly used LS method for removing batch effect. Combat removes batch effect by pooling information from multiple genes with similar expression characteristics in each batch and making least square estimations for each gene (Lazar et al., 2013b).

In this Thesis an IA has been performed including 7 different CRC studies. Two broadly used preprocessing methods (RMA and fRMA) for Affymetrix arrays and two standard BER processes (Batch mean centering and Combat) have been applied trying to find an adequate balance between eliminating batch effect and preserving the expression signal to the maximum.

1.3. Nutritional strategies in cancer based on molecular effects:

Several recent studies show that 25%-70% of patients visiting an oncology clinic for the first time are malnourished. The Prevalence of Malnutrition in Oncology (PreMiO) study over 1,952 cancer patients enrolled showed that 51% had nutritional impairment and 9% were clearly malnourished (Laviano et al., 2018). Cancer-associated malnutrition encompasses the inadequate nutritional intake leading to a depletion in body deposits of fat and lean mass, and ultimately resulting in reduced physical function (Lochs et al., 2006). It is associated to stage and commonly presents three major clinical consequences: anorexia, cachexia and sarcopenia. Eventual cancer-associated anorexia arise due to altered appetite signals concurrent with the disease (Blauwhoff-Buskermolen et al., 2016). This loss of appetite, together with physical restrictions caused by therapy or surgery (i.e. diarrhea, vomiting, malabsorption), obstructions, inflammation or molecular shift in the metabolism, can derive in a massive loss of weight of some patients. Its extreme manifestation involves the termed cancer-associated cachexia. In some types of cancer such as pancreatic, lung or CRC, cachexia arises in more than a half of all diagnosed individuals (Baracos et al., 2018). The cachectic phenotype of the last stages curses with accelerated loss of lean body mass and physical function impairment in what is known as sarcopenia (Laviano et al., 2018). Sarcopenia occurs in overweight/obese patients as well, hindering diagnosis. Malnutrition has implications in patient quality of life, worsening prognosis and survival rates (Meyerhardt et al., 2017) (Muscaritoli et al., 2017). For instance, malnourished CRC patients showed toleration to fewer cycles of chemotherapy (Aaldriks et al., 2013), different grades of malnutrition in cancer patients correlated with higher risk of toxicity to chemotherapy (Prado et al., 2016), malnourished oral cancer patients undergoing therapy achieved lower score on quality of life (QOL) scales regarding physical function (Gellrich et al., 2015). In fact, short- and long-term longitudinal studies revealed that malnourished patients displayed higher risk of fatal outcome, ranging from 2- to 5-fold, compared to patients with slight or no sign of malnourishment (Maasberg et al., 2017) (Aaldriks et al., 2013) (Pressoir et al., 2010). Infection after surgery is also associated to malnutrition. For instance, the frequently diagnosed malnutrition (based on at least one of the following four criteria: weight loss >10 % within 6 months, body mass index < 18.5 kg/m², Subjective Global Assessment Grade C, and serum albumin <3.0

g/dl.) of gastric cancer was associated with higher rates of wound area infection after surgery. It was also observed a significant rate-reduction when patients received pre-operative nutritional support to reach a minimum of 25 Kcal/kg per day (Fukuda et al., 2015).

Apart from the National Cancer Institute recommendation of increasing calorie intake to counterbalance cachexia (Nutrition in Cancer Care (PDQ®), 2019) there are no clear guidelines about dietary interventions using nutrients and/or micronutrients, or its deprivation, to improve the effectiveness or ameliorate side effects of drug-based therapies or to extent survival time of patients.

Recent evidence suggests that nutritional intervention improves outcome in cancer patients. Non-malnourished cancer patients significantly improved nutritional status and reduced post-surgical complications when received nutritional support for 14 days before surgery (Kabata et al., 2015). A systematic review including a meta-analysis over 1,400 glutamine-supplemented patients on critical illness and surgery found trends to suggest that glutamine supplementation could reduce mortality (Avenell, 2006). Nutritional supplementation of ω -3 fatty acids in patients undergoing lung cancer, improved appetite, food intake, body composition, physical function and quality of life while decreased fatigue (Van der Meij et al., 2012) (Sánchez-Lara et al., 2014). A recent prospective study of post diagnostic calcium supplementation in 1,660 nonmetastatic CRC patients displayed lower CRC-specific mortality in supplemented patients with no described side effects (Hazard ratio (HR), 0.67; 95% confidence interval (CI), 0.42–1.06; P trend = 0.047) (Yang et al., 2019). Alone or in combination with ω -3 fatty acids, glutamine, vitamins or nucleotides, arginine-based supplementation has been reported to ameliorate immune response of patient undergoing cancer, such as head and neck or esophageal. These cocktails of nutrients and micronutrients, given at supra-physiological doses, have also made known benefits in inflammatory and oxidative stress parameters of patients undergoing chemotherapy (Machon et al., 2012) (Vasson et al., 2014) (Sunpaweravong et al., 2014) (Talvas et al., 2015).

Diets as Mediterranean or Japanese have shown statistical evidence of being cancer protective in different longitudinal studies (Vecchia, 2004) (Giacosa et al., 2013) (Toledo et al., 2015) (Tsugane and Sawada, 2014). Consequently, isolating and investigating food-related compounds highly consumed in these diets, are common

practices with motivating results in cancer context. Although molecular effects of different bioactive compounds present in food are being studied nowadays, no therapeutic approaches are currently used in the clinical setting.

Since diet is increasingly recognized as a key factor associated with most cancer types worldwide, especially those related to the gastrointestinal (GI) duct (CRU, 2015) and plays an important role in cancer genesis and development, diet-related approaches could be particularly helpful in the treatment of this type of tumors.

On the other hand, one of every two women diagnosed BC experiences weight gain during cancer treatment (Wahnefried et al., 1997) (Goodwin et al., 1999). Some types of BC treatments implicate decrement in the amount of estrogen or progesterone in women and the subsequent increment in fat, loss of muscle mass and significant metabolism lowering. Fatigue, edema, menopause and the use of steroid medication to palliate inflammation, pain or nausea are also reported factors that can contribute to the body weight increment (Wahnefried et al., 1997). However, heterogeneity of tumor and treatment make difficult to clarify the effect of weight gain on BC.

Obese BC patients often present hypertension, hyperlipidemia, and diabetes, also known as metabolic syndrome (MS). Complications associated to MS can be confounding factors when trying to identify the prognostic impact of obesity in BC survival (Cho et al., 2018).

Many BC subtypes have been recognized to be hormone related. Elevated levels of estrogen associated to excessive adipose tissue seems to increase the risk of developing the disease and may influence progression (Suzuki et al., 2009) (Niraula et al., 2012). Obesity also alters response to BC treatment. For instance, higher levels of leptin or insulin in obese patients can reduce the effect of aromatase inhibitors (Gnant et al., 2013); excessive adipose tissue may induce resistance to systemic therapy (Widschwendter et al., 2015) or large body surface can lead to insufficient treatment dosage (Griggs et al., 2012).

Another nutrient-based expanding line of investigation based on specific molecular effects, addresses cancer therapeutics from the restrictive point of view. Caloric restriction, time restriction feeding, intermittent fasting, even fasting mimicking diets and compounds, reveal promising findings in cancer progression, chemotherapy effectiveness or sides effects amelioration. Although the scientific evidence of beneficial

effects associated to dietary restriction are increasing, the detrimental situation of many cancer patients, leads the healthcare professionals to be reluctant to use these types of interventions and new alternatives in this field are required.

This important aspect should be considered when suggesting any biomedical strategy. A nutrient-based strategy requires to be precise at molecular level but also adequate to the patient environment and his clinical status. In this sense, two types of cancer models have been selected here to investigate the link between nutrition and cancer: colorectal cancer, a type of cancer that is frequently associated with depletion in body energetic stores and breast cancer, a type of cancer that significantly correlates with a progressive gain of weight in an important number of individuals suffering the disease.

This Thesis addresses two differential approaches suitable with each nutritional status: nutrient supplementation by bioactive compounds and nutrient deprivation by caloric restriction. On one hand, a screening of phenolic compounds (found in fruits and nuts) and derivatives molecules in different colorectal cancer cell lines, has been performed to propose any of them as a complement to standard therapy in the frequently detrimental colorectal cancer. A further analysis of fasting cycles with two different diets has been analyzed in rodents suggesting a restrictive strategy in the commonly gain-weight breast cancer framework.

1.3.1. Bioactive compounds: Phitochemicals, Phenolic compound Ellagic acid and derivatives in colorectal cancer.

Phytochemicals and food

Food contains a broad variety of components with recognized effects as promoters or inhibitors of nutrient-related diseases such as obesity, type-II diabetes and cancer. Phytochemicals comprehend one of the most relevant groups of health-promoting compounds found in plants. Since they are abundant in fruit, seeds and vegetables, they play a key role preventing these type of diseases through the diet.

It has been substantially reported the anticarcinogenic effect of some phytochemicals from food and plants in many studies. They prevent the tumorigenic action of carcinogens, suppress cancer cell proliferation and modulate inflammatory and immune response.(Kotecha et al., 2016) (González-Vallinas et al., 2013).

Furthermore, many of these components present lack of toxicity at the concentrations found in food so developing dietary supplements based on phytochemicals and their molecular targets can help, not only to prevent but also to improve pharmacological treatment once the cancer arises.

Phenolic compounds

Phenolics are phytochemical compounds that comprise, with terpenoids and alkaloids, the three largest classes of secondary metabolites from higher plants with more than 10,000 known structures so far. (Garde-Cerdán A et al., 2017, p. 58)

As a secondary metabolite, phenolic compounds contribute to the defense mechanisms against external stressful factors, UV protection and signaling, among some other important functions of the plant. Moreover, they contribute to the pigmentation, flavor and astringency of fruits and vegetables. Due to the presence of hydroxyl groups most of the phenolic compounds are highly antioxidant (Angelo and Jorge, 2007).

Structurally, phenolics are characterized by the existence of one aromatic ring with a hydroxyl group (Liu et al., 2015), originating an extraordinary broad variety of compounds, from single phenols (C_6) or hydroxybenzoic acids (C_6-C_1) to highly polymerized ($C_6-C_3-C_6$)_n skeleton structures (Waterman and Mole, 1994).

Tannins are polyphenols mainly constituted by polymers of gallic acid single structures C_6-C_1 (hydrolysable tannins) or condensed $C_6-C_3-C_6$ structures like Leucocyanidins or proanthocyanidins (condensed tannins). (Angelo and Jorge, 2007)

Ellagitannins (ET) are a class of hydrolysable tannins often found as glucose esters in different foods including berries (straw-berries, raspberries, blackberries), pomegranate, tropical fruits, nuts (walnuts, chestnuts, almonds, oak acorns, pistachios, pecans), muscadine grapes, oak barrel aged wines and spirits, and tea. (Espín et al., 2013a), (Arapitsas, 2012), (Bakkalbaşı et al., 2008).

The ET hydrolysis in the human gastrointestinal (GI) duct releases ellagic acid (EA), weakly absorbed in the gut but properly metabolized by microbiota to release different Urolithins (Espín et al., 2007), (Cerdá et al., 2005a). Tannin acyl hydrolase (Tannase) appears to be the key enzyme involved in the bacterial biotransformation of EA (Wu et al., 2015). Several urolithin aglycones are present in fecal samples while products of phase II biotransformation, particularly glucuronide and sulphate conjugates, are mainly found in plasma and urine. (García-Villalba et al., 2016) (González-Sarrías et al., 2010) (Larrosa

et al., 2010). The ellagic acid dimethyl ethers conjugated with glucuronide and sulphate are common metabolites also found in those two fluids (Tomás-Barberán et al., 2009) (Cerdá et al., 2004). Urolithins can be detected in systemic bloodstream at concentrations in the range of 0.2–20 μM (Espín et al., 2013a). It has also been reported that concentrations of ET-derived metabolites can reach the μM range in the colon, following oral intake of ET-containing products (Nuñez-Sánchez et al., 2014) (González-Sarrías et al., 2016) (Romo-Vaquero et al., 2015). Both urolithin conjugates and Di-O-methyl Ellagic acids seems to reach the human tissues after consumption of ETs, in concentration that vary considerably and do not exceeds the range of ng per g of tissue (González-Sarrías et al., 2010)

Several studies that uses quantitative analysis in human samples, revealed that urolithins production depends on single and specific phenotype. The observed differences in the amounts yielded, indicate that the individual microbiota composition and type of ingested ellagitannins could determine the rate of urolithin production (Piwowarski et al., 2016). Different criteria have been employed to categorize individuals: According to the urolithin production capacity, subjects can be classified from non-producers to high producers (Puupponen-Pimiä et al., 2013) (Li et al., 2015); According to the main type of urolithin synthesized, individuals are categorized in metabotype 0 (urolithin non-producers), metabotype A (production of urolithin A as unique final urolithin) and metabotype B (urolithin B and/or isourolithin A are produced besides urolithin A)(Tomás-Barberán et al., 2014). ET-metabolite detection in urea can be used to classify as well (Cerdá et al., 2005b)(González-Sarrías et al., 2010) (Truchado et al., 2012) (Tomás-Barberán et al., 2017)

Different strains of bacteria, *Gordonibacter pamelaee* (DSM 19378T) and *Gordonibacter urolithinifaciens* (DSM 27213T) (Selma et al., 2014a) (Selma et al., 2014b) have been recognized to be involved in urolithin production in the gut. Novel Eggerthellaceae family strains recently isolated from human feces seem to contribute generating urolithins as well, particularly isoUrolithin-A (Selma et al., 2017), setting off a promising scenario in the probiotic field for phenolic effectiveness.

Ellagic acid and its derivatives have shown to be active against several cancer hallmarks: inhibit colon cancer cell proliferation, induce cell cycle arrest, modulate some important cellular processes involved in colon cancer development such as the

inflammatory process, transformation, hyperproliferation, initiation of carcinogenesis, angiogenesis, and metastasis (table 1.4)

Table 1. 4

Phenolic compounds and in vivo derivatives included in the study and the main reported properties related to antitumor potential.

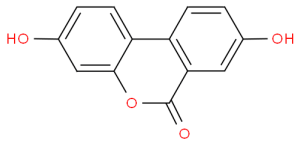
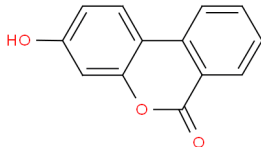
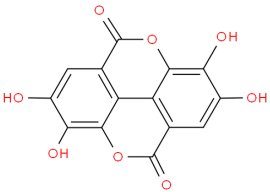
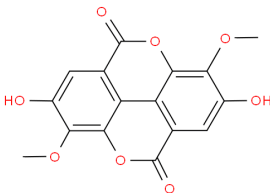
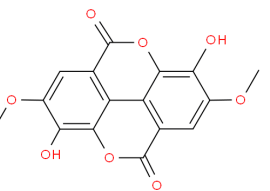
Compound	Biological Activities
<p>Uro-A CAS # 1143-70-0</p> <p>Chemical Structure</p>  <p>Uro-B CAS # 1139-83-9</p> <p>Chemical Structure</p> 	<ul style="list-style-type: none"> ○ Inhibits P450 CYP1B1-activity in 22Rv1 prostate cancer cells (Kasimsetty et al., 2009) ○ Arrested cell growth at the S- and G(2)/M-phases and MAPK signaling regulation. (González-Sarriás et al., 2009a) ○ Decreases clonogenic efficiency and cell proliferation through cell cycle arrest in the G(0)/G(1) and G(2)/M stages, followed by induction of apoptosis in HT-29 cells (Kasimsetty et al., 2010) ○ Inhibits Wnt signaling in the human 293T cell line (Sharma et al., 2010a) ○ Decreases inflammatory markers, including iNOS, COX-2, prostaglandin E synthase, and PGE2, in colonic mucosa (González-Sarriás et al., 2010) ○ Inhibits aromatase activity in breast cancer MCF-7 cells (Adams et al., 2010) ○ Inhibits cell proliferation and reduces oxidative stress status in bladder cancer (Qiu et al., 2013) ○ Modulates and is substrate for the drug efflux transporter breast cancer resistance protein (ABCG2/BCRP) (González-Sarriás et al., 2013) ○ Synergistically inhibit Androgen-Independent Prostate Cancer Cell Growth via Distinct Effects on Cell Cycle Control and Apoptosis.(Vicinanza et al., 2013) ○ Inhibits expression of the prostate-specific antigen (PSA) and the androgen receptor in prostate cancer cells (Sánchez-González et al., 2014) ○ Inhibits cell proliferation and cell cycle progression in a time- and dose-dependent manner and arrested the cells at S and G2/M phases in CRC Caco-2 and SW480 cells (González-Sarriás et al., 2014) ○ Inhibits cell proliferation and cell cycle progression by a cell cycle arrest at the G1 phase, and urolithins caused cell cycle arrest at the G2/M phase and upregulated p21 expression(Cho et al., 2015a) ○ Potentiates the anticancer effects of 5-fluorouracil chemotherapy on human colon cancer Caco-2, SW-480 and HT-29 cells (González-Sarriás et al., 2015) ○ Shows antiproliferative activity on HepG2 cells decreasing expression of β-catenin, c-Myc and Cyclin D1 and increase expression of p53, p38-MAPK and caspase-3 (Wang et al., 2015) ○ Exert anticancer effects against colon cancer cells via a common CDKN1A p21 up regulatory mechanism (González-Sarriás et al., 2016) ○ Up-regulates p21 in prostate cancer cells (Sánchez-González et al., 2016) ○ Inhibit phenotypic and molecular colon cancer stem cell features (Núñez-Sánchez et al., 2016) ○ Exerts strong antiproliferative activity, arrested cell cycle at S and G2/M phases and induced apoptosis in human colon cancer cells (Caco-2) (González-Sarriás et al., 2017) ○ Impair cell proliferation, arrest the cell cycle, induce apoptosis in UMUC3 bladder cancer cells (Liberal et al., 2017) ○ Shows antiproliferative effect by regulating the Lin28a/let-7a axis on hepatocellular carcinoma HepG2.2.15 cells (Qiu et al., 2018) ○ Exert anti-inflammatory activity mediated through the Aryl Hydrocarbon Receptor in human colon cancer cells (Caco-2) (Muku et al., 2018) ○ Induces autophagy, inhibits metastasis in human sw620 colorectal cancer cells (Zhao et al., 2018)

Table 1. 4 (Continue)

Phenolic compounds and in vivo derivatives included in the study and the main reported properties related to antitumor potential.

Compound	Biological Activities
<p>EA (Continue) CAS # 476-66-4 Chemical Structure</p> 	<ul style="list-style-type: none"> ○ Induces apoptosis via mitochondrial pathway in colon cancer Caco-2 cells but not in normal colon cells. (Larrosa et al., 2006) (Mertens-Talcott et al., 2006) ○ Inhibits proliferation by a cell cycle arrest at the S- and G(2)/M-phases and MAPK signaling regulation in Caco-2 cells (González-Sarrías et al., 2009b) (Cho et al., 2015b) ○ Exhibits anti-inflammatory property by iNOS, COX-2, TNF-α, and IL-6 downregulation due to inhibition of NF-κB and exerts its chemo preventive effect on colon carcinogenesis in rats (Umesalma and Sudhandiran, 2010) ○ Inhibits Wnt signaling in a human 293T cell line (Sharma et al., 2010b) ○ Prevents colon carcinogenesis in rats induced by 1,2-dimethylhydrazine through inhibition of the AKT/phosphoinositide-3 kinase pathway (Umesalma and Sudhandiran, 2011) (Yousef et al., 2016) ○ Induces apoptosis up regulating p53 expression in rats (Umesalma et al., 2014) ○ Induced apoptosis via the Akt signaling pathway in HCT-15 colon adenocarcinoma cells (Umesalma et al., 2015) ○ Ameliorates Cisplatin-induced nephrotoxicity and gonadotoxicity through a mechanism involving modulation of oxidative stress (Goyal et al., 2019)
<p>3,3'-DiOMEA CAS # 2239-88-5 Chemical Structure</p> 	<ul style="list-style-type: none"> ○ Exhibits antimutagenic activity in <i>S. typhimurium</i> (Smart et al., 1986) ○ Exhibits anti-PLA2 activity, an enzyme that stimulates the growth of the human pancreatic cancer cell line, and correlates with HER2 overexpression and mediates estrogen-dependent breast cancer cell growth (Da Silva et al., 2008)
<p>4,4'-DiOMEA CAS # 3374-77-4 Chemical Structure</p> 	<ul style="list-style-type: none"> ○ Exhibits antimutagenic activity in <i>S. typhimurium</i> (Smart et al., 1986) ○ Inhibits Colon Cancer Cell Growth through a mechanism involving Wnt16 (Ramírez de Molina et al., 2015)
<p>CAS, Chemical Abstracts Service; AKT, Protein Kinase B; MAPK, mitogen-activated protein kinase; COX-2; Cyclooxygenase 2; CDKN1A, Cyclin dependent kinase 1 A (p21); IGF-II, Insulin like growing factor II; bFGF, basic fibroblast growth factor; IL, interleukin; iNOS, inducible nitric oxide synthase; LPS, lipopolysaccharide; NF-κB, nuclear factor k-light-chain-enhancer of activated β cells; NO, nitric oxide; PARP, ADP ribose polymerase; ROS, reactive oxygen species; TNF-α, tumor necrosis factor-α; VEGF, vascular endothelial cell growth factor. pro-matrix metalloproteinase-2 (pro-MMP-2 vascular endothelial growth factor</p>	

1.3.2. Caloric restriction and fasting in breast cancer.

Partial or whole food deprivation have been extensively studied as a form of preventive or assisted treatment against cancer (Fernandes et al., 1976) (Weindruch and Walford, 1982) (Klurfeld et al., 1989) (Kritchevsky, 2001) (Colman et al., 2009) (Omar et al., 2010) (Brandhorst et al., 2013a). More than one hundred years ago, Moreschi observed that tumors transplanted into caloric restricted fed mice grew slower than those fed ad libitum (Moreschi, 1909).

Specifically related to BC, Tannenbaum was the first that observed the implication of reducing calorie intake in the minor size of breast tumors (Tannenbaum A, 1940).

Different combinations in the lap of time that restriction lasts and the proportion of nutrient suppressed lead to classify the more generally referred to as dietary restriction (DR) in three main different entities:

Caloric restriction (CR), in mice is usually described as a 20-40% reduction in calorie intake irrespective of its caloric source.(de Cabo et al., 2014) (Brandhorst and Longo, 2016a).

Fasting, consist in a more severe restriction of nutrients or the total lack of food (not water), usually for a shorter period of time, to avoid malnutrition. Depending on the frequency and the extent of the fasting cycles, authors differentiate between intermittent fasting (IF) and periodic fasting (PF). The difference underlays severity of the treatment in term of time and frequency. In rodent models, IF treatments usually encompass alternation between 24h ad-libitum fed of mice and 24h fasting. In PF treatment, fasting cycles last 2 or more days and mice access to normal feeding for one week or more after each restriction cycle, to recover weight. (Longo and Mattson 2014)

Another important group of DRs that has shown good results in animal models involves isocaloric diets that restraint specific nutrients in favor to others. Two relevant examples of these approaches are the Ketogenic diet (KD) and methionine restricted diet (MRD). KD encompasses a high-fat low-carbohydrates diet that rises ketonic bodies synthesis and has been reported to improve anticancer therapy in animal models with specific solid tumors, e.g. glioma, astrocytoma, pancreas, prostate, breast, colon, gastric and lung (Vidali et al., 2015) (Allen et al., 2014) (Seyfried et al., 2008). MRD limits the

sulfur amino acid methionine which seems to impair BC growth and carcinogenesis (Jeon et al., 2016) (Cavuoto and Fenech, 2012) (Durando et al., 2010) (Cellarier et al., 2003)

CR has been proven to be an effective intervention associated with the reduction of BC incidence and tumor size, and better survival in animal models (Tannenbaum A, 1940) (Klurfeld et al., 1989) (Kritchevsky et al., 1989) (Cleary et al., 2007) (Lee et al., 2012c) (Morgan E. Levine et al., 2014) (Brandhorst et al., 2017).

Generally, CR rises rodent life span by up to 60 % and delays cancer onset and improves stress resistance (Fernandes et al., 1976) (Mattson, 2005) (Mattson and Wan, 2005) (Simpson et al., 2017). Nevertheless, there is reported evidence of genetic-associated variability in CR response and specific genetic backgrounds may reverse effects, even anticipate tumor appearance and reduce longevity (Forster et al., 2003) (Liao et al., 2010)

The translationality of CR benefits to human cancer is unclear and obviously difficult. In a 23-year longitudinal study in primates undergoing 30% CR, Colman shows a decrease in cancer incidence by more than 50% in relation to control group (Colman et al., 2009), whereas in a 20-year longitudinal study performed at the National Institute of Aging, Mattison was unable to find significant differences between macaques in the control group and those in the old-beginners CR group, suggesting that not only the CR but also the early application of the intervention may be required to reduce cancer onset (Mattison et al., 2012).

The molecular mechanisms of DR have been profoundly investigated and reviewed throughout last years (Lu et al., 2019) (Madeo et al., 2019) (Kopeina et al., 2017) (Ingram and de Cabo, 2017) (Brandhorst and Longo, 2016b) (Lopez-Guadamillas et al., 2016a) (Tucci, 2012) suggesting different pathways with key implication in some cancer hallmarks (figure 1.8).

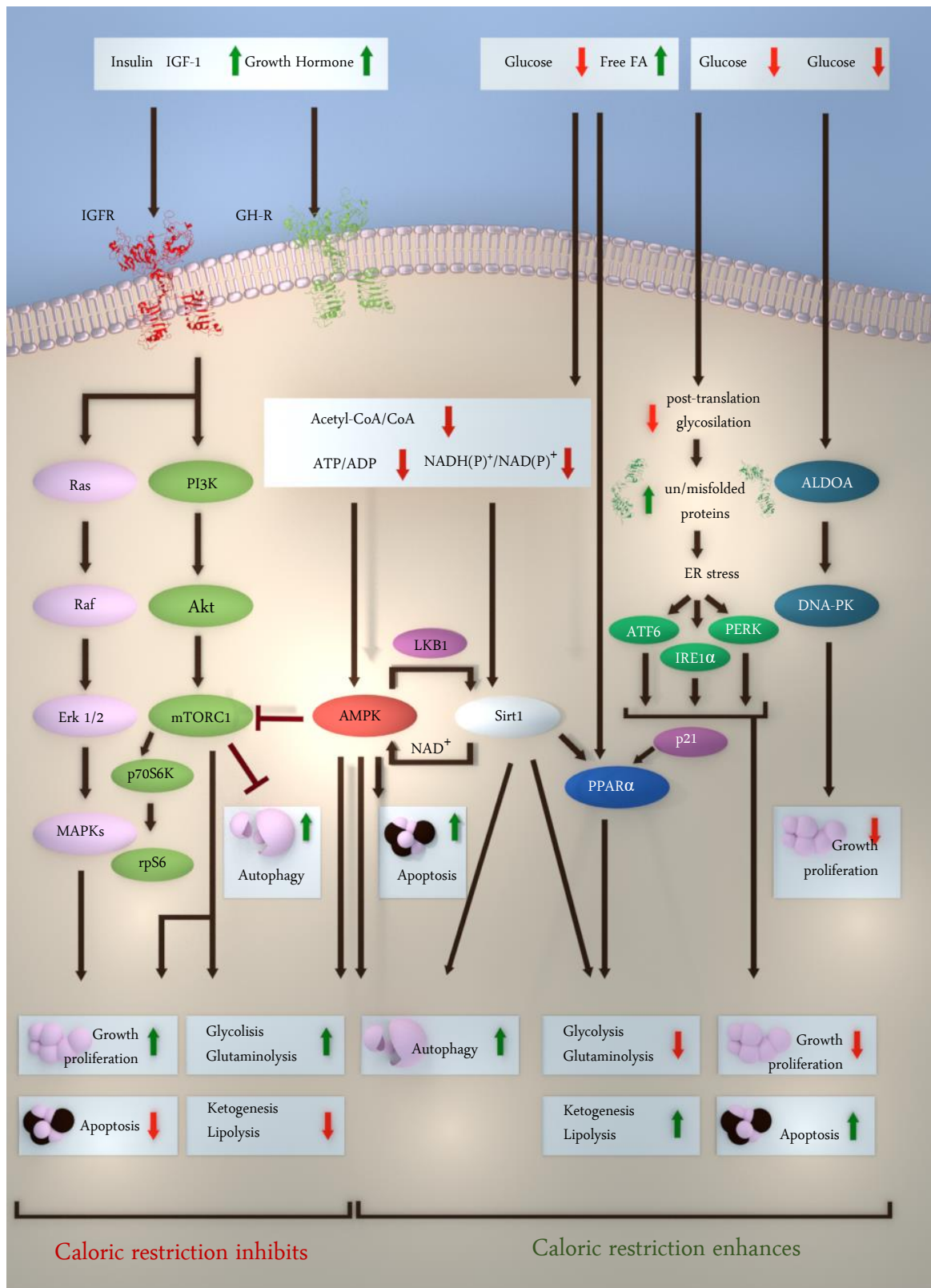


Figure 1.8. Major pathways implicated in cancer altered by caloric restriction in mammals. Figure adapted from Kopeina et al., 2017, and several reviews and papers (Lu et al., 2019) (Ma et al., 2018) (Lopez-Guadamillas et al., 2016b) (Brandhorst and Longo, 2016b).

CR and proliferative pathways

The drop of nutrients by CR outcomes in various biochemical changes leading to further metabolic adaptations that essentially consist in the sequential mobilization of internal energetic deposits. Metabolism is an extraordinary broad and complex process with thousands pathways and multiple interactors implicated. In mammals, some key processes with high implication in cancer progression encompass the decrement in levels of plasmatic glucose, the immediate alterations of acetyl-CoA/CoA, NAD(P)H/NAD(P)⁺ and ATP/ADP ratios and the decrement in the concentrations of growth factors (GFs) such as insulin-like growth factor 1 (IGF-1). Besides glucose and GF reduction, CR modulates hormonal response in different ways depending on severity and extend, which also affects plasmatic levels of a wide number of hormones such as leptin, Growth hormone (GH), insulin, glucagon, etc. (Brandhorst and Longo, 2016b) (Baljinnyam et al., 2011) (Fontana et al., 2010).

GH and IGF-1 are leading extracellular controllers of cell growth and proliferation in postnatal (Hanahan, Weinberg, 2000) and their targeting, a very active area of research (Christopoulos et al., 2015). A number of anti IGF-1 MA and TK inhibitors have been developed and currently tested in numerous clinical trials with unsuccessful results so far because of the extreme toxicity due to ubiquity of IGF-1 receptors along different tissues (Yee, 2018). Thus, one of the main advantages of CR seems to relay in its capacity of downregulating pathways triggered by this GFs.

Probably, the two most heavily studied axes in this context may be the PI3K/AKT/mTORC1 and the Ras/Raf/MAPK. They are both major signal transduction pathways that control cell growth and proliferation in response to extracellular stimulation of IGF-1, insulin and GH, among some others. Due to diverse DNA alterations (e.g., chromosomal rearrangement, SCNA, gain of function mutations in genes that constitutively activate the pathway, e.g. *PI3KCA*, *AKT1*, *HERC2* or loss of function mutations in tumor suppressor genes involved in pathway inhibition e.g. *TP53*, *PTEN*) these cascades are frequently amplified in different BC subtypes, principally those encompassing endocrine-resistant response (Steelman et al., 2016).

As occurs with IGF-1, targeting of various components of this pathway have achieved high interest in the research field including PI3K, AKT, mTORC1 (Ma, 2015) (Yamamoto-Ibusuki et al., 2015) as well as crucial downstream constituents involved in

ribosome biogenesis and protein translation (Steelman et al., 2016) (Toker and Marmiroli, 2014) (Karthik et al., 2015).

The activation of the tumor suppressor activity of AMP-dependent kinase (AMPK), a master regulator of cell metabolism and energy homeostasis, is another mechanism that inhibits cancer cell proliferation by CR. Lower levels of glucose reduce ATP/ADP and acetyl-CoA/CoA ratios increasing AMPK phosphorylation. This AMPK activation contributes to diminish cell growth and proliferation by phosphorylating inhibitors of oncogenic mTORC1 (Meynet and Ricci, 2014).

Besides acting as a tumor suppressor, AMPK has a dual role in carcinogenesis since higher levels of AMPK have been associated with chemotherapy resistance in many cancer types (Wang et al., 2016). Furthermore, AMPK expression has been correlated with some clinicopathological factors of poor prognosis in BC (Al-Maghrabi et al., 2017).

Autophagy

Starvation promotes autophagy, a catabolic pathway to disassemble unnecessary or dysfunctional cellular components for recycling. In starvation, autophagy is associated to cellular survival by maintaining energy levels to assure homeostasis (Kuma et al., 2004) (Mattson et al., 2017)

Autophagy has opposite implications in carcinogenesis. It helps to avoid accumulation of damaging components and metabolites which contributes to cell recycling and genome stability but can also induce tumor progression, since autophagy fosters adaptation to hypoxia and nutrient-reduced environment inside the tumor (Mizushima et al., 2008).

It has been widely evidenced that the activation of AMPK by CR induces cancer cell autophagy (Kopeina et al., 2017) (Mihaylova and Shaw, 2011). This process is also promoted in most type of cancer by a heavily studied family of deacetylases referred to as silent mating-type information regulation family or Sirtuins (SIRTs), that regulates epigenetic gene silencing. An extraordinary paper published by Lu and coworkers reflect the implications of different SIRTs and the crosstalk among them by CR in cancer context (Lu et al., 2019). SIRT1, a NAD⁺ dependent deacetylase, is activated by the alterations in NAD(P)H/NAD(P) ratios and the shifts in hormonal status by CR. This activation prompts the deacetylation of pro autophagic transcription factors (TF), autophagy related proteins

and proteins implicated in TF compartmentalization (Kopeina et al., 2017) (Huang et al., 2015).

However, *SIRT1* reveals different patterns of expression in BC depending on cancer subtype. Its overexpression correlates with luminal and HER2+ subtypes and reduced expression appears in the TPN subtype. It has also been reported an inverse correlation between SIRT1 expression and BC aggressiveness which suggest a dual function of SIRT1 as a tumor suppressor or oncogene (Rifaï et al., 2017) (Jin et al., 2018).

Angiogenesis

Angiogenesis is the development of new blood vasculature from existing vessels through sprouting, proliferation, and migration of endothelial cells (ECs). The expression of vascular endothelial growth factor (VEGF) command this process, particularly emphasized in cancer by the need of fueling tumor growth and further metastasis and the low oxygen microenvironment surrounding. VEGF binds on ECs cell-surface TK receptor VEGFR2, triggering signal transduction via the PI3K and MAPK pathways (Longchamp et al., 2018)

The data reported by different authors appear to hold the assumption that CR decreases tumor angiogenesis in rodents undergoing cancer. (O'Flanagan et al., 2017a) (Lashinger et al., 2011) (De Lorenzo et al., 2011) (Mukherjee et al., 2002). Fall in glucose and glutamine and reduced VEGF levels found in the serum of mice, are suggested to be key causes of the decrease in DR-associated angiogenesis. However, recent studies have revealed that DR in specific sulfur amino acids contribute to increase angiogenesis by promoting an increment in VEGF levels leading to higher micro vessel density after CR (Longchamp et al., 2018). This may indicate that CR-associated antiangiogenic effects rely on the combination of macronutrients rather than the number of calories reduced, specially the proportion of proteins included in the diet and the type of amino acids which conform their structure.

Metabolic alterations

Cancer cells consume high levels of glucose and glucogenic amino acids such as glutamine to fuel aerobic glycolysis diverting oxidative phosphorylation (Warburg effect). A restriction in glycolysis and glutaminolysis occurs during CR concurrently with an increased lipolysis and ketonic bodies (KB) synthesis or ketogenesis. (Kopeina et al., 2017). One of the key mechanism underlying this seems to rely in the stimulation by CR of an

enzyme directly involved in FFA metabolism, Peroxisome proliferator-activated receptor α (PPAR α). Tumor suppressor p21 seems to foster this stimulation under restriction of nutrients (Lopez-Guadamillas et al., 2016b) . PPAR α regulates the transcription of genes driving FFAs oxidation and KBs. Inhibition of glycolysis through PPAR α stimulation may have anti-cancer features as long as increases mitochondrial activity and reactive oxygen species (ROS) production, which has been fully associated with cell apoptosis (Vamecq et al., 2012)

Another reported consequence of higher levels of FFA though PPAR α -mediated lipolysis, encompasses the inhibition of the mTORC1 cascade, which originates apoptosis by targeting the same mechanism implicated in the upstream PI3K/AKT axe (Kopeina et al., 2017) (Laplante and Sabatini, 2013).

Others mechanism of anticarcinogenic effect by CR

An additional event proposed to be implicated in the anticarcinogenic effect of CR is the suppressed post-translation glycosylation activity of proteins due to glucose withdrawal. As a consequence of drop in glycosylation , a subsequent accumulation of unfolded or misfolded proteins in the endoplasmic reticulum (ER) occurs, which lead to ER stress and induce cancer cell apoptosis (Scheuner et al., 2001) (Zhang and Kaufman, 2006).

CR can also repress tumor growth by activating the ALDOA/DNA-PK/p53 signaling pathway (Ma et al., 2018). Fructose-1,6-bisphosphate aldolase A (ALDOA) is an enzyme that catalyzes C₆ fructose-1,6-bisphosphate detachment into two C₃-skeleton glyceraldehyde 3-phosphate and dihydroxyacetone phosphate during glycolysis. ALDOA promotes DNA-dependent protein kinase (DNA-PK) leading to augment tumor suppressor TP53 phosphorylation (Ma et al., 2018) (Lu et al., 2019). Beyond promising results by CR in animal models, little is known about this novel pathway and its implication in BC modulation.

CR and chemotherapy

The mechanism by which many anti-cancer agents introduce DNA damage in the transformed cells is highly toxic to normal cells with high rates of replacement. CR, in the setting of anti-tumoral therapy, has the capability to foster adaptative processes of normal cells to counterbalance the stress caused by toxic treatments. A great number of

researches support the evidence that the combination of stress stimuli and CR acts in a synergistic way against cancer cell, while reduce deleterious side effects on normal ones. This phenomenon is called differential stress resistance (DSR) (Kopeina et al., 2017) (Brandhorst and Longo, 2016b) (Martín-Montalvo et al., 2011)

Furthermore, CR promotes the transcription of several genes involved in cell protection against xenobiotics and damaging metabolites such as ROS. The transcription factor NF-E2-related factor (Nrf2) is upregulated under nutrient deprivation via PPAR α induction (Martín-Montalvo et al., 2011). Nrf2 is implicated in the activation of detoxification enzymes and regulates lipid and glucose metabolism enhancing cellular protection (Menegon et al., 2016).

Despite the proven effects of the combination CR and anticancer treatments in different cell lines and animal models (Raffaghello et al., 2008) (Johnson et al., 2009) (Lee et al., 2012a) (de Groot et al., 2015) (Dorff et al., 2016) (O'Flanagan et al., 2017b), the response in humans undergoing cancer is still unelucidated. Table 1. 5 shows the clinical trials identified so far that combines different types of DR in breast cancer patients.

Status	Treatment	Diet	NTC
Completed	Effects of short-term fasting on tolerance to chemotherapy	Fasting	NCT01304251
Active, not recruiting	Caloric Restriction in Treating Patients with Stage 0-I Breast Cancer Undergoing Surgery and Radiation Therapy	CR	NCT01819233
Recruiting	Caloric Restriction and Exercise for Protection from Anthracycline Toxic Effects	50% CR	NCT03131024
Active, not recruiting	Caloric Restriction Before Surgery in Treating Patients with Endometrial, Prostate, or Breast Cancer	CR	NCT02983279
Not yet recruiting	Diet Restriction and Exercise-induced Adaptations in Metastatic Breast Cancer	DR + exercise	NCT03795493
Not yet recruiting	Prevention of Breast Cancer Recurrence Through Weight Control, Diet, and Physical Activity intervention	DR	NCT02035631
Recruiting	Intermittent Fasting Accompanying Chemotherapy in Gynecological Cancers	Fasting	NCT03162289
Active, not recruiting	Short-Term Fasting During Chemotherapy in Patients with Gynecological Cancer- a Randomized Controlled Cross-over Trial	Fasting	NCT01954836
Recruiting	Controlled Low Calorie Diet in Reducing Side Effects and increasing Response to Chemotherapy in Patients with Breast or Prostate Cancer	CR	NCT01802346
Recruiting	Dietary Restriction as an Adjunct to Neoadjuvant Chemotherapy for HER2 Negative Breast Cancer	FMD	NCT02126449

Table 1.5. Clinical trials involving different types of dietary restriction in patients with breast cancer. Legend: FMD Fasting mimicking diet, DR, dietary restriction; CR, caloric restriction.

The Fasting Mimicking Diet.

The most reported unfavorable effect of CR is the down-regulation of the immune system with reduction of the amount of specific cytokines in plasma, antigen-specific lymphocytes, increment in CD8+ T-cells populations and lymphoid atrophy (Christadoss et al., 1984) (Howard et al., 1999) (González-Torres et al., 2013) (Colman et al., 2009). It has also been reported a significant delay in wound healing concurrent with neutropenia associated to CR, a non-recommendable effect for cancer patients undergoing surgery (Kim and Demetri, 1996). Furthermore, some authors have highlighted the implication of DR in fertility impairment (Bates, 1985) (Selesniemi et al., 2008) but further researches indicate that nutrient deprivation in mammals transiently downregulates fertility while

upregulates systems involved in germline protection. This suggests a standby mechanism until conditions improve, and then restore fertility (Tilly and Sinclair, 2013)

CR is problematic from the practical point of view in cancer therapeutics, especially when treating with old and delicate patients undergoing chemotherapy with exacerbated immune depression. Consequently, sort PF or IF have been designed as dietary alternatives showing positive benefits against cancer while reducing the limitations of CR (Brandhorst et al., 2013b). Nevertheless, interventions still remain difficult to adapt and recently a fasting mimicking diet (FMD) have been proposed by the group of Longo and coworkers as a short-term strategy enabling the patients to eat while mimics water-only fasting with similar benefit but without all its burden (Brandhorst et al., 2015a) (Buono and Longo, 2018).

FMD is a plant-based diet program designed to attain fasting-like effects while providing micronutrient nourishment (vitamins, minerals, etc.)(Brandhorst et al., 2013b)

Whether this dietary intervention has similar benefits as chronic caloric restriction is not fully understood but results in 16-month-old C57BL/6 mice fed with FMD significantly reduced hematopoietic tumor incidence and delayed onset, versus an isocaloric diet in the control group (Brandhorst et al., 2015a).

This diet has been tested in different models. A later publication reported that FMD-cycles combined with targeted therapy drug Doxorubicin, stimulates the hematopoietic system and enhances CD8-positive-dependent cytotoxicity which increase effectiveness of T-cell against cancer cells, both in young breast-cancer and melanoma murine models (Di Biase et al., 2016).

FMD also regulates microbiota and reduce glucose and IGF-1 levels, in serum which may help to explain its benefits in antiproliferative effects in cancer context (Rangan et al., 2019)

FMD has been tested in this thesis. Initially, downstream cascade of mTORC1, a key complex involved in nutrient sensing and cancer proliferation, has been analyzed in order to investigate the eventual modulation by FMD in comparison with SD, under intermittent fasting conditions. Furthermore, this work explores the implication of fasting cycles under FMD and SD in tumor size and metastasis trying to elucidate whether diet composition and not only restriction influences breast cancer progression

2. Hypotesis

2. Hypothesis

The differential expression of genes involved in cell metabolism and/or nutrition sensis could be associated to prognosis of cancer patients, which might be useful to identify populations susceptible of being modulated by nutritional factors.

Precision nutrition strategies, including bioactive compounds or caloric restriction, could be used to target metabolic pathways with an impact in response to chemotherapy.

3. Objectives

3. Objectives

3.1. Identification of genes involved in nutrient sensing or cell metabolism associated with CRC prognosis and patient survival.

3.2. Identification of potential precision strategies in cancer focused on molecular nutrition.

3.2.1. Nutritional strategies based on the inclusion of bioactive compounds: Identification of bioactive compounds with potential beneficial effect in CRC

3.2.2. Nutritional strategies based on the inhibition of tumor nutrient requirements: Identification of the inhibition of tumor progression and metastatic burden in BC through fasting strategies.

4. Materials and methods

4.1. In silico analysis: Identification of genes involved in nutrient sensing or cell metabolism associated with CRC prognosis and patient survival.

CRC in-silico model was built using datasets from genome-wide expression microarrays corresponding to different CRC studies obtained from public repositories. After evaluating the quality of the microarrays, datasets were integrated into a large integrative meta dataset (IMD) of 1,273 CRC samples using different preprocessing methods and Batch effect removal (BER) tools. BER was assessed by PCAs, dendrograms and a linear regression model. The preprocessed IMD that showed best BER was used to perform a subsequent differential expression analysis meant to identify genes that significantly alter their expression between early stages (I and II) and late stages (III and IV). Following, top hit candidates from previous analysis were tested in both univariate and multivariate survival analysis to evaluate their correlation with prognosis and patient survival. After adjusting the model by the confounding variables available and validating it in two external datasets, a gene set enrichment analysis was performed with top hit genes obtained in the survival analysis meant to identify enriched pathways related to nutrient sensing or cell metabolism. The association between level of expression of best candidate genes in normal colorectal epithelial tissue and tumoral tissue was assessed as well.

Genome-wide expression datasets used in this study

A large IMD was built, comprising datasets from different CRC studies, all available at the Gene Expression Omnibus repository (NCBI-GEO, 2017). Datasets included genome-wide expression microarray data corresponding to tumoral samples obtained with the platform Affymetrix GeneChip U133 Plus 2.0 for Homo sapiens. The samples were selected under the following criteria of inclusion:

- Presence of raw expression signal (non-processed intensities).
- Only primary tumor samples with no radio or chemotherapy treatment applied prior to surgery.
- Existence of phenotypic information regarding outcome in terms of overall survival (OS), disease specific survival (DSS) and/or relapse free survival (RFS) time. The samples that did not have any survival information were discarded from the study.

- Inclusion of cancer stage information.

Seven datasets of CRC samples (Table 4.1) were included, corresponding to 7 series with the following GEO accession numbers: GSE14333, GSE17536, GSE31595, GSE33113, GSE38832, GSE39084 and GSE39582. From a total of 1,407 samples only 1,273 were considered in the meta dataset. The remaining 134 were discarded due to lack of quality detected in the quality control (QC) of microarrays or errors in records or annotations.

For the external validation, two independent datasets were used. A cohort of 269 CRC samples including RNA-seq gene expression profiling and survival data (Cancer Genome Atlas Network, 2012) and a second cohort of CRC samples from the platform SurvExpress called "Colon-Metabase-Uniformized", including 482 CRC samples (Aguirre-Gamboa et al., 2013) (Table 4.2)

GEO dataset	Sample Source	Sample description	Samples	Pubmed PMID.	Author and year of study	Samples discarded	Samples processed
GSE14333	Royal Melbourne Hospital, Western Hospital and Peter MacCallum Cancer Center, Australia. H. Lee Moffitt Cancer Center, USA.	Primary colorectal cancers	290	19996206	Jorissen RN et al. (2009)	64	226
GSE17536	Moffitt Cancer Center, USA	CRC patients	177	19914252	Smith JJ et al. (2010)	0	177
GSE31595	Roskilde Hospital, Denmark	Patients with stage II and III colorectal cancer	37	ON-going	Thorsteinsson M et al. (2011)	0	37
GSE33113	Academic Medical Center (AMC) in Amsterdam, The Netherlands.	Primary tumor resections from stage II colorectal patients	90	22496204	Kemper K et al. (2012)	0	90
GSE38832	Vanderbilt University Medical Center, USA	Tumor collected from colorectal patients	122	25320007	Tripathi MK et al. (2014)	0	122
GSE39084	Toulouse Hospital, France	Sporadic early onset primary colorectal carcinomas	70	25083765	Kirzin S et al. (2014)	1	69
GSE39582	Institut G. Roussy (Villejuif), Hospital Saint Antoine (Paris), the Hospital G. Pompidou (Paris), Hospital Hautepierre (Strasbourg), Hospital Purpan (Toulouse), Institut P. Calmettes (Marseille) and Centre Antoine Lacassagne (Nice), France.	Colorectal cancer samples	566	23700391	Marisa L et al. (2013)	4	552
Total			1407			134	1273

Table 4.1 Integrative meta dataset (IMD) used in this study. Seven data sets of CRC microarrays obtained with the platform Affymetrix GeneChip U133 Plus 2.0 for Homo sapiens available in GEO, were considered for inclusion.

Characteristics	CRC patients								
	Training group			Validation group I			Validation group II		
	n° of Patients (%)			n° of Patients (%)			n° of Patients (%)		
Total sample size (n)		1273	100%		482	100%		269	100%
Age at Diagnosis (years)									
Mean		66.48			64.34			68.9	
Sd		13.63			13.51			11.94	
Age Range		22-97			19-92			35-90	
≤50		142	12.4%		68	14.1%		20	7.4%
50–70		480	41.8%		222	46.1%		115	42.8%
≥70		527	45.9%		192	39.8%		134	49.8%
Sex									
Female		540	46.9%		224	46.5%		130	48.3%
Male		611	53.1%		258	53.5%		139	51.7%
Stage									
I	55.1%	116	9.4%	44.4%	74	15.4%	59.5%	55	20.4%
II		566	45.8%		140	29.0%		105	39.0%
III	47.8%	443	35.8%	55.6%	145	30.1%	40.5%	67	24.9%
IV		148	12.0%		123	25.5%		42	15.6%
Location of Primary tumor									
Right (proximal)		371	42.0%		92	30.2%		86	31.7%
Transverse (proximal)					22	7.2%		18	6.7%
Left(distal)		472	53.4%		142	46.6%		92	34.2%
Rectum		38	4.3%		48	15.7%		75	27.9%
Other									
Lynch syndrome		8							
Outcome									
Overall survival on exitus		881	69.2%		256	53.1%		244	90.7%

Table 4.2. Phenotypical data of patients used in the present study. The table displays the phenotypical data of the IMD, and the two studies used for external validation. The IMD (1273 patients) was used as a Training group. Validation group I comprises a cohort of 482 CRC samples from the platform SurvExpress called "Colon-Metabase-Uniformized" (Aguirre-Gamboa et al., 2013) and Validation group II comprises a cohort of 276 colorectal carcinomas that had been studied using RNA-seq gene expression profiling and include survival data for only 269 (Cancer Genome Atlas Network, 2012).

All data processing, statistical modelling and graphical analysis were performed using R language (R Core Team, 2017) and the integrated development environment (IDE) RStudio Version 1.1.463 (Allaire, 2012). Most of the R packages used were downloaded from the Bioconductor website at bioconductor.org that provides tools for the analysis and comprehension of high-throughput genomic data.

The R package GEOquery (Davis and Meltzer, 2007) was used to download and operate the microarray compressed files, specifically the `getGEOSuppFiles()` and `getGEO()` functions. File uncompressing and renaming was performed with the `untar()` and `gunzip()` functions.

Text editing and reformatting for standardization was executed using jEdit software v 4.4 (www.jedit.org). Edited tab delimited files were subsequently imported into the R environment for statistical analysis.

For CRC stage unification among Dukes, Asler-Colles, TNM, etc., the tables detailed in the paper "TNM and Modified Dukes staging along with the demographic characteristics of patients with colorectal carcinoma" (Akkoca et al., 2014), were used. Times to outcome were re-calculated into month-based periods.

QC of microarrays was performed by Probe Level Model analysis using normalized Unscaled Standard Error [NUSE] plot and exploratory data analysis (EDA) using microchip images of natural scale and log-scale intensities comparison, MA-plots and boxplots of unprocessed log scale probe intensities. (Figure 4.2 displays representative examples of graphical exploratory data analysis representatives images).

Probe sets homogeneity was determined by Normalized Unscaled Standard Error (NUSE) plot. A NUSE plot represents normalized standard error estimates from the Probe-Level Model (PLM) fit which computes expression measures on a probe set by probe set basis. The function `fitPLM()` inside the `affyPLM` package (Bolstad, 2011) was used to fit the PLM and a to create the `PLMset` class objects. `PLMset` objects were subsequently used in the `NUSE()` function (`affyPLM`) to draw the NUSE plots. (Figure 4.1). A box plot of NUSE values is drawn for each array in the IMD aiming to check whether all distributions are centered near 1 and whether a microarray shows a higher spread of the NUSE distribution than the other arrays. Only arrays with median distribution centered under 1.1, were included in final IMD.

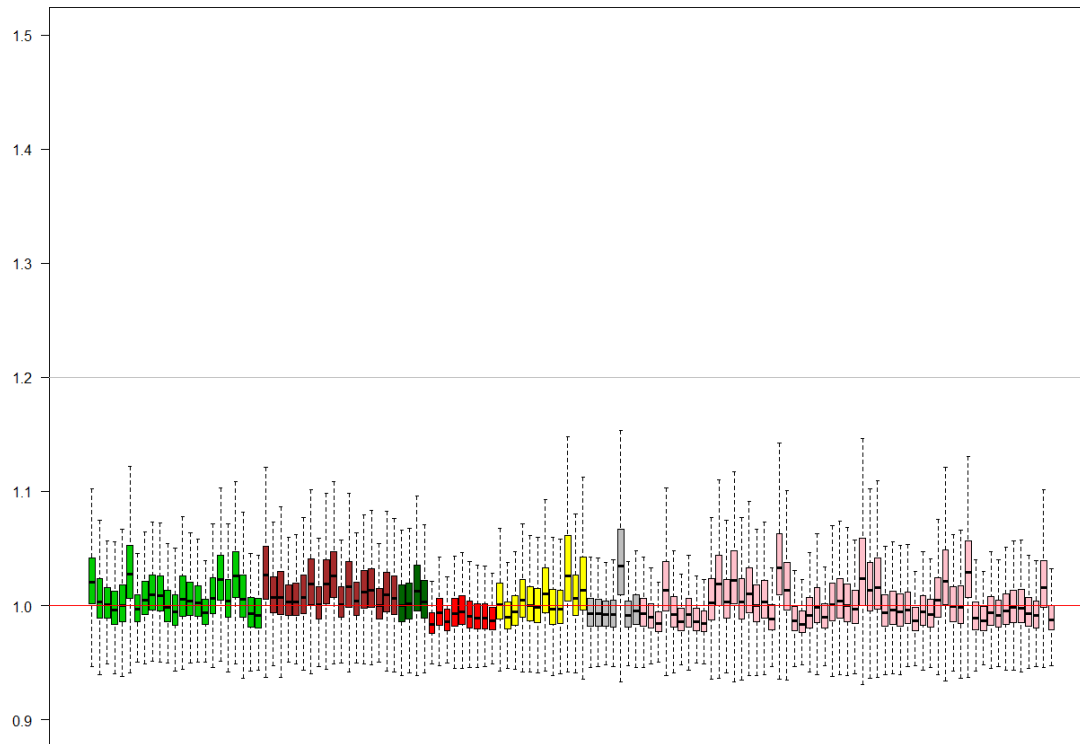


figure 4. 1. Example of NUSE boxplot for quality control of microarrays. With only 127 microarrays (10% random sampling from the total IMD for easy viewing). Most arrays are centered near 1. Each box represents a microarray, each color illustrates a different batch. Only arrays with median distribution centered under 1.1, were included in the final integrative meta dataset.

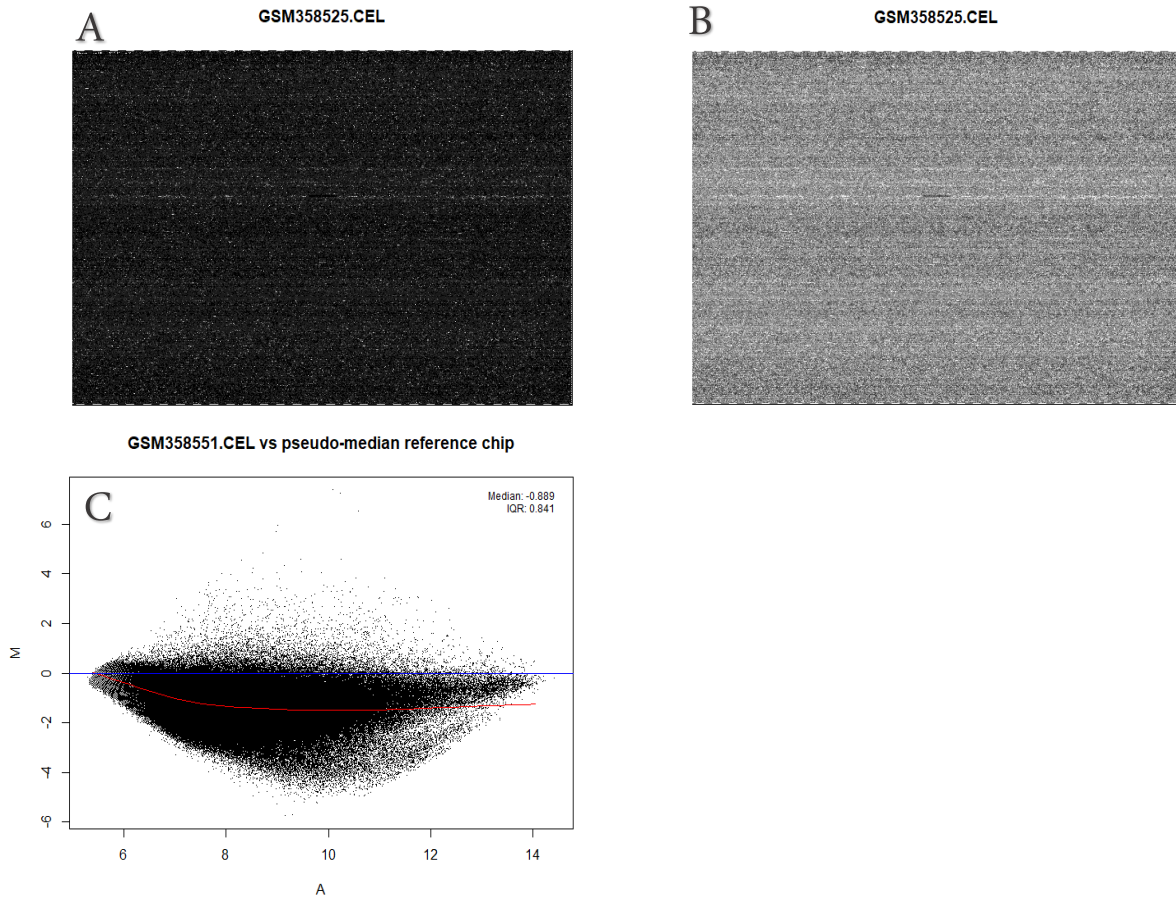


figure 4. 2. Representative examples of graphical exploratory data analysis. It shows two types of spatial images: (A) Microchip images of natural scale and (B) log-scale intensities of an array. Spatial images are artificial visualizations of a microarray that are created to visually detect spatial trends or biases; and (C). MA-plot. MA plot allows pairwise comparison of the log-intensity of each microarray to a reference median one, meant to identify intensity-dependent biases. In a non-problematic microarray, MA-plot is centered on the $y=0$ axis from low to high intensities.

4.1.1. Dataset Integration and batch effect removal.

For dataset integration in the IMD, the following preprocessing and batch effect removal methods were assayed: RMA; RMA plus ComBat; fRMA; fRMA plus Combat and fRMA plus scaling of the data using mean-centered expression values. fRMA method was computed with a self-made specific frozen parameter vector built from a random sampling proportional to batch-size and stage-group (I-II vs III-IV). The `makeVectorsAffyBatch()` function from the `affy` package (Gautier et al., 2004), was employed to build the vector. A Chip Definition File (CDF) v21 downloaded from the

website Brainarray (University of Michigan, USA) was used for updated-gene mapping (<http://brainarray.mbni.med.umich.edu/Brainarray/Database/CustomCDF/>).

AffyBatch objects were built using the `ReadAffy()` function from the `affy` package. fRMA preprocessing was performed using the function `frma()` from `frma` package (McCall et al., 2010). RMA preprocessing was performed using the `justRMA()` function of the `affy` package. All series were integrated into a single dataset with the `merge()` function available through the `InSilicomerging` package (Taminau et al., 2013) and the Combat method was implemented alternatively for later comparison. Scaling and mean-centering were fulfilled once the fRMA preprocessed IMD was constructed.

Gene annotation was performed applying the `AnnotationDECO()` function from the `DECO` R package v 0.99 (Campos-Laborie et al., 2016).

4.1.2. Batch effect removal evaluation.

BER was evaluated by correlation plots, hierarchical clustering of microarrays, principal component analysis (PCA) and linear regression (Martinez-Romero et al., 2018). Five `ExpressionSet` objects were created, one per preprocessing method, using the `Biobase()` package (Huber et al., 2015).

Correlation among arrays was evaluated on each IMD by the creation of correlation heatmaps (pair-wise Pearson correlations among microarrays were qualitatively presented as a colored matrix) and further hierarchical clustering of microarrays. Hierarchical clustering was performed in two steps: first, the distances between all pairs of arrays were calculated and second, a decision tree was created from these distances by repeatedly grouping the arrays that were closest to each other.

PCA was carried out using the `prcomp()` function in the `Stats` R package v 3.7.0 (R Core Team, 2017).

As a final testing for BER evaluation, a linear regression of the averaged expression value per batch was fitted on each five IMDs. Each batch was computed as explanatory variable in the model and coefficients and p-values compared.

4.1.3. Differential expression analysis

The expression levels of probe sets corresponding to arrays from tumors in early stages (I and II) versus tumors in advanced stages (III and IV) were considered in a Differential Expression Analysis performed to identify altered genes (adjusted $p < 0.05$) in either direction: genes up-regulated with the progression of the disease or genes down-regulated with the progression of the disease. The Linear Models for Microarrays, LIMMA package (Ritchie et al., 2015) was used to accomplish the hypothesis contrast.

Using the `model.matrix()` and `lmFit()` functions, a linear model was fitted to the expression data, for each probe set, in the IMD that showed best BER. Subsequently, the empirical Bayes method through the `eBayes()` function for differential expression was used to estimate eBayes values and to perform a moderated t-test between early and late stage samples.

4.1.4. Survival analysis

Differentially expressed genes identified in previous analysis were then ranked by adjusted p-values as described in (Martinez-Romero et al., 2018) and a second analysis was performed using 2,707 candidate genes to look for eventual association between gene expression and survival. The first step consisted in defining for each gene two separated Kaplan-Meier distributions of high and low gene expression along samples and compare them. Gene expression level of 1273 samples were sorted in ascending order and split in every sample between quantile 25% and 75% assigning a two-level factor (High and low expression) and storing data in a vector (group assignation vector [GAV]).

Kaplan-Meier (KM) objects were created computing both overall survival time and status (death or censored) using `Survfit()` function from `Survival` R package (Therneau and Grambsch, 2013).

A Cox proportional hazard (Coxph) regression model was fitted using `coxph()` and the GAV was included as explanatory variable for every cutting point.

Log rank test was then performed testing for equality of survival curves and associated Chi-square p-value recorded. The minimum p-value was selected to accomplish final group assignation of high and low expression and then fitting the Coxph model. The correspondent hazard ratios were recorded for each gene and candidates were ranked by p-value. A stringent cut-off value (adjusted $p < 0.0003$) was used to select

the genes that were considered successful candidates. This allowed the identification of genes in which the high or low expression correlated with poor survival. All analyses were adjusted by age and sex.

To assess stability and robustness of markers, a further cross-validation of the top-ranked genes was carried out. This internal cross-validation was done by a recurrent algorithm testing validity for each gene by 80% random sampling with replacement along 100 iterations.

External validation of top hit genes was carried out by applying same process in two datasets (See Validation group I and II, table 4.2)

To explore the potential improvement in CRC risk prediction of a multigenic signature, further multivariate survival analysis of 100 top markers and combinations of top 10 markers (2 to 10 gene collections) were performed using a regularized Cox proportional-hazards regression model with L_1 norm penalty (Gui and Li, 2005). The `coxnet` algorithm (Simon et al., 2011) in the R `glmnet` package (Friedman et al., 2009) was used to determine the risk score or prognostic index (PI) of each patient. A 10-fold cross-validation was applied to identify the optimal penalizing parameter λ and subsequently estimate the β coefficients associated to each gene. Those coefficients were used to predict the PI. GAVs were built following the same strategy used in the univariate analysis (minimum p-value).

4.1.5. Gene expression profiles of epithelial CRC samples vs CRC tumor samples.

To simplify further diagnostic in the clinic, the level of expression in normal colon tissue of top hit genes was tested by gathering a collection of 25 normal epithelium colorectal samples included in both series GSE33113 and GSE39582 and performing a de novo integration of the whole IMD, using same parameters and methods previously described. Normality of top hit genes distribution was tested using qqnorm plots and Shapiro-Wilk tests. Since normality was not proofed, subsequent paired Wilcox rank test was carried out to compare the levels of expression of the top hit genes with the expression from 25 normal colon samples obtained from same individuals. A subsequent unpaired Wilcox rank test was accomplished to contrast expression from iterative random 25-sampling (1000i) obtained from remaining 1248 individuals versus expression in the normal tissue. Both analyses yielded similar results

4.1.6. Geneset enrichment analysis (GSEA)

Geneset enrichment analysis tool located in Reactome.org was used for the identification of enriched pathways by top hit genes associated to poor prognosis found in previous assays.

4.2. In vitro analysis: Identification of bioactive compounds with potential beneficial effect in CRC.

4.2.1. Phenolic Compounds and Derived Metabolites

Phenolic compounds gallic acid, dihydrocaffeic acid, homovanillic acid, ellagic acid and derived metabolites 4-O-methylgallic acid and 3-O-methylgallic acid were purchased from Sigma-Aldrich (St. Louis, MO). Derivatives 3,3'-Di-O-methylellagic acid (3,3'-DiOMEA; 99% purity) and 4,4'-di-O-methylellagic acid (4,4'-DiOMEA; 99% purity) were provided by Bertin Pharma (Montigny le Bretonneux, France). Derivatives Uro-A and Uro-B, both with purity higher than 95%, were supplied by the Centro de Edafología y Biología Aplicada del Segura, Consejo Superior de Investigaciones Científicas, CEBAS-CSIC (Murcia, Spain).

4.2.2. Cell Culture

HT-29, SW-620 human colon cancer cells, 4T1 breast cancer and CCD18Co normal human colon cells, were supplied by American Type Culture Collection, ATCC (Manassas, VA). Chemo resistant cell termed SW-620-5FuR corresponds to a cell line derived from SW-620 submitted to incremental concentrations of chemo drug 5-Fluorouracil up to 150 μ M over 15 months, as previously described (González-Vallinas et al., 2013).

HT-29, SW-620, 4T1 and SW-620-5FuR, were cultured at 37°C with 5% CO₂ and 95% humidity in Dulbecco's modified Eagle's medium (Gibco/Invitrogen, Grand Island, NY) supplemented with 10% fetal bovine serum (Gibco/Invitrogen), 2 mM glutamine (BioWhittaker; Lonza Group, Basel, Switzerland) and 1% antibiotics/antifungal agents (containing 10,000 U/ml penicillin base, 10,000 μ g/ml streptomycin base, and 25,000 ng/ml amphotericin B; Gibco/Invitrogen). CCD18Co cells were cultured in Eagle's minimal essential medium (American Type Culture Collection) at standard condition 37°C with 5% CO₂ and 95% humidity. Mediums were supplemented with 10% fetal bovine serum (Gibco/Invitrogen) and 1% antibiotics/antifungal agents (containing 10,000 U/ml penicillin base, 10,000 μ g/ml streptomycin base, and 25,000 ng/ml amphotericin B; Gibco/Invitrogen). Cells were kept sub confluent, and media were changed 3 times a week. The 4T1 cell used for establishing the BC primary tumor in the mice were not maintained in vitro more than two months to maintain full malignancy and metastatic capabilities. Dimethyl sulfoxide (DMSO) was used as solvent in all stock and serial

solutions for each phenolic based treatment. DMSO concentration never exceeded 0.2 μ l of DMSO per ml of final solution in culture media.

4.2.3. Cell Viability Assays

For testing cell feasibility after 72 hours with polyphenol-based treatments, SW-620, SW-620-5FuR, HT-29, and CCD18Co cells were seeded in 24-well plates at exponential growth phase using 500 μ l/well cell suspension with a density between 15×10^3 and 60×10^3 cells.

After 24 hours, media was replaced by treatment covering serial concentrations of each polyphenol diluted in previously cited solution, or culture medium with DMSO in control cells. At 0-hour (baseline) and after 72-hour treatment, 3-(4,5-dimethylthiazol-2-yl)-2,5-diphenyltetrazolium bromide (MTT) assay was performed using 50 μ l/well of MTT (5 mg/ml in phosphate-buffered saline) (Sigma-Aldrich). Three hours after incubation at 37°C, MTT-containing media was removed and the MTT reduced to purple colored formazan by cell mitochondrial dehydrogenase was solubilized in 200 μ l/well DMSO. Formazan absorbance, which proportionally correlates with the number of viable cells (Tested compounds shall not alter mitochondrial enzyme activity), was measured one hour after solubilization, at 560 nm using a spectrophotometer microplate reader (Biochrom Asys UVM 340 Reader; ISOGEN, De Meern, The Netherlands).

At least two independent experiments were performed in triplicate for testing each compound. Proportion of viable cells was calculated both prior and post treatment.

The concentrations corresponding to the IC_{50} parameters (inhibition of 50% of cell viability), GI_{50} (inhibition of 50% of cell proliferation), TGI (total inhibition of proliferation) and LC_{50} (50% cell death) were calculated according to the descriptions of the American National Institute of Health (NIH) (Boyd and Paull, 1995)

4.2.4. RNA Extraction and Quantification

SW-620 colon cancer cells (1.7×10^5 cells per well) were seeded in six-well plates for overnight incubation under standard culture conditions. After 24 hours medium was replaced with 0 (nontreated), 5, 20, and 50 μ M concentrations of 4,4'-DIOMEA, three replicates per tested concentration. Culture medium was discarded 72 hours after treatment and total RNA was isolated from each plate using the RNeasy Mini Kit (Qiagen, Germantown, MD) following the manufacturer's instructions. For total RNA including

miRNA, miRNeasy Mini Kit from same supplier was used following manufacturer instruction.

RNA quantity and quality were checked by UV spectroscopy (NanoDrop 2000 Spectrophotometer; Thermo Scientific, Waltham, MA).

The experiment was independently repeated four times in the same conditions and total RNA from each experiment was independently analyzed.

4.2.5. Gene Expression Assays

A comparative microarray gene expression analysis between nontreated and 5 μ M 4,4'-DiOMEA-treated SW-620 colon cancer cells for 72 hours was performed at the Genomic Service Facility at the Spanish National Center for Biotechnology (Madrid, Spain). RNA integrity was determined using a 2100 Bioanalyzer (Agilent Technologies, Santa Clara, CA), and 200 ng total RNA from each sample was reverse transcribed and fluorescently labeled using the one-color Low Input Quick Amp Labeling Kit (Agilent Technologies) according to the manufacturer's protocol. The complementary RNAs were prepared for hybridization in an Agilent SurePrint G3 Human 8 x 60 K (Whole Human Genome Microarray Kit) platform using the one-color gene expression system following the manufacturer's protocol (Agilent Technologies).

4.2.6. Real time qPCR

Validation of microarray data was achieved using quantitative real-time polymerase chain reaction (PCR) analysis for measuring the transcript levels in the selected group of differentially regulated genes. Total RNA was extracted using the RNeasyMini Kit (Qiagen) following the manufacturer's instructions, and 1 μ g total RNA was reverse transcribed by a High-Capacity cDNA Reverse Transcription Kit (Applied Biosystems). TaqMan assays for gene expression (Applied Biosystems, Foster City, CA), which contain the specific primer and TaqMan probe for each gene, were used. Quantitative PCR was accomplished in real time and in triplicate on the 7900 HT Real-Time PCR System (Applied Biosystems) according to the manufacturer's instructions. Glyceraldehyde 3-phosphate dehydrogenase gene expression in each sample was used as an endogenous reference for the relative quantification of transcripts.

RQ Manager software (Applied Biosystems) was used for data extraction and analysis. To calculate the relative expression of each gene, the $2^{-\Delta\Delta C_t}$ threshold cycle method was performed as previously described (Ramírez de Molina et al., 2007, 2008).

4.2.7. Top-Fop tranfection assay

Wnt can activate several key signaling cascades including the canonical Wnt/ β -catenin pathway. Canonical pathway requires β -catenin while the other axes signal independently of it (Nusse, 2005) (Polakis, 2000). In the canonical pathway, the transcription of Wnt target genes starts when nuclear β -catenin molecules translocate to the nucleus and form a complex with TCF/LEF. This complex binds to TCF/LEF binding sites of the promoters of these target genes, and then transactivates the process (Ku et al., 2016). In order to detect Wnt activity, a series of Wnt reporters have been developed such as the TOP/FOP reporter assay. TOP-FLASH (Catalog # 21-170, Merk Millipore) is a transfection grade T-cell factor (TCF) reporter plasmid comprising two sets (with the second set in the reverse orientation) of three copies of the TCF binding site (wild type) upstream of the Thymidine Kinase (TK) minimal promoter and Luciferase open reading frame. FOP-FLASH (Catalog # 21-169, Merk Millipore) is a transfection grade T cell factor (TCF) reporter plasmid comprising two full and one incomplete copy of the TCF binding site (mutated) followed by three copies in the reverse orientation, upstream of the Thymidine Kinase (TK) minimal promoter and firefly luciferase open reading frame. This plasmid serves as a negative control to TOP-FLASH. (Figure 4.3.A)

For monitoring β -catenin/TCF/LEF activity, a dual luciferase reporting assay was performed according to the following protocol.

50,000 SW620 cells were seeded in triplicated to form sub confluent cultures in M-24 plates adding 0.5 mL culture media per well.

Then, cells were transfected using a mix of 0.8 μ l of Lipofectamine 2000 (Invitrogen), 100 μ l Optimen (Promega) per well. 600ng/well of a firefly luciferase TOP-FLASH or FOP-FLASH plasmid was co-transfected with 20ng/well of a control plasmid, pRL-SV40 renilla luciferase reporter plasmid (Promega)(Figure 4.3.B). 380 ng/well of pcDNA3 plasmid were included as carrier DNA.

After overnight incubation, medium was replaced with 0.5mL of fresh medium containing 20 μ M 4,4'DiOMEA (treated culture) or same concentration of DMSO (control culture).

After 48h on standard condition, dual luciferase was measured: the experimental signal from firefly luciferase and the control signal from renilla luciferase. Sequential readings of both firefly and renilla luciferase reporter activities were performed in a GloMax® multidetection Luminometer (Promega) using the Dual-Luciferase® Reporter Assay System (Promega) according to manufacturer's instructions.

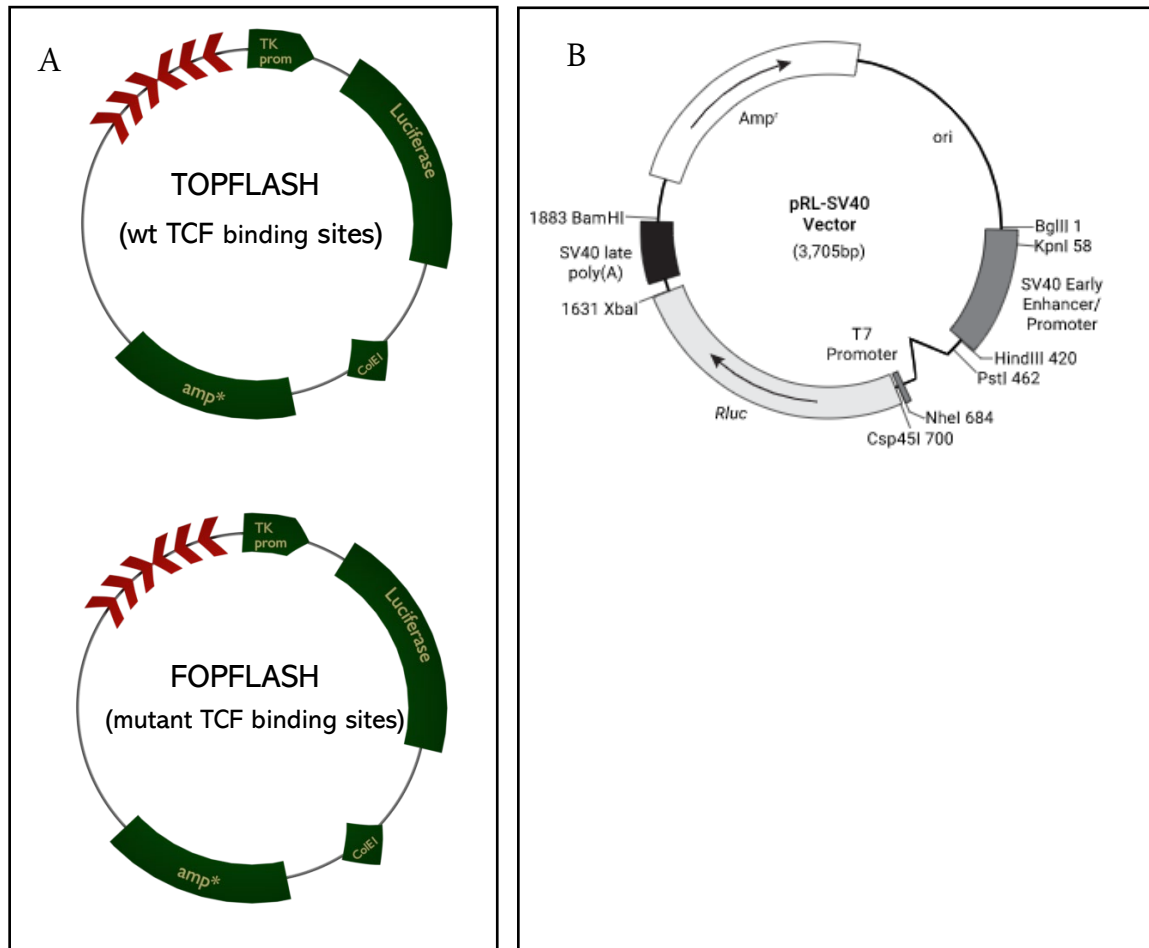


Figure 4.3 Plasmids used to transfect SW620 CRC cells for monitoring β -catenin/TCF/LEF activity after 24 hr. treatment with 20 μ M 4,4'DiOMEA, TOP/FOP and dual luciferase detection was performed using transfection grade T cell factor (TCF) reporter plasmid TOPFLASH and FOPFLASH and the pRL-SV40 vector. A) TOPFLASH plasmid comprises two sets (with the second set in the reverse orientation) of three copies of the TCF binding site (wild type) upstream of the Thymidine Kinase (TK) minimal promoter and Luciferase open reading frame. FOP-FLASH comprises two full and one incomplete copy of the TCF binding site (mutated) followed by three copies in the reverse orientation, upstream of the Thymidine Kinase (TK) minimal promoter and firefly luciferase open reading frame. This plasmid serves as a negative control to TOPFLASH. (Merk Millipore). B) The pRL-SV40 plasmid was used as an internal control reporter vector. It contains the SV40 enhancer and early promoter elements to provide high-level expression of Renilla luciferase in co-transfected mammalian cells (Promega)

4.2.8. miRNAs Expression Assay

The analysis of the miRNAs modulation of SW620 CRC cells under 4,4' DiOMEA was performed using qRT-PCR by mean of microfluid TaqMan Array panels Human MicroRNA A+B Cards Set v3.0 (Applied Biosystems), containing the specific Taqman® assays for the quantitative expression analysis of 754 miRNAs plus three endogenous controls and one negative control assay.

RT-PCR of miRNAs was carried out with the TaqMan miRNA Reverse Transcription and the primers Megaplex Primers Pools, human pools set v3.0, according to the manufacturer's instructions (Applied Biosystems). Subsequently, the TaqMan Universal PCR Master Mix No AmpErase UNG (Applied Biosystems) was employed together with the panels to carry out the qPCR in the 7900 HT equipment (Applied Biosystems), following the protocol indicated by the manufacturer. The results were analyzed by the $2^{-\Delta\Delta Ct}$ method (Livak and Schmittgen, 2001).

4.2.9. Cell Culture, Protein Extraction and Quantification

The protein extraction from cell cultures started by washing the cells with PBS and afterwards lysing them with a buffer solution containing 50 mM Tris-HCl, 1 mg/mL sodium dodecyl sulfate (SDS), 1 mg/mL deoxycholic acid, 0.1 mM Ethylene diamine tetra acetic acid (EDTA), 0.1 mM Ethylene glycol-bis(β aminoethylether) -N,N,N',N'-tetracetic acid (EGTA), 10 mM NaF, 10 mM $\text{Na}_4\text{P}_2\text{O}_7$, 10 $\mu\text{L}/\text{mL}$ Igepal CA-630, 1 mM Na_3VO_4 (Sigma-Aldrich), 1 mg/mL Complete Protease Inhibitor Cocktail, and 0.27 mg/mL AEBSF (Roche). The supernatant was collected after lysate centrifugation for 15 min at 13,500 g. High protein concentration samples were processed by an alternative method using Laemmli buffer (60 mM Tris-HCl at pH 6.8, 10% glycerol (Sigma-Aldrich) and 2% SDS) to obtain cell lysates. All samples were subsequently submitted to a 5 min at 95°C heating cycle for denaturation. The protein quantification was completed by using the Bio-Rad kit DC Protein Assay (Bio-Rad Laboratories, Hercules, CA) according to supplier's specifications.

4.2.10. Western Blot analysis

25-50 μg of total protein was separated by 8-14% density polyacrylamide SDS-Page gel electrophoresis (BioRad, Hercules, CA) under reducing conditions and transferred onto nitrocellulose membranes (BioRad, Hercules, CA) before blocking unspecific sites with 5% milk in PBS with 0.05 % of tween-20. The membranes were incubated overnight at 4°C with either one of the primary antibodies specified in table 4.3.

Subsequently membranes were incubated with secondary horse radish peroxidase-conjugated antibodies anti-mouse (antibody AP130P, 1:40,000 dilution, Millipore Corporation, Billerica, MA, USA) or anti-rabbit (antibody AP106P, 1:20,000 dilution, Millipore Corporation) for one hour at room temperature. Detection was performed using the Clarity Western ECL Substrate (BioRad Laboratories). Data image output from the chemiluminescence enhanced membrane was scanned and subsequently translated to 8-bit and analyzed directly with ImageJ software for protein quantification.

Target protein	MW (kDa)	Dilution	Supplier	Reference	Host Specie
AKT	60	1:1000	Cell Signaling	9272S	Rabbit
p-AKT (Ser473)	60	1:1000	Cell Signaling	9217s	Rabbit
mTOR	289	1:1000	Cell Signaling	2972S	Rabbit
p-mTOR (Ser2448)	289	1:1000	Cell Signaling	2971S	Rabbit
P70 S6 Kinase	75	1:1000	Cell Signaling	9202S	Rabbit
p-P70 S6K (T389)	75	1:1000	Cell Signaling	9205S	Rabbit
S6 Ribosomal protein	32	1:1000	Cell Signaling	2217S	Rabbit
P-S6 Ribosomal protein (S240-244)	32	1:1000	Cell Signaling	5364S	Rabbit
Nrf2	68	1:5000	Abcam	ab62352	Rabbit
p-Nrf2 (S40)	68	1:5000	Abcam	ab76026	Rabbit
SLC2A3	54	1:8000	Abcam	ab41525	Rabbit
Wnt16	41	1:3000	GeneTex	GTX128468	Rabbit

Table 4.3. Primary antibodies used in Western Blot analysis

4.2.11. Cell Migration Assay

Cell migration was analyzed by wound healing assay (Moreno-Bueno et al., 2009). 50,000 SW-620 cells cultured in M24 plates and once confluence was reached, a wound was done by scratching the monolayer surface carefully and washed with PBS. After addition of culture media (control culture) and 5 μ M of 4,4' DiOMEA and EA solution (treated culture) and incubate, sequential pictures of same surface of the wound were taken every 12 hours until its closure using a Leica DM IL microscope, with a 10X Plan Fluotar objective. Pixel quantification by software TScratch 1.0 of control cells and treated was performed. Data represent average open area ratio at 48 and 72 hrs divided by the average open area at 0 hrs of three independent experiments, with three replicates per tested concentration. (Two-tailed unpaired t.test, $\alpha=0.05$).

4.2.12. Mitochondrial respiration and glycolytic function monitoring.

Mitochondrial respiration and glycolytic functions were analyzed by monitoring Oxygen consumption rate (OCR) and extracellular acidification rate (ECAR) of non-treated and treated cultures (5 and 20 μ M). A XF96 Seahorse Extracellular Flux Analyzer (Agilent Technologies) was used to perform the experiment. According to previous titration, 50,000 SW620 cells per well were plated into a XF96 multiwell-plate. After 24 hr and several washes, culture media was replaced with base media supplemented with 2 mM pyruvate, 2 mM glutamine and 10mM glucose (Agilent technologies) in order to supply substrate-rich environment for the cell to perform normal glycolysis and respiration. 60 min ahead the assay, cells were incubated in a non-CO₂ atmosphere at 37 °C. Basal measurements of respiration and acidification were recorded of both control and treated cells and rates were calculated at intervals of 7 minutes. Afterwards, an oxidative phosphorylation uncoupler, carbonilcyanide p-triflouro methoxy phenylhydrazone (FCCP) (Agilent technologies) at a concentration of 0,3 μ M was added to the media to record the maximal respiration of cells. For the FCCP preparation and injection, XF Cell Mito Stress Test kit Kit ref 103015-100 instructions were followed. FCCP is a potent oxidative phosphorylation uncoupler that disrupts ATP synthesis by transporting protons across mitochondrial inner membranes depolarizing membrane potential (Heytler and Prichard, 1962). Previous titration showed FCCP concentrations of 0.2 to 0,5 μ M as the optimal range to be used in SW620 cell cultures. Same data was collected following injection of the drug (3 measures of OCR ECAR) and spare respiratory capacity (SRC) calculated.

Phenotype test report was subsequently obtained using Seahorse manufacturer Wave software 2.6.0 (Agilent Technologies)

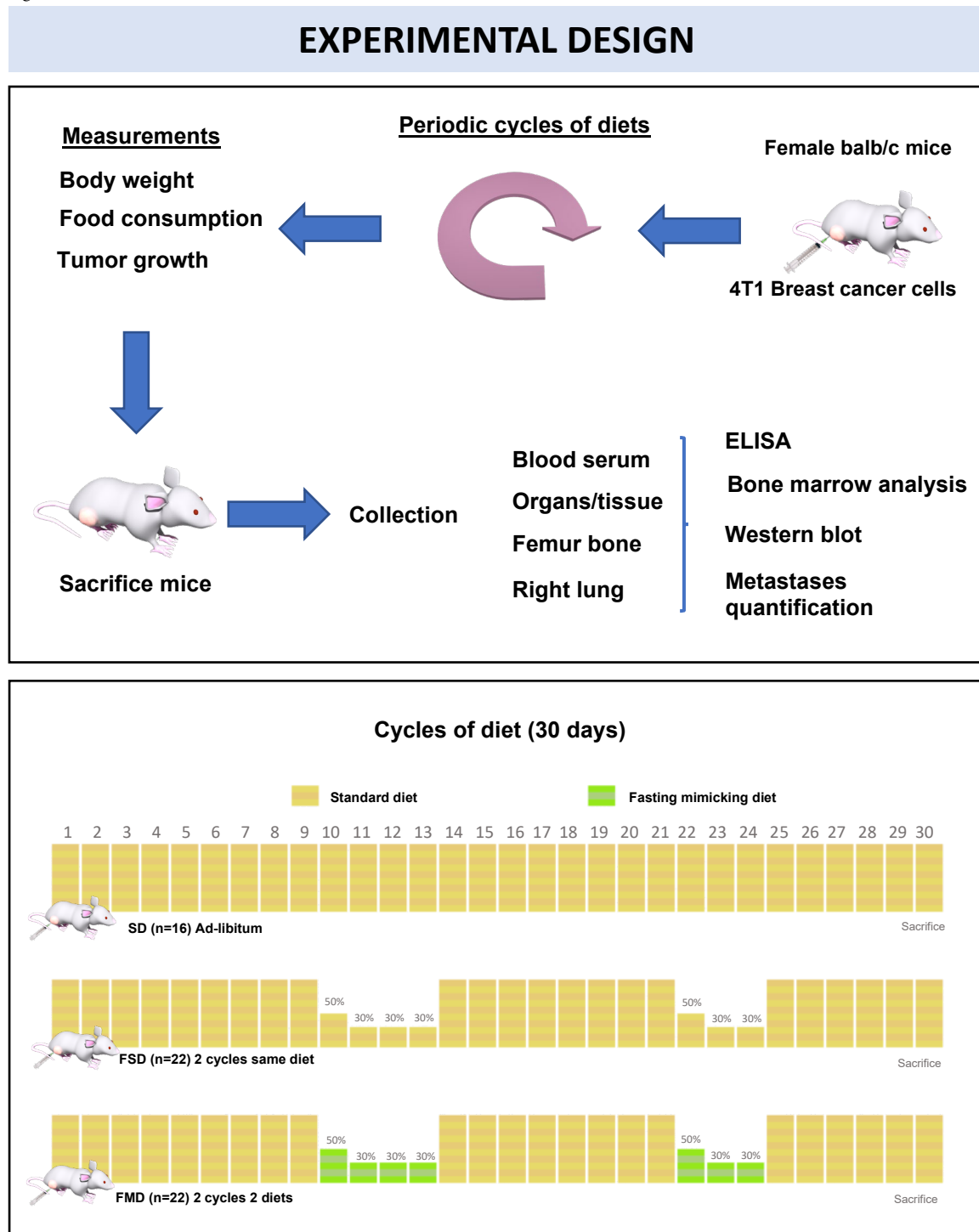


Figure 4.4. flowchart representing the experimental design to test fasting cycles with different diets in breast cancer murine models. 60 female Balb/c mice were single housed at 8 weeks of age and injected 4 weeks later with 2×10^5 4T1 Breast cancer cells subcutaneously in the fourth mammary gland. Thereafter mice were randomized into three groups: i) "Standard Diet" SD group (n=16): mice were fed ad-libitum (AL); ii) "Fasting Mimicking Diet" FMD group (n=22): mice underwent 2 cycles of 4-3 days of fasting followed by 8-6 days of AL refeeding, respectively. On day 1 of fasting, mice received a pellet of FMD containing 50% of the daily calories of AL controls. On days 2-4, the FMD pellet contained 30% of the daily calories; and iii) "Fasting Standard Diet" FSD group (n=22): mice underwent the same feeding paradigm than FMD but were fed SD during the fasting cycles. On day 1 of fasting, mice received a pellet of SD containing 50% of the daily calories. On days 2-4, the FMD pellet contained 30% of the daily calories. At the end of the study (30 days after injection, day 6 of refeeding), mice were sacrificed, and tissues were harvested. 13 mice (2-SD, 5-FMD, 6-FSD) developed tumor ulceration and were euthanized before the end of the study to fulfill the endpoint criteria of the animal protocol.

4.3. In vivo analysis: Identification of the inhibition of tumor progression and metastatic burden in BC through fasting strategies.

60 mice were initially randomized in 3 groups, one of them feed ad-libitum on standard diet (SD) and the two others submitted to short fasting cycles with a specific diet each, Fasting Mimicking Diet (FMD) and Fasting Standard Diet (FSD). A flowchart captured in figure 4.4 briefly explains the experimental design.

Figure 4.4



All the work was performed in the Biomedical Research Center, National Institutes of Health NIH, NIA, Translational Gerontology Branch Laboratory at Johns Hopkins Bayview Campus, Baltimore, MD, USA.

4.3.1. Animals

60 female 8-week-old BALB/c (wild-type) mice purchased from Jackson Laboratories were single housed in duplexes (#15 Single Housed Duplexed Cage; Dimensions 22.2 x 30.8 x 16.24 cm; Thoren Caging Systems, Hazeltown, PA, USA). Nestlet for enrichment and autoclaved corncob bedding was included in each duplex. The experiment was performed at the NIA Biomedical Research Center vivarium (Baltimore, MD, USA), under pathogen-free setting in rooms maintained at 22-22°C, 30 to 70% relative humidity and 12 hr day/light cycles (Artificial light supply from 6:00 AM to 6:00 PM). Free access to individual bottles of municipal tap water treated by reverse osmosis and hyper chlorinated (2-3 ppm) was provided. Low velocity HEPA filtered air was pumped through sealed shelf plenums directly into the cages through holes practiced above each cage filter top.

All animal protocols were approved by the Animal Care and Use Committee (352-TGB-2018) of the National Institute on Aging, National Institutes of Health. Baltimore, MD, USA. Animals were inspected twice a day for health issues. Euthanasia criteria were established on an independent valuation by veterinarians according to the Association for Assessment and Accreditation of Laboratory Animal Care International (AAALAC) guidelines.

4.3.2. Diets

All animals were fed ad-libitum (AL) irradiated AIN-93G Envigo Teklad purified diet (TD.94045 Envigo,MI, USA) for 4 weeks prior to injecting the breast cancer cells. Thereafter mice were randomized into three groups maintaining between groups tumor size homogeneity and fed as specified bellow:

1) Standard Diet (SD) group (n=16): mice were fed ad-libitum (AL); 2) Fasting Mimicking Diet (FMD) group (n=22): mice underwent 2 cycles of 4-3 days of fasting followed by 8-6 days of AL refeeding, respectively. On day 1 of cycle, mice received a pellet of FMD containing 50% of the daily calories of AL controls. On days 2-4, the FMD pellet was reduced to the 30% of the daily calories; and 3) Fasting Standard Diet (FSD) group (n=22): mice underwent the same feeding paradigm (2 cycles of 4-3 days of fasting with same reductions in caloric intakes followed by 8-6 days of AL refeeding) but the composition of the food consisted in AIN-93G Standard

For calculating dietary proportions, food consumption of 16 animals randomly selected and fed ad-libitum on SD were monitored before starting point. An average daily intake of 2.35 gr chow per mouse was used subsequently as baseline to calculate calorie requirements. Manufacturer indicates a caloric charge of 3,76 kcal/gr of AIN-93G so an ad-libitum daily caloric intake reference of 8.85 kcal per animal was estimated as caloric baseline. The AIN-93G macronutrient proportion of proteins, carbohydrates and fats (P:C:F) is 25:58:17 (TD.94045 Envigo,MI, USA).

The day 1 of each cycle every animal was transferred into a fresh cage to avoid coprophagy, supplied with new tap water and fed a diet including 4.43 kcal (50% of baseline) of total digestible energy. The day 2-4 rations were reduced to a daily amount of 2.67 kcal (30% of baseline) per animal. After fasting, mice were re-fed ad libitum for 8 days until following restriction cycle. Restricted food diets were isocaloric. FSD group was fed AIN-93G chow and FMD group FMD chow. Mice on restricted diet consumed all the supplied food while on the cycles.

The FMD is based on a nutritional diet consisting on a mix of various low-calorie broth powders, a vegetable medley powder, extra virgin olive oil, and essential fatty acids, all inside a hydrogel matrix to achieve binding and to allow cage feeder dispensation (Brandhorst et al., 2015b). The macronutrient distribution of FMD is 6:65:29 (P:C:F). No

animal proteins are included in the chow composition and the caloric charge per gram including hydrogel is 2.90 Kcal, some 30% fewer than the standard diet used as control.

4.3.3. Establishing and monitoring BC tumor

Every Balb/c mouse were subcutaneously inoculated with 2×10^5 4T1 breast cancer cells diluted with 100 μ l serum-free medium at the age of 12-weeks-old, 4 weeks after reception from Jackson Labs. Tumor onset was monitored after injection by primarily palpating injection area and subsequently measuring dimensions with a Vernier caliper every 3 to 4 days. None of the primary tumors reached a mean tumor diameter (TD) of 16 mm and neither any animal became moribund (IACUC guidelines) but 13 mice (2-SD, 5-FMD, 6-FSD) showed tumor ulceration and were euthanized and removed from the experiment fulfilling criteria of the animal protocol. Animal weight and food consumption data was also recorded every 3 days during ad libitum feeding time and every day while on food restriction time.

4.3.4. Sacrifice, collection of tissues, lysates and protein extraction, metastasis analysis.

At the end of the study (30 days after injection), mice were sacrificed, and tissues were harvested, snap-frozen in liquid nitrogen and stored at -80°C . Lungs were analyzed for metastasis by ex-vivo injecting indian ink through the trachea, which was detained in Fekete's solution to count tumor nodules. (Pulaski and Ostrand-Rosenberg, 2001). Metastasis counting was performed by three independent researcher and results included average values of all three recordsets.

Frozen tissues were disrupted and homogenized for 3 min at 30 MHz using high-speed shaking in a QIAGEN TissueLyser II equipment. Samples were processed in batches of 20 units using 2-mL-Eppendorf Safe-Lock micro test tubes with one stainless steel bead per tube in presence of a 450 μ L solution including Pierce[®] RIPA buffer (Thermo Scientific, Rockford, IL), protease inhibitor cocktails (PIC) 1, PIC 2 and PIC 3 (Sigma-Aldrich St-Louis, MO) phosphatase inhibitor phenylmethylsulfonyl fluoride (PMSF, Thermo Scientific, Rockford, IL) and lysine deacetylase inhibitors (10 μ M trichostatin A, 10 μ M nicotinamide, and 50 μ M butyric acid, all from Sigma-Aldrich, St-Louis, MO). Total protein extracts were quantified with BCA assay (Thermo Scientific, Rockford, IL), dissolved in NuPAGE buffer (Thermo Scientific, Rockford, IL) and denatured by boiling for 5 min at 100°C .

5. Results

5.1. Identification of genes involved in nutrient sensing or cell metabolism associated with CRC prognosis and patient survival.

5.1.1. Identification of 765 genes associated with differential survival among CRC patients.

5.1.1.1. Data integration: RMA plus Combat and fRMA plus Combat achieved effective BER among the five methods tested

Hierarchical clustering correlation heatmap in figure 5.1 shows adequate batch effect removal in those IMD that has been pre-processed with RMA or fRMA only when the Combat algorithm was applied (5.1.B and 5.1.D). The figures represent association between 210 random samples from 7 different batches identified by a different colour, shown in the upper side bar of each plot (30 samples from each batch). This unsupervised analysis displays samples clustered together when batch effect remains after pre-processing with RMA, fRMA and fRMA plus mean centering (5.1.A, C and E). The heatmap indicates clear colour shuffling and lack of clusters when applying the other two methods.

Figure 5.2 displays score plot of the first two principal components (PCA) of 1,273 CRC samples normalized with the 5 different methods 5.2.A (RMA method) and 5.2.C (fRMA) clearly identify clusters by colours suggesting a strong batch effect remaining after pre-processing. By contrast, PCA data provided by the other 3 procedures (5.2.B, D and E, RMA plus Combat, fRMA plus Combat and fRMA plus mean-centered scaling methods respectively) show an adequate mix of all the samples.

Table 5.1 displays coefficients obtained from regressing gene expression on array batch per pre-processing method. The largest p-values indicating lack of significant difference and no batch effect were achieved when regressing the arrays in where RMA plus Combat and fRMA plus Combat algorithms were used.

Since no more datasets were previewed to be added, the IMD pre-processed with RMA plus Combat was selected (and fRMA plus Combat discarded) for further differential expression, survival and GSEA analysis.

5.1.1.2. 765-candidate genes correlated with low survival were identified

Differential expression analysis performed in the IMD using LIMMA, revealed that a substantial number of genes, more than one tenth of the entire genome, significantly alter their expression when cancer progresses between early stages (I and II) and late stages (III and IV). 2,707 genes out of 20,079 CDF-mapped genes were differentially expressed between those two conditions (adjusted p-value < 0.05).

Univariate KM survival analysis using the expression level of those 2,707 genes identified 765 genes that mark survival differences among samples in either direction (i.e. 429 genes whose high expression correlated with bad prognosis and 336 genes whose low expression correlated with same outcome). Supplemental table S1.

Table 5.1 presents the top 50 genes selected as best survival markers of CRC: the first part of the table corresponds to the top 25 genes, where up-regulation correlates with shorter survival and higher risk (HR > 1); the second part of the table displays the top 25 genes, where up-regulation corresponds to longer survival and lower risk (HR < 1). The genes were ranked by their p-values and the HR values calculated for the whole dataset. As indicated previously (See materials and methods), the stability and robustness of the gene survival markers were assessed by 80% random sampling along 100 iterations. For the final ranking only genes achieving significance under cut-off value in more than 80 cases out of 100, were considered as successful candidates.

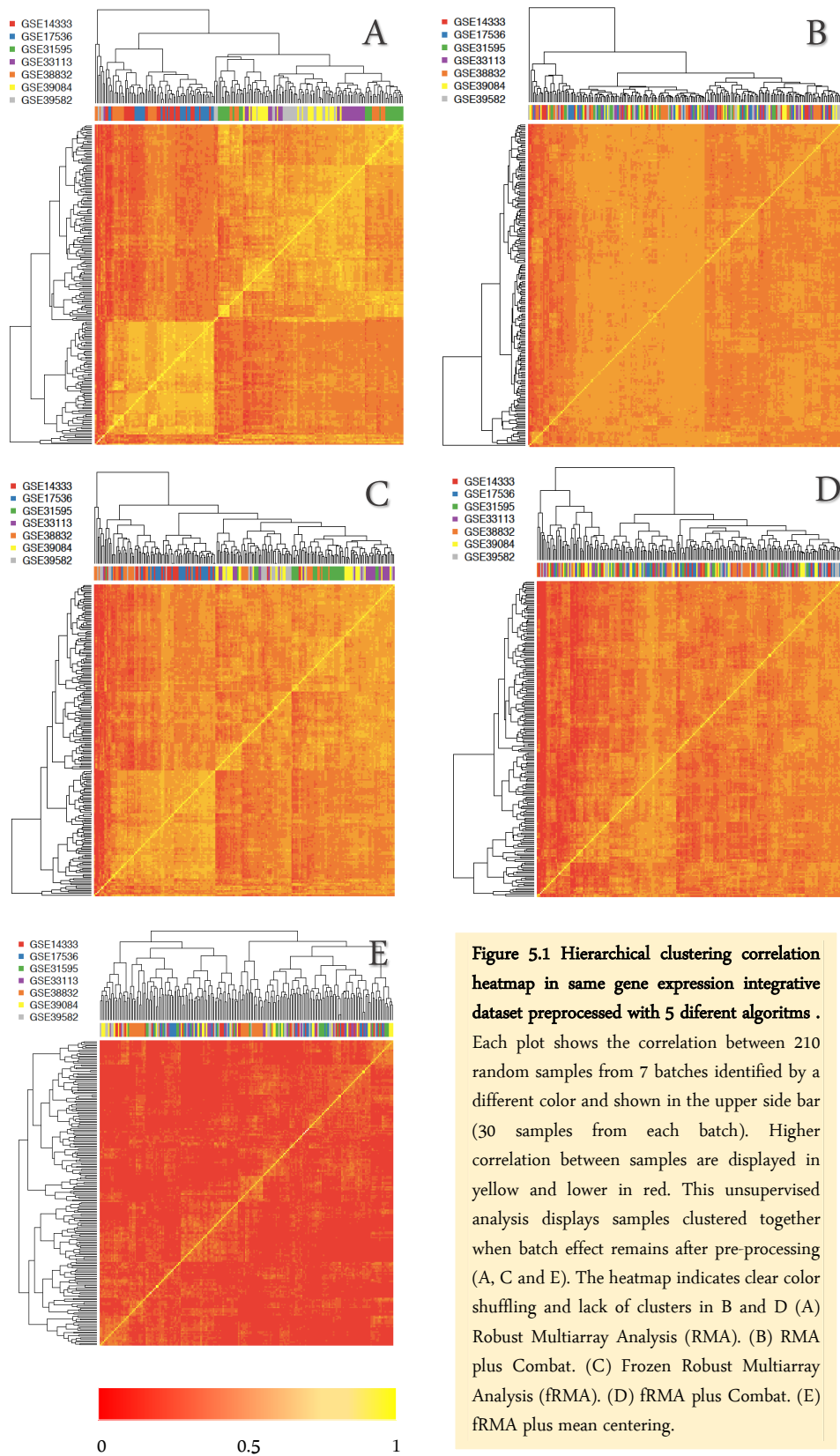


Figure 5.1 Hierarchical clustering correlation heatmap in same gene expression integrative dataset preprocessed with 5 different algorithms .

Each plot shows the correlation between 210 random samples from 7 batches identified by a different color and shown in the upper side bar (30 samples from each batch). Higher correlation between samples are displayed in yellow and lower in red. This unsupervised analysis displays samples clustered together when batch effect remains after pre-processing (A, C and E). The heatmap indicates clear color shuffling and lack of clusters in B and D (A) Robust Multiarray Analysis (RMA). (B) RMA plus Combat. (C) Frozen Robust Multiarray Analysis (fRMA). (D) fRMA plus Combat. (E) fRMA plus mean centering.

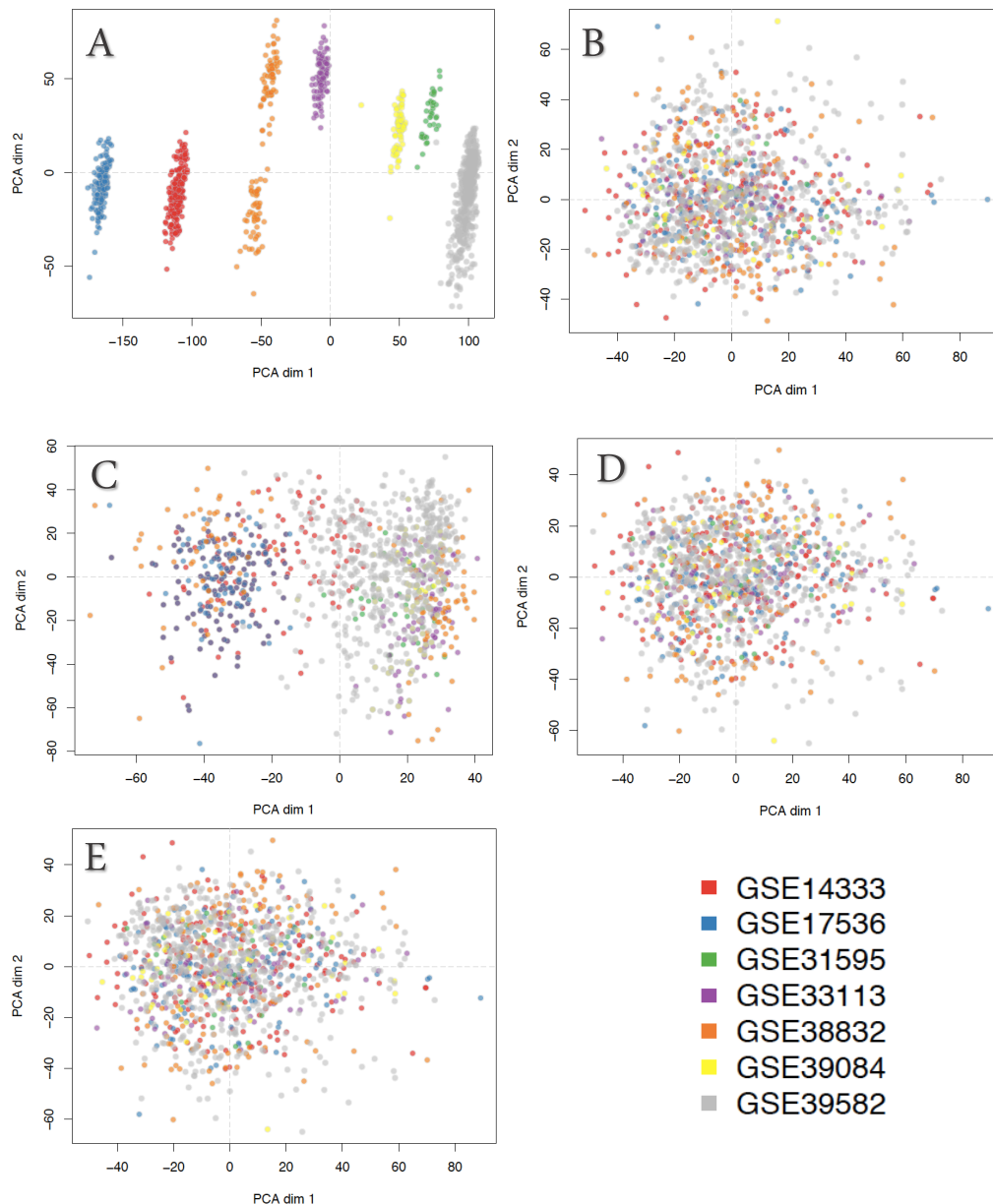


Figure 5.2. Score plot of the first two principal components (PCA) of 1,273 CRC samples corresponding to 7 independent studies integrated with 5 different preprocessing methods. Batches are identified by colors. (A) Robust Multiarray Analysis (RMA). (B) RMA plus Combat. (C) Frozen Robust Multiarray Analysis (fRMA). (D) fRMA plus Combat. (E) fRMA plus mean centered expression values. PCA of the global gene expression profile of each sample converts the signal of each sample using an orthogonal transformation in linearly uncorrelated variables called principal component or dimension. Each plot presents the values of the two main dimensions (dim 1 versus dim 2). PCA in plot A (RMA) and C (fRMA) clearly identifies batches suggesting a strong batch effect remaining after normalization. By contrast, plots of PCA data provided by the other 3 procedures (B, D and E, RMA plus Combat, fRMA plus Combat and fRMA plus mean-centered scaling respectively) captures an adequate mix of all the samples suggesting adequate batch effect removal.

Table 5.1.

A) RMA					
Coefficients:	Estimate	Std. Error	t value	P-value	Factor effect
Intercept (GSE 14333)	6.925	0.014	512.610	<2e-16	
GSE17536	0.387	0.019	20.230	<2e-16	yes
GSE31595	-1.212	0.019	-63.440	<2e-16	yes
GSE33113	-0.577	0.019	-30.210	<2e-16	yes
GSE38832	-0.355	0.019	-18.570	<2e-16	yes
GSE39084	-0.978	0.019	-51.180	<2e-16	yes
GSE39582	-1.375	0.019	-71.970	<2e-16	yes
B) RMA plus Combat					
Coefficients:	Estimate	Std. Error	t value	P-value	Factor effect
Intercept	6.219	0.013	473.582	<2e-16	
GSE17536	0.000	0.019	0.001	0.999	no
GSE31595	0.002	0.019	0.122	0.903	no
GSE33113	0.001	0.019	0.051	0.959	no
GSE38832	-0.001	0.019	-0.033	0.973	no
GSE39084	0.002	0.019	0.092	0.927	no
GSE39582	0.001	0.019	0.029	0.977	no
C) FRMA					
Coefficients:	Estimate	Std. Error	t value	P-value	Factor effect
Intercept	6.535	0.015	450.434	<2e-16	
GSE17536	-0.011	0.021	-0.553	0.580	no
GSE31595	0.089	0.021	4.329	0.000	yes
GSE33113	0.071	0.021	3.455	0.001	yes
GSE38832	0.054	0.021	2.641	0.008	yes
GSE39084	0.096	0.021	4.695	0.000	yes
GSE39582	0.089	0.021	4.336	0.000	yes

Table 5.1 (Continue).

D) FRMA plus Combat					
Coefficients:	Estimate	Std. Error	t value	P-value	Factor effect
Intercept	6.590	0.014	457.338	<2e-16	
GSE17536	0.000	0.020	0.001	1.000	no
GSE31595	0.002	0.020	0.093	0.926	no
GSE33113	0.001	0.020	0.072	0.942	no
GSE38832	0.000	0.020	0.019	0.985	no
GSE39084	0.002	0.020	0.089	0.929	no
GSE39582	0.000	0.020	0.007	0.994	no

E) FRMA Mean Centered					
Coefficients:	Estimate	Std. Error	t value	P-value	Factor effect
Intercept	-0.000	0.000	-1.638	0.101	
GSE17536	0.000	0.000	1.264	0.206	Low*
GSE31595	0.000	0.000	0.288	0.773	no
GSE33113	0.000	0.000	1.605	0.108	yes
GSE38832	0.000	0.000	1.449	0.147	yes
GSE39084	-0.000	0.000	-0.076	0.940	no
GSE39582	0.000	0.000	1.395	0.163	yes

Table 5.1 Coefficients obtained from regressing gene expression on array batch per preprocessing method The methods applied were: (A) RMA; (B) RMA plus ComBat; (C) fRMA; (D) fRMA plus ComBat; (E) fRMA plus scaling of the data using mean-centered expression values. The linear regression is done to evaluate the “batch effect” (i.e. considering that the tested factors are the fact of “belonging” to a given dataset). Thus, when the p-value of the factors are significant (< 0.05), the “batch effect” remains on the overall expression signal. *A marginal low significance was considered when p-values were < 0.20 in the case E. The largest p-values indicating lack of significant difference and no factor effect were achieved for both RMA plus Combat and fRMA plus Combat algorithms. The largest p-values indicating lack of significance and no factor effect were achieved for both RMA plus Combat and fRMA plus Combat algorithms. A marginal low significance was considered when p-values were < 0.20 in the case E

Gene	Accession number	Hazard Ratio	Nsinf	Avg. HR (100i)	p-val (KM)
<i>DCBLD2</i>	ENSG00000057019	2.02	99	2.105577851	0.0000000000
<i>PTPN14</i>	ENSG00000152104	1.99	99	2.081980089	0.0000000000
<i>LAMP5</i>	ENSG00000125869	1.99	93	2.046377013	0.0000000000
<i>TM4SF1</i>	ENSG00000169908	1.96	93	2.030914773	0.0000000010
<i>NPR3</i>	ENSG00000113389	1.95	97	2.136437795	0.0000000020
<i>LEMD1</i>	ENSG00000186007	1.95	85	1.936983243	0.0000000030
<i>LCA5</i>	ENSG00000135338	1.89	97	2.020869585	0.0000000030
<i>CSGALNACT2</i>	ENSG00000169826	1.91	92	1.974005294	0.0000000080
<i>SLC2A3</i>	ENSG00000059804	1.93	89	1.993164569	0.0000000140
<i>GADD45B</i>	ENSG00000099860	1.92	97	2.074130061	0.0000000180
<i>SCEL</i>	ENSG00000136155	1.88	87	1.928223891	0.0000000180
<i>SIX4</i>	ENSG00000100625	1.89	91	1.950776377	0.0000000190
<i>AKAP12</i>	ENSG00000131016	1.85	95	2.09190669	0.0000000280
<i>COLEC12</i>	ENSG00000158270	1.84	92	1.940993256	0.0000000280
<i>PDLIM3</i>	ENSG00000154553	1.84	91	1.985228488	0.0000000470
<i>ITGB5</i>	ENSG00000082781	1.82	88	1.910536646	0.0000000490
<i>GULP1</i>	ENSG00000144366	1.81	88	1.911473199	0.0000000500
<i>SCG2</i>	ENSG00000171951	1.81	93	2.033681411	0.0000000510
<i>AHNAK2</i>	ENSG00000185567	1.80	87	1.895908709	0.0000000660
<i>CYP1B1</i>	ENSG00000138061	1.84	85	1.883705242	0.0000000750
<i>PRKD1</i>	ENSG00000184304	1.74	87	1.872420442	0.00000004510
<i>SPARCL1</i>	ENSG00000152583	1.74	85	1.862917692	0.00000004710
<i>CDKN2B</i>	ENSG00000147883	1.73	84	1.846935684	0.00000007170
<i>MLLT11</i>	ENSG00000213190	1.70	84	1.812843086	0.0000019890
<i>CD36</i>	ENSG00000135218	1.69	85	1.891001875	0.0000027510

Gene	Accession number	Hazard Ratio	Nsinf	Avg. HR (100i)	p-val (KM)
<i>EPHB2</i>	ENSG00000133216	0.43	100	0.426450798	0.0000000000
<i>DUS1L</i>	ENSG00000169718	0.49	98	0.481106549	0.0000000000
<i>NUAK2</i>	ENSG00000163545	0.51	96	0.495293636	0.0000000010
<i>FANCC</i>	ENSG00000158169	0.51	95	0.497635109	0.0000000020
<i>CISD3</i>	ENSG00000277972	0.51	87	0.511094605	0.0000000020
<i>TIMM13</i>	ENSG00000099800	0.53	95	0.510758919	0.0000000030
<i>AGMAT</i>	ENSG00000116771	0.52	95	0.514839807	0.0000000050
<i>MYB</i>	ENSG00000118513	0.52	93	0.508188656	0.0000000060
<i>CHDH</i>	ENSG00000016391	0.53	90	0.51951104	0.0000000060
<i>FHDC1</i>	ENSG00000137460	0.52	96	0.505062052	0.0000000080
<i>ZBED3</i>	ENSG00000132846	0.52	88	0.522153296	0.0000000090
<i>NOL9</i>	ENSG00000162408	0.54	92	0.52661077	0.0000000150
<i>GAR1</i>	ENSG00000109534	0.50	99	0.47897017	0.0000000170
<i>FAM83F</i>	ENSG00000133477	0.54	93	0.51778748	0.0000000190
<i>TXN2</i>	ENSG00000100348	0.53	88	0.527441942	0.0000000360
<i>GALK1</i>	ENSG00000108479	0.55	88	0.524508995	0.0000000360
<i>MLEC</i>	ENSG00000110917	0.55	96	0.476092921	0.0000000450
<i>MAPKAPK3</i>	ENSG00000114738	0.55	92	0.520129905	0.0000000480
<i>CASP1</i>	ENSG00000137752	0.56	87	0.523042004	0.00000001800
<i>MCCC2</i>	ENSG00000131844	0.57	93	0.515787771	0.00000001830
<i>BEND3</i>	ENSG00000178409	0.55	88	0.529440815	0.00000001930
<i>CISH</i>	ENSG00000114737	0.55	87	0.508288272	0.00000002160
<i>LARS2</i>	ENSG00000011376	0.55	91	0.528494178	0.00000002390
<i>CDC25A</i>	ENSG00000164045	0.57	90	0.53902196	0.00000004810
<i>L3MBTL4</i>	ENSG00000154655	0.54	90	0.506115452	0.00000006060

Table 5.2: Genes selected as top-50 best survival markers of colorectal cancer (CRC). The upper part of the table includes the top-25 genes whose UP-regulation correlates with shorter survival and higher risk (i.e. Hazard Ratios, HR > 1); the bottom part of the table shows the top-25 genes whose UP-regulation correlates with longer survival and lower risk (Hazard Ratios, HR < 1). The genes were ranked by their adjusted p values and the Hazard Ratio values calculated with 1,273 samples sourced from all datasets. To provide the results with more stability, a cross-validation of top hits were accomplished by testing the algorithm in randomized 80 % samples with replacement along one hundred iterations. Only genes that obtained a significant adjusted p-value in more than 80 iterations out of 100, were included in the ranking. Legend: Hazard ratio, the HR obtained in first KM analysis considering all datasets; Nsinf, number of iterations using 80% random sampling achieving significance (cut-off: p-value < 0.0003); Avg HR (100i), average HR in 100 iterations; pval (KM), p-value corresponding to log rank test including all datasets (95%CI and remaining relevant data in supplemental table 2)

Figure 5.3 shows the Kaplan-Meier analysis of top two genes related to the survival profiles of the two groups of risk according to level of expression in either side, up-regulation (red) correlated to poor survival (Fig. 5.3.A) and down-regulation (green) correlated to poor survival (Fig. 5.3.B). Figures 5.3.C and D display the distribution of expression levels increasingly ordered. Each dot represents a CRC patient and the colours evidence the segregated group performed by the recurrent algorithm used to find de minimum adjusted p-value (red for group of patients with higher level of gene expression and green for patients with low level).

Notched boxplots in Fig 5.3. E and F, shown the distribution groups of two genes and two risk levels. The variability in the populations are very similar in terms of range (whiskers) and interquartile range (boxes). Notches do not overlap and a very low p-value in both t-test indicates a very significant difference between level of expression of *DCBLD2* and *EPHB2* for the two groups.

The separation of the two populations in both cases is very significant, with KM p-values bellow $1.0e-10$ and HR of 2.02 (95%CI: 1.65-2.48) for the binomial gene-overexpression-short-survival and 0.43 (95%CI: 0.35-0.52) for gene-repression-short-survival. High level of *EPHB2* seems to be CRC protective and high levels of *DCBL2* increase the hazard ration by more than 2, leading to sorter survival time.

The list of survival markers genes obtained from the meta-dataset containing 1,273 samples was subsequently externally validated in two series. Figure 5.4 shows validation of gene *EPHB2* as a representative example of the validation process in two external series selected for that purpose (See materials and methods 4.2.6).

Of the top-10 genes, for the case of up-regulation associated with poor survival, 7 genes were validated (*PTPN14*, *LAMP5*, *TM4SF1*, *LCA5*, *CSGALNACT2*, *SLC2A3* and *GADD45B*). Of the top-10 found for down-regulation associated with poor survival, 6 genes were validated (*EPHB2*, *DUS1L*, *NUAK2*, *FANCC*, *MYB* and *CHDH*).

Figure 5.3

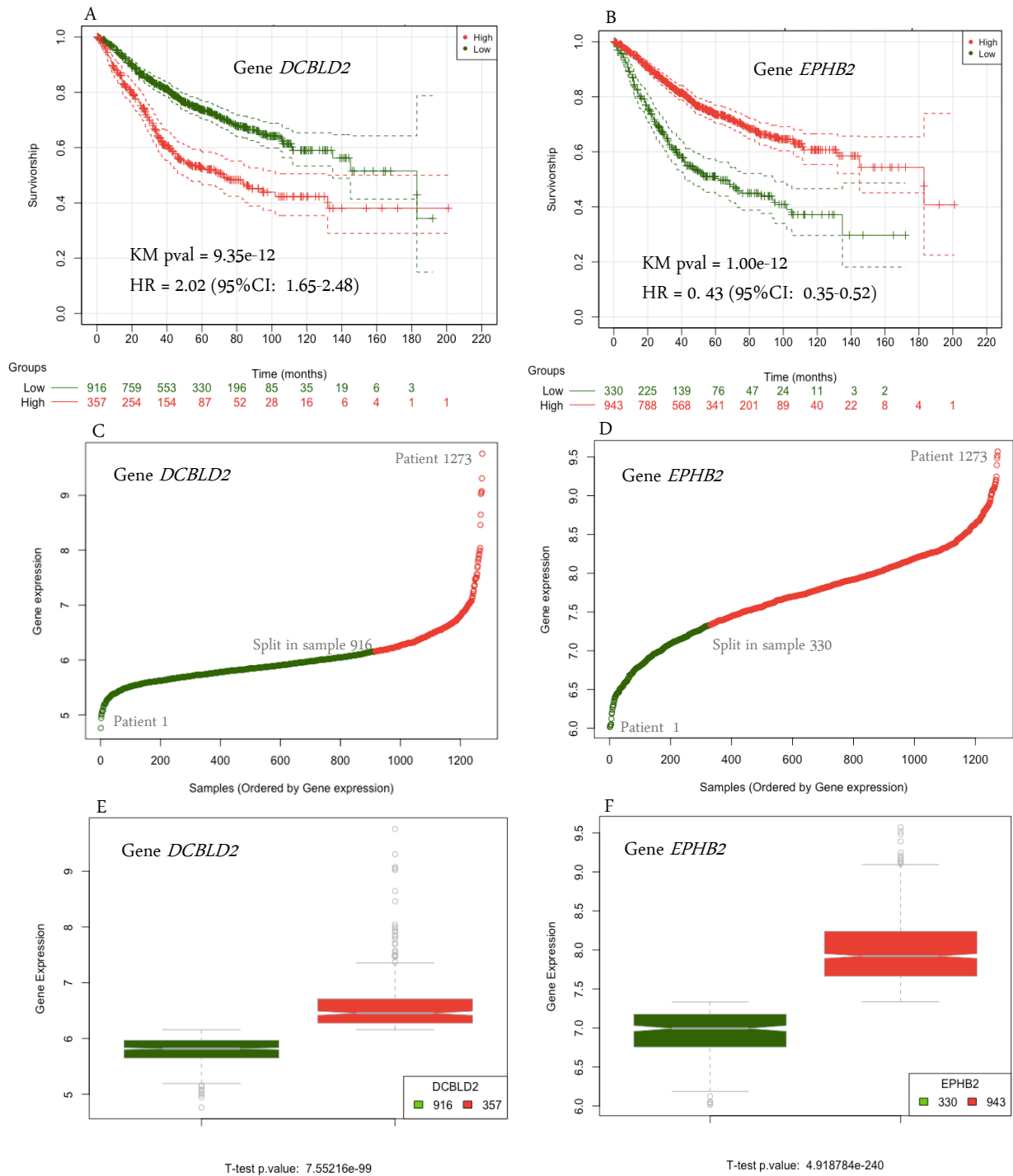
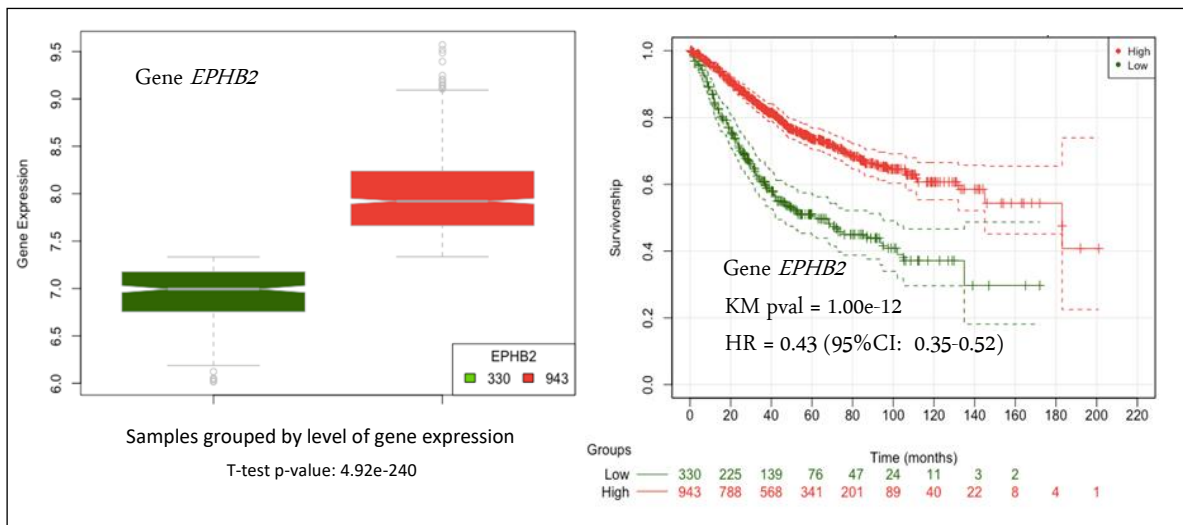


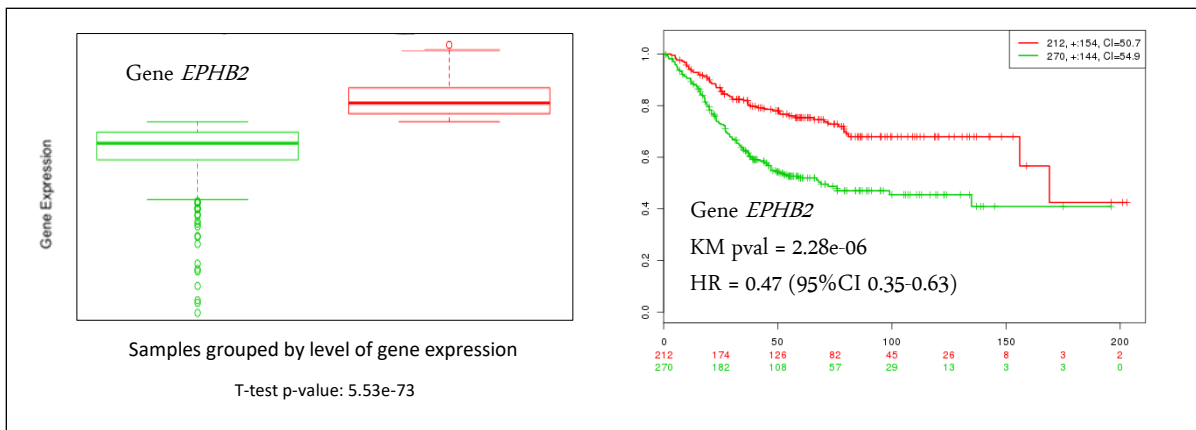
Figure 5.3: Plots of survival analysis using 1273 samples from human colorectal cancer (CRC) patients. Only top two genes shown, *DCBLD2* and *EPHB2*. The patients are separated in two groups (high expression in red and low expression in green): Plots in A and B display Kaplan -Meier distributions. Plots in C and D shows level of gene expression increasingly ordered (each dot represent a patient. Change of color indicates where the algorithm split the samples for group assignment. E) and F) reflects boxplot of the two groups and a highly significant p-value of a doubled sided unpaired t.test. In the case of *DCBLD2* high expression correlates with short survival time HR = 2.02 (95%CI: 1.65-2.48); and in the case of *EPHB2* the low expression correlates with shorter survival time HR = 0.43 (95%CI: 0.35-0.52).

A) Training series: 1,273 samples (microarrays)

Figure 5.4



B) Validation series I: 482 samples (microarrays from Colon-Metabase-unif)



C) Validation series II: 269 samples (RNA-seq from the TCGA)

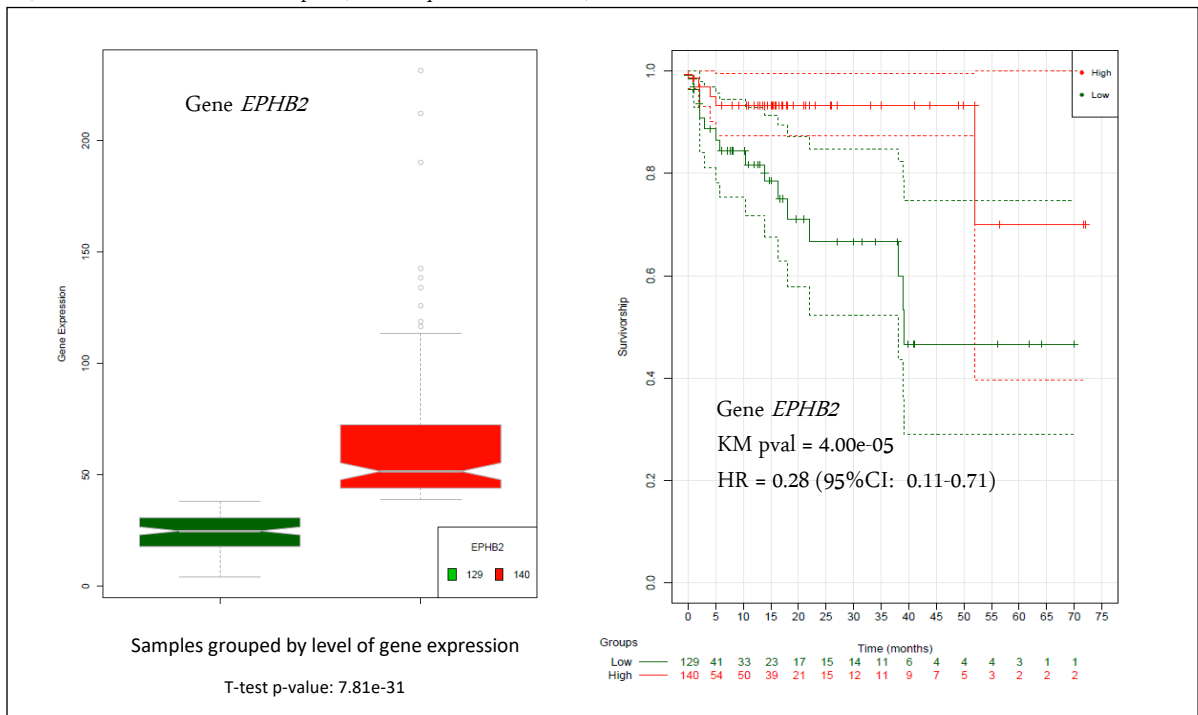


Figure 5.4 Validation of previous KM analysis corresponding to top hit gene *EPHB2*. Fig. 5.4.A display previous *EPHB2* analysis for better comparison referred to as training series. Validation of survival data was performed in two independent set of samples taken from the CRC dataset selected “Colon-Metabase-Uniformized” (validation serie I Fig.5.4.B) including 482 samples with overall survival data and genome-wide expression determined with Affymetrix microarrays and The Cancer Genome Atlas series for CRC (Validation serie II 5.4.C), that included 269 colorectal carcinomas with survival information and RNA-seq expression profiling. Results in the three series shows similar trend for gene *EPHB2* highlighting a much more protective HR of 0.28 (95%CI: 0.11-0.71) in the RNA-seq series. Boxplot in the left side of each figure represents groups of samples assignation according to gene expression level.

5.1.2. Identification of one major pathway (IGFBP signalling), deeply involved in cell nutrition and highly modulated by caloric restriction.

Geneset enrichment analysis (Table 5.3) displays 11 significantly enriched pathways with FDR (<0.05) corresponding to a hypergeometric test using the 765-candidate geneset. The Regulation of Insulin-like Growth Factor (IGF) transport and uptake by Insulin-like Growth Factor Binding Proteins (IGFBPs), is one of the enriched pathways. This axe is profoundly involved in nutrient sensing and proliferation.

Table 5.3

Pathway name	Pathway identifier	Gene pathway				
		Found	Total	Ratio	pValue	FDR
Extracellular matrix (ECM) organization	R-HSA-1474244	47	329	0.0232	0.000	0.000
ECM proteoglycans	R-HSA-3000178	19	79	0.0056	0.000	0.001
Non-integrin membrane-ECM interactions	R-HSA-3000171	16	61	0.0043	0.000	0.001
Integrin cell surface interactions	R-HSA-216083	19	86	0.0061	0.000	0.001
Assembly of collagen fibrils and other multimeric structures	R-HSA-2022090	16	67	0.0047	0.000	0.002
Regulation of Insulin-like Growth Factor (IGF) transport and uptake by Insulin-like Growth Factor Binding Proteins (IGFBPs)	R-HSA-381426	21	127	0.0090	0.000	0.013
Post-translational protein phosphorylation	R-HSA-8957275	19	109	0.0077	0.000	0.013
Degradation of the extracellular matrix	R-HSA-1474228	23	148	0.0105	0.000	0.013
Laminin interactions	R-HSA-3000157	9	31	0.0022	0.000	0.025
Chondroitin sulfate biosynthesis	R-HSA-2022870	8	25	0.0018	0.000	0.027
Collagen formation	R-HSA-1474290	17	104	0.0073	0.000	0.045

Table 5.3 Pathway enrichment analysis Results after performing a hypergeometric test of 765 top hit candidate genes showed eleven overrepresented pathways that achieved statistical significance (FDR<0.05). Of note, the pathway R-HSA-381426 “Insulin-like Growth Factor (IGF) transport and uptake by Insulin-like Growth Factor Binding Proteins (IGFBPs)”, with an FDR=0.013, was enriched. This node is profoundly involved in cell nutrient sensing and consistently modulated by caloric restriction (Reactome database)

5.1.3. *SLC2A3*, *NPR3* and *LCA5* involvement in patient survival

5.1.3.1. The *SLC2A3*, *NPR3* and *LCA5* geneset achieved best risk identification among patient of CRC in early stage I and II

Multivariate survival analysis performed with the combinatory of top ten genes, shows that the best separation of survival curves in all-stage samples was obtained when computing the 7-gene combination *DCBLD2*, *LAMP5*, *TM4SF1*, *NPR3*, *LEMD1*, *LCA5*, *CSGALNACT2* (HR: 2.68; CI:2.58-2.78; p-val: 0.31e-05). Table 5.4 shows those combinations that displayed higher hazard ratio in different stages.

Since a gene signature requires predictive value in those stages where is more needed, preferably early than late ones, all gene sets were analysed computing samples of stage I and II. The gene combination *SLC2A3*, *NPR3* and *LCA5* achieved best results predicting risk when processing early stage (I-II) samples (HR: 3.60; CI: 3.431.73-7.83; p-val.:0.0024])

Final multivariate survival analysis performed computing top 100 candidate genes allowed to identify the genes that were the most influential factors in this risk analysis. Supplemental table S5 displays the β factors assigned to each gene.

ALL STAGES (n=1273)				
Gene signature (HG symbol)	HR	CI (95%)		p-val (KM)
<i>DCBLD2, LAMP5, TM4SF1, NPR3, LEMD1, LCA5, CSGALNACT2</i>	2.68	2.58	2.78	0.0000031
<i>DCBLD2, PTPN14, TM4SF1, LEMD1, LCA5, CSGALNACT2</i>	2.54	2.43	2.64	0.0000052
<i>SLC2A3, NPR3, LCA5, LAMP5, CSGALNACT2</i>	2.31	2.20	2.41	0.0001140
<i>SLC2A3, NPR3, LCA5, LAMP5</i>	2.34	2.24	2.44	0.0000519
<i>SLC2A3, NPR3, LCA5</i>	2.36	2.25	2.46	0.0000056
STAGE II & III (n=1009)				
Gene signature (HG symbol)	HR	CI (95%)		p-val (KM)
<i>DCBLD2, LAMP5, TM4SF1, NPR3, LEMD1, LCA5, CSGALNACT2</i>	2.85	2.73	2.96	0.0000052
<i>DCBLD2, PTPN14, TM4SF1, LEMD1, LCA5, CSGALNACT2</i>	2.75	2.63	2.87	0.0000024
<i>SLC2A3, NPR3, LCA5, LAMP5, CSGALNACT2</i>	2.02	1.90	2.14	0.0004610
<i>SLC2A3, NPR3, LCA5, LAMP5</i>	2.23	2.11	2.35	0.0003440
<i>SLC2A3, NPR3, LCA5</i>	2.22	2.10	2.34	0.0008660
STAGE I & II (n=682)				
Gene signature (HG symbol)	HR	CI (95%)		p-val (KM)
<i>DCBLD2, LAMP5, TM4SF1, NPR3, LEMD1, LCA5, CSGALNACT2</i>	2.88	2.72	3.03	0.0024200
<i>DCBLD2, PTPN14, TM4SF1, LEMD1, LCA5, CSGALNACT2</i>	2.85	2.69	3.00	0.0017400
<i>SLC2A3, NPR3, LCA5, LAMP5, CSGALNACT2</i>	3.06	2.89	3.22	0.0057100
<i>SLC2A3, NPR3, LCA5, LAMP5</i>	3.30	3.13	3.47	0.0045700
<i>SLC2A3, NPR3, LCA5</i>	3.60	3.43	3.77	0.0018702

Table 5.4 Multivariate survival analysis. A multivariate survival analysis performed with combinations of top 10 hits, grouping then from 2 to 10-gene collections. Best separation of survival curves was achieved with 7-gene signature *DCBLD2, LAMP5, TM4SF1, NPR3, LEMD1, LCA5, CSGALNACT2* yielding a Hazard Ratio of 2.68 (CI: 2.58-2.78 p-val.:0.31e-05). Signature *SLC2A3, NPR3* and *LCA5* achieved highest risk differences when only samples in early stage were processed (I and II) (HR: 3.60; CI: 3.43-3.77; p-val.:0.0018702)].

Description	Value
$\beta(\text{NPR3})$	0.3535
$\beta(\text{LCA5})$	0.9781
$\beta(\text{SLC2A3})$	0.1292

Table 5.5: β Coefficients after performing the multivariate Cox regression considering the gene signature *SLC2A3*, *NPR3*, *LCA5* as explanatory variable and using samples of stage I and II only. Mean values after cross validation.

Forest plot in figure 5.5 captures the survival analysis of the 3-gene signature *SLC2A3*, *NPR3* and *LCA5* performed in each independent dataset, reaching hazard ratios above 4.5 in two out of seven studies. The study GSE14333 only includes patients in stage I and II and the study GS33113 includes patients in stage I and II, 18 patients in stage III and none in stage IV. 266 patients out of a total of 552 included in study GSE39582 correspond to stage III and IV. The distribution of ages and genders are similar in all studies analyzed (Table 4.2). The variability in the results obtained from each study, highlights the

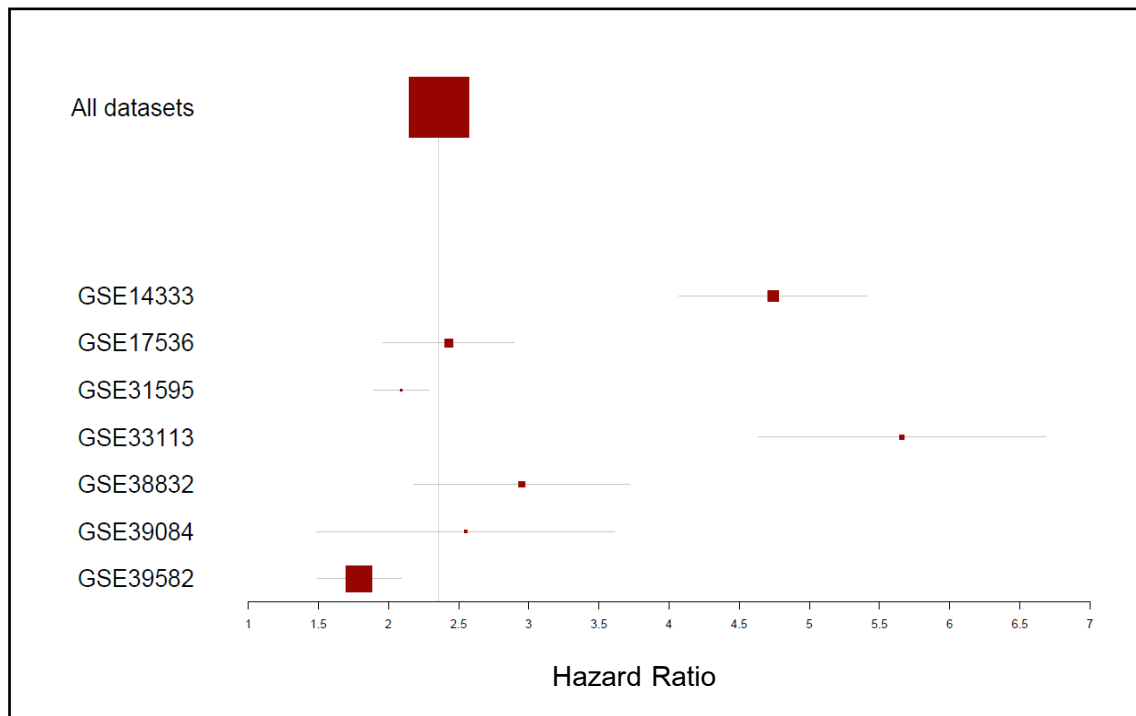


Figure 5.5: Forest plot representing the hazard ratio of the 3-gene signature *SLC2A3*, *NPR3*, *LCA5* in each independent dataset, reaching values above 4.5 in two of the seven studies analyzed. The study GSE14333 only includes patients in stage I and II and the study GS33113 includes patients in stage I and II, 18 patients in stage III and none in stage IV. 266 patients out of a total of 552 included in study GSE39582 corresponds to patients in stage III and IV. The distribution of ages and genders are similar in all studies analyzed (see table in material and methods). This confirms that the gene signature *SLC2A3*, *NPR3*, *LCA5* better identifies risk when samples from early stages are computed.

importance of building large integrated datasets to appreciate relevant generalized changes or trends in the population of a specific class.

5.1.3.2. Difference of top-hit-gene expression levels between tumoral and epithelial tissue in the cohort of 1273 samples analyzed.

To support potential further diagnostic in the clinic, the behavior in normal colon tissue of top hit genes was compared to explore eventual association between the geneset expression in both types of tissues, tumoral and epithelial. In general, tumoral tissue displays higher levels of mRNA than the epithelial (Figure 5.6). Heatmap and table 5.7 shows results of iterative Wilcoxon-rank tests exploring differential expression between genes from both tissues. Random iterative selection of 25 samples from tumor (1000i) were compared to 25 colon epithelial samples. Genes with low numbers of significant results are shown in red and genes with high number are shown in green, e.g. *GADD45B*, which only achieved significant difference between tissues in 14 samplings (25 patients each) out of 1000 random groups tested. This suggest association between levels of expression of *GADD45B* and *NUAK2* in both tumor and epithelium. Further, levels of expression of *DUS1L* or *PTPN14* were significantly different in all 1000 samplings contrasted, indicating poor association between tissues in the expression of these genes.

Table 5.6

Gene	Significant Tests (1000i)	Expression level association
<i>GADD45B</i>	14	High
<i>NUAK2</i>	19	
<i>NPR3</i>	26	
<i>FHDC1</i>	35	
<i>FANCC</i>	60	
<i>MYB</i>	71	
<i>LCA5</i>	184	
<i>LAMP5</i>	211	
<i>CHDH</i>	340	
<i>AGMAT</i>	377	
<i>TM4SF1</i>	665	
<i>CSGALNACT2</i>	887	
<i>CISD3</i>	933	
<i>SLC2A3</i>	947	
<i>TIMM13</i>	961	
<i>DCBLD2</i>	964	
<i>EPHB2</i>	992	
<i>LEMD1</i>	999	
<i>DUS1L</i>	1000	
<i>PTPN14</i>	1000	

Table 5.6 Association between level of expression in tumor and normal colon epithelium. Unpaired Wilcoxon-rank test was accomplished to compare gene expression level from iterative 25 random sampling (1000i) obtained from 1273 tumors versus expression in the 25 normal tissue samples. Central column shows number of test achieving significant difference out of 1000 iteration. Genes with low numbers of significant test are shown in red and genes with high number are shown in green. *GADD45B* or *NUAK2* only achieved significant difference between tissues in 14 samplings of 25 patients out of 1000 random groups tested. This suggest association between levels of expression of *GADD45B* and *NUAK2* in both tumor and epithelium. Levels of expression of *DUS1L* or *PTPN14* were significantly different in all 1000 samplings contrasted, indicating poor association between tissues in the expression of these genes

Figure 5.6 Distribution comparison of expression signal corresponding to twenty top-ranked genes in 25 samples from normal colorectal epithelium (green boxplots) versus 25 samples from CRC tumor (red boxplots). The genes in boxplot A are the top-10 best survival marker genes found to be up-regulated for poor and the genes in plot B are the top-10 best survival marker genes found up-regulated for good prognosis

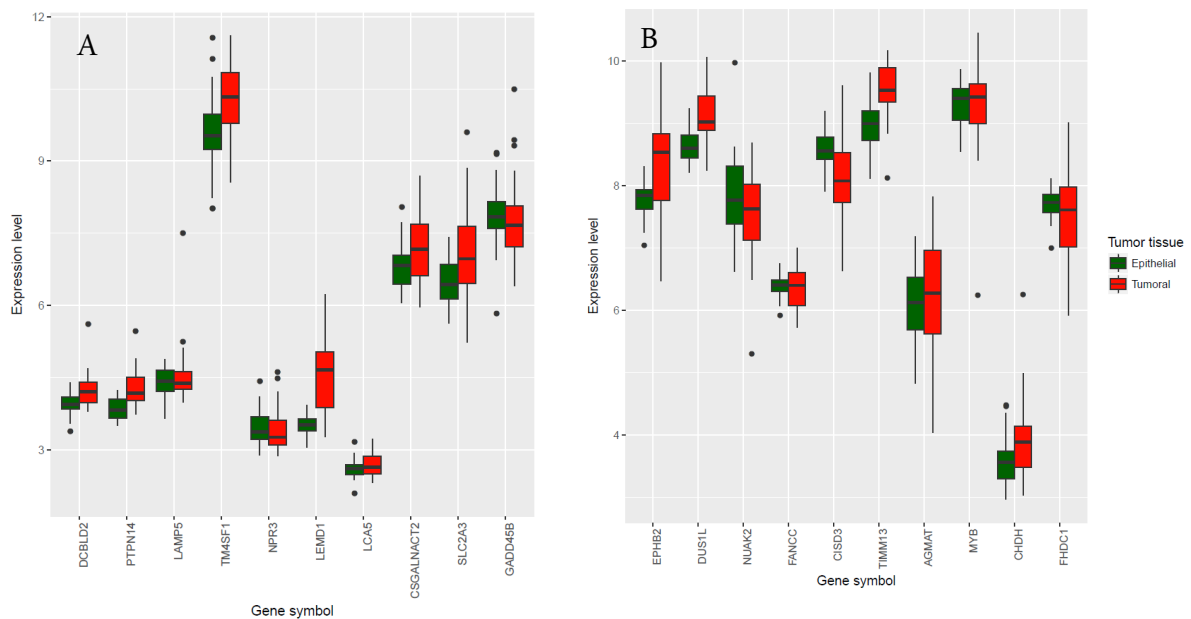


Figure 5.6

5.1.3.3. The *SLC2A3*, *NPR3* and *LCA5* gene set identifies patients with the most aggressive mesenchymal CRC subtype

To explore whether the gene signature *SLC2A3*, *NPR3* and *LCA5* was able to identify any particular CRC subtype, a hierarchical clustering following a similar strategy to the one used to assay batch effect removal, was carried out using the expression level of the 3-gene signature from 569 CRC samples. These samples included molecular subtype among the phenotypical information of the tumours. The samples were categorized in 6 different subtypes, C1 to C6 (Marisa et al., 2013). Despite it has two more subtypes, this classification is similar to the previously described in the introduction as "Consensus Molecular Subtype" and the C4 subtype clearly overlaps the highly aggressive, mesenchymal like CMS4 (Guinney et al., 2015).

The heatmap in figure 5.7 shows a clear cluster corresponding to C4 subtype (cyan colour) in the left side of the plot suggesting that this gene signature could molecularly identify that poor prognosis group.

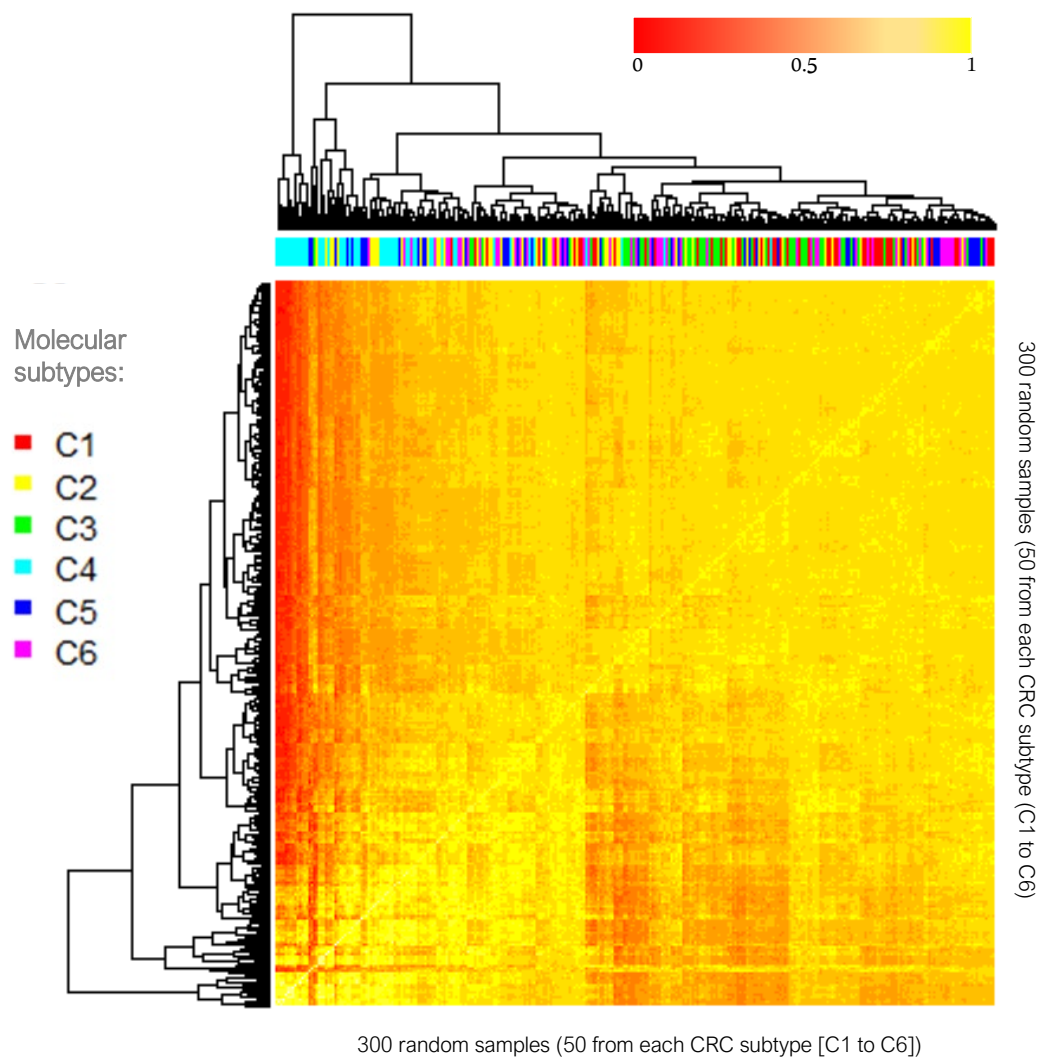


Figure 5.7 Hierarchical clustering correlation heatmap of 1273 microarrays to identify cluster corresponding to any specific CRC subtype (C1 to C6). The plot shows the Pearson's correlation between 300 random samples from 6 molecular subtypes C1 to C6 (Marisa et al., 2013) identified by six different colors and shown in the upper side bar (50 samples from each subtype). Higher correlation between samples are displayed in yellow and lower in red. Correlation index was calculated using Euclidean distance from expression level of 3 genes *SLC2A3*, *NPR3* and *LCA5* (569 CRC samples). C4 subtype samples are clearly clustered together (cyan color in the left part of the sidebar). This subtype shows highly aggressive mesenchymal like phenotype and overlaps poor prognosis consensus molecular subtype 4 (CMS4), previously described in the introduction to this Thesis (Guinney et al., 2015)

5.2. Identification of potential precision strategies in cancer focused on molecular nutrition.

5.2.1. Nutritional strategies based on the inclusion of bioactive compounds: Screening of bioactive compounds with potential beneficial effect in CRC.

5.2.1.1. Identification of the Ellagic Acid derivative 4,4' Di-O-Methyl Ellagic Acid (4,4'DIOMEA) as an effective agent in the inhibition of the proliferation of colon cancer cells.

The growth inhibitory effect of 10 different phenolic compounds and derived metabolites in a preliminary screening on HT-29 cells was analyzed by MTT assay (Table 4.1). 6 out of the 10 compounds tested (homovanillic acid, dihydrocaffeic acid, gallic acid, 4-Omethylgallic acid, 3-O-methylgallic acid, and Uro-B) had no effect on cell viability in the CRC lines tested at the assayed concentrations (1–100 μ M).

By contrast, 4 of the 10 analyzed compounds (EA, 3,3'-DiOMEA, 4,4'-DiOMEA, and Uro-B) displayed antiproliferative activity in CRC cell lines under the assayed conditions (Table 5.7).

4,4'-DiOMEA is the most effective agent against CRC cells within the members of the EA family tested, which was confirmed using an additional human colon CRC-derived cell line (SW-620) (Table 5.7).

5.2.1.2. 4,4'DIOMEA inhibits viability of CRC cells resistant to the chemo-therapeutic drug 5-FU

The phenolic compounds were tested in the 5-FU resistant SW620 cell line (SW620-5FuR), previously developed by the group (See materials and methods). The data collected in preceding experiments regarding cell sensitivity of both SW620 and SW620-5FuR to drug 5-FU determined an IC₅₀ value of 7.1 \pm 1.3 μ M for the SW620 line and an IC₅₀ value over 5,000.0 μ M for the SW620-5FuR cell line (Table 5.7).

MTT assay results show that SW-620-5FuR cells seems to be sensitive to EA; 3,3'-DIOMEA; 4,4'-DiOMEA as can be observed in Table 5.7, being 4,4'-DIOMEA the strongest molecule against this line, with an IC₅₀ in the range of 30.

Polyphenol	Cell line			
	HT-29	SW-620	SW-620-5FuR	CCD18Co
	[IC ₅₀ (μM)]			
5-FU	-	7.1±1.3	>5,000.0	<3.0
EA	95.0±10.4	79.0±4.0	45.0±5.0	37.50±2.5
3,3'DIOMEA	106.0±3.3	72.5±2.5	145.0±5.0	47.5±2.5
4,4'DIOMEA	7.6±1.5	5.8±1.6	28.8±3.2	59.5±4.55
Urolithin A	38.5±3.5	26.0±1.0	-	-

1 Data represent mean ± s.e.m. of at least two independent experiments, with three replicates per test concentration.
- not determined

Table 5.7: Anti-proliferative activity [IC₅₀ (μM)] of different polyphenols in several CRC cell lines: HT-29, SW-620, colon cancer resistant to 5-FU SW-60-5FuR and normal colon epithelium CCD18Co.

Compounds were also assayed in epithelial colon CCD18Co cells with the intention of analyze the behavior of these compounds in normal tissue. 4,4' DIOMEA was the only agent that showed an IC₅₀ of larger magnitude in epithelial cells than the one required in tumoral and chemo resistant lines, which may suggest the presence of a therapeutic window.

EA and 3,3'-DiOMEA exhibited relatively low sensitivity against colon cancer cells (IC₅₀ >70 μM) and their growth inhibitory activity was almost 2-fold compared to normal cells (IC₅₀ ≈ 40 μM). 4,4'-DiOMEA displayed effectiveness against both HT-29 and SW-620 colon cancer cells (IC₅₀ ≤ 10 μM), a concentration in which normal cells are lowly affected by the compound (IC₅₀ ≈ 60μM) suggesting this derivate as a promising candidate in colon cancer therapy (Table 5.7).

Figure 5.8 shows dose-response curves of the cell viability assays after 72 h treatment of SW620 colon cancer cells with increasing concentrations of EA and its derivatives (3,3'-Di-O-Methylellagic and 4,4'-Di-O-Methylellagic).

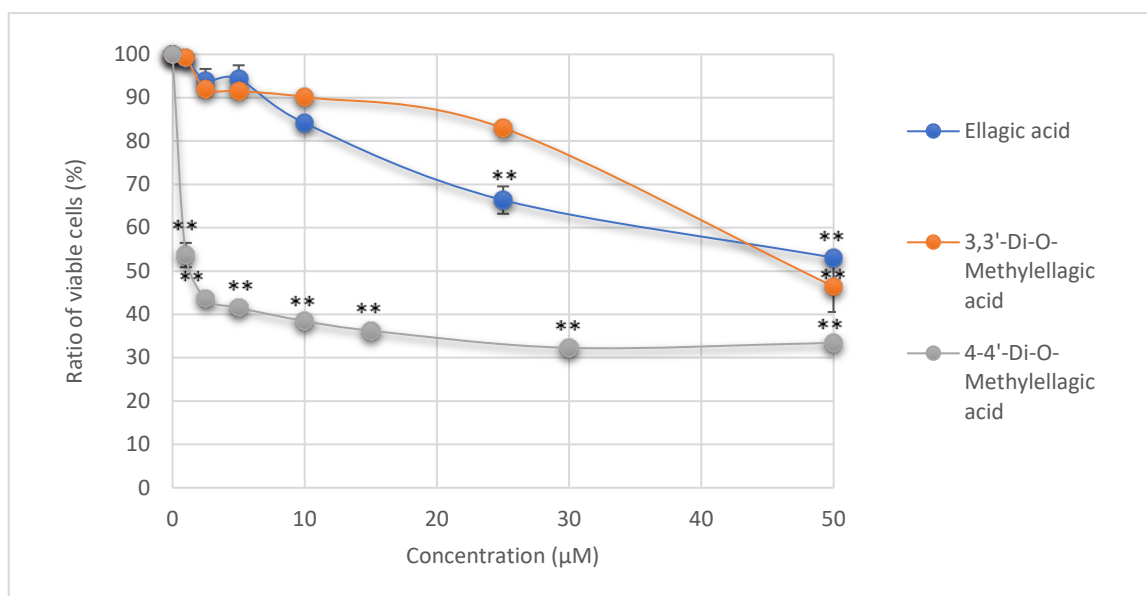


Figure 5.8 Dose-response curves after treating SW620 CRC cell line with EA and derivatives. 4,4'-Di-O-Methylellagic acid strongly induces human CRC cell growth inhibition. Curves show cell viability assays after 72 h treatment of SW620 colon cancer cells with increasing concentrations of EA and its derivatives 3,3'-Di-O-Methyl ellagic acid and 4,4'-Di-O-Methyl ellagic acid. Data represent mean \pm s.e.m. of at least two independent experiments each performed in triplicate. The results were analyzed by analysis of variance (ANOVA) with Bonferroni and Tukey as post hoc tests.

5.2.1.3. The Antiproliferative Activity of 4,4'-DiOMEA is not associated to antioxidant Activity

FRAP and DPPH antioxidant assays were performed to analyze whether the antiproliferative phenotype of CRC cells under these phenolics was mediated by their antioxidant capacity or should be modulated by antioxidant-based mechanisms. Results shown in figure 5.9 confirm the previously reported antioxidant capacity of EA with a very steep slope in the graphic but 4,4'-DiOMEA does not show this activity in any cell line tested.

Interestingly, 3,3'-DiOMEA and 4,4'-DiOMEA display different antioxidant capacity despite their similar chemical structure.

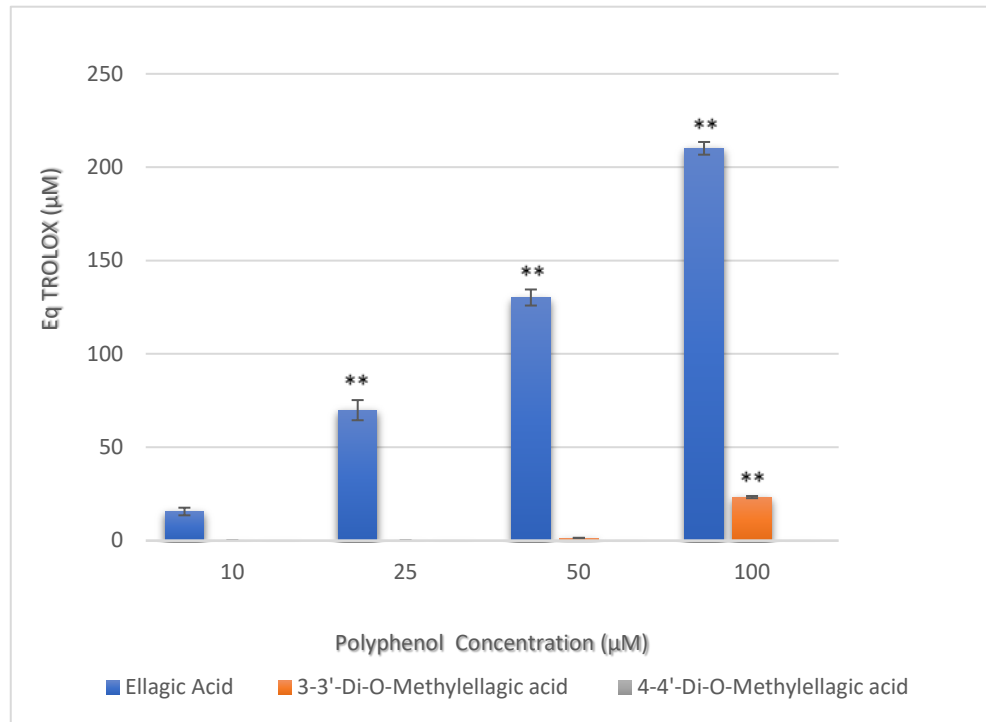


Figure 5.9. Antioxidant activity of EA and derivatives 3,3'DiOMEA and 4,4'DiOMEA. FRAP Assay shows less antioxidant activity in the methylated species in comparison with EA. 4,4' DiOMEA does not display any antioxidant capacity. Data represent mean \pm s.e.m. of equivalent of TROLOX.

5.2.1.4. The Antiproliferative Activity of 4,4'-DiOMEA might be mediated by the inhibition of the Wnt signaling cascade.

A comparison between full transcriptomes of SW-620 cells treated at 5 μ M vs control was performed by means of microarray technology in order to analyze the molecular mechanism underlying the anticarcinogenic effect of 4,4'-DiOMEA. A subsequent hypothesis contrast using Limma, was performed to identify DEG and the FDR correction was applied previously to rank all genes by fold change and correspondent p-

value. A restringing threshold of 2-fold was used to identify 11 genes whose altered expression achieved statistical significance (data in table 5.8).

A subsequent Gene set enrichment analysis was carried out using The Gene Ontology Database meant to identify any relevant cancer pathway significantly enriched by the candidates. Table 5.9 shows the top ranked axes and the p-values associated to their correspondent hypergeometric test, showing the proliferative Wnt signaling cascade among those pathways significantly enriched with better FDR (0.0112).

Wnt signaling is one of the most frequently activated pathways associated to cancer hallmarks such as proliferation or epithelial-to-mesenchymal transition (EMT) in different type of cancers (Polakis, 2000) (Camps et al., 2013) and 4,4'DIOMEA repress *Wnt16* expression according to the microarray results (table 5.8). KEGG, Reactome and Cytoscape databases were also consulted to identify functional interactions, transcription factors and relevant networks in which the candidates might be molecularly involved. Table 5.9 shows the most relevant interactors found in the analysis.

Gene	Accession number	Fold Change	logControl	StdErr (logControl)	logExperiment	StdErr (logExperiment)	p-value (limma)	Description
<i>RHBDL1</i>	NM_001278720	- 2.54	13.67	0.10	12.33	0.70	0.039	Homo sapiens rhomboid, veinlet-like 1 (Drosophila) (<i>RHBDL1</i>), transcript variant 1
<i>A4GALT</i>	NM_017436	- 2.49	14.02	0.30	12.71	0.50	0.016	Homo sapiens alpha 1,4-galactosyltransferase (<i>A4GALT</i>)
<i>WNT16</i>	NM_057168	- 2.30	7.14	0.70	5.94	0.10	0.050	Homo sapiens w ingless-type MMTV integration site family, member 16 (<i>WNT16</i>), transcript variant 1
<i>PCSK1N</i>	NM_013271	- 2.19	14.66	0.30	13.53	0.50	0.029	Homo sapiens proprotein convertase subtilisin/kexin type 1 inhibitor (<i>PCSK1N</i>)
<i>PAPPA</i>	NM_002581	- 2.12	7.36	0.60	6.27	0.10	0.033	Homo sapiens pregnancy-associated plasma protein A, pappalysin 1 (<i>PAPPA</i>)
<i>WDR52</i>	NM_001164496	4.50	6.40	0.10	8.57	1.20	0.039	Homo sapiens WD repeat domain 52 (<i>WDR52</i>), transcript variant 1
<i>MUSK</i>	NM_005592	2.46	6.47	0.10	7.77	0.70	0.044	Homo sapiens muscle, skeletal, receptor tyrosine kinase (<i>MUSK</i>), transcript variant 1
<i>GRHL1</i>	NM_198182	2.20	6.50	0.10	7.64	0.50	0.013	Homo sapiens grainyhead-like 1 (Drosophila) (<i>GRHL1</i>)
<i>GTF2I</i>	ENST00000473333	2.10	6.17	-	7.24	0.30	0.002	General transcription factor Iii
<i>SLC22A8</i>	ENST00000451262	2.06	7.13	0.10	8.18	0.30	0.002	Solute carrier family 22 (organic anion transporter), member 8
<i>S100A5</i>	NM_002962	2.05	7.95	0.20	8.98	0.40	0.013	Homo sapiens S100 calcium binding protein A5 (<i>S100A5</i>)

Table 5.8: Differentially expressed genes identified after treating SW-620 colon cancer cells with phenolic 4,4'DiOMEA.

Microarray analysis of SW620 CRC cells treated during 72 h with 5 μ M of commercial 44'DiOMEA was performed to identify DEG. A threshold of 2-fold absolute change in gene expression was used to consider significant. Results include (log) fold changes, log-intensity values (control: logControl; and experiment: logExperiment), standard errors (StdErr) and p-values for Limma package (linear models for microarray data).

Biological Process	Reference Support	p-value (Hyp)	p-value (Hyp)*	Genes
Tripeptide transport	2	0.0012	0.0377	<i>SLC22A8</i>
Regulation of synaptic growth at neuromuscular junction	2	0.0012	0.0377	<i>MUSK</i>
Stress-induced premature senescence	5	0.0031	0.0419	<i>WNT16</i>
Regulation of gene expression	3160	0.0021	0.0424	<i>EIF3K,MUSK,GRHL1,BARX1,CHD4,GTF2I,WNT16</i>
Response to methotrexate	4	0.0025	0.0431	<i>SLC22A8</i>
Vasculature development	468	0.0028	0.0433	<i>FZD9,GTF2I,EPHB4</i>
Oxidative stress-induced premature senescence	3	0.0018	0.0453	<i>WNT16</i>
Cardiovascular system development	693	0.0008	0.0467	<i>FZD9,GTF2I,WNT16,EPHB4</i>
KEGG Pathways	Reference Support	p-value (Hyp)	p-value (Hyp)*	Genes
Basal cell carcinoma	55	0.0005	0.0047	<i>WNT16,FZD9</i>
Melanogenesis	98	0.0016	0.0074	<i>WNT16,FZD9</i>
Wnt signaling pathway	149	0.0037	0.0112	<i>WNT16,FZD9</i>
Glycosphingolipid biosynthesis - globo series	14	0.0086	0.0193	<i>A4GALT</i>
Pathways in cancer	324	0.0167	0.0300	<i>WNT16,FZD9</i>
Basal transcription factors	39	0.0237	0.0355	<i>GTF2I</i>
Hedgehog signaling pathway	56	0.0338	0.0435	<i>WNT16</i>
Bile secretion	71	0.0427	0.0480	<i>SLC22A8</i>
Transcription factors	Reference Support	p-value (Hyp)	p-value (Hyp)*	Genes
CP2	178	0.0002	0.0132	<i>CHD4,RHBDL1,PAPPA</i>
PAX4	164	0.0001	0.0208	<i>RBMS3,CHD4,PAPPA</i>
E12	1805	0.0006	0.0225	<i>A4GALT,MUSK,GTF2I,WNT16,RHBDL1,SLC22A8</i>
AP4	1119	0.0005	0.0250	<i>RBMS3,MUSK,FZD9,CHD4,CRHBP</i>
TEF-1	384	0.0016	0.0495	<i>RBMS3,MUSK,CHD4</i>

Table 5.9: Bioinformatic analysis of biological processes, pathways and transcription factors significantly altered by 44'DiOMEA in SW-620 colon cancer cells according to microarray data. The list shows the most altered cellular functions and molecular networks in colon cancer cells treated with 44'DiOMEA under conditions in which it exerts anti-proliferative activity according to microarray data. p-value (Hyp) represents the p-value of the hypergeometric test used in this analysis. p-value (Hyp)* represents the p-value of the hypergeometric test adjusted for False discovery rate (FDR) correction. These data were obtained from Gene Ontology, KEGG pathways and GSEA databases.

The downregulation of *Wnt16* by 4,4'-DiOMEA was later validated by quantitative real-time PCR in a dose-dependent manner, showing decreased levels of mRNA correlating with incremental concentration of compound (Figure 5.10).

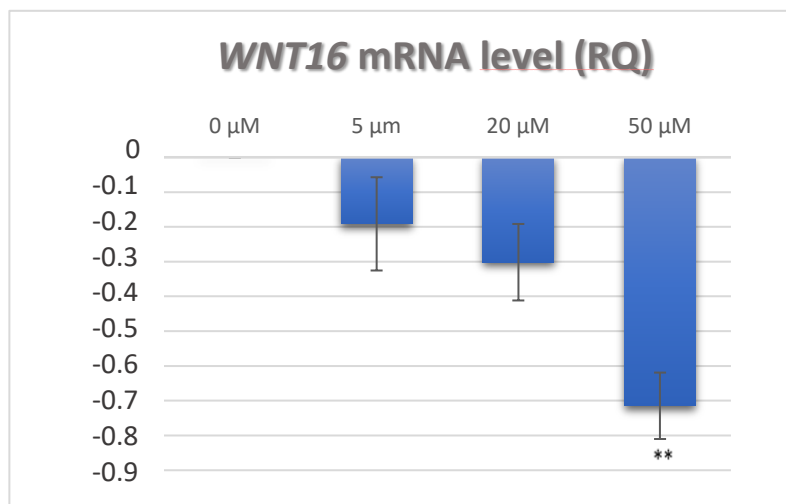


Figure 5.10: *WNT16* expression in human SW-620 CRC cells treated with different concentrations of 4,4'-DiOMEA. Relative quantification for *WNT16* in SW-620 cells treated with 5, 20, and 50 μM 4,4'-DiOMEA in relation to nontreated cells normalized to the endogenous control (glyceraldehyde 3-phosphate dehydrogenase).

5.2.1.5. SW-620 CRC cells treated with 20 μM 4,4'DIOMEA do not lower levels of downstream Wnt signal, β-catenine

Wnt signaling encompass different transduction pathways triggered by binding Wnt ligands to their membrane receptor and activating genes implicated in different development processes required for embryonic progress and tissue maintenance and regeneration in adults (Liu et al., 2008). Inadequate activation of the Wnt pathway is involved in the progression of numerous tumors, supporting an important role of this pathway in promoting cancer (Brennan and Brown, 2004). Mutations in the Wnt/β-catenin signaling pathway trigger a great number of sporadic CRC; thus, one approach for CRC therapy is to inhibit Wnt activity (Lazarova and Bordonaro, 2012a).

Wnt can activate several key signaling cascades including the canonical Wnt/β-catenin pathway, and the noncanonical Wnt pathways such as the PCP (planar cell polarity), c-Jun amino-terminal kinase (JNK), Rho, and calcium signaling pathway (Moon et al., 2004) (Reya and Clevers, 2005). The main difference between canonical and

noncanonical signaling relies in the role played by the protein β -catenin. Canonical pathway requires this protein while the other axes signal independently of it (Nusse, 2005) (Polakis, 2000). To detect activity of Wnt canonical signaling under 4,4'DIOMEA, the TOP/FOP plasmid was transfected into both control SW-620 and treated cells (20 μ M, 72 hr). Renilla luciferase was used to measure transfection efficiency and firefly luciferase to properly quantity levels of β -catenine. A higher luciferase intensity should be expected in low Wnt activity cells like those treated with the compound of interest.

Graph in figure 5.11 (A) shows that Treated SW-620 cells do not display a decrease in β -catenin levels (firefly luciferase normalized to renilla intensity) in comparison with cells non treated with the phenolic compound.

In figure 5.11 (B) the negative controls (FOP) display slight activity, in the two group of cells, control vs treated, whereas figure 5.11 (C) shows that transfection of plasmids containing the reporters TOP occurs more effectively than the transfection of the plasmids with the negatives control FOP.

To obtain the net ratios (fig 5.11.A), the signal of luciferase reporter (TOP) is normalized to the negative reporter (FOP).

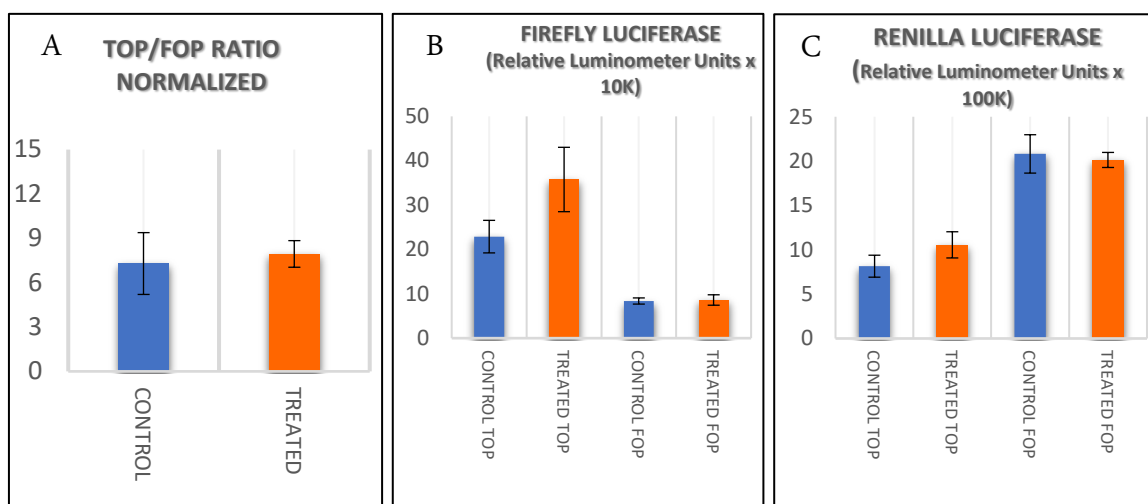


Figure 5.11 Results of the TOP/FOP assay performed on SW-620 CRC cells treated with 4,4'DIOMEA as a reporter of Wnt/ β -catenine activity. A) TOP/FOP ratio display an increment (non-significative) in luciferase signal levels (firefly luciferase normalized to renilla intensity) in the treated cells in comparison with cells non treated with the phenolic, indicating no significant differences in Wnt/ β -catenine activity. (B) Plot showing levels of negative controls (FOP). (C) Plot showing levels of transfection control (renilla luciferase). It is shown that transfection of plasmids containing the reporters TOP occurs more effectively than the transfection of negatives control FOP.

Epithelium-mesenchymal transition (EMT) is a process by which epithelial cells lose their epithelial characteristics and gain migratory and invasive abilities to acquire a mesenchymal-like phenotype (Cano and Portillo, 2010)

Since Wnt signaling is deeply involved in the EMT process of cancer cells, a combination of EMT markers detection by RT-qPCR and cell motility behavior by wound healing assay were performed in monolayer SW620 cultures to explore whether the phenolic might contribute to modulate EMT.

Downregulation of E-cadherin is one of the crucial leading events for EMT and is considered a hallmark of the process (Moreno-Bueno et al., 2009) although a great number of factors and signals seems to be involved in the transition. Based mainly in the finding of different authors regarding EMT, the markers stated in table 5.10 were selected for RT-qPCR analysis mean to detect the eventual repression of the EMT process by the 4,4' DIOMEA.

Gene name	Marker
N-Cadherin	Mesenchimal
Vimentine	Mesenchimal
E-Cadherin	Epithelial
Keratin 18	Epithelial
Na ⁺ /K ⁺ ATPase β 1	Epithelial
Snail	Mesenchimal
β -Catenin	Mesenchimal

Table 5.10 Genes selected for EMT analysis and related phenotype

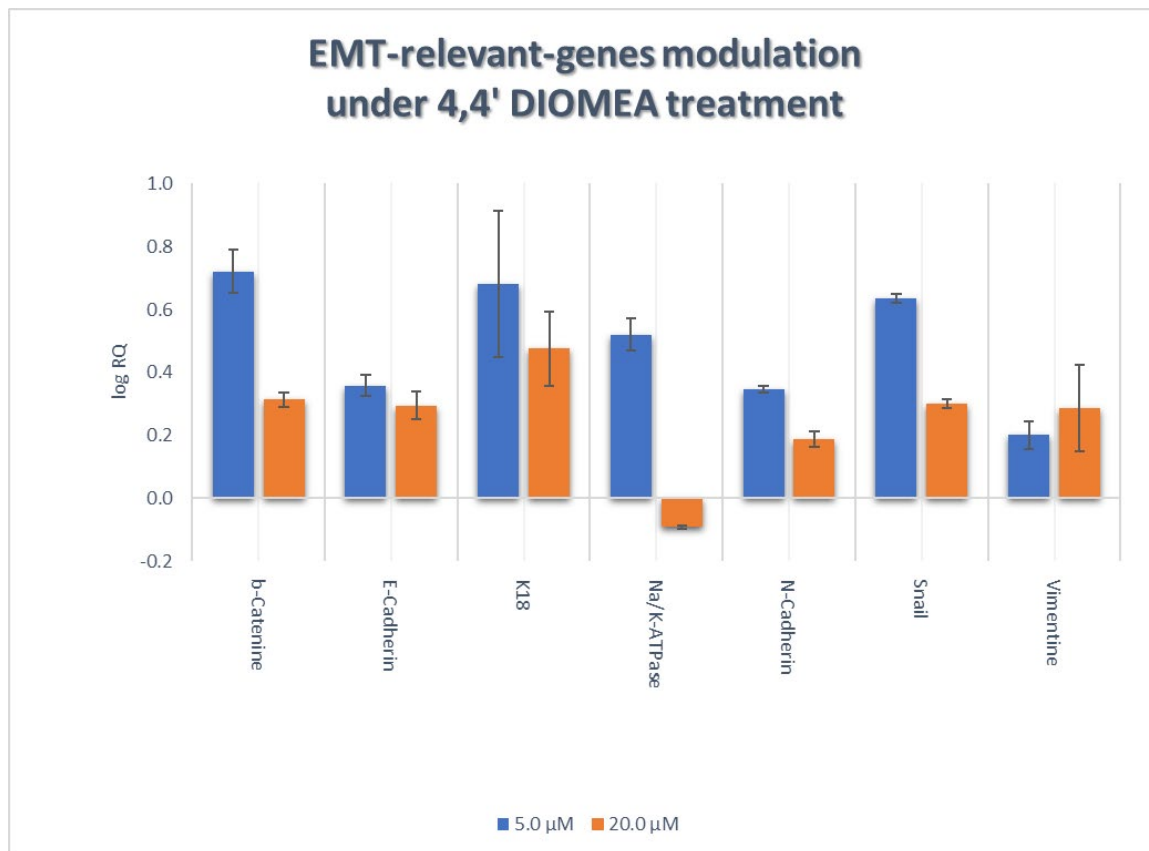


Figure 5.12 RT-qPCR analysis showing the SW-620 cells mRNA levels of the epithelial markers E-Cadherin, K18 and Na⁺/K⁺ATPase β1, the mesenchymal markers N-Cadherin, Vimentin, and EMT inducers Snail and β-catenin upon 72 hours of treatment with 4,4'DIOMEA (5 μM and 20 μM). The increment in epithelial markers (except for the marker Na⁺/K⁺ATPase β1 in cells treated at 20 μM) is counterbalanced by the increment in mesenchymal markers as well, which lead to an uncertain conclusion about EMT modulation by the phenolic derivative. The increment in β-catenin confirms previous results of TOP/FOP transfection assay to monitor Wnt signaling. Two-tailed unpaired t.test ($\alpha=0.05$) was performed to detect significant differences between control and treated groups (n=2).

Figure 5.12 shows contradictory results regarding EMT since both increment in epithelial and mesenchymal markers were achieved. Drop in E cadherin levels, which is one of the most robust marker of EMT was reversed by the treatment with 4,4' DIOMEA suggesting eventual inhibition of EMT, but the concurrent increment in mesenchymal markers contradicts this finding. RT-qPCR results also confirmed the increment in mRNA levels of β-Catenin in the line with the previous data collected by the TOP/FOP transfection assay.

Trying to understand these contradictory results, a functional assay was performed aimed to detect alteration in migration of CRC cells treated with 4,4' DIOMEA. A wound healing assay was carried out, testing different concentrations of the compound in SW620 cells. The protocol previously referred in material and methods to test cell migration (Moreno-Bueno et al., 2009), was accomplished and results brought up non-significant differences between treated with 4,4'DIOMEA (5 μ M and 20 μ M) and control cells.

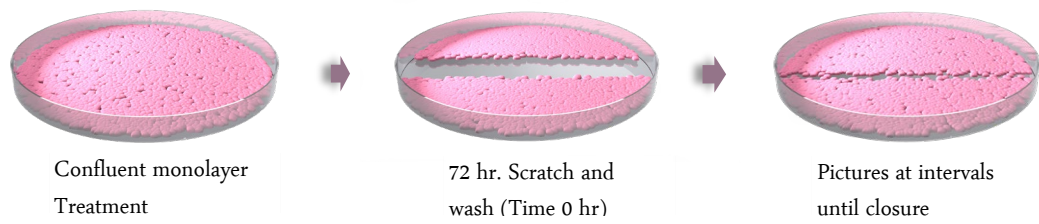
The phenolic compound Ellagic Acid was also tested using same concentrations to compare efficiency between the precursor EA and its in-vivo derivative but neither differences were achieved.

Figure 5.13 A) captures representative cartoon of wound healing assay and B) captures representative pictures at different timepoints (only 5 μ M shown) and the transformed image by the software used for grey-scale pixel quantification, TScratch 1.0 (Gebäck et al., 2009). Control cells (most left column of images) seems to show a much more cohesive unidirectional migration than the one shown by cells treated with Ellagic Acid and 4,4DIOMEA (right two columns of the panel). Quantification did not detect statistical dissimilarities between treated and control groups at any concentration tested.

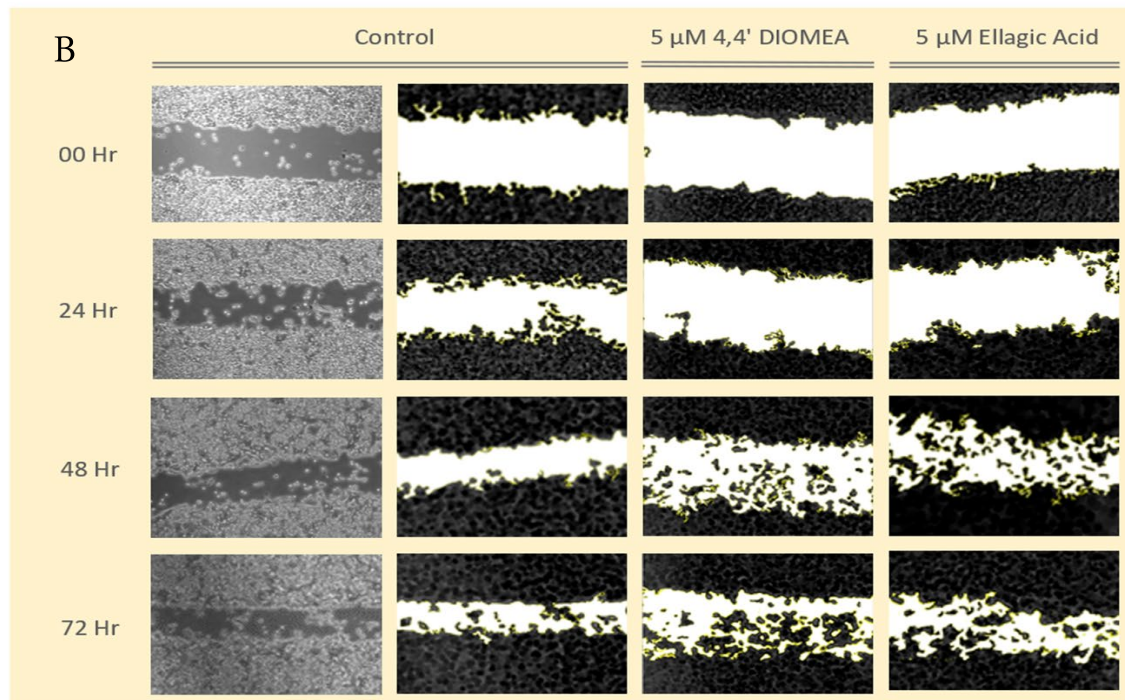
Figure 5.13.C

WOUND HEALING ASSAY

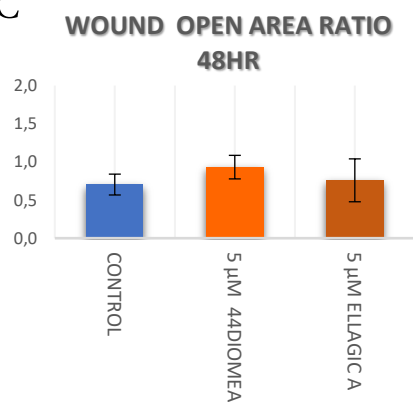
A



B



C



D

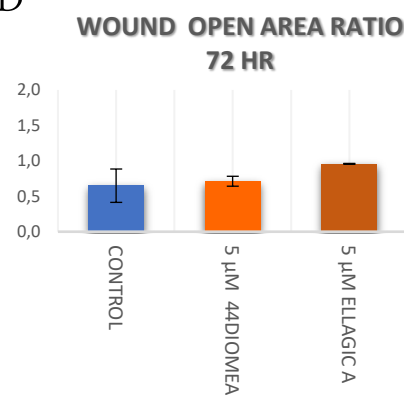


Figure 5.13: Wound Healing Assay. A) Cartoon representatives of main steps in wound healing assay. B) Representative pictures of wound in control cells at time 0hr, 24, 48 and 72 hr (left column). Image transformed for pixel quantification by software TScratch 1.0 of control cells and treated (center and right columns). The two columns on the most right shows a slightly random migration at 48 and 72 hr. in comparison with control (more cohesive unidirectional behavior)

C) D) Pictures Quantification. Data represent avg. open area ratio at 48 and 72 hr (Divided by avg. area at 0 hr) \pm sd. of two independent experiments, with three replicates per tested concentration. (Two-tailed unpaired t.test, $\alpha=0.05$).

5.2.1.6. Epigenetic analysis of 754 miRNA in CRC SW-620 cells. Modulation by 4,4' DIOMEA.

In order to investigate the eventual role of several miRNAs in the mechanism of action of 4,4' DIOMEA, the differential levels of expression of 754 miRNAs after treatment of CRC cells with two concentration of the compound (5 and 20 μM), were tested by means of TLDA cards, following the protocol previously detailed in materials and methods. In a first filtering considering only those miRNA showing dose-dependent response, a set of 33 candidates were selected, 15 of them experienced treatment-mediated over-expression and 18 underwent treatment-mediated repression. Figure 5.15 displays the 33 candidates and related log RQ.

The miRNA set was subsequently ranked by its folding change and restringing thresholds of 2 (for the miRNA upregulated) and 0.5 (for the miRNAs downregulated) were applied to bring up a final list of 9 candidate miRNAs for further validation by RT-qPCR (table 5.11).

Special relevance display two top candidates: The miRNA-203 (Fig 5.14.A), since its epigenetic silencing is essential for EMT and cancer stem cells properties (Deng et al., 2016) (Taube et al., 2013) (Liao et al., 2015) and oncogenic miR-96 (Fig 5.14.B), directly implicated in DNA mismatch repair deficiency (Sarver et al., 2009) and associated to bad prognosis in CRC (Xu et al., 2012).

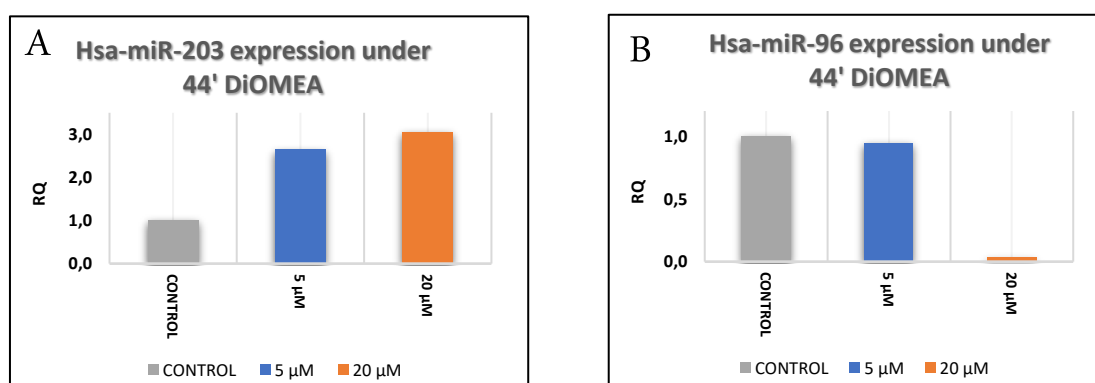


Figure 5.14. Level of expression of miRNA 203 and miRNA 96 after performing a Taqman Low Density Array (TLDA) analysis on SW-620 CRC cells treated with 4,4' DIOMEA at different concentrations . Plots display miRNA levels of top hit miR-203 and miR-96 after 72 hr treatment with 4,4' DIOMEA. A) miRNA-203 expression level. Its epigenetic silencing is essential for EMT and cancer stem cells properties (Deng et al., 2016) (Taube et al., 2013) (Liao et al., 2015) B) miRNA-96 expression level. It has been reported that oncogenic miR-96 is directly implicated in DNA mismatch repair deficiency (Sarver et al., 2009) and associated to bad prognosis in CRC (Xu et al., 2012)

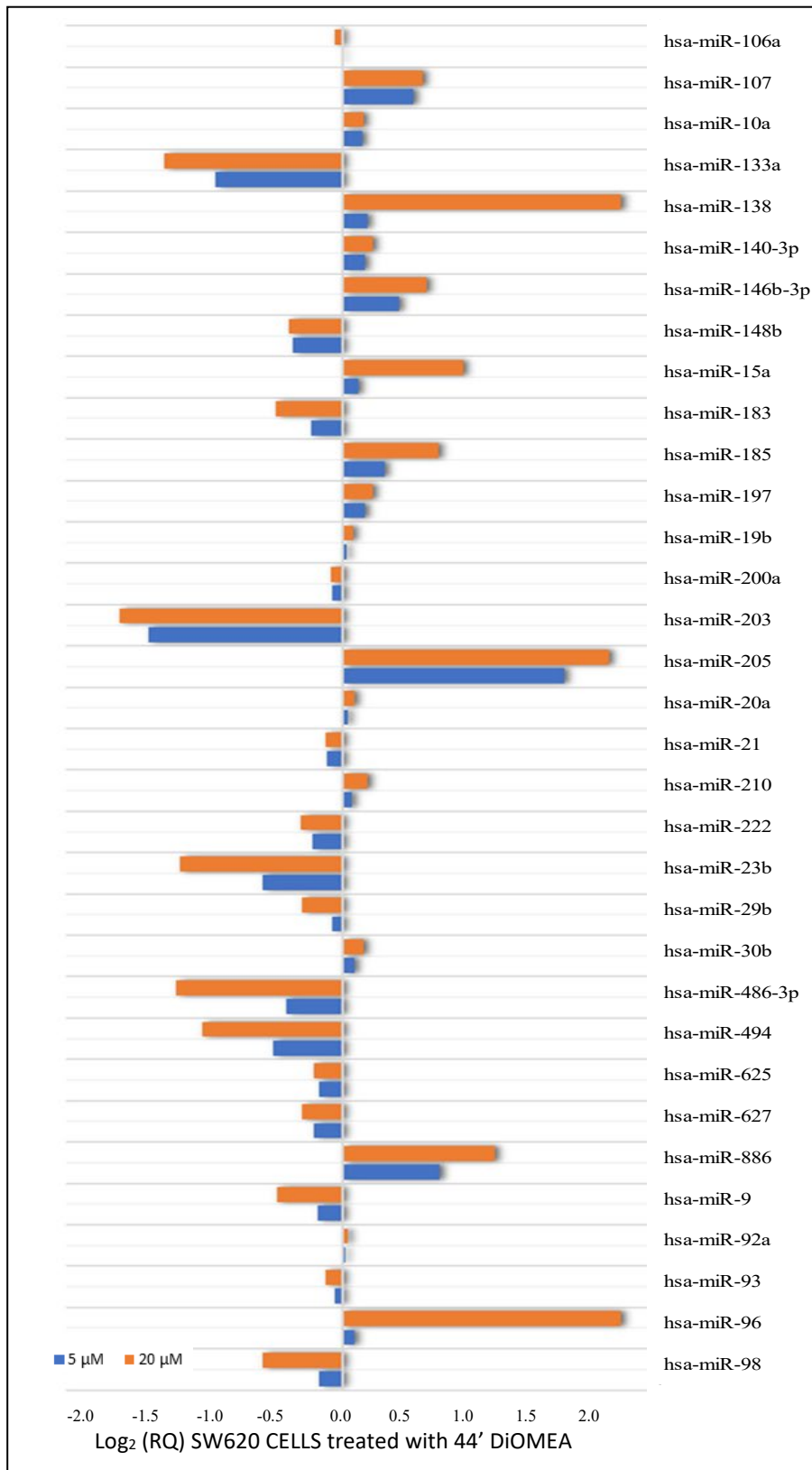


Figure 5.15 TLDA analysis results showing the expression levels of 33 miRNA from SW620 CRC cells that responded to 4,4'DIOMEA treatment in a dose dependent way. (72 hr treatment with 4,4'DIOMEA at 5 μM [blue] and 20 μM [orange].)

miRNA	4,4' DIOMEA Concentration	$\Delta\Delta C_t$	RQ	Log RQ
hsa-miR-138-4395395	0 μ M	-	1.00	-
hsa-miR-138-4395395	5 μ M	0.17	0.89	- 0.05
hsa-miR-138-4395395	20 μ M	2.00	0.25	- 0.60
hsa-miR-205-4373093	0 μ M	-	1.00	-
hsa-miR-205-4373093	5 μ M	1.60	0.33	- 0.48
hsa-miR-205-4373093	20 μ M	1.91	0.27	- 0.58
hsa-miR-886-5p-4395304	0 μ M	-	1.00	-
hsa-miR-886-5p-4395304	5 μ M	0.70	0.62	- 0.21
hsa-miR-886-5p-4395304	20 μ M	1.09	0.47	- 0.33
hsa-miR-96-4373372	0 μ M	-	1.00	-
hsa-miR-96-4373372	5 μ M	0.08	0.95	- 0.02
hsa-miR-96-4373372	20 μ M	4.93	0.03	- 1.48
hsa-miR-133a-4395357	0 μ M	-	1.00	-
hsa-miR-133a-4395357	5 μ M	- 0.92	1.89	0.28
hsa-miR-133a-4395357	20 μ M	- 1.29	2.45	0.39
hsa-miR-203-4373095	0 μ M	-	1.00	-
hsa-miR-203-4373095	5 μ M	- 1.41	2.65	0.42
hsa-miR-203-4373095	20 μ M	- 1.61	3.05	0.48
hsa-miR-23b-4373073	0 μ M	-	1.00	-
hsa-miR-23b-4373073	5 μ M	- 0.58	1.49	0.17
hsa-miR-23b-4373073	20 μ M	- 1.18	2.26	0.35
hsa-miR-486-5p-4378096	0 μ M	-	1.00	-
hsa-miR-486-5p-4378096	5 μ M	- 0.41	1.33	0.12
hsa-miR-486-5p-4378096	20 μ M	- 1.20	2.30	0.36
hsa-miR-494-4395476	0 μ M	-	1.00	-
hsa-miR-494-4395476	5 μ M	- 0.51	1.42	0.15
hsa-miR-494-4395476	20 μ M	- 1.02	2.02	0.31

Table 5.11. TLDA analysis showing modulation of the expression level of top miRNAs by 4,4' DiOMEA at different concentrations. SW620 CRC cells were treated for 72 hr with two concentrations of 4,4'DIOMEA. The table displays top miRNAs that were modulated in a dose dependent way.

5.2.1.7. Analysis of cell bioenergetics after 4,4' DIOMEA treatment.

One of the cancer hallmarks in close relationship with nutrition comprise the cancer-associated metabolic deregulation. Cancer profoundly modifies energy balance. The metabolic reprogramming of the cancer cells underly the need of fueling uncontrolled growth and proliferation. Traditionally, the most studied alteration in the metabolism of cancer cell encompasses the heavily studied “Warburg effect”. Under presence of oxygen (aerobic conditions), normal cell glycolysis ends up with pyruvate entering the mitochondria for an oxidative phosphorylation yielding ATP and carbon dioxide. If oxygen is not present, anaerobic conditions, glycolysis dispatch less pyruvate to the mitochondria and the cell produce most of the ATP in a cytosolic fermentation to lactate. Normal cells ferment glucose to make ATP in low oxygen environment. Otto Warburg discovered that cancer cell reprograms the metabolism to accomplish fermentation even under aerobic conditions (Warburg, 1956) (Figure 5.16).

Glycolysis encompass the biochemical reaction that converts a 6-carbon molecule of glucose into two 3-carbon molecules of pyruvate yielding ATP and NADH^+ , but the term is used in its broadest sense to refer the process only when a subsequent pyruvate reduction to lactate in the fermentation reaction take place.

Although the Warburg effect has governed much of the viewpoint on altered cancer metabolism over the last years, glucose cannot supply all the necessary resources for cancer to progress, in fact not all transformed cells show glycolytic phenotype and depressed mitochondrial activity. Another blend of metabolic deregulation in cancer is the elevated glutaminolysis, meant to use glutamine rather than or together with glucose as energy supply and building-blocks provider for cancer cells to grow and proliferate (Dang, 2010). The de-novo fatty acid synthesis and related pathways aimed to supply energy or deliver lipidic components for anabolic processes such as cell membrane building, is another trait of metabolic deregulation of transformed cells (Mashima et al., 2009).

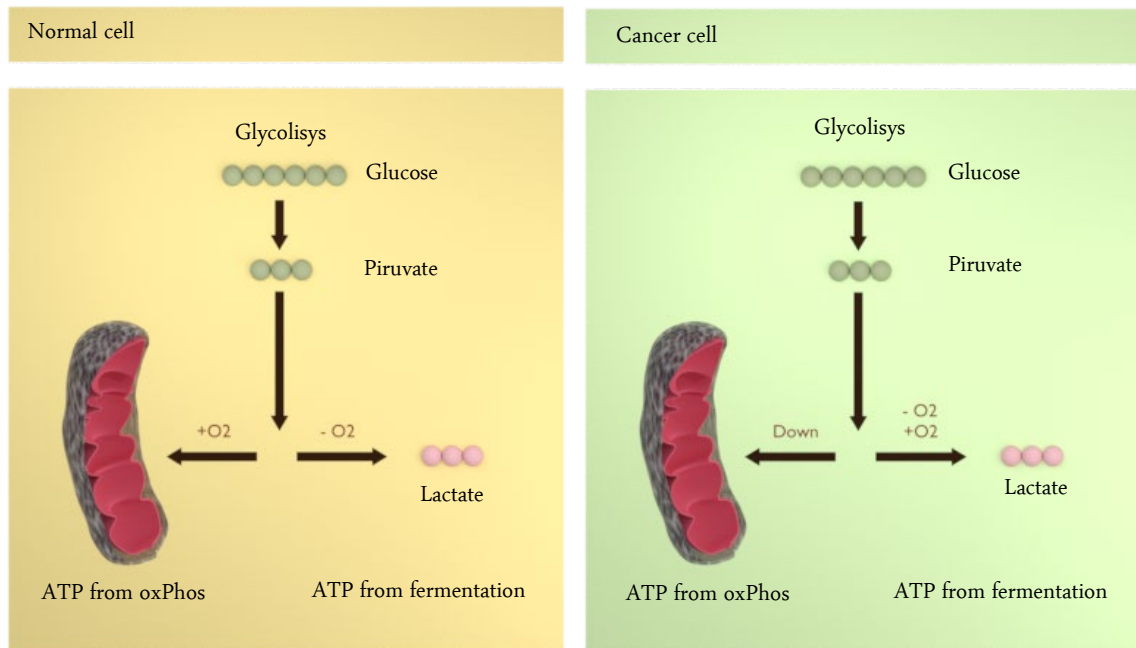


Figure 5.16 Representation of the Warburg effect. One of the key metabolic reprogramming in cancer cells together with glutaminolysis and de-novo fatty acids synthesis, among others. Under the presence of oxygen (aerobic conditions), glycolysis of most normal cells ends up with pyruvate entering the mitochondria for an oxidative phosphorylation (oxPhos) yielding ATP and carbon dioxide. If oxygen is not present (anaerobic conditions) glycolysis dispatch less pyruvate to the mitochondria and the cell produce most of the ATP in a cytosolic fermentation to lactate. Differentiated non-transformed cells ferment glucose to make ATP in low oxygen environment. Otto Warburg discovered that cancer cell reprograms the metabolism to accomplish fermentation under aerobic conditions and use this reaction as one of the main pathways to produce ATP (Warburg, 1956)

To investigate the eventual modulation of mitochondrial activity by 4,4'-DIOMEA, the Extra-Cellular Acidification Rate (ECAR) and the Oxygen Consumption Rate (OCR) were monitored in the surrounding media of both cultures of SW-620 CRC non treated cells and SW-620 CRC cells treated for 72 hr with 4,4'-DIOMEA. The equipment used for this purpose was an extracellular flux analyzer (See materials and methods). The concentration tested were the IC₅₀ and twice the IC₅₀ achieved in the previous MTT cell viability assays for the 4,4'-DIOMEA phenolic.

This analysis was performed in two different situations, a basal nutrient-rich metabolic setting and a stressed nutrient-rich metabolic situation in which a high energy demand is simulated. By adding a metabolic perturbation agent to the culture media, (carbonyl cyanide-4-[trifluoromethoxy] phenylhydrazone [FCCP]), protons freely flow through the mitochondrial membrane due to a FCCP-mediated H⁺ permeability. This flow disrupts the existing membrane potential (mito Ψ) which uncouples respiration from ATP synthesis by the electron transport chain complex V. Without this system regulating respiration, any oxidizable substrates present in the medium can be oxidized only limited by the maximum OCR achieved by the cell (Winer and Wu, 2014). By measuring OCR after FCCP injection, the maximum OCR is obtained and a parameter referred to as spare respiratory capacity (SRC) can be therefore calculated by the difference between basal and maximum OCR. Lowering this parameter by compounds such as the phenolics may impair cancer cell viability since it seems to exist strong correlation between enhanced SRC and apoptotic death-resistance (Nickens et al., 2013), furthermore attenuated SRC has been reported to increase vulnerability to oxidative stress and cell death in some types of cancer (Sriskanthadevan et al., 2015).

Figure 5.17 A shows the averaged OCR and ECAR phenotype plot of CRC SW-620 cells that have been non-treated and treated with 4,4'-DIOMEA at two concentrations (IC₅₀ and 2xIC₅₀). Graph shows a slight change in the metabolic profiles towards a less oxidative phosphorylation once the phenolic is applied, in stressed setting, but the high variability in the data obtained does not permit drawing clear conclusions. Figure 5.17.B and C displays OCR and ECAR of the three conditions tested and figure 5.18 reflects a dose-dependent decrement in SRC after treating the cells. This suggests that the compound does not modify bioenergetics when CRC cells are in rich nutrient basal environment, but it seems that it could impair mitochondrial activity when cells undergo stress, displaying a less flexible metabolic phenotype.

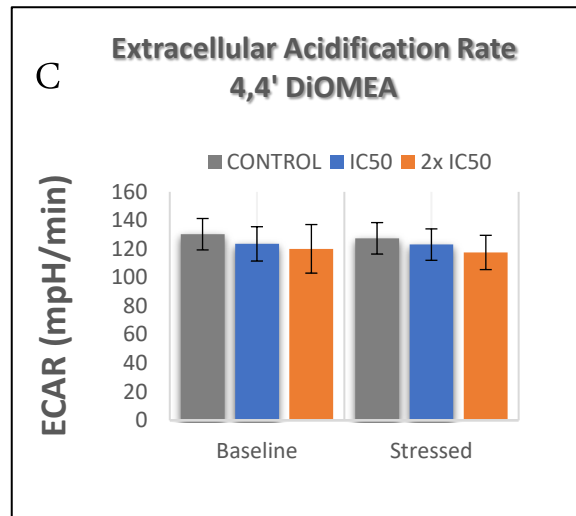
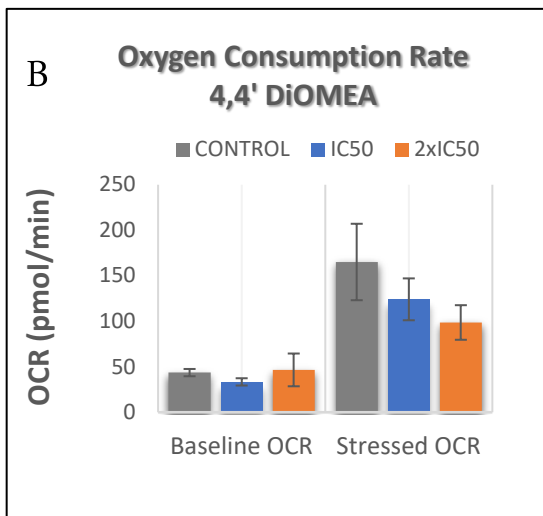
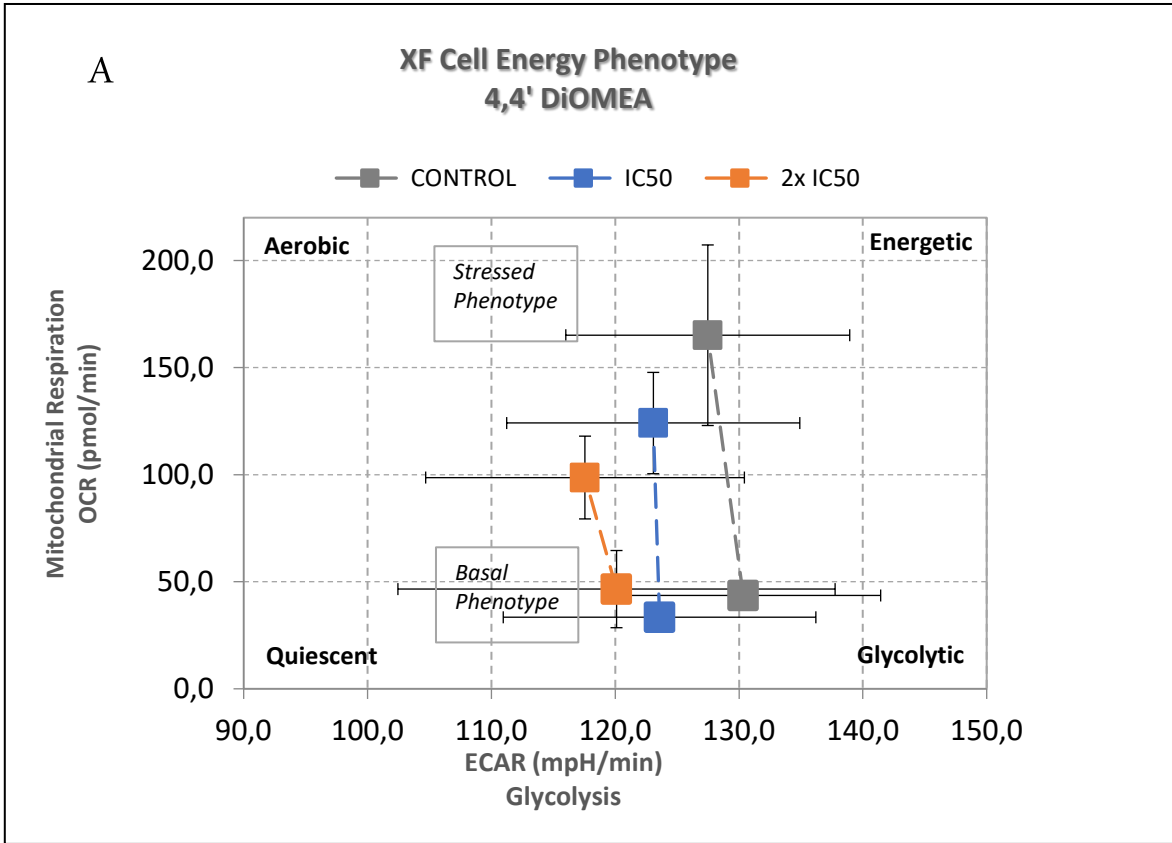


Figure 5.17 Energy Phenotype analysis on CRC SW-620 cells after 4,4'DiOMEA treatment at two concentrations. (IC50 and 2xIC50). A) Energy phenotype represents the utilization of both major energy producing pathways (mitochondrial, respiration and glycolysis), to meet their energy demand. Energy Phenotype comprises a baseline phenotype, a stressed phenotype (High energy demand), and a metabolic potential (Dot line) The plot shows four energetic status: Quiescent: The cell is not very energetic for either metabolic pathway, Energetic: The cell utilizes both metabolic pathways; Aerobic: The cell utilizes predominantly mitochondrial respiration; Glycolytic: The cell utilizes predominantly glycolysis. Despite seem to show a slightly tendency to a less oxidative phosphorylation in stressed setting, SW620 cells do not significantly alter the bioenergetic phenotype after adding 4,4'DiOMEA. Figure 5.17 B and C displays OCR and ECAR of SW620 cells under the three conditions tested (control; 4,4'DiOMEA at IC50; 4,4' DiOMEA at 2xIC50).

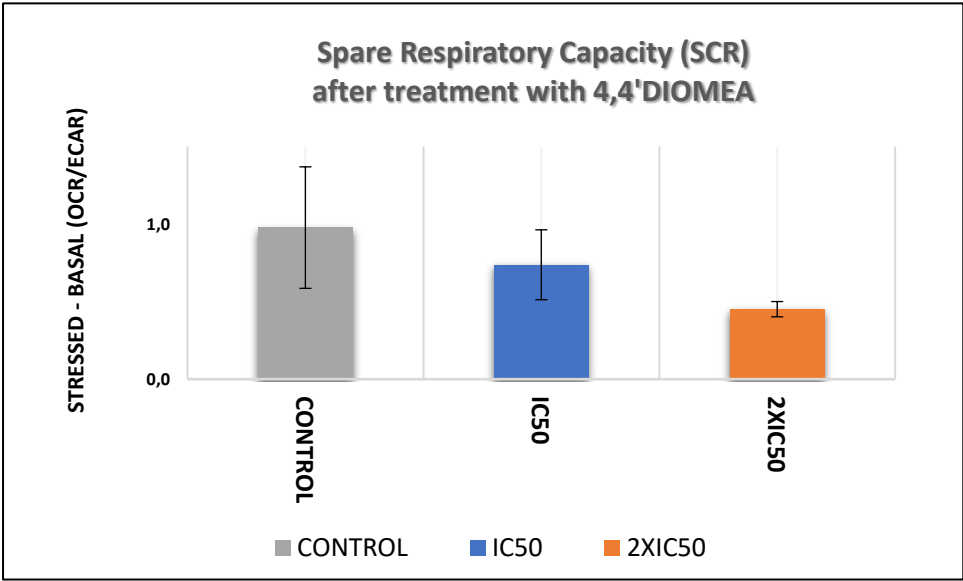


Figure 5.18. Spare respiratory capacity of CRC SW620 cells after treatment with concentrations of 4,4'DiOMEA equivalent to the IC_{50} and $2xIC_{50}$. The bars show a dose-dependent decrement in SRC after treating the cells with the compound.

**5.2.2. Nutritional strategies based on the inhibition of tumor nutrient requirements:
Intermittent Fasting as a potential precision nutrition strategy in BC**

5.2.2.1. Fasting cycles decrease growth of BC primary tumor in 4T1-induced breast cancer Balb/c mice.

Nutritional deficiencies often appear in many CRC patients, which make them suitable for nutritional strategies based on the inclusion of bioactive compounds. Contrary, BC is frequently associated with weight gain and metabolic syndrome, which could rationalize precision nutrition strategies based on caloric restriction. To further study this approach, female mice inoculated with BC cells underwent a nutritional intervention based on fasting cycles.

Figure 5.19 shows monitored body weight of mice along the experiment and reveals significant differences until third day post fasting-cycle and a progressive recovery to almost normal weight within one week after each interval.

Figure 5.20.A (See next page) displays tumor size measured weekly and before and after each fasting cycle (dark area of the graphic). It reveals significant differences of tumor sizes between both FMD and FSD groups compared to control group, however, there is no difference between diets in fasted animals. This suggests that the reduction in calories impairs tumor growth, but the diet composition tested (FMD and FSD) does not seem to have significant effect in the tumor size when fasting. The tumor size changes after the first fasting interval and differences improve significantly after the second cycle. Figure 5.20 B shows significant differences in tumor weight in the same way that occurs with size. Figure 5.20 C displays most representative pictures of tumors from animals of each diet group, i.e. FMD, FSD and SD showing clear differences in size between fasted groups and control group.

Regarding the length of the fasting cycles, the plot reveals that the second interval (one day shorter than the previous gap) has more incidence in the tumor impairment than the first cycle.

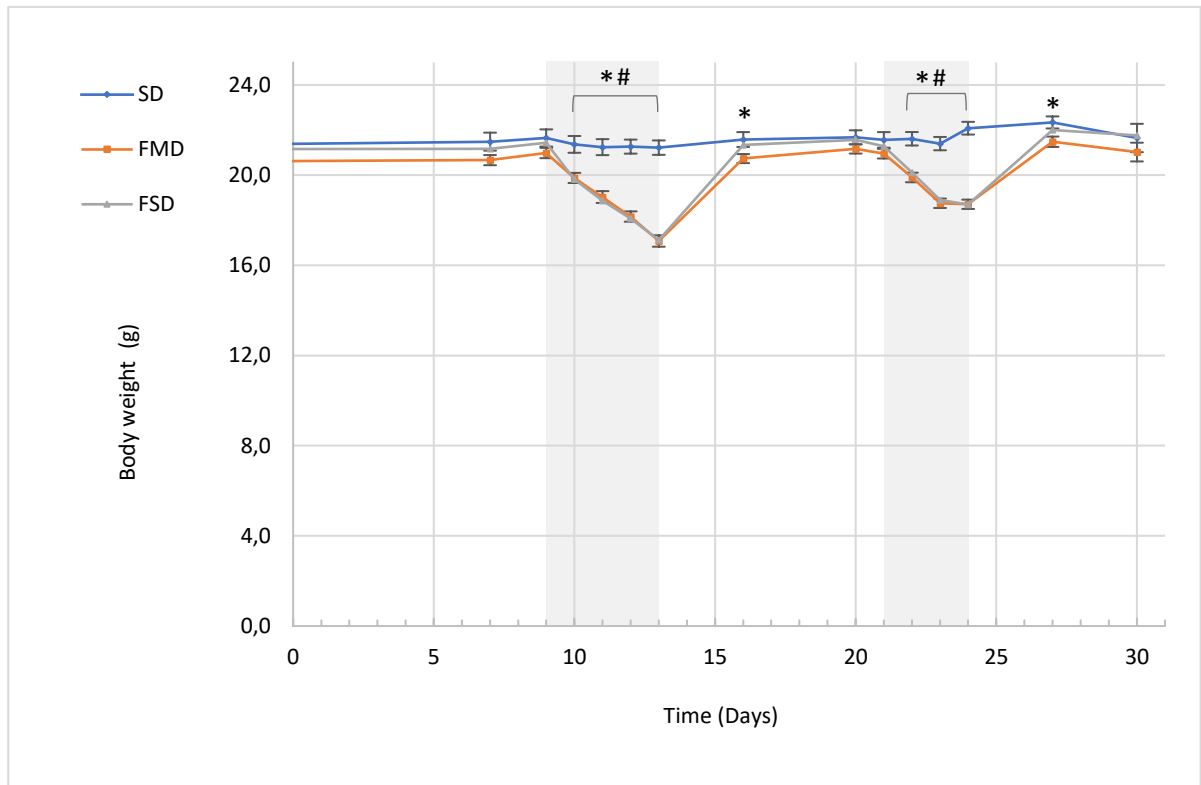


Figure 5.19 Body weight trajectories of mice fed SD, FSD and FMD. Graph includes averages of all animals at each time point until the end of the study. (* SD vs FMD, # SD vs FSD).

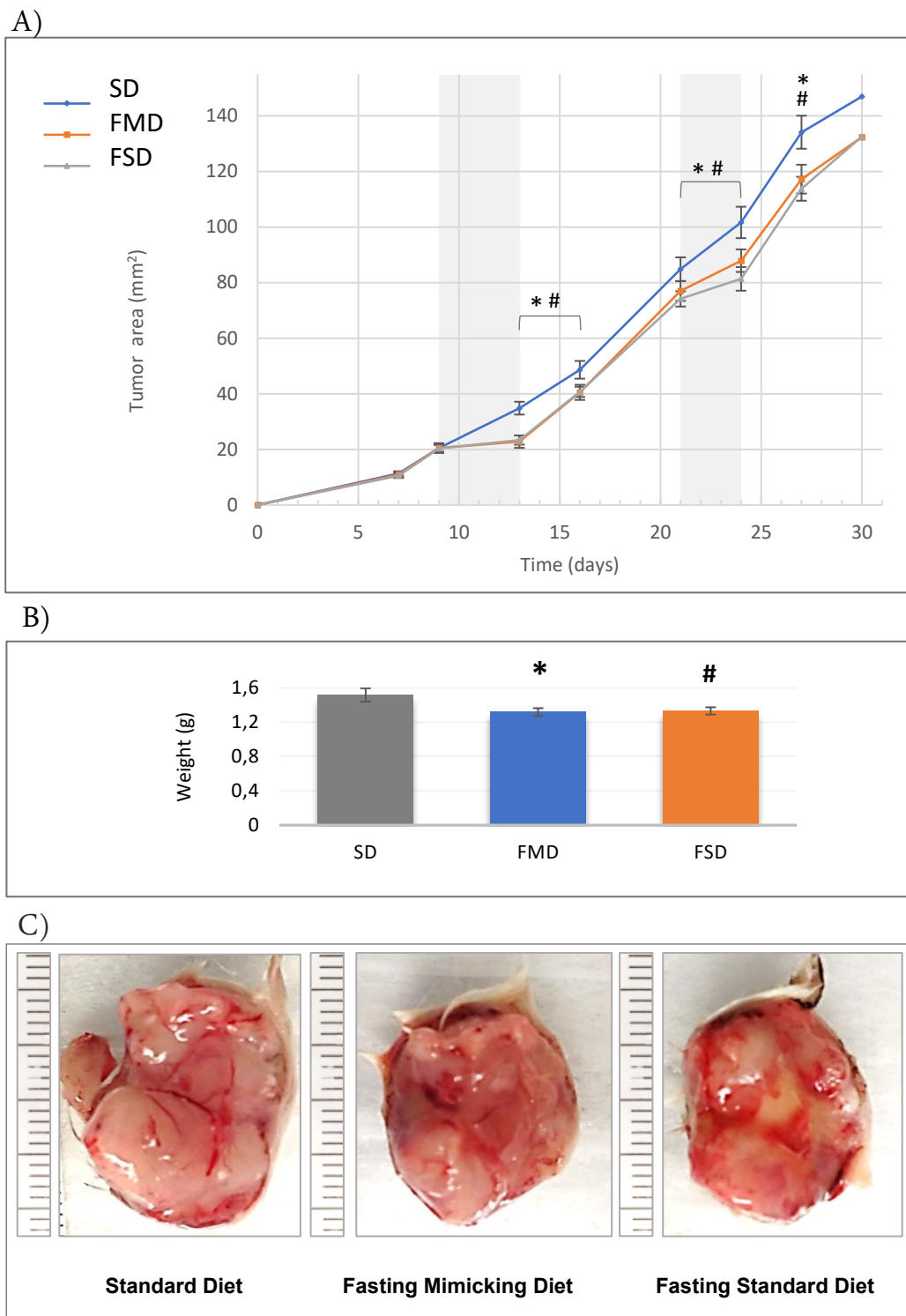


Figure 5.20 Breast tumor size measurements of mice fed SD, FSD and FMD. A) Graph includes all animals at each time point until the study termination. Tumor area (length x width) was measured with an electronic caliper. (* SDvsFMD, # SDvsFSD). B) Tumor weight. (* SDvsFMD, # SDvsFSD). C) Most representative pictures of tumors from animals of each diet group in where different size can be appreciated between fasted and ad-libitum fed animals but not between FMD and FSD.

5.2.2.2. Fasting cycles increase BC lung metastatic burden despite reduction in tumor size.

A)



B)

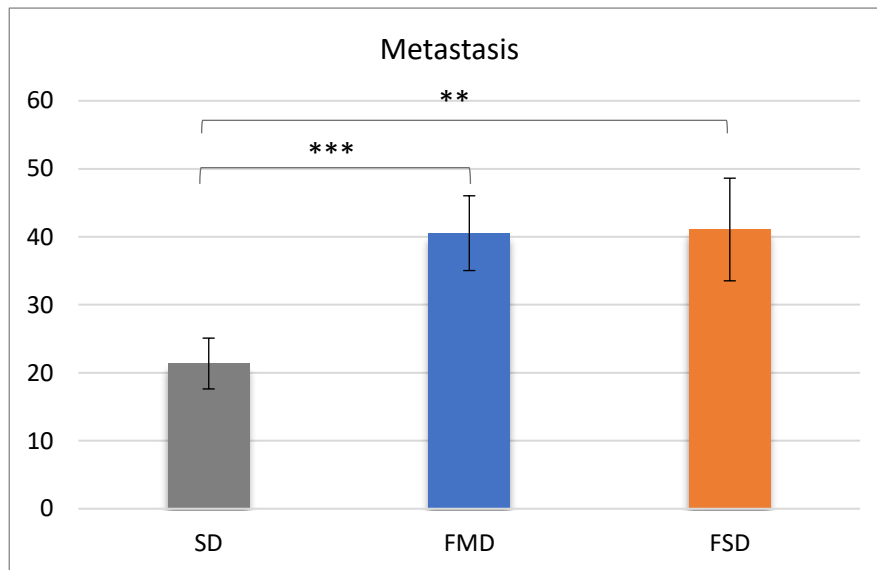


Figure 5.21. Lung metastatic nodules of mice fed SD, FSD and FMD. A) Image representation of lung metastatic nodules of animals from the three groups (SD, FSD and FMD). An intratracheal injection with India ink solution was performed to contrast tumor metastases in the right lung (n=45). An increment in the numbers of metastasis can be appreciated in both fasted groups compared to standard diet group. B) Bars-Plot representing metastatic nodules differences among groups. Despite tumor reduction in fasted groups a highly significant increment between FMD and FSD compared to the control SD has been achieved.

To analyze whether fasting diets elicit beneficial response in metastasis, an intratracheal injection with indian ink solution was performed in each mouse to contrast tumor metastases in the right lung (n=45). The counting of three independent researcher revealed an unexpected strong association between fasting and an increment in the number of metastatic nodes. Moreover, the FMD fed animals did not show differences in metastasis compared to the group on FSD. This similarities in the results of both groups undergoing fasting suggest that the augment in the metastatic burden is mediated by the number of calories restricted and the length of the fasting intervals, whereas the composition of these diets does not seem to affect in the process (Figure 5.21).

5.2.2.3. Fasting cycles: Molecular mechanism of action

As was pointed out in the introduction to this work, one of the key pathways involved in caloric restriction to inhibit cancer proliferation involves the downregulation of IGF1/PI3K/AKT/mTOR/p70/S6K/rpS6 and its modulation by fasting cycles in murine models fed on two different diets.

A clear explanation of this cascade is described in a deep review regarding ribosomal protein S6 (rpS6) and its implication in a broad variety of molecular processes (Ruvinsky and Meyuhas, 2006). In brief, this cascade starts with the activation of the dimerized receptor tyrosine kinase by GFs which activates class I phosphatidylinositol 3-kinase (PI3K). Two kinases, 3-phosphoinositide-dependent kinase 1 (PDK1) and protein kinase B (Akt) are recruited by PIP3 to the plasma membrane (Brazil and Hemmings, 2001), and then PDK1 phosphorylates and activates Akt (Belham et al., 1999). Activated Akt triggers a cascade of events leading to the activation of the mammalian target of rapamycin complex 1 (mTORC1) (Ruvinsky and Meyuhas, 2006). Active mTORC1 phosphorylates two translational regulators, S6 kinase (S6K) and eukaryotic initiation factor 4E (eIF-4E)-binding protein (4E-BP1, 2, and 3) (Hay and Sonenberg, 2004). Activation of S6Ks requires also phosphorylation by PDK1 in a reaction where binding of PDK1 to PIP3 is not required (Alessi et al., 1998). At the end of this cascade, activated S6Ks phosphorylates different substrates being ribosomal protein S6 (rpS6) one of them (Meyuhas and Drazan, 2009). Among some other functions, rpS6 have been suggested as one of the best indicators of mTOR cascade blockade (Tabernero et al., 2008) (Majumder et al., 2004) (Torres-Arzayus et al., 2004).

p70S6K is amplified in some breast carcinomas (Couch et al., 1999). Mostly, for tumors that have an amplification of p70S6K, there is a concurrent increment in the level of p70S6K protein (Couch et al., 1999). In several models of BC, mTORC1 pathway has been proposed to be a major signaling transduction node responsible for controlling metastasis (Akar et al., 2010). It has also been proposed that the activation of S6K1 or high S6 phosphorylation in primary BC tumors might be implicated in developing relapse and/or metastases (Khotskaya et al., 2014).

As a first approach to investigate the molecular mechanism underlying the effectiveness of fasting under the two diets compared to the group fed standard diet, Western blot analysis from tumoral and lung tissue were carried out using antibodies against diverse proteins of this pathway.

Despite both phosphorylated and non-phosphorylated proteins AKT, mTOR, p70S6K, and rpS6 were analyzed in both lung and tumor tissue, only consistent results were obtained in ribosomal protein S6. Figure 5.22 to 5.24 shows preliminary results of Western Blots regarding assays from samples of non-phosphorylated AKT, mTOR and p70S6K and the ratio after quantification of the phosphorylated/non-phosphorylated levels of rpS6 protein performed with tumor tissue from 8 animals per group of diet.

Fasted mice (FMD and FSD groups) show non-significant decrement in levels of active p70S6K but display significant inactivation of rpS6, which suggest a downregulation of the mTOR cascade. It has not been reported rpS6 involvement in cell proliferation, only in regulation of cell size, glucose homeostasis and protein synthesis (Ruvinsky et al., 2005). However, it might be indicative of mTOR inactivation which would explain the inhibition in proliferation and tumor shrinkage.

Finally, the results do not show differences between fasted and standard diets indicating that caloric restriction (and not diet composition) mainly explains this antiproliferative phenotype.

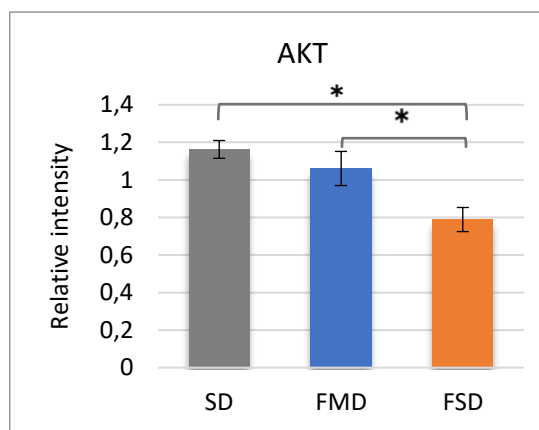
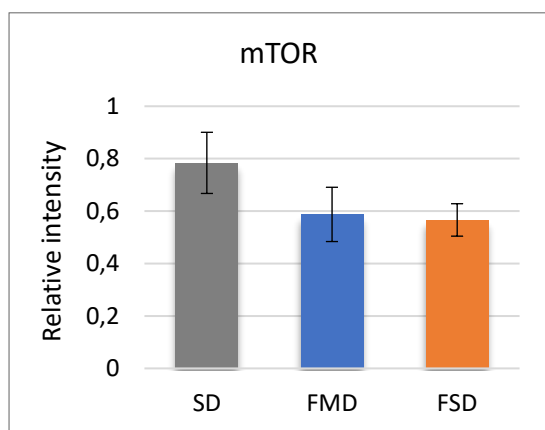
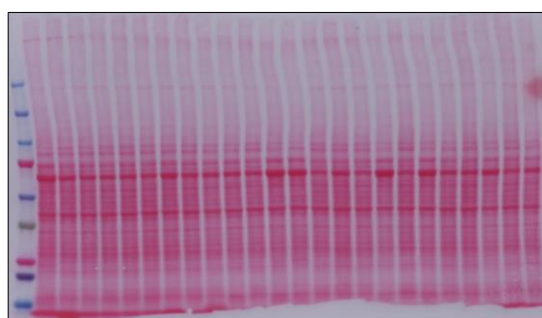
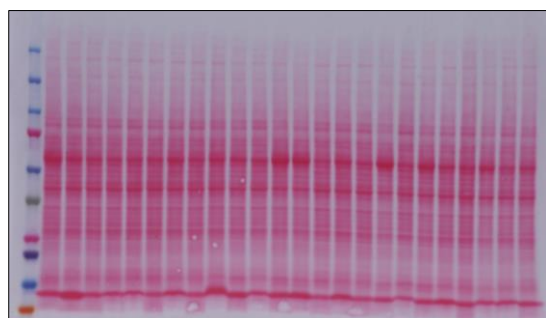
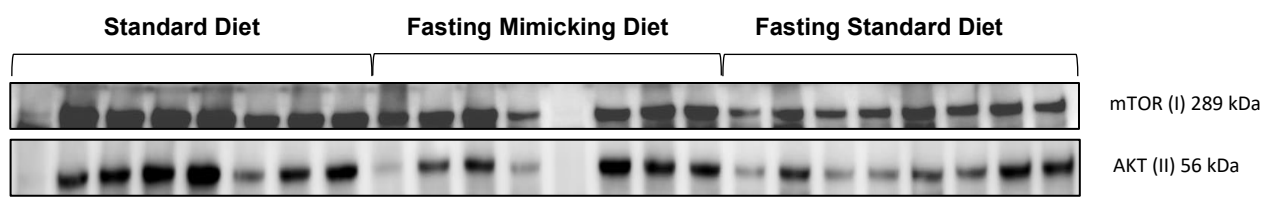


Figure 5.22. Western blot analysis in tumoral tissue from mice fed SD, FSD and FMD including mTOR and AKT proteins. Plots display level of protein corresponding to 8 mice per group of diet, SD: Standard diet, FMD: Fasting mimicking Diet, FSD: Fasting Standard Diet. Roman numerals identify the Ponceau staining image correspondent to each gel. ImageJ software was used to quantify the protein's relative intensity. p value of <math><0.05</math> (Unpaired two-sided t-test) was considered significant. (*p-value < 0.05)

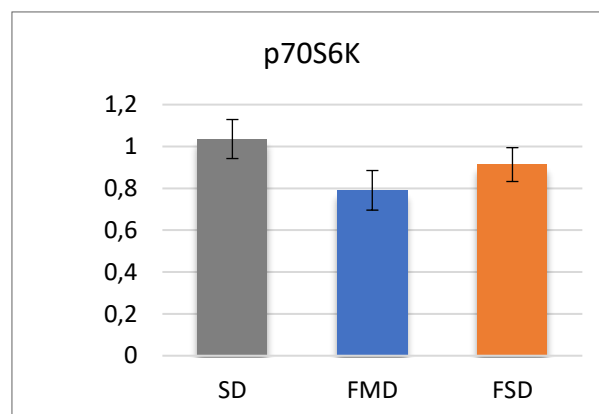
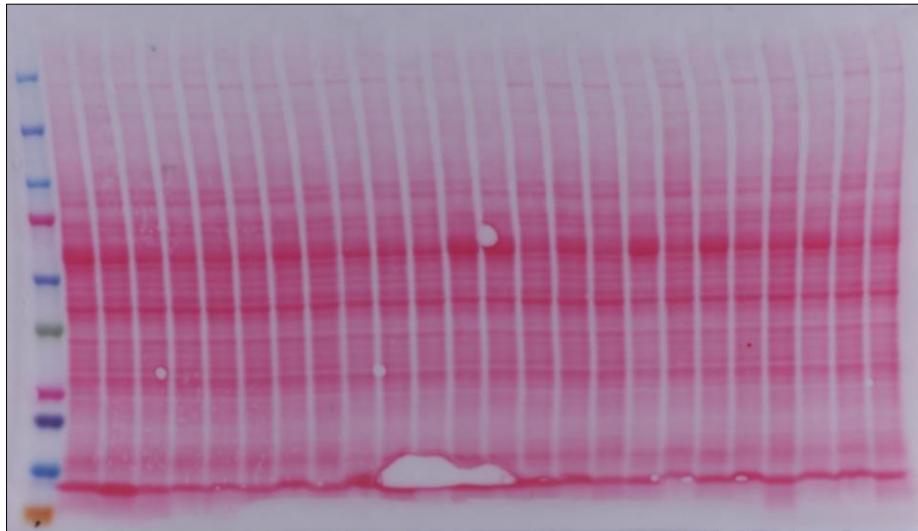
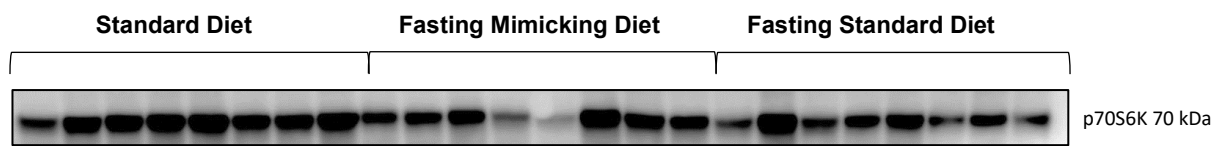
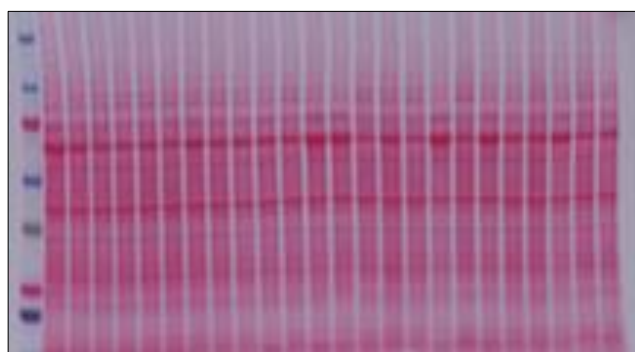
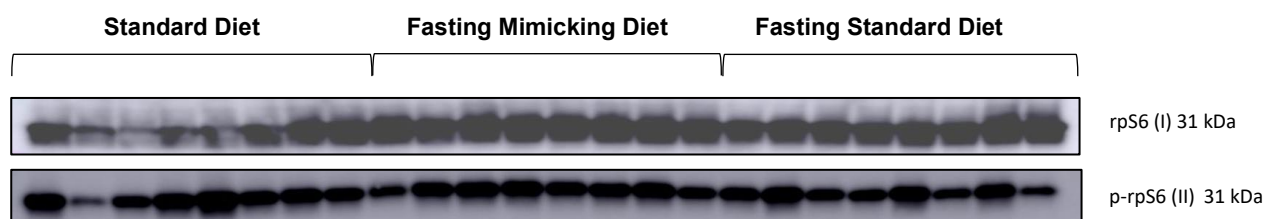
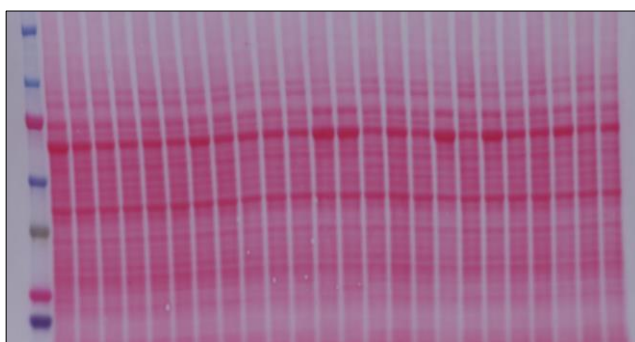


Figure 5.23. Western blot analysis of protein p70S6K in tumoral tissue from mice fed SD, FSD and FMD.

Plot displays level of protein corresponding to 8 mice per group of diet, SD: Standard diet, FMD: Fasting mimicking Diet, FSD: Fasting Standard Diet. ImageJ software was used to quantify the protein's relative intensity. p value of <math><0.05</math> (Unpaired two-sided t-test) was considered significant. (*p-value < 0.05)



Gel I



Gel II

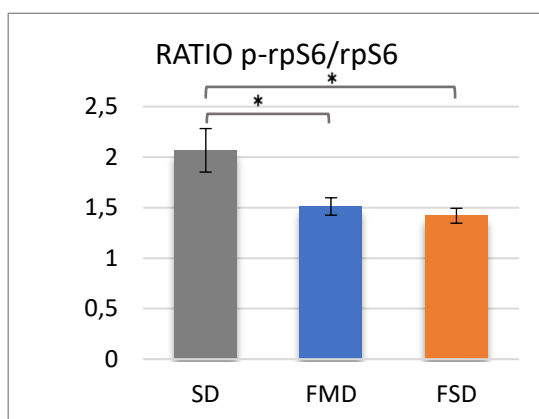


Figure 5.24. Western blot analysis in tumoral tissue from mice fed SD, FSD and FMD including rpS6 and p-rpS6 proteins. Image corresponding to 8 mice per group of diet (SD, FMS, FSD). ImageJ software was used to quantify the protein's relative intensity. Roman numerals identify the Ponceau staining image correspondent to each gel. Plot representing ratio between levels of phosphorylated and non-phosphorylated rpS6 protein. p value of <0.05 (Unpaired two-sided t-test) was considered significant. (*p-value < 0.05).

5.3. Comparative analysis of different nutritional strategies throughout *in vivo*, *in vitro* and *in silico* results

Levels of proteins of top hit gene identified as biomarker of survival in the *in-silico* analysis *SLC2A3* and the gene identified to be inhibited by the phenolic compound 4.4'DiOMEA in the *in-vitro* analysis were examined in tumoral tissue from mice fed on standard , fasting mimicking and fasting standard diet to identify eventual modulation by the caloric restriction and a plant-based diet. Figure 5.25 and 5.26 display the results of the Western blot analysis and correspondent quantifications

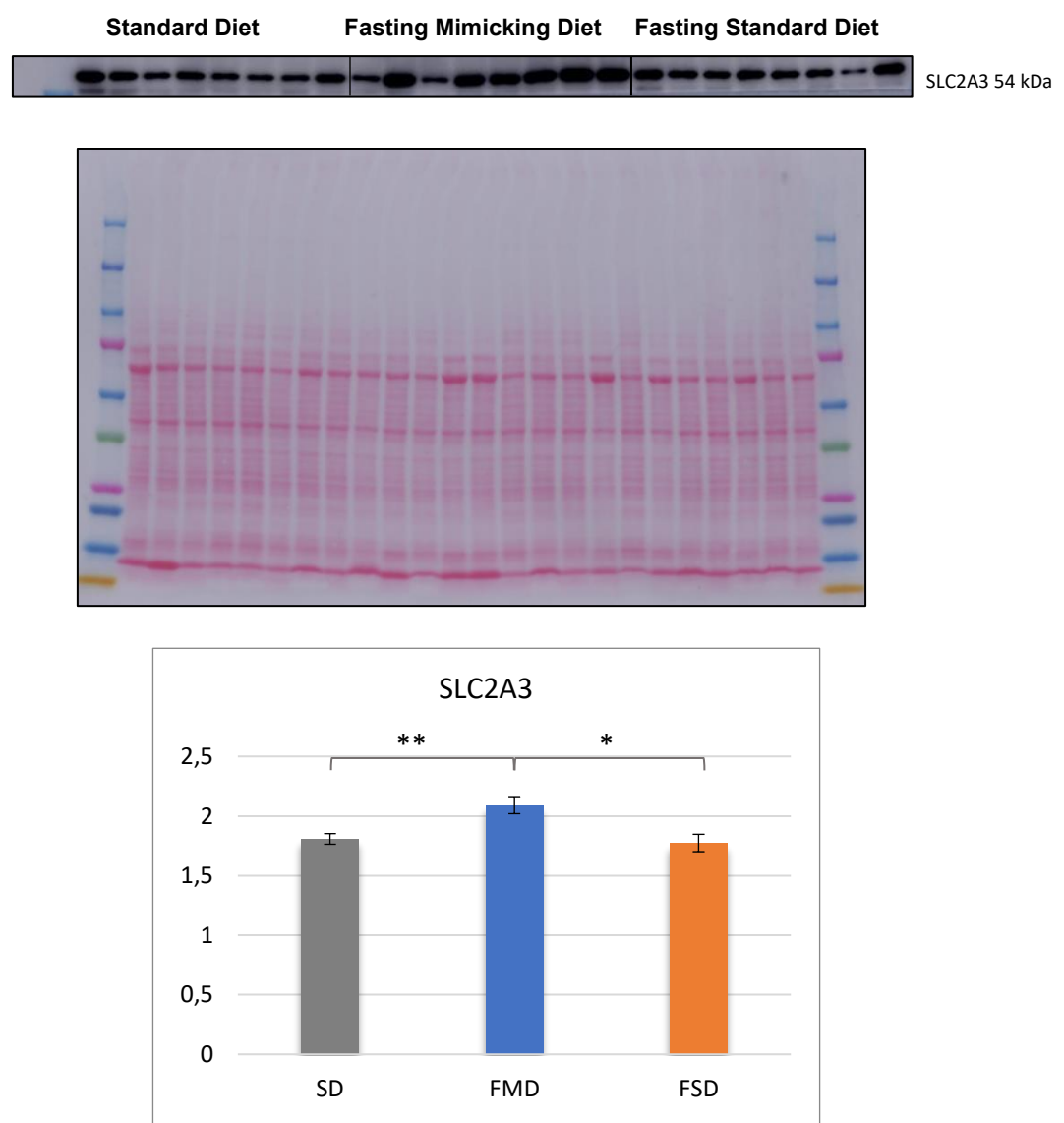


Figure 5.25. Western blot analysis of protein SLC2A3 in tumoral tissue from mice fed SD, FSD and FMD.

Plot displays level of protein corresponding to 8 mice per group of diet, SD: Standard diet, FMD: Fasting mimicking Diet, FSD: Fasting Standard Diet. ImageJ software was used to quantify the protein's relative intensity. p value of <0.05 (Unpaired two-sided t-test) was considered significant. (*p-value < 0.05).

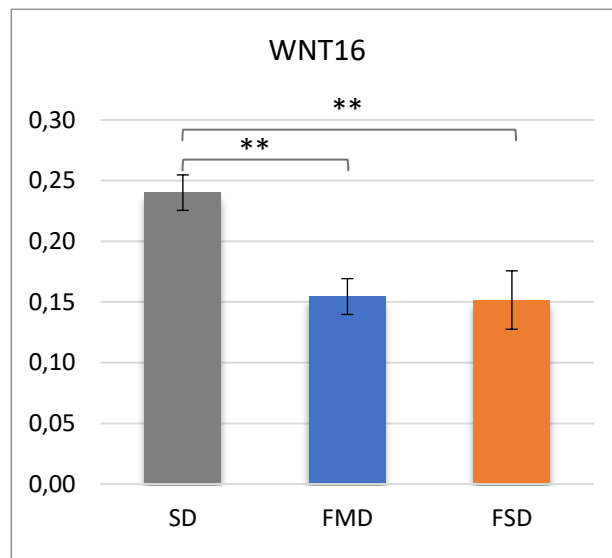
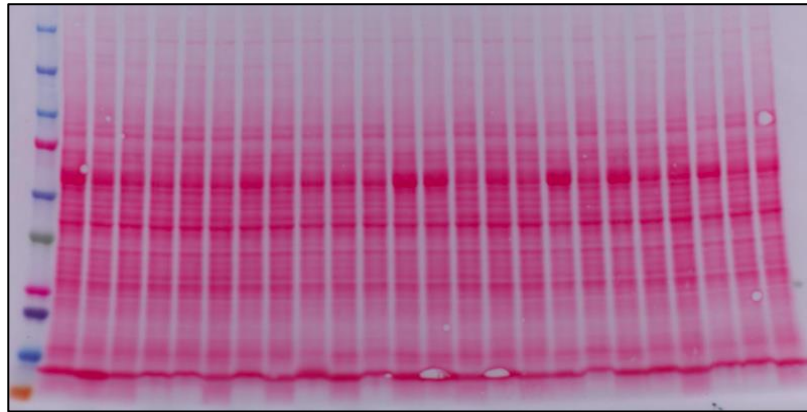
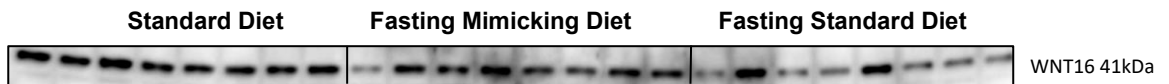


Figure 5.26. Western blot analysis of protein Wnt16 in tumoral tissue from mice fed SD, FSD and FMD.

Plot displays level of protein corresponding to 8 mice per group of diet, SD: Standard diet, FMD: Fasting mimicking Diet, FSD: Fasting Standard Diet. ImageJ software was used to quantify the protein's relative intensity. p value of <math><0.05</math> (Unpaired two-sided t-test) was considered significant. (*p-value <math><0.05</math>).

6. Discussion

6.1. Identification of genes involved in nutrient sensing or cell metabolism associated with CRC prognosis and patient survival

One important concept to take into consideration when accomplishing survival analysis is the selection of the statistical model to be used. Survival models consider 'time to event' as response variable while include one or several explanatory variables. The R survival package used in this Thesis contains different parametric and non-parametric models. Briefly, parametric models are fitted using `survreg()` and a non-parametric models are fitted using `coxph()`. Model selection mainly depends on the data structure and the target of the analysis. If the model is fitted for prediction, then the use of parametric `survreg()` becomes a must, because `coxph()` does not extrapolate beyond the last observation. Both techniques can be productively used depending on the particular question being asked. Crawley suggest typical questions addressed with `coxph()`: How much does the risk of dying decrease if a treatment is given?. In contrast, parametric techniques are routinely used for answering the following questions: What proportion of patients will die in x years based on data from an experiment that ran for just months? (Michael J Crawley, 2013)

Age-specific hazard has been considered in the survival analysis by including the Weibull distribution, since hazard changes with age regardless other factors. Weibull age-specific hazard model is very flexible because it can deal with hazards that increase with age in an accelerating or decelerating manner.

Another aspect to be considered in survival analysis is the fact that Coxph produces overfitted models when computing a large number of explanatory variables in multivariate survival analysis. In this Thesis, this issue has been addressed by using a Lasso penalized Cox regression model particularly convenient when the model has computed the top 100 genes at the same time to identify the weight of each gene in the survival risk score.

The selection of one preprocessing method to avoid batch effect is another important aspect when accomplishing integrative analysis. The use of different methodologies may lead to different biological results. The Venn diagram displayed in figure 6.1, shows a good example of this issue. The data analyzed corresponds to the same

IMD of 1273 CRC samples preprocessed with fRMA in where different BER algorithms has been applied (fRMA, fRMA plus Combat and fRMA plus mean centering). A later hypothesis contrast performed using LIMMA to identify genes deferentially expressed among early and late stages ($p\text{-val} < 0.01$) obtains dissimilar number of DEG depending on the BER method applied. In the IMD preprocessed with fRMA alone, more candidates were found to be significant in comparison with those brought up when computing IMDs using fRMA plus Combat and fRMA plus mean centering. Batch effect removal modifies the data and could lead to biological information missing, thus should be managed with caution.

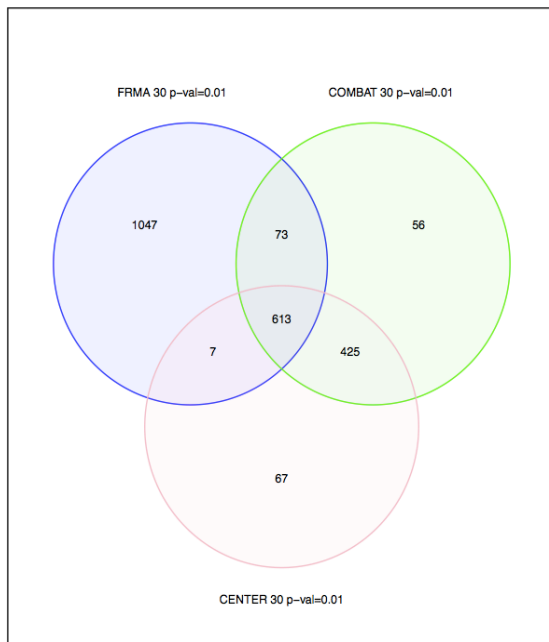


Figure 6.1. Venn diagram showing different hits after performing LIMMA analysis using same gene expression microarrays preprocessed with 3 different methods (fRMA, fRMA+Combat, fRMA+Mean centering). (fRMA in blue, fRMA plus Combat in green and fRMA plus mean centering in red). A LIMMA analysis was performed in the three IMDs to identify genes deferentially expressed between early and late stages ($p\text{-val} < 0.01$). Despite the three IMDs contains same probesets and same samples, Venn diagram shows only 613 genes common to the three IMD.

The work of this Thesis addressed a question regarding the implication of nutrient-sensing or metabolism related genes in cancer survival for subsequent exploration of their modulation by different nutritional strategies. The examination of 1273 transcriptomes of CRC samples and the application of the stringent cut-off values (adjusted $p < 0.0003$) revealed 765 differentially expressed genes (DEG) that marked strong correlation between level of mRNA and survival time.

Besides the functional implication in a specific pathway, the consistency of some survival markers found here is widely supported by previous discoveries: top hit *EPHB2*, a receptor tyrosine kinase for ephrin ligands, has been considered to be a CRC tumor

suppressor and solid prognostic factor (Batlle et al., 2005) (Oba et al., 2001) (Jubb et al., 2005); *LAMP5* has been included in a multigenic assay to predict recurrence after surgery (Lee et al., 2014); Discoidin CUB And LCCL Domain Containing 2 (*DCBLD2*), member of a family of neuropilin-like proteins, has been identified as CRC biomarker (Pagnotta et al., 2013); growth arrest and DNA-damage-inducible 45 beta (*GADD45B*) is a gene associated with cell cycle regulation, DNA repair and apoptosis. Its overexpression has been recently correlated with worse survival in CRC (Wang et al., 2012). Moreover, a recent integrative analysis of multiple CRC subtype classifiers reported that one of the three highest scoring genes included in several classifiers was *GADD45B* (Sztupinski and Gyórfy, 2016)

Among the less studied genes found in the 765 prognosis markers proposed here, CDGSH iron sulfur domain 3 (*CISD3*) is probably one of the best candidates for further research in the nutrient-cancer scenario. Its overexpression indicates to be strongly cancer-preventive (HR 0.51 [95%CI:0.41-0.63] p=1.8E-10).

CISD3 is highly expressed in colon, duodenum and small intestine and codes for CISD3 protein, one of the three members of the iron-sulfur (Fe-S) NEET family. This family of mitochondrial proteins is involved in iron and ROS homeostasis (Lipper et al., 2018). There has been growing interest in the products of *CISD1* and *CISD2* because they are key regulators of mitochondrial function and lipid homeostasis and they are directly involved in obesity, cardiovascular disease, cancer and aging (Kusminski et al., 2012). Meanwhile, the importance of the inner mitochondrial isoform 3 is still lowly explored in cancer field which may suggest new opportunities for novel investigation.

The Geneset enrichment analysis identified 11 overrepresented pathways (table 5.2) according to the functional annotation of those 765 genes, mostly describing changes in the motile behavior of the cell i.e., cell adhesion, extracellular matrix organization, integrin, laminin, chondroitin, collagen formation. These results were likely presumed since expression level from samples in early-stage vs late-stage were contrasted to identify the DEG. In early stages (I-II) the tumor is still local whereas late stages (III-IV) encompass full activation of the invasive and migrative mechanisms to spread malignancy.

Beyond this sort of axes, a pathway with major implication in nutrient sensing and cancer proliferation was revealed to be highly enriched as well. Pathway R-HSA-381426,

"The Regulation of Insulin-like Growth Factor transport and uptake by Insulin-like Growth Factor Binding Proteins". A group of genes i.e., *APOE*, *CYR61*, *FBN1*, *FN1*, *FSTL1*, *FSTL3*, *IGF1*, *IGFBP3*, *IGFBP4*, *IGFBP7*, *LAMC1*, *LGALS1*, *LTBP1*, *MXRA8*, *SCG2*, *SPARCL1*, *SPP1*, *TIMP1*, *TIMP2*, *VCAN*, included in the CRC survival markers whose overexpression correlates with bad prognosis, were identified to be active members of this biochemical pathway.

As described in previous pages, IGFs have a fundamental role in carcinogenesis since they trigger diverse pathways involved in cell proliferation. Decreasing IGF seems to be one of the key mechanism implicated in the anticarcinogenic benefits of caloric restriction. In the bloodstream and in local tissues, most IGFs molecules are bound by one of the six members of the IGF-binding protein (IGFBP) family. Most IGFs are found in complexes with IGFBPs, which seems to increase time in the body, modulate accessibility of IGFs to receptors, decrease insulin like effects of IGFs, and perform signaling processes independently of IGFs. Mainly, IGFs become active when are released from the IGF:IGFBP complexes by proteolysis mechanisms. However, IGFs may also show activity when still bound to some IGFBPs (Allard and Duan, 2018) (Guler et al., 1989) (Jones and Clemmons, 1995) (Hwa et al., 1999).

The three genes proposed as survival prognosis signature (*LCA5*, *NPR3* and *SLC2A3*) due to the strong correlation between upregulation and poor survival of CRC patients in early stages (HR: 3.60; CI: 3.43-3.77; p=0.00187]), have different level of implication in nutrient sensing or cell metabolism.

Solute Carrier Family 2 Member 3 (*SLC2A3* or *GLUT3*) is a gene located in chromosome 12 that belongs to *SLCA2* or *GLUTs* family. There are currently 14 members of GLUTs in humans plus 4 pseudogenes in chromosomes 1,2, 5 and 8 (Mueckler and Thorens, 2013). The first class of genes (class I) are known as the classical glucose transporters and they including *GLUT 1–4* and *GLUT 14*(Adekola et al., 2012).

SLC2A3 is highly expressed in human bone marrow, placenta, gall, urinary bladder and brain (NCBI). CRC tumors with higher levels of expression of this gene correlates with shorter survival times of patients (HR 1.93 [95%CI:1.56-2.39] p=1.4E-09). *SLC2A3* codes for the GLUT3 protein, implicated in sugar transport across the cell membrane with high affinity for glucose but not fructose. It has also been reported binding with less affinity galactose, mannose, maltose, xylose and dehydroascorbic acid (Simpson et al., 2008) .

Traditionally, GLUT 3 has been recognized as a neuronal glucose transporter due to substrate specificity and high expression of *SLC2A3* in the brain, but further studies have made moving beyond that thinking since GLUT3 has been identified in a wide variety of cell types, particularly those with high requirements of glucose, including sperm, preimplantation embryos, circulating white blood cells and diverse tumoral cell lines (Simpson et al., 2008). This ubiquity of GLUT3 in human tissues does not appear in many experimental models such as monkeys, rats, or mice, where the pattern of expression of GLUT3 is profuse only in brain.

Despite glucose transport and the *GLUTs* family have been profoundly studied in cancer due to high glucose consumption exhibited by transformed cells, *GLUT3* is one of the less studied isoforms in CRC context (Watanabe et al., 2010) (Adekola et al., 2012) (Medina and Owen, 2002) (Simpson et al., 2008). In brain, glucose uptake is facilitated by GLUT3 that controls the transport of glucose into the neuron by high affinity and high capacity, and by the heavily studied GLUT1 responsible for glucose transportation across the blood-brain barrier. GLUT3 appears to be responsible for basal glucose transportation in humans together with GLUT1, mainly due to the ubiquitous distribution of GLUT3 in human tissues. Moreover, research in rodents suggest that, in contrast to GLUT1, glucose concentrations do not regulate expression of GLUT3 since levels of both mRNA and protein does not drop in presence of high concentrations of glucose. (Simmons, 2017).

Recent discoveries regarding GLUT3 regulation in CRC has identified this carrier as a Yes-Associated Protein 1 (YAP1) regulated gene involved in glucose metabolism, invasion and metastasis. YAP1 is a transcriptional regulator that controls organ size in diverse species acting as a downstream regulator in the Hippo pathway. GLUT3 activates YAP triggering glycolytic gene expression, including GLUT3 itself. In late stage CRC patients, this pathway deregulation can induce GLUT3 expression and increased glycolytic capacity. Moreover, GLUT3 and YAP silencing effectively inhibits CRC aggressiveness and metastasis (Kuo et al., 2019)

Caveolin 1 (CAV1) is another protein related to GLUT3 with implications in glucose metabolism. This scaffolding protein is the main component of the caveolae plasma membranes found in most cell types and is involved in multiple functions such as cholesterol transportation, membrane trafficking or signal transduction through the interaction with a wide variety of ligands (Liu et al., 2002). It has been reported to increase

aerobic glycolysis in CRC cells via activation of *SLC2A3* transcription. Reduction of CAV1 levels decreases glucose uptake, ATP level and lactate accumulation in the cell triggering autophagy through the AMPK-TP53/p53 pathway (Ha and Chi, 2012).

The implication of *SLC2A3* in Vitamin C transport across the membrane is another important aspect to consider in the nutrition-cancer scenario. Preliminary studies in the 1970s conducted by Nobel laureate Pauling Linus, described vitamin C on prolonging the survival of patients with terminal cancer (Cameron and Pauling, 1976) (Cameron and Pauling, 1978). The mechanistic understanding of the anticancer activity of Vitamin C is still unelucidated. The interaction between ascorbate radicals and transition metals has been proposed as a presumed molecular mechanism, since involves the formation of ROS which induce cancer cell apoptosis (Chen et al., 2005). More recent studies have shown that aerobic glycolysis greatly enhances vitamin C-induced toxicity in multiple cancer cell lines through a mechanism involving the hypoxia-inducible factor (HIF) pathway. HIF enhances vitamin C uptake by different transporters including the GLUTs. Resulting higher intracellular levels induce higher oxidation, ATP exhaustion, ROS level increment and cellular apoptosis (Tian et al., 2014).

SLC2A3 has been profoundly studied in the brain, where it seems not to be regulated by extracellular glucose availability but further studies in tissues with high demand for glucose, like tumors, seems to be particularly interesting in the nutritional field, for instance, testing different combinations of glucose restriction and vitamin C supplementation at the same time to explore competence for the carrier, intracellular availability, cytotoxicity and the molecular mechanism driving the implication of *SLC2A3* in cellular apoptosis.

Leber congenital amaurosis 5 (*LCA5*), the second gene of the proposed CRC prognostic signature has not been studied in cancer framework. Located in chromosome 6, this gene is mainly expressed in testis, thyroid and ovary. It encodes a protein that is thought to be involved in centrosomal or ciliary functions (Gupta et al., 2015). This finding drives to hypothesize implication of *LCA5* in processes of abnormal division of cancer cells during mitosis. Mutations in *LCA5* lead to retinal dystrophy and an eye disorder named LCA (Genetics Home Reference, 2019). Despite this gene has no evidenced involvement in nutrient sensing or metabolism, Palmer and coworkers have identified in a 4,176 cohort GWAS, a single nucleotide polymorphism (rs196701) in *LCA5* which seems to alter glucose

and insulin homeostasis and the risk of suffering type 2 diabetes (Palmer et al., 2015). CRC patients with higher level of expression of this gene present shorter survival times (HR 1.89 [95%CI:1.55-2.31] $p=3.25E-10$). Since its role in cancer is unknown, further research about this gene seems to be specially fascinating in CRC, so far.

Natriuretic Peptide Receptor 3 (NPR3) or Natriuretic Peptide Receptor C/Guanylate Cyclase C (Atrial natriuretic Peptide Receptor C) is the last gene of the signature. This gene encodes one of three natriuretic peptide receptors. Guanylin, uroguanylin and lymph guanylin are three natriuretic peptides (NP) discovered initially in the GI tract. They contribute to regulate electrolyte and water transport in both intestinal and adrenal epithelium by means of cyclic GMP (cGMP)-dependent mechanisms (Beltowski, 2001). Uroguanylin is believed to be the key intestinal NP, since its expression is strongly conditioned by the content of dietary salt (Potthast et al., 2001). NPR3 is in charge of clearing circulating and extracellular NP through endocytosis of the receptor to alter circulating levels of these peptides (Chang et al., 1989) (Wilkins et al., 1997).

Besides the natriuretic functionality, Guanylin peptides regulate intestinal epithelial cell growth. Cl^- secretion is known to be linked to the guanylyl cyclase-C signaling pathway and this pathway seems to be implicated in CRC proliferation (Laney Jr et al., 1992).

NPR3 has been identified as a marker of intestinal metaplasia, dysplasia, and adenocarcinoma of the GI duct (Carrithers et al., 1996) (Birbe et al., 2005). Camici reviewed the physiological aspect of NPs and describes activation of the second messenger cGMP by NPR3 to increase colon epithelial cell proliferation by triggering a signaling pathway with different ion channels, phosphodiesterases and kinases involved (Camici, 2008). However, mice lacking NPR3 in the multiple intestinal neoplasia mouse model essentially confirmed a decline in the number of polyps (and no change in polyp size), suggesting a compensatory mechanism of cell apoptosis associated to loss of NPR3 (Mann et al., 2005).

This link between NP-NPRs resulting in modulation of intracellular second messenger cGMP and CRC proliferation could be specially sensible to diet, particularly diet poor in some electrolytes enhancing this cascade such as Na^+ . Furthermore, given that the colon is highly proliferative, understanding how NPR3 regulates cancer cell division under

conditions where food is restricted could be particularly revealing in the precision nutrition and cancer framework.

As occurs with the previous two genes of the signature CRC patients with higher level of expression of *NPR3* present shorter survival times (HR 1.95 [95%CI:1.59-2.39] $p=1.56E-10$).

It is important to remark the ability of this three gene signature (*SLC2A3*, *LCA5* and *NPR3*) to identify the CRC subtype associated with worse survival, the CMS4 or mesenchymal like phenotype. CMS4 displays higher chromosomal instability as measured by SCNA counts, is enriched in signatures associated with the activation of transforming growth factor β (TGF β) signaling, angiogenesis, matrix remodeling pathways and pathways of the complement inflammatory system. CMS4 encompasses a gene expression profile compatible with stromal infiltration and higher admixture with non-cancer cells, as measured by the significant overexpression of proteins implicated in stromal invasion, mesenchymal activation, and complement pathways (Guinney et al., 2015).

Hypothesizing, the relationship about the signature and the molecular subtype could be led by *NPR3*. This gene has been reported as a biomarker of metastatic CRC in lymph nodes when patients on CRC stage II and no histologic sign of lymph node invasion develop recurrent disease, likely because of hidden micro-metastases (Cagir et al., 1999). Moreover, its implication in volume homeostasis is narrowly linked with the inflammatory response and CMS4 displays pathways of the inflammatory system significantly altered.

It has been described that the induction of *SLC2A3* facilitates metabolic adaptation to nutrient deprivation in brain tumor-initiating cells (Flavahan et al., 2013) and it is responsible for TGF β -induced EMT in non-small cell lung cancer (Masin et al., 2014), although the implication in CRC is still unelucidated. The capacity of *SLC2A3* to identify CMS4, could involve the previously mentioned Hippo cascade, by which Glut3 promotes invasiveness and stemness in YAP-dependent manner. Activation of YAP sequentially transactivates Glut3 which seems to enhance expression of a group of genes involved in aerobic glycolysis and metastatic phenotype (Kuo et al., 2019).

LCA5 has not been studied in cancer context and its ability to identify CMS4 is unknown. Conjecturing, the association of the SNP *rs196701* in *LCA5* with altered glucose and insulin homeostasis and the risk of suffering type 2 diabetes could suggest an alleged

metabolic link between this gene and the EMT-like phenotype presented by the CMS4, but this has to be explored.

Summarizing, the results presented in this work provide a set of genes that marks survival among CRC patients and an open list of 765 differentially expressed genes when tumor delocalizes that provide prognostic strength. By integrating data from different microarray experiments, a reliable large-scale model of genomic data (with more than 1200 samples) is available for biological questioning. The size brings robustness and contributes to overcome the limitations of relatively weak statistical power when results come from evaluating small datasets. The proposed list includes genes widely studied in CRC and previously annotated in biological databases such as *EPHB2* or *LAMP5*, which provides reliability to the method applied, but also genes far less known or without recognized implication in the disease such as *LCA5* or *CISD3*. This allows to hypothesize about novel nodes in cancer biology. Furthermore, the regression fitted considering the top 100 genes, paves the way for building other risk predictors or researching putative cancer-related networks, pathways or any other functional interactions by focusing in the genes with higher weight in the model. The involvement of these genes in nutrient sensing opens a question regarding their putative role as potential biomarkers of molecular nutrition strategies. Of course, this is only an open gate for further research in the field.

6.2. Identification of potential precision strategies in cancer focused on molecular nutrition.

6.2.1. Nutritional strategies based on the inclusion of bioactive compounds: Screening of bioactive compounds with potential beneficial effect in CRC.

The beneficial activity of EA is significantly affected by its low bioavailability. Gut microbiota has been acknowledged to metabolize EA yielding the derivatives molecules that play an active role in CRC inhibition. This work tries to identify the structures with higher anticancer activity among those metabolites. It has revealed strong differences within derivatives regarding their antiproliferative effects in CRC. Particularly one, the 4,4'-DIOMEA, has demonstrated to be the most effective compound of all tested (lower IC₅₀) inducing cell viability inhibition in a dose-dependent manner. This inhibitory effect of 4,4'-DiOMEA was around 13-fold higher than that exerted by the precursor EA and the other methylated specie tested, the 3,3'-DiOMEA (See the dose response curve displayed in table 5.5).

The structure-activity divergences among the compounds in the CRC cell lines tested may indicate that the hydroxyl group substitutions are key factors in the antiproliferative capacity of each molecule. EA, 4,4' DIOMEA and 3,3' DIOMEA present similar chemical structure but the two methoxy groups present in the last two molecules, reduce polarity, suggesting easier passage across the cell membrane in comparison to EA. Moreover, MTT results reflect better performance when the methoxy group is present in 4,4'-position suggesting further implication of the methoxy group location in the molecular interaction with other components in the cell.

Attention should also be drawn to the fact that different hydroxyl substitutions of Urolithin-A and Urolithin-B resulted in a considerably dissimilar inhibition of cell proliferation. This suggest that the additional hydroxyl group at 8-position in Urolithin-A is essential for this biological activity of the molecule.

Nor the molecular size, neither the presence of a lactone ring, seems to have implication in the antiproliferative activity of this group of compounds. Urolithins are smaller dibenzopyran-6-one derivatives formed by the opening and decarboxylation of

one of the lactone rings of EA and the sequential removal of different hydroxyl groups (Ramirez de Molina et al., 2015). 4,4'-DiOMEA was more active than Urolithin-A, and this was more active than both EA and its 3,3'-DiOMEA derivative.

Microarray analysis revealed that the downregulation of Wnt16 signaling might be involved in the antiproliferative effect of 4,4'-DiOMEA. This result is consistent with previous knowledge reporting modulation of the Wnt pathway by ETs, EA and Urolithins in cancer cells (Sadik and Shaker, 2013) (Sharma et al., 2010b) (Espín et al., 2013b). The main advantage of 4,4'-DiOMEA in comparison with other phenolics tested here is that it seems to be much more effective inhibiting the pathway (13fold EA).

The WNT gene family is comprised of fundamentally associated genes that encode secreted signaling proteins (more than 19 Wnt isoforms identified so far). These ligands are implicated in several canonical and non-canonical Wnt signaling cascades and numerous crosslinks which are tightly regulated by multiple mechanisms including post-translational modification of Wnts, antagonist binding (to Wnts or their receptors), and regulation of the availability of Wnt receptors. This sort of networks lead to multiple cell phenotypes (Malinauskas and Jones, 2014).

Similar to β -catenin in the canonical Wnt pathway, the calcium-responsive transcription factor Nuclear Factor of Activated T-cells (NF-AT) has been suggested as a potential target in noncanonical Wnt cascades. (Murphy and Hughes, 2002), (Saneyoshi et al., 2002). These pathways, called the Wnt/calcium pathways or the Wnt/planar cell polarity pathway to distinguish from the canonical Wnt/ β -catenin pathway (Kühl et al., 2000) are also activated by Wnt ligands, leading to the transcription of genes involved in cytoskeleton reconfiguration, growth and proliferation (Zhan et al., 2017) (Jessen, 2009) (Staal et al., 2008). Wnt16 ligand can signal via both canonical and non-canonical cascades (Gori et al., 2015).

Figure 6.2 displays the main nodes implicated in the canonical Wnt/ β -catenin pathway (Veeman et al., 2003) and figure 6.3 capture non-canonical Wnt signaling showing the extraordinary complexity of this network (Zhan et al., 2017).

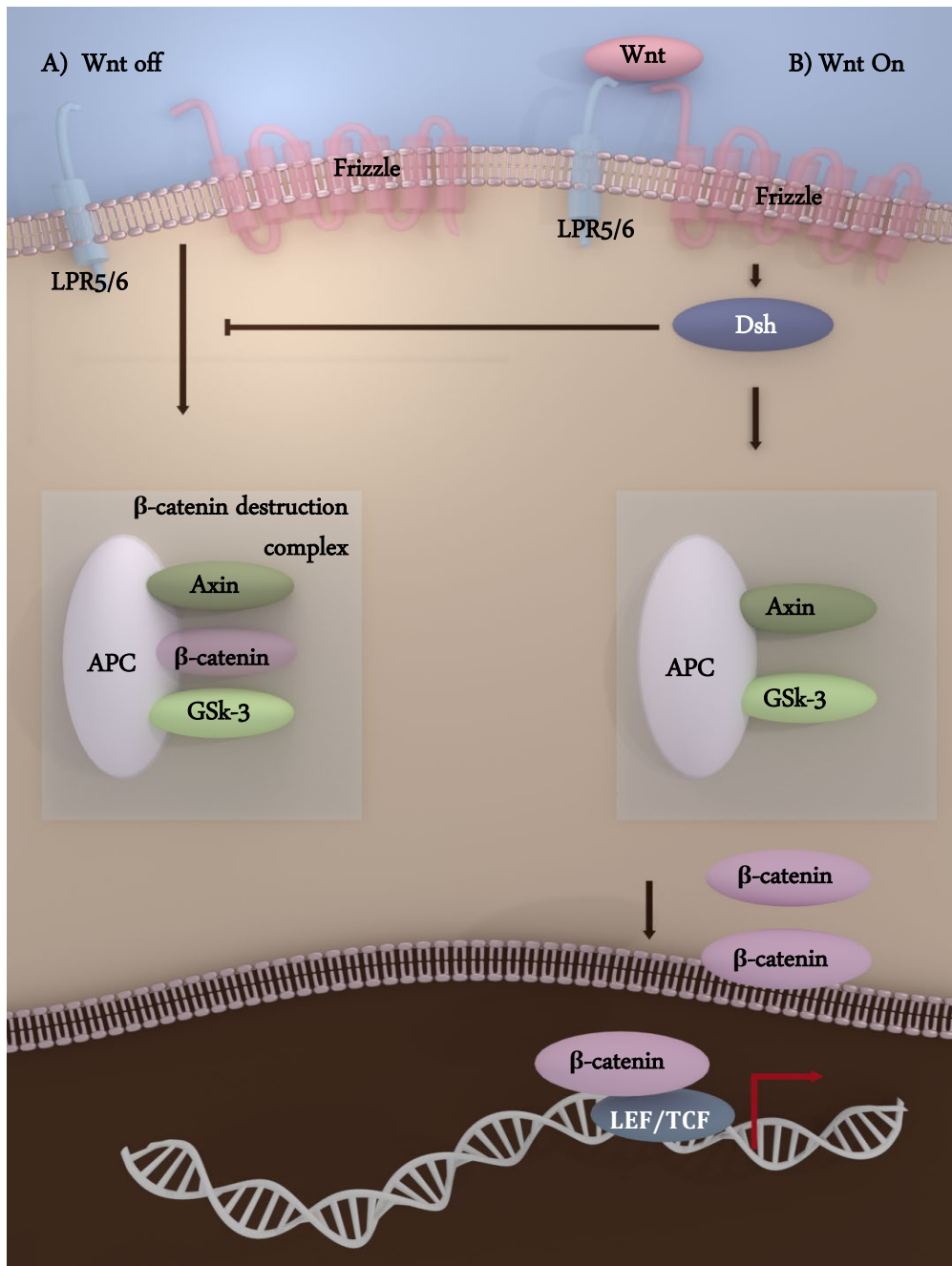


Figure 6.2 Canonical Wnt signaling in vertebrates. A) Non activated and B) activated (Adapted from Veeman et al., 2003) Wnt ligands binds to Frizzled and LRP5/6 coreceptors activating Dishevelled (Dsh). Dsh inhibits β -catenin destruction complex comprising APC, Axin, and GSK-3. If complex is not destroyed by the ubiquitin-proteasome pathway, free β -catenin entries into the nucleus where it recruits transactivators to HMG box DNA binding proteins of the LEF/TCF family.

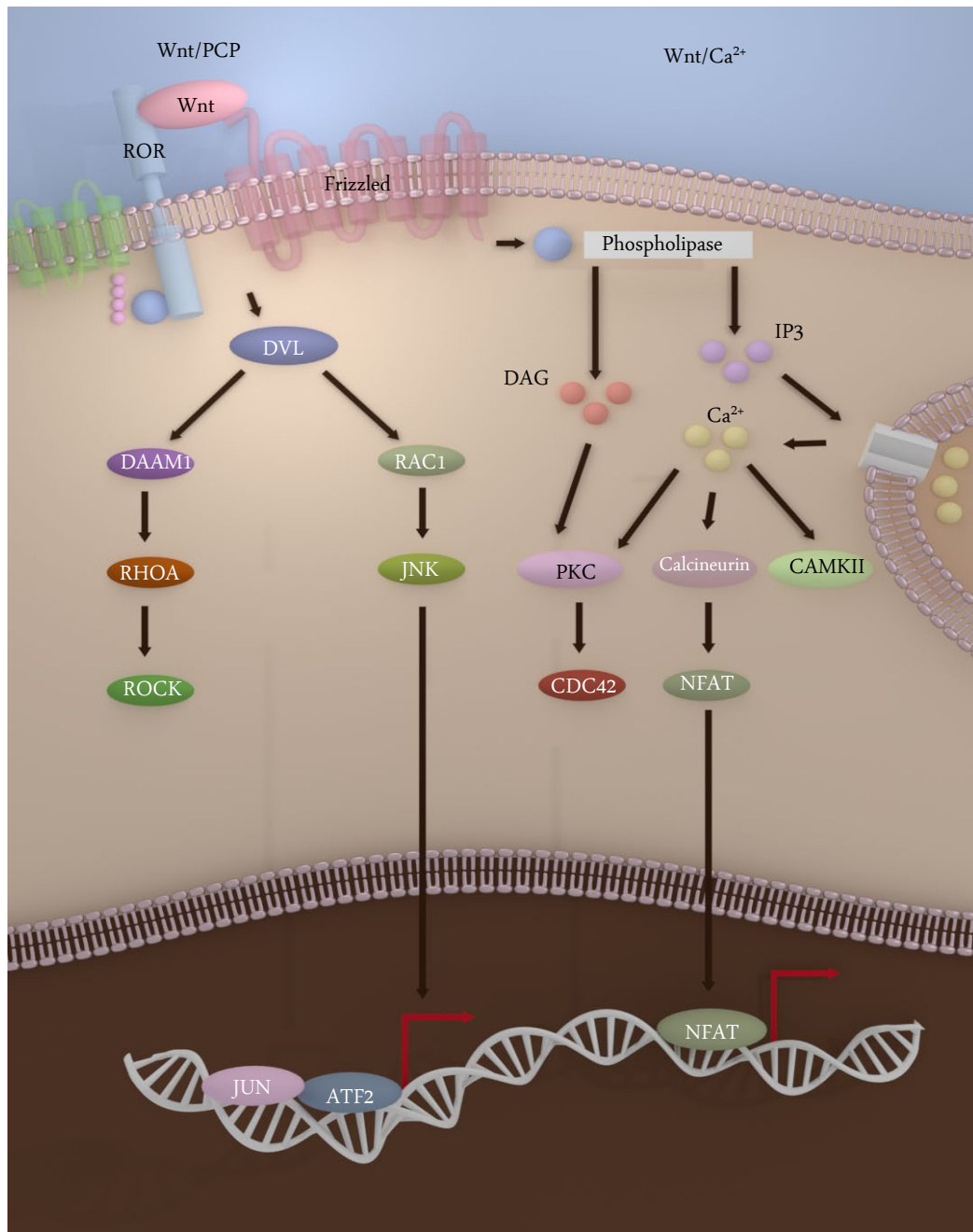


Figure 6.3. Non-Canonical Wnt signaling in mammals (Adapted from Zhan et al., 2017.)
 Non-canonical Wnt signaling or β -catenin-independent Wnt signal transduction. During Wnt/PCP signaling, Wnt ligands bind to the ROR-Frizzled receptor complex. Then Dvl is recruited and activated. Dvl binds to Rho by de-inhibition of the cytoplasmic protein DAAM1 (Dvl associated activator of morphogenesis 1). Rac1 and Rho together trigger ROCK (Rho kinase) and JNK producing diverse transcriptional responses, for example via ATF2 (activating transcription factor 2). Wnt/Ca²⁺ signaling start by G-protein activation of phospholipase C resulting in calcium fluxes to the cytoplasm which activates the phosphatase, calcineurin. Calcineurin induces de-phosphorylation of NFAT, subsequently translocation to the nucleus and final transcriptional regulation of NFAT dependent genes.

The member of the WNT family *Wnt16* comprises two transcript variants which seem to be the final products of discrete promoters and not to be splice variants from a single one (Correa-Rodríguez et al., 2016). They are differentially expressed in normal tissues. Variant B is expressed only in the pancreas, whereas variant A is expressed more ubiquitously, mainly in the spleen, brain, kidney, heart placenta, and slightly in the digestive system. Many studies have reported the role of *Wnt16* gene in bone development and disease (Zheng et al., 2016) (Alam et al., 2015). *Wnt16* stimulates tumor growth and promotes resistance to chemotherapy in different cancer types (Johnson et al., 2013)

The results of this thesis, particularly the TOP/FOP transfection assay and the RT-qPCR assay, revealed no decrement of β -catenin levels, a read-out of the canonical Wnt signaling pathway, after treating different CRC cell lines with 4,4'DIOMEA.

This unchanged level of β -catenin, despite the presence of lower levels of *Wnt16*, may suggest another interactor implicated in the inhibition of cell proliferation. It has been reported that overexpression of non-canonical Wnt signaling can enhance or antagonize with the canonical pathway (Veeman et al., 2003). Given that many WNT ligands can signal through both axis depending on the cellular status (nature of receptors/co-receptors involved, presence of co-activators, antagonists, etc.) which induce distinct phenotypes, results showing unaltered levels of β -catenin in the treated CRC cells suggest that 4,4'DiOMEA could activate a non-canonical Wnt pathway through *Wnt16*. Probably measuring levels of NFAT phosphorylation could contribute to clarify this hypothesis, or at least suggest a hint of an eventual crosslinking between the canonical and non-canonical signaling.

There was no clear conclusion regarding the inhibition of epithelium-mesenchymal-transition in different CRC cell lines under treatment with 4,4' DiOMEA. The EMT process is associated with the canonical pathway of Wnt and involves a more aggressive cell phenotype (Moustakas and Heldin, 2007) (Huber et al., 2005). RT-qPCR assays of the expression of 8 EMT marker genes were unable to reveal significant alteration in EMT activity but confirmed previous TOP/FOP results; β -catenin, an epithelial marker, remained unaltered in treated cells. Neither motile behavior tested by wound healing assay, showed significant changes between treated and non-treated cells.

Wnt16 is deeply involved in chemotherapy resistance. High expression of this gene in the tumor microenvironment diminishes the cytotoxic effects of chemotherapy. It has been proposed as a mechanism by which drug resistance augments after consecutive cycles of chemotherapy (Sun et al., 2012). 4,4'-DiOMEA showed an IC_{50} of larger magnitude in epithelial cells than the one required in both SW620 and chemo-resistant SW620 cell lines. This suggests the presence of a therapeutic window, at least when it comes to epithelial preservation. Taking these two skills together, 4,4'-DiOMEA could be particularly effective as a coadjuvant agent since it could overcome resistance by increasing drug cytotoxicity whereas lower doses of chemotherapy should be required, protecting normal epithelium from damaging.

Another interesting aspect of this work encompasses oxidation. FRAP and DHPP assays display poor antioxidant capacity of 4,4'-DiOMEA. Moreover, the inhibition of mitochondrial activity monitored by the Seahorse Extra flux analyzer in stressed settings after 4,4'-DiOMEA treatment could be caused by multiple causes, maybe oxidative-mediated pathways. Structurally, 4,4'-DiOMEA does not seem to be antioxidant, neither oxidant, but its modulation of mitochondrial respiration could suggest a hint towards that line of investigation. It could be interesting analyzing ROS production after treatment as a putative explanation linking inhibition in proliferation to inhibition in mitochondrial activity. ROS can be indicative of pro or anticarcinogen activity. It has been reported that increasing ROS promotes EMT and cancer cell aggressiveness (Wu, 2006). On the other hand, increasing oxidative phosphorylation in mitochondria has been widely hypothesized as one of the targets for cancer therapeutics, since it has been strongly associated to ROS accumulation and further apoptosis (Marchetti et al., 2015)(Omar et al., 2010) (Ferreira, 2010) (Samudio et al., 2009). In this line of investigation, molecules such as 3-bromopyruvate, lonidamine or the dichloroacetate (DCA), have shown anticancer effectiveness affecting cancer cells' metabolism and mitochondrial deregulation (Pelicano et al., 2006). (Michelakis et al., 2008) (Johnstone et al., 2013) (Sutendra and Michelakis, 2013) (Szczyka et al., 2017) (Cheng et al., 2019).

Although further studies are needed for better understanding of the molecular characteristics responsible for the anticancer activity of 4,4'-DiOMEA in different CRC cell lines, our results seem to reveal 4,4'-DiOMEA as a promising complementary agent in colorectal cancer therapy.

6.2.2. Nutritional strategies based on the inhibition of tumor nutrient requirements: Intermittent Fasting as a potential precision nutrition strategy in BC

To fulfill the last objective and give response to the hypothesis of whether the differences in diet composition during fasting inhibit processes of tumor proliferation and metastasis, a Bal/c murine model was selected, in where transplantable mammary tumor cells, 4T1, were injected.

The adequacy of this TPN breast cancer model for analyzing metastasis has been widely proved due to the tumorigenic and invasive characteristics of the tumor that, unlike other tumor models, can spontaneously and rapidly reach distant organs such as liver, lung, brain, and bone which permits to start detecting the tumor within less than 7 days from injection and gather metastatic data in less than 30 days. The 4T1 mammary carcinoma cells were originally isolated from a single spontaneously arising mammary tumor of a BALB/c mouse (Dexter et al., 1978) (Aslakson and Miller, 1992).

The pattern of metastasis of 4T1 and the anatomical location after injection is very similar to that of human mammary cancer (Pulaski and Ostrand-Rosenberg, 1998). Moreover, this murine model has been extensively used in caloric restriction experiments (Brandhorst et al., 2013b) (Morgan E. Levine et al., 2014) (Suzuki et al., 2012) (Zhuang et al., 2014).

This Thesis provides evidence that intermittent fasting significantly decreases breast tumor size and weight in this model, which is consistent with similar studies and fully substantiated by literature (De Lorenzo et al., 2011) (Lee et al., 2012b) (Di Biase et al., 2016) . However, the difference in diet composition (standard diet [SD] versus a low in sugar, rich in vegetables and unsaturated fats and lack of animal protein [FMD]), did not achieved significant differences regarding tumor size and tumor weight between the two groups of mice undergoing fasting.

Contrary to expectations, this study did not find a significant reduction in metastasis in the fasted animals. In fact, the number of lung metastasis counted in both fasted groups strongly increased (Avg. \approx 45%), compared to the number counted in the

animals fed *ad-libitum*. In this regard, diet composition neither achieved significant differences between FSD and FMD group.

The BC metastasis decrement associated to restriction in nutrients, has been reported in different studies in the last decades. Kari et al. evidenced that functional disruption of the IGF-1 receptor dropped BC metastasis in immune deficient nude mice by suppressing cellular adhesion and invasion (Kari et al., 1999) . De Lorenzo and coworkers designed a similar study to the one used in this Thesis to investigate the effects of a 40% CR on metastases, in female 8 week-old BALB/c mice, using the 4T1 BC cells (De Lorenzo et al., 2011). They exposed that CR alone seems to reduce the number and size of lung nodules in both spontaneous and experimental metastases.

A few years later Simone et al. reported similar results in female 8 week-old 4T1-BALB/c mice using a combination of 30% CR with ionizing radiation (Simone et al., 2016).

On the other hand, and besides breast cancer models, Ershler and coworkers previously proved that the number of pulmonary metastases increased in mice on 30% CR, while growth of primary B16 melanomas were reduced (Ershler et al., 1986).

The main difference between the above-mentioned studies and the one presented in this Thesis is remarkable: All those studies encompass less severe protocols in calories restricted in comparison with the 70% IF (4 and 3 days fasting) tested here.

Strong fasting reduces IGF-1 drastically. The 75% reduction in serum IGF-1 caused by a 2 to 5 day fast in mice and humans cannot be achieved by a more moderate CR, which does not reduce IGF-1 levels in humans unless the protein intake is also restricted (Clemmons and Underwood 1991; Fontana, Weiss et al. 2008; Lee, Safdie et al. 2010). Even when combined with protein restriction, chronic CR only causes a small reduction of IGF-I in humans (Fontana, Weiss et al. 2008).

One main evidenced difference between diverse degrees of caloric restrictions involves glucose levels in serum. In an outstanding Thesis about dietary strategies in cancer context, Brandhorst reports decreases in glucose levels in Female CD-1 mice, aged 12-15 weeks, under nutrient deprivation, some of them could be considered as fasting (40%, 60%, 80%, 90% and 100% reduction in calories [48 hr. intervention]). Interestingly, this work shows that the percentage of calories restricted positively correlates with glucose levels. Besides total fasting, that showed the higher reduction of glucose (70%), lower levels of blood glucose were achieved in mild restriction (40% restriction) following

a positive trend to a maximum level of glucose when 90% calories were restricted. This results could be indicative of higher levels of catabolism and tissue destruction concurrent with higher levels of nutrient restriction. Levels of IGF-1 did not show significant differences among different degrees of restriction. (Brandhorst, 2013).

The results reported by Brandhorst could give us a hint about the unexpected outcome regarding metastasis in comparison with other studies. The above mentioned studies (reporting decrement of metastasis associated to CR), were performed under mild caloric restriction which seems to encompass lower glucose levels and that could be explained by lower catabolism, since more nutrients are supplied. In contrast, a more extreme restriction like the 70% IF of the present study produce higher levels of glucose, which could be indicative of higher tissue catabolism. This higher catabolism would explain, at least in part, the CR-associated tumor shrinkage and could be responsible of promoting a migrative phenotype as a survival mechanism of cancer cell to find nutrients beyond the restrictive environment of the tumor. More precisely, a question arises: Does an extreme nutrient-limitation, resulting in tumor reduction concurrent with increment in metastasis, induce a proliferative-to-invasive phenotype shift?".

The malignancy of a tumor is measured not by its size, but by its ability to invade and metastasize. Understanding what makes a tumor cell metastatic is a major concern in cancer research (Jang and Hill, 1997).

The mechanism by which exposure to microenvironmental stress, such as lack of nutrients, affects the metastatic ability of cancer cells is not known. In an extraordinary work García-Jiménez and Goding approach the link between cell starvation and metastasis (García-Jiménez and Goding, 2019).

Invasion could be proposed as a conserved strategy in response to nutrient deprivation. It comprises the process by which cells from the primary tumor occupy surrounding tissue and then enter blood or lymphatic vasculature, for further colonization and proliferation in new locations (Coghlin and Murray, 2010; Klein, 2009; Lambert et al., 2017). Motility confers an evolutive advantage to look for nutrients in those environments where are limited rather than waiting inactively for them to arrive. Many unicellular organisms use motility to restore supply-demand balance under nutrient limitations (Carey et al., 2018).

Suggesting similar behavior seems to be too simple when it comes to mammalian cells that respond more complexly and coordinately to nutritional stimuli, but cancer profoundly deregulates proliferative signaling which increase nutrients demand (García-Jiménez and Goding, 2019). The exacerbated aerobic glycolysis is also a blend associated to resources expenditure in cancer framework. It is not efficient compared to oxPhos in terms of ATP production, so more sugar is required to obtain same amount of energy. The glycolysis-concomitant increment in gluconeogenesis, the augmented energy expenditure due to cancer-associated inflammation, the deregulation of immune response, even the activation of futile cycles to produce heat in white-adipose-tissue browning (a common trait of cachexia), are good examples as contributors to this status of high-demand. On the other side of this model, nutrient supply governed by a delayed chaotic angiogenesis may not be sufficient to cover source requisitions by the tumor(Nagy et al., 2009). For instance, it has been reported that poor blood flow in the newly built capillaries leads to lower amino acids and glucose levels in the tumor area. An abundant anabolic amino acid in blood such as glutamine, can display lower levels in the tumor microenvironment (Pan et al., 2016). The nitric oxide precursor amino acid, arginine, can also be depleted due to the need of increasing blood flow in the new vasculature (Fukumura and Jain, 1998). Decrement in the amount of some immune-response-associated essential amino acids, is also a trait linked to some types of cancer (Sullivan et al., 2018) (Timosenko et al., 2016) (Platten et al., 2012). This supply-demand setting proposes a cellular competition for resources and a subsequent adaptation to satisfy imbalance. The sequence EMT, invasion, migration and metastasis might be one suitable nutrient-based adaptative strategy of cancer cell to counterbalance resources deficit.

García-Jiménez and Goding strongly suggest starvation in the tumor micro-environment as drivers of cancer metastasis (García-Jiménez and Goding, 2019). Under energy-limiting conditions a key mechanism to decrease nutrient demand encompasses protein-synthesis inhibition. mTORC1 regulates protein synthesis. By phosphorylating S6Ks and eukaryotic translation initiation factor 4E (eIF4E)-binding protein (4E-BP1), mTORC1 can promotes protein translation. Nutrient limitation activates AMPK which reduce translation by restricting mTORC1 complex (Ng et al., 2012) (Sancak et al., 2008) (Saxton and Sabatini, 2017). Protein translation is also modulated by regulation of the eukaryotic translation initiation factor 2 (eIF2). The phosphorylation of Ser51 located in

the smallest α subunit of eIF2 α by GCN2 reduce protein translation in response to stress such as imbalance in nutrient supply-demand (Muaddi et al., 2010).

Besides this mechanism to inhibit protein synthesis by eIF2 α phosphorylation, increasing evidence suggests that invasion is linked eIF2 α phosphorylation. Activation of the eIF2 α kinase (PERK) is associated to EMT-phenotype and triggers EMT and invasion in BC (Nagelkerke et al., 2013) (Feng et al., 2014), pancreatic cancer (Dekervel et al., 2017) and melanoma (Falletta et al., 2017). Increased p-eIF2 α is also known to drive invasion in chronic leukemia (Podszywalow-Bartnicka et al., 2016). Starvation promotes a translation reprogramming through phosphorylation of eIF2 α (reversible by the action of phosphatases such as GADD34) that leads to a proliferative-to-invasive phenotypic transition of cancer cells. However, the mechanism by which changes in the translation of specific mRNAs towards migration over proliferation needs to be unraveled (García-Jiménez and Goding, 2019) . Figure 6.4 displays a representation of the control of the translation reprogramming by eIF2 α phosphorylation, described by García-Jiménez and Goding.

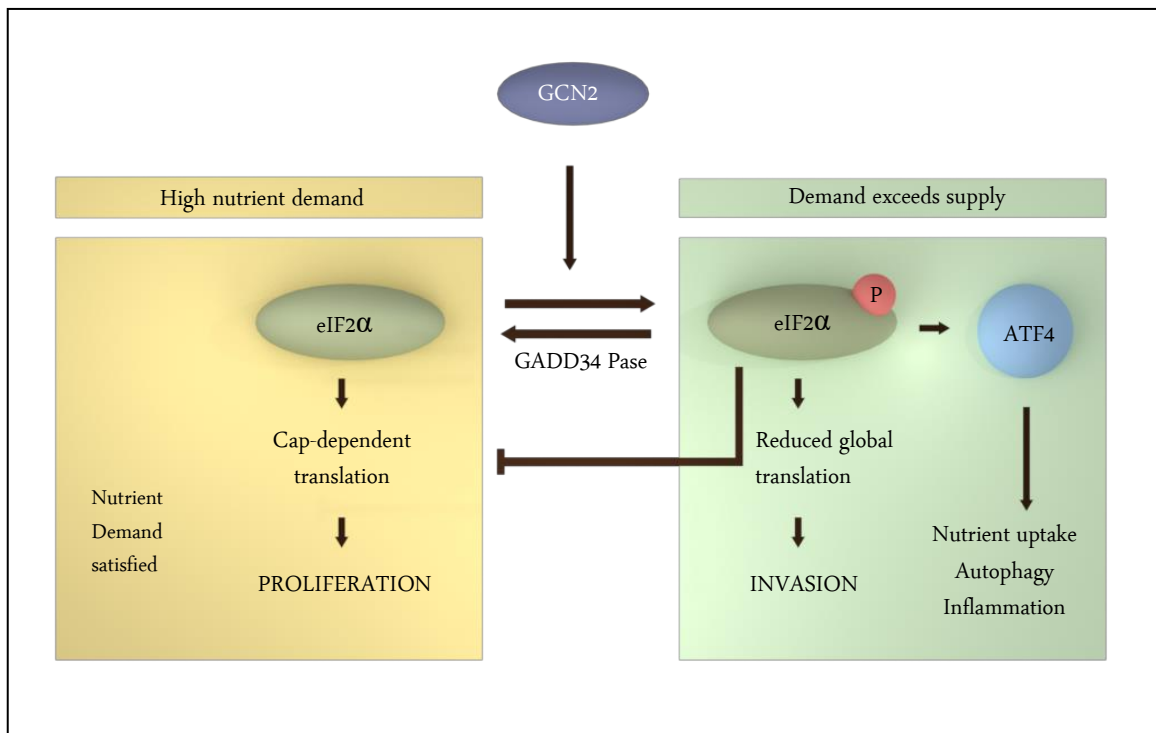


Figure 6.4. Control of Translation Reprogramming by eIF2 α Phosphorylation. (Adapted from García-Jiménez and Goding, 2019). eIF-2-alpha kinase GCN2 senses nutrient limitation and phosphorylates translation initiation factor eIF2 α . GADD34 reverses phosphorylation. To decrease nutrient demand, p-eIF2 α inhibits global translation. To increase nutrient supply, p-eIF2 α increases translation of specific mRNAs including transcription factor for nutrient uptake and autophagy. P-eIF2 α also drives invasion, promoting cells to leave nutrient-poor settings and searching for new environments to restore nutrient supply.

The hypothesis of whether the extreme lack of nutrients triggered this transition towards invasiveness, through phosphorylation of eIF2 α (which could justify the metastasis increment), and at the cost of inhibiting cell proliferation (which could explain the tumor reduction), appears to be a reasonable option which deserves to be explored.

Another approach to this issue focuses in the specific tissue where metastasis occur, the lungs, and addresses the increment from a more clinical perspective. Is there any alteration associated to lung tissue and nutrient deprivation that could molecularly promote metastasis?

In an extensive paper, Wilson et al. widely approach the effect of diet on lung-associated diseases. They summarized the impact of nutrition on the integrity of normal lung structure approaching mechanism of lung injury and repair, surfactant alterations and the pulmonary defense system, and suggest a potential association between starvation and damage in the lung (Wilson et al., 1985).

Further biochemical and morphological evidence of changes in the structure of the lung have been reported, particularly in collagen and elastin, when rodents were submitted to severe calorie-protein restriction (Riley and Thakker-Varia, 1995). Remarkably, the results in animal models agree with injuries in pulmonary tissue reported in young patients with anorexia nervosa (Overby and Litt, 1988) (Coxson et al., 2004).

The mechanism explaining this association seems to relay in different causes. The weakening of pulmonary defense system is one of them.

Elastase is a serine proteinase secreted by neutrophils and macrophages during inflammation, it destroys bacteria and host tissue. One mechanism to counteract this proteinase convey a group of anti-proteinases, the SERPINA superfamily. One member of this superfamily, α 1-antitrypsin (AAT) or SERPINA1 coats lungs protecting them from elastase. This enzyme maintains lung integrity. Congenital AAT deficiency typically leads to severe emphysema in humans. In its absence, elastase is free to break down elastin, which contributes to the elasticity of the lungs, resulting in respiratory complications such as emphysema, or chronic obstructive pulmonary disease (COPD) (Law et al., 2006).

It has been reported that caloric restriction decrease levels of AAT in mice (Wilson et al., 1985). It is not clear whether this AAT reduction by nutrient deficiency is enough to damage tissue. In this regards an oxidative action has been proposed as the mechanism driving inefficiency of AAT. When the methionine residue of the elastase binding site of AAT is oxidized, this anti-proteinase become inactive to block activity of elastase (Johnson and Travis, 1979). This help to explain the high incidence of lung damage in smokers.

In the experiment performed in this Thesis, severe fasting cycles could decrease AAT leaving lung tissue unprotected for the elastase to act leading to lung injury and fostering metastasis dissemination. Since the half-life of mature elastin in rodents is approximately 6 months (Dubick et al., 1981), time of recovery between fasting cycles (9 days feeding ad-libitum) would be insufficient for tissue repairing and an accumulative effect should be produced (Figure 6.5).

The antioxidant hypothesis would not explain the increment in the metastatic burden in fasted groups since one of the diets (FMD) includes an important load of antioxidants from vegetables and no difference in metastasis were found compared to the standard diet (FSD).

Notwithstanding, the results of this work need to be contrasted but the evidence of whether the metastasis increased under fasting condition by lack of protection against own immune system in the lungs, could be an attractive explanation to this unexpected result.

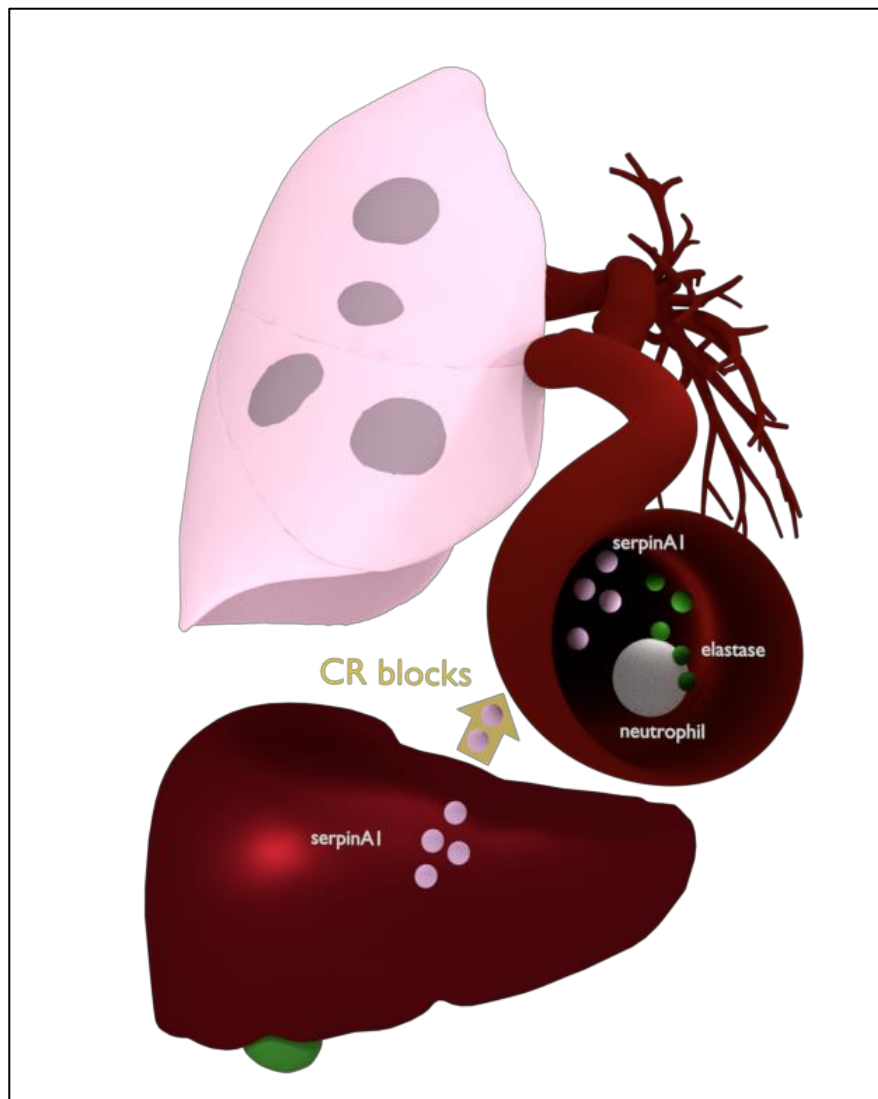


Figure 6.5. Cartoon representing the hypothesis of CR-mediated increment in BC cancer metastasis in the lung due to lack of protection against own immune system. One member of SERPIN superfamily produced in the liver, α 1-antitrypsin (AAT) or SERPINA1 coats lungs protecting them from enzymes secreted by inflammatory cells such as neutrophil elastase. It has been reported that caloric restriction decreases levels of AAT in mice (Wilson et al., 1985) Reduction of AAT could leave lung tissue unprotected for the elastase to act leading to lung injury and fostering metastasis dissemination.

6.3. Comparative analysis of different nutritional strategies throughout in vivo, in vitro and in silico results

As a final approach to the link between nutrition and cancer, this Thesis tackles a comparative analysis comprising main findings in the three different studies performed.

Levels of one gene product identified as prognostic biomarker of CRC in the in-silico analysis (*SLC2A3*) and one gene product identified in the in-vitro analysis to mediate in the antiproliferative effect of the phenolic acid 4,4'-DiOMEA, (Wnt16), were analyzed in the tumoral tissue of mice submitted to different nutritional strategies, in order to evaluate their modulation by caloric restriction and diet composition.

6.3.1. Modulation of *SLC2A3* in BC tumor by IF

It has been previously described in this work that high expression of *SLC2A3*/GLUT3 in CRC (through the phosphorylation of YAP1, an active member of the Hippo pathway), correlates with bad prognosis of CRC patients. *SLC2A3* overexpression increases the transcription of EMT genes and promotes cell migration and invasion in different in-vitro CRC models. Furthermore, knockout of GLUT3 using the CRISPR/Cas9 systems significantly reduced cell migration and invasion in CRC (Kuo et al., 2019b) and a recent study has shown that YAP promotes GLUT3 transcription in glioma (Cosset et al., 2017).

To verify whether the unexpected increment of metastasis observed in fasted animals could involve the Hippo pathway in BC, levels of *SLC2A3* were analyzed by Western blot assays in mice under fasting conditions. Results showed significant increment of this carrier only in animals fasted and fed FMD but not FSD. From this results it seems that diet composition modulates the receptor. A combination of antioxidant rich diet with restriction in nutrient significantly increase GLUT3 which would be a hint of metastasis increment through the Hippo pathway, but further results in animal under nutrient restriction on standard diet did not show GLUT3 increment. This result reveals that metastasis increment in the lung of fasted mice after IF is independent of GLUT3 overexpression. Diet seems to modulate levels of *SLC2A3* in the tumoral tissue but not fasting.

6.3.2. Modulation of Wnt16 in BC tumor by IF

Wnt pathway has been proposed to be one of the cell sensors for nutritional signaling, and therefore, seems to be “at the crossroads of nutritional regulation” (Sethi and Vidal-Puig, 2008). Lazaroba and Bordonaro suggest that the likely physiological behavior of Wnt signaling is dual regarding nutrient availability: Should be "on" in the presence of nutrients encompassing moderate levels of activation to maintain cell proliferation and should be “off” in the absence of nutrients, suppressing cell proliferation (Lazarova and Bordonaro, 2012b).

Diet composition appears to be implicated in Wnt modulation, particularly in cell lines where this route is frequently mutated such as CRC cells. For instance, high fiber intake which encompasses higher concentrations of short chain fatty acids such as butyrate, hyper-activates Wnt transcriptional activity in CRC cells with mutations in the Wnt pathway, but not in cells without such mutations (Lazarova et al., 2004) (Bordonaro et al., 2008). Changes of Wnt signaling are linearly correlated to the levels of CRC cell apoptosis. This finding suggests that it is not only the Wnt activation but also the intensity of the change what leads cell fate when it comes to cell proliferation. The presence of glucose also prone autocrinal activation of Wnt signaling (Anagnostou and Shepherd, 2008)

Lack of nutrients, on the other hand, may inhibit the Wnt signaling. There is evidence that Wnt signaling is silenced in colonic cells in the absence of nutrients and induced in the presence of metabolites (Bordonaro et al., 2007)

In contrast to CRC, Wnt pathway mutations are hardly detected in BC tumors. However, several sources of evidence reveal that loss of expression of negative pathway regulators seems to be under the Wnt pathway alterations in BC tumors. Although the implication of Wnt16 in BC is largely unknown, many Wnt ligands and receptors have been reported to be expressed in human BC cell lines and tumors (Howe and Brown, 2004). Furthermore, β -catenin is often detected stabilized and within the nucleus of BC cells and seems to be associated with poor prognosis (Ryo et al., 2001) (Lin et al., 2000). All these considerations suggest that WNT signaling may recurrently be de-regulated in BC.

In this Thesis, Wnt16 modulation by both caloric restriction and diet composition were assayed in the BC tumoral tissue in order to start exploring the eventual activation/inactivation of Wnt signaling in this type of cancer by this isoform. Levels of ligand were significantly lower ($p < 0.01$) in the two cohorts of mice undergoing caloric restriction compared to the control but no differences were achieved regarding diet composition. It seems that under strong nutrient restraint, the proliferative mechanism induced by Wnt16 remains inactive, preserving resources for other cellular tasks, maybe migration. The protective function of metabolites derived from a vegetable- and fiber-rich diet seems not to be so relevant concerning Wnt activation when a strong nutrient restriction is present. Probably, a metabolomic study from breast and tumoral tissue samples could give a better picture to clarify whether any anticarcinogenic metabolite such as butyrate for colon could reach the breast tumor. This could contribute to identify differential Wnt-associated activity. However, the beneficial modulation by diet seems not to be so evident when lack of nutrients exists.

7. Conclusions

Conclusions

- 7.1.** More than one tenth of the entire human genome shows significantly altered levels of expression once cancer spreads beyond the tumor. Integrative analysis of different independent datasets provides information of the most relevant genes commonly related to clinical outcome.
- 7.2.** Integrative analysis of 7 datasets including 1273 CRC cancer patients revealed two sets of genes that are candidate prognostic markers for CRC, showing either up-regulation or down-regulation correlated with poor prognosis. The top 10 up-regulated genes found as survival markers of poor prognosis in late stages III and IV (i.e. low survival) were: *DCBLD2*, *PTPN14*, *LAMP5*, *TM4SF1*, *NPR3*, *LEMD1*, *LCA5*, *CSGALNACT2*, *SLC2A3* and *GADD45B*.
- 7.3.** Regarding early stages (I-II), a 3-genes signature (*SLC2A3*, *NPR3* and *LCA5*) was identified as a strong biomarker of survival (HR: 3.60; CI: 3.43-3.77; p-val.:0.00187]). This gene signature is related to nutrient sensing and cell metabolism.
- 7.4.** The phenolic acid derivative 4,4'DiOMEA is able to inhibit cell viability of different CRC cell lines, including a 5 fluorouracil-resistant CRC cell line. It is more effective (13-fold) than its precursor ellagic acid.
- 7.5.** The antiproliferative effect of 4,4DiOMEA in CRC cancer cells seems to be mediated through downregulation of Wnt16, although it does not result in a significant reduction of the invasive properties of cancer cells.
- 7.6.** Caloric restriction by intermittent fasting decreases tumor size in vivo in BC-induced young female Balb/c mice. However, intermittent fasting increases lung metastasis in this model, irrespective the diet composition tested.

Conclusiones

- 7.1. Más de una décima parte del genoma humano muestra niveles de expresión significativamente alterados, una vez que el cáncer se disemina fuera del tumor. El análisis integrativo de datos independientes proporciona información de los genes más relevantes relacionados con desenlace clínico.
- 7.2. Por medio del análisis integrativo de los datos de 7 estudios independientes, incluyendo muestras tumorales de 1273 pacientes con cáncer colorrectal (CCR), se identificaron dos conjuntos de genes candidatos como marcadores de pronóstico en CCR. Dichos genes muestran asociación entre altos (o bajos) niveles de expresión y pronóstico desfavorable del paciente. Los 10 genes que muestran mejor asociación entre altos niveles de expresión y mal pronóstico (baja supervivencia) en estadios tardíos III y IV son: *DCBLD2*, *PTPN14*, *LAMP5*, *TM4SF1*, *NPR3*, *LEMD1*, *LCA5*, *CSGALNACT2*, *SLC2A3* y *GADD45B*
- 7.3. Con respecto a los estadios tempranos (I-II), se identifica una firma genética (*SLC2A3*, *NPR3* y *LCA5*) como claro biomarcador de supervivencia en CCR (HR: 3.60; IC: 3.43-3.77; p-val.:0.00187]). Esta huella genética está relacionada con la detección celular de nutrientes y el metabolismo celular.
- 7.4. El derivado del ácido fenólico 4,4'Di-O-Metil ácido elágico inhibe la viabilidad celular de diferentes líneas de CCR, incluida una línea resistente a 5 fluorouracilo. El 4,4'Di-O-Metil ácido elágico muestra una eficacia inhibitoria 13 veces mayor que la molécula precursora, el ácido elágico.
- 7.5. El efecto anti proliferativo en células de CCR demostrado por el 4,4'Di-O-Metil ácido elágico, parece estar mediado por la regulación negativa de *Wnt16*. Esta regulación negativa no resulta en una reducción significativa de las propiedades invasivas de las células cancerígenas.
- 7.6. La restricción calórica por medio del ayuno intermitente disminuye el tamaño del tumor in vivo en ratones Balb/c, hembras, jóvenes, con CM inducido. Sin embargo, el ayuno intermitente aumenta la metástasis pulmonar en este modelo, independientemente de la composición de la dieta probada.

8.Perspectives.

One of the main issue emerging in almost every field of science is the extraordinary amount of data that new technologies are daily providing. Public repositories are extraordinarily useful but many times the user get lost in that mare magnum of information. A correct approach to any biological question should start by reviewing the huge volume of information rather than going directly to generate new data. Bioinformatics and more specific integrative analysis can substantially help in this aspect. It can indicate the correct path to follow, or at least suggest which one not to follow, making research more straight forwarding, more efficient. The road towards identifying a gene involved in ocular dystrophy as Leber Congenital Amaurosis 5 (*LCA5*) as a CRC prognosis biomarker, would be probably much longer without the help of bioinformatic tools.

Of course, the result of this Thesis is only a first approach to the subject. Building a risk predictor including the 3-gene signature *SLC2A3*, *NPR3* and *LCA5* could be a reasonable pathway to follow. Firstly, requires identifying cofounding variables in survival models to discard eventual gene modulation by them. Human CRC gene expression microarrays or RNA-Seq datasets with phenotypical and histopathological information should be needed. Analyzing modulation of tissue-specific endogenous genes and normalizing levels of expression of this gene signature could help to rationalize the use of the predictor in the clinic. A further molecular validation of the DEG signature in several CRC cell lines of different stages would give consistency to this finding, for instance, by contrasting expression from tumoral SW480 vs metastatic SW620 CRC cell line samples.

Another interesting line of investigation could be opened by exploring bibliography regarding the top 100 genes with higher β factors shown in the multivariate survival analysis. This would contribute to identify those genes less studied in CRC and enquire about their implication in the disease. It is also meaningful to explore the transcriptome of those patients living remarkably longer, particularly, by analyzing levels of expression of those 765 genes proposed as prognosis biomarkers. This could give us a hint of the genetic behavior in these outliers and identify putative targets for patients with shorter survival or a more aggressive phenotype.

Regarding the inhibition of the proliferation shown by 4,4'-DiOMEA, the precise molecular mechanism of action has not been unraveled in this work, so further research is required. It seems to downregulate *Wnt16*, but β -catenin levels remain unchanged. Exploring non canonical Wnt signaling, for instance the Wnt/Calcium pathway, could help identifying further interactors involved in the Wnt mediated antiproliferative effect of the 4,4' DiOMEA. It is also important to investigate modulation of *Wnt16* in different CRC cell lines at protein level, by Western blot assay. It might be interesting to confirm the antiproliferative activity identified in the MTT assays by a more precise flow cytometer, identify eventual cell cycle arrest, analyze genes involved in apoptosis, explore the modulation of major oncogenes or tumor suppressor by different concentrations of this phenolic, analyze aggressiveness modulation by Trans well Migration Assay. Moreover, the dose-dependent modulation by 4,4'-DiOMEA of oncogenic miR96 and tumor suppressor miR203 achieved in the comparison of the Taqman Low Density Array (TLDA) should be validated by RT-qPCR analysis and could give a hint about putative epigenetic modulation by the phenolic.

Another interesting approach relies in the fact that 4,4' DiOMEA does not show antioxidant activity. There are no pro-oxidative enriched pathways found in the GSEA performed using only DEG genes after treating the cells with the phenolic. It might be quite revealing to perform a second GSEA using a less restrictive list of genes and another bioinformatic tool such as the Broad Institute Software GSEA or similar. This new analysis could reveal enrichment of others biochemical pathways involved in the antiproliferative effect of the 4,4' DiOMEA, maybe pro-oxidative, ROS producing or pro-apoptotic routes.

One important shortcoming of this work encompasses the fact that 4,4'-DiOMEA has shown to be a very difficult compound to handle with low solubility in culture media and propension to form aggregates. Thus, a correct vehiculation of the bioactive compound 4,4' DiOMEA is essential for its effectiveness against tumoral cells using, for instance, liposomes or micelles (Molina et al., 2013) (Martí et al., 2014). The importance of developing delivery system with new formulation leading to improve bioavailability and efficiency are aspects widely approached in biomedicine. In this regard, lipid-based delivery systems have been reported to be

excellent bioactive vehicles to increase phytochemical bioavailability. Fish oils from certain shark species as ratfish liver oil (RLO) possesses a high content in Alkylglycerols (AKG), which have shown anticarcinogenic and immunomodulatory effects (Molina et al., 2013) (Corzo-Martínez et al., 2016). They seem to foster stability during gastric digestion and improve the intestinal bio accessibility and bioavailability as well. Results of an intervention in humans recently published by our group using specific alkylglycerols (AKG) from RLO together with one anticarcinogenic extract of *Rosmarinus officinalis* (RE), display both higher bioavailability and bioaccessibility and a synergistic effect when is vehiculated with AKGs (Gómez de Cedrón et al., 2019). Testing whether the same synergy occurs with 4,4' DiOMEA could be a good approach to improve efficacy.

Another important limitation regarding the 4,4'DiOMEA is the extremely expensive price of this compound which justifies the exploration of new ways of synthesizing the molecule at a lower cost. In this sense, one interesting approach could be exploring the possibility of enzymatically produce 4,4' DiOMEA *in-vitro* from not expensive EA, using different enzymes to catalyze the reaction, such as methyl transferases or catechol-O-methyl transferases and, obviously evaluating quality of final products and the yield in the process.

The unexpected results achieved in murine models under IF regarding higher metastatic burden suggest being cautious when addressing precision nutrition strategies based on caloric restriction in BC patients, particularly in late stage IV. It is required to confirm results by repeating the entire experiment under the same feeding paradigm. Probably, a cohort of mice feed FMD ad-libitum should be included in the experiments since outcomes obtained are unable to discriminate diet-composition specific effects from fasting associated effects.

Examining levels of Serpina1 in BC tumoral tissue could clarify the hypothesis exposed about whether the increment in lung metastasis is linked to a fasting-associated lack of protection in lungs against own immune system. Testing levels of eIF2 α phosphorylation would pave the way to explain whether the extreme lack of nutrients triggers a transition from cell proliferation towards cell invasiveness supporting the phenotype shown of tumoral shrinkage and higher number of metastasis.

Cancer therapeutic has shown solid advances within last few years, mainly in early diagnosis. But still many cancer subtypes continue to be untreatable. This is mostly due to inter- and intra-tumor heterogeneity, both in primary lesions and distal metastasis. For this reason, it is important to make a comprehensive approach and from different perspectives, that allows to know the characteristics of each lesion and the status of each patient, in order to find the most appropriate treatment in each case. Nutrition displays a plethora of opportunities to improve integral treatment of cancer. Omics technologies play an important role in understanding the molecular mechanism underlying this heterogeneity.

The crosslinking of these considerations, among several others, might contribute to transform normal nutrition in patient-based precision nutrition, which could improve treatment efficacy or, at least, ameliorate patient's quality of life. It seems to be an unquestionable line of research. Of course, knowing its potential requires broad and deep research in the field.

9. Bibliography

- Aaldriks, A.A., van der Geest, L.G., Giltay, E.J., le Cessie, S., Portielje, J.E., Tanis, B.C., Nortier, J.W., Maartense, E., 2013. Frailty and malnutrition predictive of mortality risk in older patients with advanced colorectal cancer receiving chemotherapy. *J Geriatr Oncol* 4 (3): 218–226.
- Abdelrahim, M., Safe, S., Baker, C., Abudayyeh, A., 2006. RNAi and cancer: Implications and applications. *J. RNAi Gene Silenc. Int. J. RNA Gene Target. Res.* 2, 136.
- ACS, 2018. Colorectal Cancer Stages [WWW Document]. Am. Cancer Soc. URL <https://www.cancer.org/cancer/colon-rectal-cancer/detection-diagnosis-staging/staged.html> (accessed 2.28.19).
- ACS, 2015. Breast Cancer Risk Factors You Cannot Change | Genetic Risk Factors [WWW Document]. URL <https://www.cancer.org/cancer/breast-cancer/risk-and-prevention/breast-cancer-risk-factors-you-cannot-change.html> (accessed 3.4.19).
- Adams, L.S., Zhang, Y., Seeram, N.P., Heber, D., Chen, S., 2010. Pomegranate Ellagitannin-Derived Compounds Exhibit Anti-proliferative and Anti-aromatase Activity in Breast Cancer Cells In Vitro. *Cancer Prev. Res. Phila. Pa* 3, 108–113. <https://doi.org/10.1158/1940-6207.CAPR-08-0225>
- Adekola, K., Rosen, S.T., Shanmugam, M., 2012. Glucose transporters in cancer metabolism. *Curr. Opin. Oncol.* 24, 650–654. <https://doi.org/10.1097/CCO.0b013e328356da72>
- Aguirre-Gamboa, R., Gomez-Rueda, H., Martínez-Ledesma, E., Martínez-Torteya, A., Chacolla-Huaranga, R., Rodriguez-Barrientos, A., Tamez-Peña, J.G., Treviño, V., 2013. SurvExpress: An Online Biomarker Validation Tool and Database for Cancer Gene Expression Data Using Survival Analysis. *PLoS ONE* 8, e74250. <https://doi.org/10.1371/journal.pone.0074250>
- Aibar Santos, S., 2015. Bioinformática aplicada a datos genómicos para la caracterización de subtipos de cáncer: estudios integrativos en hemopatías malignas.
- Akar, U., Ozpolat, B., Mehta, K., Lopez-Berestein, G., Zhang, D., Ueno, N.T., Hortobagyi, G.N., Arun, B., 2010. Targeting p70S6K prevented lung metastasis in a breast cancer xenograft model. *Mol. Cancer Ther.* 9, 1180–1187.
- Akkoca, A.N., Yanık, S., Özdemir, Z.T., Cihan, F.G., Sayar, S., Cincin, T.G., Çam, A., Özer, C., 2014. TNM and Modified Dukes staging along with the demographic characteristics of patients with colorectal carcinoma. *Int. J. Clin. Exp. Med.* 7, 2828–2835.
- Alam, I., Alkhouli, M., Gerard-O’Riley, R.L., Wright, W.B., Acton, D., Gray, A.K., Patel, B., Reilly, A.M., Lim, K.-E., Robling, A.G., 2015. Osteoblast-specific overexpression of human WNT16 increases both cortical and trabecular bone mass and structure in mice. *Endocrinology* 157, 722–736.
- Allaire, J., 2012. RStudio: integrated development environment for R. Boston MA 770.
- Allard, J.B., Duan, C., 2018. IGF-binding proteins: why do they exist and why are there so many? *Front. Endocrinol.* 9, 117.
- Allen, B.G., Bhatia, S.K., Anderson, C.M., Eichenberger-Gilmore, J.M., Sibenaller, Z.A., Mapuskar, K.A., Schoenfeld, J.D., Buatti, J.M., Spitz, D.R., Fath, M.A., 2014. Ketogenic diets as an adjuvant cancer therapy: History and potential mechanism. *Redox Biol.* 2, 963–970. <https://doi.org/10.1016/j.redox.2014.08.002>
- Al-Maghrabi, J., Al-Sakkaf, K., Qureshi, I.A., Butt, N.S., Damnhory, L., Elshal, M., Al-Maghrabi, B., Aldahlawi, A., Ashoor, S., Brown, B., Dobson, P., Khabaz, M.N.,

2017. AMPK expression patterns are significantly associated with poor prognosis in breast cancer patients. *Ann. Diagn. Pathol.* 29, 62–67.
<https://doi.org/10.1016/j.anndiagpath.2017.05.012>
- Anagnostou, S.H., Shepherd, P.R., 2008. Glucose induces an autocrine activation of the Wnt/ β -catenin pathway in macrophage cell lines. *Biochem. J.* 416, 211–218.
- Anbazhagan, R., Osin, P.P., Bartkova, J., Nathan, B., Lane, E.B., Gusterson, B.A., 1998. The development of epithelial phenotypes in the human fetal and infant breast. *J. Pathol.* 184, 197–206. [https://doi.org/10.1002/\(SICI\)1096-9896\(199802\)184:2<197::AID-PATH992>3.0.CO;2-J](https://doi.org/10.1002/(SICI)1096-9896(199802)184:2<197::AID-PATH992>3.0.CO;2-J)
- Angelo, P.M., Jorge, N., 2007. Phenolic compounds in foods - a brief review. *Rev. Inst. Adolfo Lutz Impreso* 66, 01–09.
- Arapitsas, P., 2012. Hydrolyzable tannin analysis in food. *Food Chem.* 135, 1708–1717.
<https://doi.org/10.1016/j.foodchem.2012.05.096>
- Arriaga, M.E., Vajdic, C.M., Canfell, K., MacInnis, R.J., Banks, E., Byles, J.E., Magliano, D.J., Taylor, A.W., Mitchell, P., Giles, G.G., Shaw, J.E., Gill, T.K., Klaes, E., Velentzis, L.S., Cumming, R.G., Hirani, V., Laaksonen, M.A., 2019. The preventable burden of breast cancers for premenopausal and postmenopausal women in Australia: a pooled cohort study. *Int. J. Cancer.* <https://doi.org/10.1002/ijc.32231>
- Aslakson, C.J., Miller, F.R., 1992. Selective events in the metastatic process defined by analysis of the sequential dissemination of subpopulations of a mouse mammary tumor. *Cancer Res.* 52, 1399–1405.
- Avenell, A., 2006. Glutamine in critical care: current evidence from systematic reviews. *Proc. Nutr. Soc.* 65, 236–241. <https://doi.org/10.1079/PNS2006498>
- Bakkalbaşı, E., Menteş, Ö., Artik, N., 2008. Food Ellagitannins—Occurrence, Effects of Processing and Storage. *Crit. Rev. Food Sci. Nutr.* 49, 283–298.
<https://doi.org/10.1080/10408390802064404>
- Baljinnyam, E., De Lorenzo, M.S., Vatner, D.E., Vatner, S.F., Abarzúa, P., Rabson, A.B., 2011. Caloric restriction reduces growth of mammary tumors and metastases. *Carcinogenesis* 32, 1381–1387. <https://doi.org/10.1093/carcin/bgr107>
- Baracos, V.E., Martin, L., Korc, M., Guttridge, D.C., Fearon, K.C.H., 2018. Cancer-associated cachexia. *Nat. Rev. Dis. Primer* 4, 17105.
<https://doi.org/10.1038/nrdp.2017.105>
- Bastiaannet, E., Sampieri, K., Dekkers, O.M., de Craen, A.J.M., van Herk-Sukel, M.P.P., Lemmens, V., van den Broek, C.B.M., Coebergh, J.W., Herings, R.M.C., van de Velde, C.J.H., Fodde, R., Liefers, G.J., 2012. Use of Aspirin postdiagnosis improves survival for colon cancer patients. *Br. J. Cancer* 106, 1564–1570.
<https://doi.org/10.1038/bjc.2012.101>
- Bates, W.G., 1985. Body Weight Control Practice as a Cause of Infertility. *Clin. Obstet. Gynecol.* 28, 632.
- Batlle, E., Bacani, J., Begthel, H., Jonkeer, S., Gregorieff, A., van de Born, M., Malats, N., Sancho, E., Boon, E., Pawson, T., Gallinger, S., Pals, S., Clevers, H., 2005. EphB receptor activity suppresses colorectal cancer progression. *Nature* 435, 1126–1130. <https://doi.org/10.1038/nature03626>
- Beltowski, J., 2001. Guanylin and related peptides. *J. Physiol. Pharmacol.* 52.
- Birbe, R., Palazzo, J.P., Walters, R., Weinberg, D., Schulz, S., Waldman, S.A., 2005. Guanylyl cyclase C is a marker of intestinal metaplasia, dysplasia, and

- adenocarcinoma of the gastrointestinal tract. *Hum. Pathol.* 36, 170–179.
<https://doi.org/10.1016/j.humpath.2004.12.002>
- Blauwhoff-Buskermolen, S., Ruijgrok, C., Ostelo, R.W., de Vet, H.C., Verheul, H.M., de van der Schueren, M.A., Langius, J.A., 2016. The assessment of anorexia in patients with cancer: cut-off values for the FAACT–A/CS and the VAS for appetite. *Support. Care Cancer* 24, 661–666.
- Boland, C.R., Goel, A., 2010. Microsatellite Instability in Colorectal Cancer. *Gastroenterology* 138, 2073–2087.e3.
<https://doi.org/10.1053/j.gastro.2009.12.064>
- Bolstad, B., 2011. affyPLM: Model Based QC Assessment of Affymetrix GeneChips.
- Bolstad, B.M., Irizarry, R.A., Åstrand, M., Speed, T.P., 2003. A comparison of normalization methods for high density oligonucleotide array data based on variance and bias. *Bioinformatics* 19, 185–193.
<https://doi.org/10.1093/bioinformatics/19.2.185>
- Bordonaro, M., Lazarova, D.L., Sartorelli, A.C., 2008. Hyperinduction of Wnt activity: a new paradigm for the treatment of colorectal cancer? *Oncol. Res. Featur. Preclin. Clin. Cancer Ther.* 17, 1–9.
- Bordonaro, M., Lazarova, D.L., Sartorelli, A.C., 2007. The activation of beta-catenin by Wnt signaling mediates the effects of histone deacetylase inhibitors. *Exp. Cell Res.* 313, 1652–1666.
- Boyd, M.R., Paull, K.D., 1995. Some practical considerations and applications of the national cancer institute in vitro anticancer drug discovery screen. *Drug Dev. Res.* 34, 91–109. <https://doi.org/10.1002/ddr.430340203>
- Brandhorst, 2013. Thesis. Dietary- and fasting-based interventions as novel approaches to improve the efficacy of cancer treatment.
- Brandhorst, S., Choi, I.Y., Wei, M., Cheng, C.W., Sedrakyan, S., Navarrete, G., Dubeau, L., Yap, L.P., Park, R., Vinciguerra, M., Di Biase, S., Mirzaei, H., Mirisola, M.G., Childress, P., Ji, L., Groshen, S., Penna, F., Odetti, P., Perin, L., Conti, P.S., Ikeno, Y., Kennedy, B.K., Cohen, P., Morgan, T.E., Dorff, T.B., Longo, V.D., 2015a. A Periodic Diet that Mimics Fasting Promotes Multi-System Regeneration, Enhanced Cognitive Performance, and Healthspan. *Cell Metab.* 22, 86–99.
<https://doi.org/10.1016/j.cmet.2015.05.012>
- Brandhorst, S., Choi, I.Y., Wei, M., Cheng, C.W., Sedrakyan, S., Navarrete, G., Dubeau, L., Yap, L.P., Park, R., Vinciguerra, M., Di Biase, S., Mirzaei, H., Mirisola, M.G., Childress, P., Ji, L., Groshen, S., Penna, F., Odetti, P., Perin, L., Conti, P.S., Ikeno, Y., Kennedy, B.K., Cohen, P., Morgan, T.E., Dorff, T.B., Longo, V.D., 2015b. A Periodic Diet that Mimics Fasting Promotes Multi-System Regeneration, Enhanced Cognitive Performance, and Healthspan. *Cell Metab.* 22, 86–99.
<https://doi.org/10.1016/j.cmet.2015.05.012>
- Brandhorst, S., Harputlugil, E., Mitchell, J.R., Longo, V.D., 2017. Protective effects of short-term dietary restriction in surgical stress and chemotherapy. *Ageing Res. Rev.* 39, 68–77. <https://doi.org/10.1016/j.arr.2017.02.001>
- Brandhorst, S., Longo, V.D., 2016a. Fasting and Caloric Restriction in Cancer Prevention and Treatment. *Recent Results Cancer Res. Fortschritte Krebsforsch. Progres Dans Rech. Sur Cancer* 207, 241–266. https://doi.org/10.1007/978-3-319-42118-6_12

- Brandhorst, S., Longo, V.D., 2016b. Fasting and Caloric Restriction in Cancer Prevention and Treatment. *Recent Results Cancer Res. Fortschritte Krebsforsch. Progres Dans Rech. Sur Cancer* 207, 241–266. https://doi.org/10.1007/978-3-319-42118-6_12
- Brandhorst, S., Wei, M., Hwang, S., Morgan, T.E., Longo, V.D., 2013a. Short-term calorie and protein restriction provide partial protection from chemotoxicity but do not delay glioma progression. *Exp. Gerontol., Calorie Restriction and Fasting; Challenges and Future Directions for Research* 48, 1120–1128. <https://doi.org/10.1016/j.exger.2013.02.016>
- Brandhorst, S., Wei, M., Hwang, S., Morgan, T.E., Longo, V.D., 2013b. Short-term calorie and protein restriction provide partial protection from chemotoxicity but do not delay glioma progression. *Exp. Gerontol.* 48, 1120–1128. <https://doi.org/10.1016/j.exger.2013.02.016>
- Brennan, K.R., Brown, A.M., 2004. Wnt proteins in mammary development and cancer. *J. Mammary Gland Biol. Neoplasia* 9, 119–131.
- Brinton, L.A., Hoover, R., Fraumeni Jr, J.F., 1983. Reproductive factors in the aetiology of breast cancer. *Br. J. Cancer* 47, 757–762. <https://doi.org/10.1038/bjc.1983.128>
- Buono, R., Longo, V.D., 2018. Starvation, Stress Resistance, and Cancer. *Trends Endocrinol. Metab. TEM* 29, 271–280. <https://doi.org/10.1016/j.tem.2018.01.008>
- Cagir, B., Gelmann, A., Park, J., Fava, T., Tankelevitch, A., Bittner, E.W., Weaver, E.J., Palazzo, J.P., Weinberg, D., Fry, R.D., 1999. Guanylyl cyclase C messenger RNA is a biomarker for recurrent stage II colorectal cancer. *Ann Intern Med* 131, 805–812.
- Calon, A., Lonardo, E., Berenguer-Llargo, A., Espinet, E., Hernando-Momblona, X., Iglesias, M., Sevillano, M., Palomo-Ponce, S., Tauriello, D.V.F., Byrom, D., Cortina, C., Morral, C., Barceló, C., Tosi, S., Riera, A., Attolini, C.S.-O., Rossell, D., Sancho, E., Batlle, E., 2015. Stromal gene expression defines poor-prognosis subtypes in colorectal cancer. *Nat. Genet.* 47, 320–329. <https://doi.org/10.1038/ng.3225>
- Cameron, E., Pauling, L., 1978. Supplemental ascorbate in the supportive treatment of cancer: reevaluation of prolongation of survival times in terminal human cancer. *Proc. Natl. Acad. Sci.* 75, 4538–4542.
- Cameron, E., Pauling, L., 1976. Supplemental ascorbate in the supportive treatment of cancer: Prolongation of survival times in terminal human cancer. *Proc. Natl. Acad. Sci.* 73, 3685–3689.
- Camici, M., 2008. Guanylin peptides and colorectal cancer (CRC). *Biomed. Pharmacother.* 62, 70–76.
- Campos-Laborie, F.J., Risueño, A., Ortiz-Estévez, M., Rosón-Burgo, B., Droste, C., Fontanillo, C., Loos, R., Sánchez-Santos, J.M., Trotter, M.W., De Las Rivas, J., 2016. DECO: decompose heterogeneous population cohorts for patient stratification and discovery of sample biomarkers using omic data profiling. *Bioinformatics.*
- Camps, J., Pitt, J.J., Emons, G., Hummon, A.B., Case, C.M., Grade, M., Jones, T.L., Nguyen, Q.T., Ghadimi, B.M., Beissbarth, T., Difilippantonio, M.J., Caplen, N.J., Ried, T., 2013. Genetic Amplification of the NOTCH Modulator LNX2 Upregulates the WNT/ β -Catenin Pathway in Colorectal Cancer. *Cancer Res.* 73, 2003–2013. <https://doi.org/10.1158/0008-5472.CAN-12-3159>

- Cancer Genome Atlas Network, 2012. Comprehensive molecular characterization of human colon and rectal cancer. *Nature* 487, 330–337. <https://doi.org/10.1038/nature11252>
- Cano, A., Portillo, F., 2010. An emerging role for class I bHLH E2-2 proteins in EMT regulation and tumor progression. *Cell Adhes. Migr.* 4, 56–60.
- Carey, J.N., Metttert, E.L., Roggiani, M., Myers, K.S., Kiley, P.J., Goulian, M., 2018. Regulated stochasticity in a bacterial signaling network permits tolerance to a rapid environmental change. *Cell* 173, 196–207. e14.
- Carrithers, S.L., Barber, M.T., Biswas, S., Parkinson, S.J., Park, P.K., Goldstein, S.D., Waldman, S.A., 1996. Guanylyl cyclase C is a selective marker for metastatic colorectal tumors in human extraintestinal tissues. *Proc. Natl. Acad. Sci. U. S. A.* 93, 14827–14832.
- Cavuoto, P., Fenech, M.F., 2012. A review of methionine dependency and the role of methionine restriction in cancer growth control and life-span extension. *Cancer Treat. Rev.* 38, 726–736. <https://doi.org/10.1016/j.ctrv.2012.01.004>
- cBioportal, 2019. cBioPortal for Cancer Genomics [WWW Document]. URL http://www.cbioportal.org/study?id=brca_tcga%2Cbrca_metabric%2Cbrca_bccrc%2Cbrca_broad%2Cbrca_sanger%2Cbrca_bccrc_xenograft_2014%2Cbrca_igr_2015%2Cbrca_mbcproject_wagle_2017 (accessed 3.5.19).
- Cellarier, E., Durando, X., Vasson, M.P., Farges, M.C., Demiden, A., Maurizis, J.C., Madelmont, J.C., Chollet, P., 2003. Methionine dependency and cancer treatment. *Cancer Treat. Rev.* 29, 489–499. [https://doi.org/10.1016/S0305-7372\(03\)00118-X](https://doi.org/10.1016/S0305-7372(03)00118-X)
- Cerdá, B., Espín, J.C., Parra, S., Martínez, P., Tomás-Barberán, F.A., 2004. The potent in vitro antioxidant ellagitannins from pomegranate juice are metabolised into bioavailable but poor antioxidant hydroxy-6H-dibenzopyran-6-one derivatives by the colonic microflora of healthy humans. *Eur. J. Nutr.* 43, 205–220. <https://doi.org/10.1007/s00394-004-0461-7>
- Cerdá, B., Periago, P., Espín, J.C., Tomás-Barberán, F.A., 2005a. Identification of Urolithin A as a Metabolite Produced by Human Colon Microflora from Ellagic Acid and Related Compounds. *J. Agric. Food Chem.* 53, 5571–5576. <https://doi.org/10.1021/jf050384i>
- Cerdá, B., Tomás-Barberán, F.A., Espín, J.C., 2005b. Metabolism of antioxidant and chemopreventive ellagitannins from strawberries, raspberries, walnuts, and oak-aged wine in humans: identification of biomarkers and individual variability. *J. Agric. Food Chem.* 53, 227–235. <https://doi.org/10.1021/jf049144d>
- Chang, M., Lowe, D.G., Lewis, M., Hellmiss, R., Chen, E., Goeddel, D.V., 1989. Differential activation by atrial and brain natriuretic peptides of two different receptor guanylate cyclases. *Nature* 341, 68–72. <https://doi.org/10.1038/341068a0>
- Chang, M.T., Bhattarai, T.S., Schram, A.M., Bielski, C.M., Donoghue, M.T.A., Jonsson, P., Chakravarty, D., Phillips, S., Kandoth, C., Penson, A., Gorelick, A., Shamu, T., Patel, S., Harris, C., Gao, J., Sumer, S.O., Kundra, R., Razavi, P., Li, B.T., Reales, D.N., Socci, N.D., Jayakumar, G., Zehir, A., Benayed, R., Arcila, M.E., Chandarlapaty, S., Ladanyi, M., Schultz, N., Baselga, J., Berger, M.F., Rosen, N., Solit, D.B., Hyman, D.M., Taylor, B.S., 2018. Accelerating Discovery of Functional Mutant Alleles in Cancer. *Cancer Discov.* 8, 174–183. <https://doi.org/10.1158/2159-8290.CD-17-0321>

- Chen, C., Grennan, K., Badner, J., Zhang, D., Gershon, E., Jin, L., Liu, C., 2011. Removing batch effects in analysis of expression microarray data: an evaluation of six batch adjustment methods. *PloS One* 6, e17238.
<https://doi.org/10.1371/journal.pone.0017238>
- Chen, Q., Espey, M.G., Krishna, M.C., Mitchell, J.B., Corpe, C.P., Buettner, G.R., Shacter, E., Levine, M., 2005. Pharmacologic ascorbic acid concentrations selectively kill cancer cells: action as a pro-drug to deliver hydrogen peroxide to tissues. *Proc. Natl. Acad. Sci.* 102, 13604–13609.
- Cheng, G., Zhang, Q., Pan, J., Lee, Y., Ouari, O., Hardy, M., Zielonka, M., Myers, C.R., Zielonka, J., Weh, K., Chang, A.C., Chen, G., Kresty, L., Kalyanaraman, B., You, M., 2019. Targeting lonidamine to mitochondria mitigates lung tumorigenesis and brain metastasis. *Nat. Commun.* 10, 2205. <https://doi.org/10.1038/s41467-019-10042-1>
- Cho, H., Jung, H., Lee, H., Yi, H.C., Kwak, H., Hwang, K.T., 2015a. Chemopreventive activity of ellagitannins and their derivatives from black raspberry seeds on HT-29 colon cancer cells. *Food Funct.* 6, 1675–1683.
<https://doi.org/10.1039/c5fo00274e>
- Cho, H., Jung, H., Lee, H., Yi, H.C., Kwak, H., Hwang, K.T., 2015b. Chemopreventive activity of ellagitannins and their derivatives from black raspberry seeds on HT-29 colon cancer cells. *Food Funct.* 6, 1675–1683.
<https://doi.org/10.1039/c5fo00274e>
- Cho, W.K., Choi, D.H., Park, W., Cha, H., Nam, S.J., Kim, S.W., Lee, J.E., Yu, J., Im, Y.-H., Ahn, J.S., Park, Y.H., Kim, J.-Y., Ahn, S., 2018. Effect of Body Mass Index on Survival in Breast Cancer Patients According to Subtype, Metabolic Syndrome, and Treatment. *Clin. Breast Cancer* 18, e1141–e1147.
<https://doi.org/10.1016/j.clbc.2018.04.010>
- Christadoss, P., Talal, N., Lindstrom, J., Fernandes, G., 1984. Suppression of cellular and humoral immunity to T-dependent antigens by calorie restriction. *Cell. Immunol.* 88, 1–8.
- Christopoulos, P.F., Msaouel, P., Koutsilieris, M., 2015. The role of the insulin-like growth factor-1 system in breast cancer. *Mol. Cancer* 14.
<https://doi.org/10.1186/s12943-015-0291-7>
- Cleary, M.P., Hu, X., Grossmann, M.E., Juneja, S.C., Dogan, S., Grande, J.P., Maihle, N.J., 2007. Prevention of mammary tumorigenesis by intermittent caloric restriction: does caloric intake during refeeding modulate the response? *Exp. Biol. Med.* Maywood NJ 232, 70–80.
- Colman, R.J., Anderson, R.M., Johnson, S.C., Kastman, E.K., Kosmatka, K.J., Beasley, T.M., Allison, D.B., Cruzen, C., Simmons, H.A., Kemnitz, J.W., Weindruch, R., 2009. Caloric restriction delays disease onset and mortality in rhesus monkeys. *Science* 325, 201–204. <https://doi.org/10.1126/science.1173635>
- Correa-Rodríguez, M., Rio-Valle, J.S., Rueda-Medina, B., 2016. Polymorphisms of the WNT16 gene are associated with the heel ultrasound parameter in young adults. *Osteoporos. Int.* 27, 1057–1061.
- Corzo-Martínez, M., Vázquez, L., Arranz-Martínez, P., Menéndez, N., Reglero, G., Torres, C.F., 2016. Production of a bioactive lipid-based delivery system from ratfish liver oil by enzymatic glycerolysis. *Food Bioprod. Process.* 100, 311–322.

- Couch, F.J., Wang, X.-Y., Wu, G.-J., Qian, J., Jenkins, R.B., James, C.D., 1999. Localization of PS6K to chromosomal region 17q23 and determination of its amplification in breast cancer. *Cancer Res.* 59, 1408–1411.
- Coxson, H.O., Chan, I.H., Mayo, J.R., Hlynsky, J., Nakano, Y., Birmingham, C.L., 2004. Early emphysema in patients with anorexia nervosa. *Am J Respir Crit Care Med* 170. <https://doi.org/10.1164/rccm.200405-651OC>
- CRU, 2015. Bowel cancer incidence statistics [WWW Document]. *Cancer Res.* UK. URL <https://www.cancerresearchuk.org/health-professional/cancer-statistics/statistics-by-cancer-type/bowel-cancer/incidence> (accessed 2.28.19).
- Da Silva, S.L., Calgarotto, A.K., Chaar, J.S., Marangoni, S., 2008. Isolation and characterization of ellagic acid derivatives isolated from *Casearia sylvestris* SW aqueous extract with anti-PLA(2) activity. *Toxicol Off. J. Int. Soc. Toxicology* 52, 655–666. <https://doi.org/10.1016/j.toxicol.2008.07.011>
- Dang, C.V., 2010. Glutaminolysis: supplying carbon or nitrogen or both for cancer cells? *Cell Cycle* 9, 3884–3886.
- Davis, S., Meltzer, P.S., 2007. GEOquery: a bridge between the Gene Expression Omnibus (GEO) and BioConductor. *Bioinformatics* 23, 1846–1847.
- de Groot, S., Vreeswijk, M.P., Welters, M.J., Gravesteyn, G., Boei, J.J., Jochems, A., Houtsma, D., Putter, H., van der Hoeven, J.J., Nortier, J.W., Pijl, H., Kroep, J.R., 2015. The effects of short-term fasting on tolerance to (neo) adjuvant chemotherapy in HER2-negative breast cancer patients: a randomized pilot study. *BMC Cancer* 15, 652. <https://doi.org/10.1186/s12885-015-1663-5>
- De Lorenzo, M.S., Baljinnyam, E., Vatner, D.E., Abarzúa, P., Vatner, S.F., Rabson, A.B., 2011. Caloric restriction reduces growth of mammary tumors and metastases. *Carcinogenesis* 32, 1381–1387. <https://doi.org/10.1093/carcin/bgr107>
- De Sousa E Melo, F., Wang, X., Jansen, M., Fessler, E., Trinh, A., de Rooij, L.P.M.H., de Jong, J.H., de Boer, O.J., van Leersum, R., Bijlsma, M.F., Rodermond, H., van der Heijden, M., van Noesel, C.J.M., Tuynman, J.B., Dekker, E., Markowitz, F., Medema, J.P., Vermeulen, L., 2013. Poor-prognosis colon cancer is defined by a molecularly distinct subtype and develops from serrated precursor lesions. *Nat. Med.* 19, 614–618. <https://doi.org/10.1038/nm.3174>
- de Cabo, R., Carmona-Gutierrez, D., Bernier, M., Hall, M.N., Madeo, F., 2014. The Search for Antiaging Interventions: From Elixirs to Fasting Regimens. *Cell* 157, 1515–1526. <https://doi.org/10.1016/j.cell.2014.05.031>
- Dekervel, J., Bulle, A., Windmolders, P., Lambrechts, D., Van Cutsem, E., Verslype, C., van Pelt, J., 2017. Acriflavine Inhibits Acquired Drug Resistance by Blocking the Epithelial-to-Mesenchymal Transition and the Unfolded Protein Response. *Transl. Oncol.* 10, 59–69. <https://doi.org/10.1016/j.tranon.2016.11.008>
- Deng, B., Wang, B., Fang, J., Zhu, X., Cao, Z., Lin, Q., Zhou, L., Sun, X., 2016. MiRNA-203 suppresses cell proliferation, migration and invasion in colorectal cancer via targeting of EIF5A2. *Sci. Rep.* 6, 28301.
- Denoix PF, 1952. Nomenclature classification des cancers. *Bull Inst Nat Hyg* 743–748.
- DeSantis, C.E., Bray, F., Ferlay, J., Lortet-Tieulent, J., Anderson, B.O., Jemal, A., 2015. International Variation in Female Breast Cancer Incidence and Mortality Rates. *Cancer Epidemiol. Prev. Biomark.* <https://doi.org/10.1158/1055-9965.EPI-15-0535>

- Dexter, D.L., Kowalski, H.M., Blazar, B.A., Fligielski, Z., Vogel, R., Heppner, G.H., 1978. Heterogeneity of tumor cells from a single mouse mammary tumor. *Cancer Res.* 38, 3174–3181.
- Di Biase, S., Lee, C., Brandhorst, S., Manes, B., Buono, R., Cheng, C.-W., Cacciottolo, M., Martin-Montalvo, A., de Cabo, R., Wei, M., Morgan, T.E., Longo, V.D., 2016. Fasting-Mimicking Diet Reduces HO-1 to Promote T Cell-Mediated Tumor Cytotoxicity. *Cancer Cell* 30, 136–146. <https://doi.org/10.1016/j.ccell.2016.06.005>
- Dinger, J., Bardenheuer, K., Minh, T.D., 2011. Levonorgestrel-releasing and copper intrauterine devices and the risk of breast cancer. *Contraception* 83, 211–217. <https://doi.org/10.1016/j.contraception.2010.11.009>
- Dorff, T.B., Groshen, S., Garcia, A., Shah, M., Tsao-Wei, D., Pham, H., Cheng, C.-W., Brandhorst, S., Cohen, P., Wei, M., Longo, V., Quinn, D.I., 2016. Safety and feasibility of fasting in combination with platinum-based chemotherapy. *BMC Cancer* 16, 360. <https://doi.org/10.1186/s12885-016-2370-6>
- Dubick, M.A., Rucker, R.B., Cross, C.E., Last, J.A., 1981. Elastin metabolism in rodent lung. *Biochim. Biophys. Acta BBA - Gen. Subj.* 672, 303–306. [https://doi.org/10.1016/0304-4165\(81\)90297-X](https://doi.org/10.1016/0304-4165(81)90297-X)
- Durando, X., Farges, M.-C., Buc, E., Abrial, C., Petorin-Lesens, C., Gillet, B., Vasson, M.-P., Pezet, D., Chollet, P., Thivat, E., 2010. Dietary methionine restriction with FOLFOX regimen as first line therapy of metastatic colorectal cancer: a feasibility study. *Oncology* 78, 205–209. <https://doi.org/10.1159/000313700>
- Eliyatkın, N., Yalçın, E., Zengel, B., Aktaş, S., Vardar, E., 2015. Molecular Classification of Breast Carcinoma: From Traditional, Old-Fashioned Way to A New Age, and A New Way. *J. Breast Health* 11, 59–66. <https://doi.org/10.5152/tjbh.2015.1669>
- Ellis IO, 2003. WHO Classification of Tumours Pathology and Genetics of Tumours of the Breast and Female Genital Organs. IARC Press, Lyon.
- EMBL-EBI, 2010. Functional genomics: An introduction to the EBI resources [WWW Document]. EMBL-EBI Train Online. URL <https://www.ebi.ac.uk/training/online/course/functional-genomics-introduction-ebi-resources> (accessed 3.6.19).
- Eroles, P., Bosch, A., Alejandro Pérez-Fidalgo, J., Lluch, A., 2012. Molecular biology in breast cancer: Intrinsic subtypes and signaling pathways. *Cancer Treat. Rev.* 38, 698–707. <https://doi.org/10.1016/j.ctrv.2011.11.005>
- Ershler, W.B., Berman, E., Moore, A.L., 1986. Slower B16 melanoma growth but greater pulmonary colonization in calorie-restricted mice. *J. Natl. Cancer Inst.* 76, 81–85.
- Espín, J.C., González-Barrio, R., Cerdá, B., López-Bote, C., Rey, A.I., Tomás-Barberán, F.A., 2007. Iberian pig as a model to clarify obscure points in the bioavailability and metabolism of ellagitannins in humans. *J. Agric. Food Chem.* 55, 10476–10485. <https://doi.org/10.1021/jf0723864>
- Espín, J.C., Larrosa, M., García-Conesa, M.T., Tomás-Barberán, F., 2013a. Biological Significance of Urolithins, the Gut Microbial Ellagic Acid-Derived Metabolites: The Evidence So Far [WWW Document]. *Evid. Based Complement. Alternat. Med.* <https://doi.org/10.1155/2013/270418>
- Espín, J.C., Larrosa, M., García-Conesa, M.T., Tomás-Barberán, F., 2013b. Biological Significance of Urolithins, the Gut Microbial Ellagic Acid-Derived Metabolites: The

- Evidence So Far [WWW Document]. *Evid. Based Complement. Alternat. Med.*
<https://doi.org/10.1155/2013/270418>
- Falletta, P., Sanchez-del-Campo, L., Chauhan, J., Effern, M., Kenyon, A., Kershaw, C.J., Siddaway, R., Lisle, R., Freter, R., Daniels, M.J., Lu, X., Tüting, T., Middleton, M., Buffa, F.M., Willis, A.E., Pavitt, G., Ronai, Z.A., Sauka-Spengler, T., Hölzel, M., Goding, C.R., 2017. Translation reprogramming is an evolutionarily conserved driver of phenotypic plasticity and therapeutic resistance in melanoma. *Genes Dev.* 31, 18–33. <https://doi.org/10.1101/gad.290940.116>
- Fearon, E.R., Vogelstein, B., 1990. A genetic model for colorectal tumorigenesis. *Cell* 61, 759–767.
- Feng, Y., Sokol, E.S., Vecchio, C.A.D., Sanduja, S., Claessen, J.H.L., Proia, T.A., Jin, D.X., Reinhardt, F., Ploegh, H.L., Wang, Q., Gupta, P.B., 2014. Epithelial-to-Mesenchymal Transition Activates PERK–eIF2 α and Sensitizes Cells to Endoplasmic Reticulum Stress. *Cancer Discov.* 4, 702–715.
<https://doi.org/10.1158/2159-8290.CD-13-0945>
- Fernandes, G., Yunis, E.J., Good, R.A., 1976. Suppression of adenocarcinoma by the immunological consequences of calorie restriction. *Nature* 263, 504.
<https://doi.org/10.1038/263504b0>
- Flavahan, W.A., Wu, Q., Hitomi, M., Rahim, N., Kim, Y., Sloan, A.E., Weil, R.J., Nakano, I., Sarkaria, J.N., Stringer, B.W., 2013. Brain tumor initiating cells adapt to restricted nutrition through preferential glucose uptake. *Nat. Neurosci.* 16, 1373.
- Fontana, L., Partridge, L., Longo, V.D., 2010. Extending healthy life span—from yeast to humans. *Science* 328, 321–326. <https://doi.org/10.1126/science.1172539>
- Fontanillo, C., 2013. Tesis: Desarrollo de algoritmos bioinformáticos para estudios de genómica funcional: aplicaciones en cáncer.
- Forster, M.J., Morris, P., Sohal, R.S., 2003. Genotype and age influence the effect of caloric intake on mortality in mice. *FASEB J. Off. Publ. Fed. Am. Soc. Exp. Biol.* 17, 690–692. <https://doi.org/10.1096/fj.02-0533fje>
- Friedman, J., Hastie, T., Tibshirani, R., 2009. glmnet: Lasso and elastic-net regularized generalized linear models. R Package Version 1.
- Fukuda, Y., Yamamoto, K., Hirao, M., Nishikawa, K., Maeda, S., Haraguchi, N., Miyake, M., Hama, N., Miyamoto, A., Ikeda, M., 2015. Prevalence of malnutrition among gastric cancer patients undergoing gastrectomy and optimal preoperative nutritional support for preventing surgical site infections. *Ann. Surg. Oncol.* 22, 778–785.
- Fukumura, D., Jain, R.K., 1998. Role of nitric oxide in angiogenesis and microcirculation in tumors. *Cancer Metastasis Rev.* 17, 77–89.
<https://doi.org/10.1023/A:1005908805527>
- Galea, M.H., Blamey, R.W., Elston, C.E., Ellis, I.O., 1992. The Nottingham prognostic index in primary breast cancer. *Breast Cancer Res. Treat.* 22, 207–219.
<https://doi.org/10.1007/BF01840834>
- Gambari, R., Brognara, E., Spandidos, D.A., Fabbri, E., 2016. Targeting oncomiRNAs and mimicking tumor suppressor miRNAs: New trends in the development of miRNA therapeutic strategies in oncology. *Int. J. Oncol.* 49, 5–32.
- García-Jiménez, C., Goding, C.R., 2019. Starvation and Pseudo-Starvation as Drivers of Cancer Metastasis through Translation Reprogramming. *Cell Metab.* 29, 254–267. <https://doi.org/10.1016/j.cmet.2018.11.018>

- García-Villalba, R., Espín, J.C., Tomás-Barberán, F.A., 2016. Chromatographic and spectroscopic characterization of urolithins for their determination in biological samples after the intake of foods containing ellagitannins and ellagic acid. *J. Chromatogr. A, Advances in Food Analysis* 1428, 162–175. <https://doi.org/10.1016/j.chroma.2015.08.044>
- Garde-Cerdán A, Gonzalo-Diago A., Pérez-Álvarez E, 2017. *Phenolic Compounds: Type, Effects and Research.*, First. ed. Nova Science Publishers, New York, NY.
- Gautier, L., Cope, L., Bolstad, B.M., Irizarry, R.A., 2004. affy—analysis of Affymetrix GeneChip data at the probe level. *Bioinformatics* 20, 307–315.
- Gebäck, T., Schulz, M.M.P., Koumoutsakos, P., Detmar, M., 2009. TScratch: a novel and simple software tool for automated analysis of monolayer wound healing assays. *BioTechniques* 46, 265–274. <https://doi.org/10.2144/000113083>
- Gellrich, N.-C., Handschel, J., Holtmann, H., Krüskemper, G., 2015. Oral cancer malnutrition impacts weight and quality of life. *Nutrients* 7, 2145–2160.
- Genetics Home Reference, G.H., 2019. Leber congenital amaurosis [WWW Document]. Genet. Home Ref. NIH. URL <https://ghr.nlm.nih.gov/condition/leber-congenital-amaurosis> (accessed 5.22.19).
- Gentleman, R., Carey, V., Huber, W., Irizarry, R., Dudoit, S., 2006. *Bioinformatics and computational biology solutions using R and Bioconductor.* Springer Science & Business Media.
- Getty, 2008. Nature Specials: Cancer genomics, in: *Nature Specials: Cancer Genomics.* p. Portrait.
- Giacosa, A., Barale, R., Bavaresco, L., Gatenby, P., Gerbi, V., Janssens, J., Johnston, B., Kas, K., La Vecchia, C., Mainguet, P., Morazzoni, P., Negri, E., Pelucchi, C., Pezzotti, M., Rondanelli, M., 2013. Cancer prevention in Europe: the Mediterranean diet as a protective choice. *Eur. J. Cancer Prev.* 22, 90. <https://doi.org/10.1097/CEJ.0b013e328354d2d7>
- Giovannucci, E., 2001. Insulin, Insulin-Like Growth Factors and Colon Cancer: A Review of the Evidence. *J. Nutr.* 131, 3109S-3120S. <https://doi.org/10.1093/jn/131.11.3109S>
- Gnant, M., Pfeiler, G., Stöger, H., Mlineritsch, B., Fitzal, F., Balic, M., Kwasny, W., Seifert, M., Stierer, M., Dubsy, P., 2013. The predictive impact of body mass index on the efficacy of extended adjuvant endocrine treatment with anastrozole in postmenopausal patients with breast cancer: an analysis of the randomised ABCSG-6a trial. *Br. J. Cancer* 109, 589.
- Goldhirsch, A., Glick, J.H., Gelber, R.D., Coates, A.S., Thürlimann, B., Senn, H.-J., 2005. Meeting Highlights: International Expert Consensus on the Primary Therapy of Early Breast Cancer 2005. *Ann. Oncol.* 16, 1569–1583. <https://doi.org/10.1093/annonc/mdi326>
- Gómez de Cedrón, M., Laparra, J.M., Loria-Kohen, V., Molina, S., Moreno-Rubio, J., Montoya, J.J., Torres, C., Casado, E., Reglero, G., Ramírez de Molina, A., 2019. Tolerability and Safety of a Nutritional Supplement with Potential as Adjuvant in Colorectal Cancer Therapy: A Randomized Trial in Healthy Volunteers. *Nutrients* 11, 2001.
- González-Sarrías, A., Espín, J.-C., Tomás-Barberán, F.A., García-Conesa, M.-T., 2009a. Gene expression, cell cycle arrest and MAPK signalling regulation in Caco-2 cells

- exposed to ellagic acid and its metabolites, urolithins. *Mol. Nutr. Food Res.* 53, 686–698. <https://doi.org/10.1002/mnfr.200800150>
- González-Sarrías, A., Espín, J.-C., Tomás-Barberán, F.A., García-Conesa, M.-T., 2009b. Gene expression, cell cycle arrest and MAPK signalling regulation in Caco-2 cells exposed to ellagic acid and its metabolites, urolithins. *Mol. Nutr. Food Res.* 53, 686–698. <https://doi.org/10.1002/mnfr.200800150>
- González-Sarrías, A., Giménez-Bastida, J.A., García-Conesa, M.T., Gómez-Sánchez, M.B., García-Talavera, N.V., Gil-Izquierdo, A., Sánchez-Álvarez, C., Fontana-Compiano, L.O., Morga-Egea, J.P., Pastor-Quirante, F.A., Martínez-Díaz, F., Tomás-Barberán, F.A., Espín, J.C., 2010. Occurrence of urolithins, gut microbiota ellagic acid metabolites and proliferation markers expression response in the human prostate gland upon consumption of walnuts and pomegranate juice. *Mol. Nutr. Food Res.* 54, 311–322. <https://doi.org/10.1002/mnfr.200900152>
- González-Sarrías, A., Giménez-Bastida, J.A., Núñez-Sánchez, M.Á., Larrosa, M., García-Conesa, M.T., Tomás-Barberán, F.A., Espín, J.C., 2014. Phase-II metabolism limits the antiproliferative activity of urolithins in human colon cancer cells. *Eur. J. Nutr.* 53, 853–864. <https://doi.org/10.1007/s00394-013-0589-4>
- González-Sarrías, A., Larrosa, M., Tomás-Barberán, F.A., Dolara, P., Espín, J.C., 2010. NF-kappaB-dependent anti-inflammatory activity of urolithins, gut microbiota ellagic acid-derived metabolites, in human colonic fibroblasts. *Br. J. Nutr.* 104, 503–512. <https://doi.org/10.1017/S0007114510000826>
- González-Sarrías, A., Miguel, V., Merino, G., Lucas, R., Morales, J.C., Tomás-Barberán, F., Alvarez, A.I., Espín, J.C., 2013. The gut microbiota ellagic acid-derived metabolite urolithin A and its sulfate conjugate are substrates for the drug efflux transporter breast cancer resistance protein (ABCG2/BCRP). *J. Agric. Food Chem.* 61, 4352–4359. <https://doi.org/10.1021/jf4007505>
- González-Sarrías, A., Núñez-Sánchez, M.Á., García-Villalba, R., Tomás-Barberán, F.A., Espín, J.C., 2017. Antiproliferative activity of the ellagic acid-derived gut microbiota isourolithin A and comparison with its urolithin A isomer: the role of cell metabolism. *Eur. J. Nutr.* 56, 831–841. <https://doi.org/10.1007/s00394-015-1131-7>
- González-Sarrías, A., Núñez-Sánchez, M.Á., Tomé-Carneiro, J., Tomás-Barberán, F.A., García-Conesa, M.T., Espín, J.C., 2016. Comprehensive characterization of the effects of ellagic acid and urolithins on colorectal cancer and key-associated molecular hallmarks: MicroRNA cell specific induction of CDKN1A (p21) as a common mechanism involved. *Mol. Nutr. Food Res.* 60, 701–716. <https://doi.org/10.1002/mnfr.201500780>
- González-Sarrías, A., Tomé-Carneiro, J., Bellesia, A., Tomás-Barberán, F.A., Espín, J.C., 2015. The ellagic acid-derived gut microbiota metabolite, urolithin A, potentiates the anticancer effects of 5-fluorouracil chemotherapy on human colon cancer cells. *Food Funct.* 6, 1460–1469. <https://doi.org/10.1039/c5fo00120j>
- González-Torres, C., González-Martínez, H., Miliar, A., Nájera, O., Graniel, J., Firo, V., Alvarez, C., Bonilla, E., Rodríguez, L., 2013. Effect of malnutrition on the expression of cytokines involved in Th1 cell differentiation. *Nutrients* 5, 579–593. <https://doi.org/10.3390/nu5020579>
- González-Vallinas, M., González-Castejón, M., Rodríguez-Casado, A., Ramírez de Molina, A., 2013. Dietary phytochemicals in cancer prevention and therapy: a

- complementary approach with promising perspectives. *Nutr. Rev.* 71, 585–599.
<https://doi.org/10.1111/nure.12051>
- Goodwin, P.J., Ennis, M., Pritchard, K.I., McCready, D., Koo, J., Sidlofsky, S., Trudeau, M., Hood, N., Redwood, S., 1999. Adjuvant Treatment and Onset of Menopause Predict Weight Gain After Breast Cancer Diagnosis. *J. Clin. Oncol.* 17, 120–120.
<https://doi.org/10.1200/JCO.1999.17.1.120>
- Gori, F., Lerner, U., Ohlsson, C., Baron, R., 2015. A new WNT on the bone: WNT16, cortical bone thickness, porosity and fractures. *BoneKEy Rep.* 4.
<https://doi.org/10.1038/bonekey.2015.36>
- Goyal, Y., Koul, A., Ranawat, P., 2019. Ellagic acid ameliorates cisplatin toxicity in chemically induced colon carcinogenesis. *Mol. Cell. Biochem.* 453, 205–215.
<https://doi.org/10.1007/s11010-018-3446-1>
- Griggs, J.J., Mangu, P.B., Temin, S., Lyman, G.H., 2012. Appropriate chemotherapy dosing for obese adult patients with cancer: American Society of Clinical Oncology clinical practice guideline. *J. Oncol. Pract.* 8, e59.
- Großhans, H., Filipowicz, W., 2008. Molecular biology: The expanding world of small RNAs. *Nature* 451, 414–416. <https://doi.org/10.1038/451414a>
- Gui, J., Li, H., 2005. Penalized Cox regression analysis in the high-dimensional and low-sample size settings, with applications to microarray gene expression data. *Bioinformatics* 21, 3001–3008. <https://doi.org/10.1093/bioinformatics/bti422>
- Guinney, J., Dienstmann, R., Wang, X., de Reyniès, A., Schlicker, A., Soneson, C., Marisa, L., Roepman, P., Nyamundanda, G., Angelino, P., Bot, B.M., Morris, J.S., Simon, I.M., Gerster, S., Fessler, E., de Sousa e Melo, F., Missiaglia, E., Ramay, H., Barras, D., Homicsko, K., Maru, D., Manyam, G.C., Broom, B., Boige, V., Perez-Villamil, B., Laderas, T., Salazar, R., Gray, J.W., Hanahan, D., Taberero, J., Bernardis, R., Friend, S.H., Laurent-Puig, P., Medema, J.P., Sadanandam, A., Wessels, L., Delorenzi, M., Kopetz, S., Vermeulen, L., Tejpar, S., 2015. The Consensus Molecular Subtypes of Colorectal Cancer. *Nat. Med.* 21, 1350–1356.
<https://doi.org/10.1038/nm.3967>
- Guler, H.-P., Zapf, J., Schmid, C., Froesch, E.R., 1989. Insulin-like growth factors I and II in healthy man. *Eur. J. Endocrinol.* 121, 753–758.
- Gupta, G.D., Coyaud, É., Gonçalves, J., Mojarad, B.A., Liu, Y., Wu, Q., Gheiratmand, L., Comartin, D., Tkach, J.M., Cheung, S.W.T., Bashkurov, M., Hasegan, M., Knight, J.D., Lin, Z.-Y., Schueler, M., Hildebrandt, F., Moffat, J., Gingras, A.-C., Raught, B., Pelletier, L., 2015. A Dynamic Protein Interaction Landscape of the Human Centrosome-Cilium Interface. *Cell* 163, 1484–1499.
<https://doi.org/10.1016/j.cell.2015.10.065>
- Ha, T.-K., Chi, S.-G., 2012. CAV1/caveolin 1 enhances aerobic glycolysis in colon cancer cells via activation of SLC2A3/GLUT3 transcription. *Autophagy* 8, 1684–1685.
- Hall, A., 1984. Oncogenes--implications for human cancer: a review. *J. R. Soc. Med.* 77, 410.
- Hanahan, Weinberg, 2000. The Hallmarks of Cancer: *Cell*. *Cell* 100, 57–70.
- Hawkins, N.J., Bariol, C., Ward, R.L., 2002. The serrated neoplasia pathway. *Pathology (Phila.)* 34, 548–555.
- Herschkowitz, J.I., Simin, K., Weigman, V.J., Mikaelian, I., Usary, J., Hu, Z., Rasmussen, K.E., Jones, L.P., Assefnia, S., Chandrasekharan, S., Backlund, M.G., Yin, Y., Khramtsov, A.I., Bastein, R., Quackenbush, J., Glazer, R.I., Brown, P.H., Green,

- J.E., Kopelovich, L., Furth, P.A., Palazzo, J.P., Olopade, O.I., Bernard, P.S., Churchill, G.A., Van Dyke, T., Perou, C.M., 2007. Identification of conserved gene expression features between murine mammary carcinoma models and human breast tumors. *Genome Biol.* 8, R76. <https://doi.org/10.1186/gb-2007-8-5-r76>
- Heytler, P.G., Prichard, W.W., 1962. A new class of uncoupling agents — Carbonyl cyanide phenylhydrazones. *Biochem. Biophys. Res. Commun.* 7, 272–275. [https://doi.org/10.1016/0006-291X\(62\)90189-4](https://doi.org/10.1016/0006-291X(62)90189-4)
- Holtorf, H., Guitton, M.-C., Reski, R., 2002. Plant functional genomics. *Naturwissenschaften* 89, 235–249. <https://doi.org/10.1007/s00114-002-0321-3>
- Howard, J.K., Lord, G.M., Matarese, G., Vendetti, S., Ghatei, M.A., Ritter, M.A., Lechler, R.I., Bloom, S.R., 1999. Leptin protects mice from starvation-induced lymphoid atrophy and increases thymic cellularity in ob/ob mice. *J. Clin. Invest.* 104, 1051–1059. <https://doi.org/10.1172/JCI6762>
- Howe, L.R., Brown, A.M.C., 2004. Wnt Signaling and Breast Cancer. *Cancer Biol. Ther.* 3, 36–41. <https://doi.org/10.4161/cbt.3.1.561>
- Huang, R., Xu, Y., Wan, W., Shou, X., Qian, J., You, Z., Liu, B., Chang, C., Zhou, T., Lippincott-Schwartz, J., Liu, W., 2015. Deacetylation of Nuclear LC3 Drives Autophagy Initiation under Starvation. *Mol. Cell* 57, 456–466. <https://doi.org/10.1016/j.molcel.2014.12.013>
- Huber, M.A., Kraut, N., Beug, H., 2005. Molecular requirements for epithelial–mesenchymal transition during tumor progression. *Curr. Opin. Cell Biol., Cell-to-cell contact and extracellular matrix* 17, 548–558. <https://doi.org/10.1016/j.ceb.2005.08.001>
- Huber, W., Carey, V.J., Gentleman, R., Anders, S., Carlson, M., Carvalho, B.S., Bravo, H.C., Davis, S., Gatto, L., Girke, T., 2015. Orchestrating high-throughput genomic analysis with Bioconductor. *Nat. Methods* 12, 115.
- Hwa, V., Oh, Y., Rosenfeld, R.G., 1999. The insulin-like growth factor-binding protein (IGFBP) superfamily. *Endocr. Rev.* 20, 761–787.
- Ijspeert, J.E.G., Medema, J.P., Dekker, E., 2015. Colorectal neoplasia pathways: state of the art. *Gastrointest. Endosc. Clin. N. Am.* 25, 169–182. <https://doi.org/10.1016/j.giec.2014.11.004>
- Ingram, D.K., de Cabo, R., 2017. Calorie restriction in rodents: caveats to consider. *Ageing Res. Rev.* 39, 15–28.
- Iorio, M.V., Croce, C.M., 2012. MicroRNA dysregulation in cancer: diagnostics, monitoring and therapeutics. A comprehensive review. *EMBO Mol. Med.* 4, 143–159.
- Irizarry, R.A., Hobbs, B., Collin, F., Beazer-Barclay, Y.D., Antonellis, K.J., Scherf, U., Speed, T.P., 2003. Exploration, normalization, and summaries of high density oligonucleotide array probe level data. *Biostatistics* 4, 249–264. <https://doi.org/10.1093/biostatistics/4.2.249>
- Jang, A., Hill, R.P., 1997. An examination of the effects of hypoxia, acidosis, and glucose starvation on the expression of metastasis-associated genes in murine tumor cells. *Clin. Exp. Metastasis* 15, 469–483. <https://doi.org/10.1023/A:1018470709523>
- Jass, J.R., 2007a. Classification of colorectal cancer based on correlation of clinical, morphological and molecular features. *Histopathology* 50, 113–130. <https://doi.org/10.1111/j.1365-2559.2006.02549.x>

- Jass, J.R., 2007b. Classification of colorectal cancer based on correlation of clinical, morphological and molecular features. *Histopathology* 50, 113–130. <https://doi.org/10.1111/j.1365-2559.2006.02549.x>
- Jeon, H., Kim, J.H., Lee, E., Jang, Y.J., Son, J.E., Kwon, J.Y., Lim, T., Kim, S., Park, J.H.Y., Kim, J.-E., Lee, K.W., 2016. Methionine deprivation suppresses triple-negative breast cancer metastasis in vitro and in vivo. *Oncotarget* 7, 67223–67234. <https://doi.org/10.18632/oncotarget.11615>
- Jessen, J.R., 2009. Noncanonical Wnt signaling in tumor progression and metastasis. *Zebrafish* 6, 21–28.
- Jin, X., Wei, Y., Xu, F., Zhao, M., Dai, K., Shen, R., Yang, S., Zhang, N., 2018. SIRT1 promotes formation of breast cancer through modulating Akt activity. *J. Cancer* 9, 2012–2023. <https://doi.org/10.7150/jca.24275>
- Johnson, D., Travis, J., 1979. The oxidative inactivation of human al-proteinase inhibitor. *J Biol Chem* 254, 4022–4026.
- Johnson, J.B., John, S., Laub, D.R., 2009. Pretreatment with alternate day modified fast will permit higher dose and frequency of cancer chemotherapy and better cure rates. *Med. Hypotheses* 72, 381–382. <https://doi.org/10.1016/j.mehy.2008.07.064>
- Johnson, L.M., Price, D.K., Figg, W.D., 2013. Treatment-induced secretion of WNT16B promotes tumor growth and acquired resistance to chemotherapy: implications for potential use of inhibitors in cancer treatment. *Cancer Biol. Ther.* 14, 90–91.
- Johnson, W.E., Li, C., Rabinovic, A., 2007. Adjusting batch effects in microarray expression data using empirical Bayes methods. *Biostatistics* 8, 118–127. <https://doi.org/10.1093/biostatistics/kxj037>
- Johnstone, T.C., Kulak, N., Pridgen, E.M., Farokhzad, O.C., Langer, R., Lippard, S.J., 2013. Nanoparticle Encapsulation of Mitaplatin and the Effect Thereof on In Vivo Properties. *ACS Nano* 7, 5675–5683. <https://doi.org/10.1021/nn401905g>
- Jones, J.I., Clemmons, D.R., 1995. Insulin-like growth factors and their binding proteins: biological actions. *Endocr. Rev.* 16, 3–34.
- Jubb, A.M., Zhong, F., Bheddah, S., Grabsch, H.I., Frantz, G.D., Mueller, W., Kavi, V., Quirke, P., Polakis, P., Koepfen, H., 2005. EphB2 is a Prognostic Factor in Colorectal Cancer. *Clin. Cancer Res.* 11, 5181–5187. <https://doi.org/10.1158/1078-0432.CCR-05-0143>
- Kabata, P., Jastrzębski, T., Kąkol, M., Król, K., Bobowicz, M., Kosowska, A., Jaśkiewicz, J., 2015. Preoperative nutritional support in cancer patients with no clinical signs of malnutrition—prospective randomized controlled trial. *Support. Care Cancer* 23, 365–370.
- Kalimutho, M., Nones, K., Srihari, S., Duijf, P.H.G., Waddell, N., Khanna, K.K., 2019. Patterns of Genomic Instability in Breast Cancer. *Trends Pharmacol. Sci.* 40, 198–211. <https://doi.org/10.1016/j.tips.2019.01.005>
- Kari, F.W., Dunn, S.E., French, J.E., Barrett, J.C., 1999. Roles for insulin-like growth factor-1 in mediating the anti-carcinogenic effects of caloric restriction. *J. Nutr. Health Aging* 3, 92–101.
- Karthik, G.-M., Ma, R., Lövrot, J., Kis, L.L., Lindh, C., Blomquist, L., Fredriksson, I., Bergh, J., Hartman, J., 2015. mTOR inhibitors counteract tamoxifen-induced activation of breast cancer stem cells. *Cancer Lett.* 367, 76–87. <https://doi.org/10.1016/j.canlet.2015.07.017>

- Kasimsetty, S.G., Bialonska, D., Reddy, M.K., Ma, G., Khan, S.I., Ferreira, D., 2010. Colon cancer chemopreventive activities of pomegranate ellagitannins and urolithins. *J. Agric. Food Chem.* 58, 2180–2187. <https://doi.org/10.1021/jf903762h>
- Kasimsetty, S.G., Bialonska, D., Reddy, M.K., Thornton, C., Willett, K.L., Ferreira, D., 2009. Effects of pomegranate chemical constituents/intestinal microbial metabolites on CYP1B1 in 22Rv1 prostate cancer cells. *J. Agric. Food Chem.* 57, 10636–10644. <https://doi.org/10.1021/jf902716r>
- Kellis, M., Wold, B., Snyder, M.P., Bernstein, B.E., Kundaje, A., Marinov, G.K., Ward, L.D., Birney, E., Crawford, G.E., Dekker, J., 2014. Defining functional DNA elements in the human genome. *Proc. Natl. Acad. Sci.* 111, 6131–6138.
- Kelsey, J.L., Gammon, M.D., John, E.M., 1993. Reproductive factors and breast cancer. *Epidemiol. Rev.* 15, 36–47.
- Khotskaya, Y.B., Goverdhan, A., Shen, J., Ponz-Sarvise, M., Chang, S.-S., Hsu, M.-C., Wei, Y., Xia, W., Yu, D., Hung, M.-C., 2014. S6K1 promotes invasiveness of breast cancer cells in a model of metastasis of triple-negative breast cancer. *Am. J. Transl. Res.* 6, 361–376.
- Kim, S.K., Demetri, G.D., 1996. CHEMOTHERAPY AND NEUTROPENIA. *Hematol. Clin.* 10, 377–395. [https://doi.org/10.1016/S0889-8588\(05\)70344-0](https://doi.org/10.1016/S0889-8588(05)70344-0)
- Klurfeld, D.M., Welch, C.B., Davis, M.J., Kritchevsky, D., 1989. Determination of degree of energy restriction necessary to reduce DMBA-induced mammary tumorigenesis in rats during the promotion phase. *J. Nutr.* 119, 286–291. <https://doi.org/10.1093/jn/119.2.286>
- Knudson, A.G., 2002. Cancer genetics. *Am. J. Med. Genet.* 111, 96–102.
- Koolman J Rohm K, 2012. *Color Atlas of Biochemistry*, 3rd ed. Georg Thieme Verlag KG, New York USA.
- Kopeina, G.S., Senichkin, V.V., Zhivotovsky, B., 2017. Caloric restriction - A promising anti-cancer approach: From molecular mechanisms to clinical trials. *Biochim. Biophys. Acta Rev. Cancer* 1867, 29–41. <https://doi.org/10.1016/j.bbcan.2016.11.002>
- Kotecha, R., Takami, A., Espinoza, J.L., 2016. Dietary phytochemicals and cancer chemoprevention: a review of the clinical evidence. *Oncotarget* 7, 52517–52529. <https://doi.org/10.18632/oncotarget.9593>
- Kritchevsky, D., 2001. Caloric restriction and cancer. *J. Nutr. Sci. Vitaminol. (Tokyo)* 47, 13–19.
- Kritchevsky, D., Welch, C.B., Klurfeld, D.M., 1989. Response of mammary tumors to caloric restriction for different time periods during the promotion phase. *Nutr. Cancer* 12, 259–269. <https://doi.org/10.1080/01635588909514025>
- Kühl, M., Sheldahl, L.C., Park, M., Miller, J.R., Moon, R.T., 2000. The Wnt/Ca²⁺ pathway: a new vertebrate Wnt signaling pathway takes shape. *Trends Genet.* 16, 279–283.
- Kuma, A., Hatano, M., Matsui, M., Yamamoto, A., Nakaya, H., Yoshimori, T., Ohsumi, Y., Tokuhiya, T., Mizushima, N., 2004. The role of autophagy during the early neonatal starvation period. *Nature* 432, 1032. <https://doi.org/10.1038/nature03029>
- Kuo, C.-C., Ling, H.-H., Chiang, M.-C., Chung, C.-H., Lee, W.-Y., Chu, C.-Y., Wu, Y.-C., Chen, C.-H., Lai, Y.-W., Tsai, I.-L., Cheng, C.-H., Lin, C.-W., 2019. Metastatic Colorectal

- Cancer Rewrites Metabolic Program Through a Glut3-YAP-dependent Signaling Circuit. *Theranostics* 9, 2526–2540. <https://doi.org/10.7150/thno.32915>
- Kusminski, C.M., Holland, W.L., Sun, K., Park, J., Spurgin, S.B., Lin, Y., Askew, G.R., Simcox, J.A., McClain, D.A., Li, C., Scherer, P.E., 2012. MitoNEET-driven alterations in adipocyte mitochondrial activity reveal a crucial adaptive process that preserves insulin sensitivity in obesity. *Nat. Med.* 18, 1539–1549. <https://doi.org/10.1038/nm.2899>
- Laiho, P., Kokko, A., Vanharanta, S., Salovaara, R., Sammalkorpi, H., Järvinen, H., Mecklin, J.-P., Karttunen, T.J., Tuppurainen, K., Davalos, V., Schwartz Jr, S., Arango, D., Mäkinen, M.J., Aaltonen, L.A., 2007. Serrated carcinomas form a subclass of colorectal cancer with distinct molecular basis. *Oncogene* 26, 312–320. <https://doi.org/10.1038/sj.onc.1209778>
- Laney Jr, D.W., Mann, E.A., Dellon, S.C., Perkins, D.R., Giannella, R.A., Cohen, M.B., 1992. Novel sites for expression of an Escherichia coli heat-stable enterotoxin receptor in the developing rat. *Am. J. Physiol.-Gastrointest. Liver Physiol.* 263, G816–G821.
- Laplante, M., Sabatini, D.M., 2013. Regulation of mTORC1 and its impact on gene expression at a glance. *J Cell Sci* 126, 1713–1719. <https://doi.org/10.1242/jcs.125773>
- Larrosa, M., García-Conesa, M.T., Espín, J.C., Tomás-Barberán, F.A., 2010. Ellagitannins, ellagic acid and vascular health. *Mol. Aspects Med., Phytochemicals and Cardiovascular Protection* 31, 513–539. <https://doi.org/10.1016/j.mam.2010.09.005>
- Larrosa, M., Tomás-Barberán, F.A., Espín, J.C., 2006. The dietary hydrolysable tannin punicalagin releases ellagic acid that induces apoptosis in human colon adenocarcinoma Caco-2 cells by using the mitochondrial pathway. *J. Nutr. Biochem.* 17, 611–625. <https://doi.org/10.1016/j.jnutbio.2005.09.004>
- Lashinger, L.M., Malone, L.M., McArthur, M.J., Goldberg, J.A., Daniels, E.A., Pavone, A., Colby, J.K., Smith, N.C., Perkins, S.N., Fischer, S.M., Hursting, S.D., 2011. Genetic Reduction of Insulin-like Growth Factor-1 Mimics the Anticancer Effects of Calorie Restriction on Cyclooxygenase-2–Driven Pancreatic Neoplasia. *Cancer Prev. Res. (Phila. Pa.)* 4, 1030–1040. <https://doi.org/10.1158/1940-6207.CAPR-11-0027>
- Laviano, A., Lazzaro, L.D., Koverech, A., 2018. Nutrition support and clinical outcome in advanced cancer patients. *Proc. Nutr. Soc.* 77, 388–393. <https://doi.org/10.1017/S0029665118000459>
- Law, R.H., Zhang, Q., McGowan, S., Buckle, A.M., Silverman, G.A., Wong, W., Rosado, C.J., Langendorf, C.G., Pike, R.N., Bird, P.I., Whisstock, J.C., 2006. An overview of the serpin superfamily. *Genome Biol.* 7, 216. <https://doi.org/10.1186/gb-2006-7-5-216>
- Lawrence, M.S., Stojanov, P., Polak, P., Kryukov, G.V., Cibulskis, K., Sivachenko, A., Carter, S.L., Stewart, C., Mermel, C.H., Roberts, S.A., Kiezun, A., Hammerman, P.S., McKenna, A., Drier, Y., Zou, L., Ramos, A.H., Pugh, T.J., Stransky, N., Helman, E., Kim, J., Sougnez, C., Ambrogio, L., Nickerson, E., Shefler, E., Cortés, M.L., Auclair, D., Saksena, G., Voet, D., Noble, M., DiCara, D., Lin, P., Lichtenstein, L., Heiman, D.I., Fennell, T., Imielinski, M., Hernandez, B., Hodis, E., Baca, S., Dulak, A.M., Lohr, J., Landau, D.-A., Wu, C.J., Melendez-Zajgla, J., Hidalgo-Miranda, A., Koren, A., McCarroll, S.A., Mora, J., Lee, R.S., Crompton, B., Onofrio, R., Parkin,

- M., Winckler, W., Ardlie, K., Gabriel, S.B., Roberts, C.W.M., Biegel, J.A., Stegmaier, K., Bass, A.J., Garraway, L.A., Meyerson, M., Golub, T.R., Gordenin, D.A., Sunyaev, S., Lander, E.S., Getz, G., 2013. Mutational heterogeneity in cancer and the search for new cancer-associated genes. *Nature* 499, 214–218. <https://doi.org/10.1038/nature12213>
- Lazar, C., Meganck, S., Taminau, J., Steenhoff, D., Coletta, A., Molter, C., Weiss-Solís, D.Y., Duque, R., Bersini, H., Nowé, A., 2013a. Batch effect removal methods for microarray gene expression data integration: a survey. *Brief. Bioinform.* 14, 469–490. <https://doi.org/10.1093/bib/bbs037>
- Lazar, C., Meganck, S., Taminau, J., Steenhoff, D., Coletta, A., Molter, C., Weiss-Solís, D.Y., Duque, R., Bersini, H., Nowé, A., 2013b. Batch effect removal methods for microarray gene expression data integration: a survey. *Brief. Bioinform.* 14, 469–490. <https://doi.org/10.1093/bib/bbs037>
- Lazarova, D.L., Bordonaro, M., 2012a. Extreme fluctuations in Wnt/beta-catenin signaling as an approach for colon cancer prevention and therapy. *Adv. Stud. Biol.* 4, 351–362.
- Lazarova, D.L., Bordonaro, M., 2012b. Extreme fluctuations in Wnt/beta-catenin signaling as an approach for colon cancer prevention and therapy. *Adv. Stud. Biol.* 4, 351–362.
- Lazarova, D.L., Bordonaro, M., Carbone, R., Sartorelli, A.C., 2004. Linear relationship between Wnt activity levels and apoptosis in colorectal carcinoma cells exposed to butyrate. *Int. J. Cancer* 110, 523–531.
- Lederberg, J., 2001. 'Ome Sweet 'Omics-- A Genealogical Treasury of Words [WWW Document]. *Sci. Mag.* URL <https://www.the-scientist.com/commentary/ome-sweet-omics---a-genealogical-treasury-of-words-54889> (accessed 5.6.19).
- Ledford, H., 2017. DNA typos to blame for most cancer mutations. *Nat. News.* <https://doi.org/10.1038/nature.2017.21696>
- Lee, C., Raffaghello, L., Brandhorst, S., Safdie, F.M., Bianchi, G., Martin-Montalvo, A., Pistoia, V., Wei, M., Hwang, S., Merlino, A., Emionite, L., Cabo, R. de, Longo, V.D., 2012a. Fasting Cycles Retard Growth of Tumors and Sensitize a Range of Cancer Cell Types to Chemotherapy. *Sci. Transl. Med.* 4, 124ra27-124ra27. <https://doi.org/10.1126/scitranslmed.3003293>
- Lee, C., Raffaghello, L., Brandhorst, S., Safdie, F.M., Bianchi, G., Martin-Montalvo, A., Pistoia, V., Wei, M., Hwang, S., Merlino, A., Emionite, L., de Cabo, R., Longo, V.D., 2012b. Fasting cycles retard growth of tumors and sensitize a range of cancer cell types to chemotherapy. *Sci. Transl. Med.* 4, 124ra27. <https://doi.org/10.1126/scitranslmed.3003293>
- Lee, C., Raffaghello, L., Longo, V.D., 2012c. Starvation, detoxification, and multidrug resistance in cancer therapy. *Drug Resist. Updat. Rev. Comment. Antimicrob. Anticancer Chemother.* 15, 114–122. <https://doi.org/10.1016/j.drug.2012.01.004>
- Lee, J., Sohn, I., Do, I.-G., Kim, K.-M., Park, S.H., Park, J.O., Park, Y.S., Lim, H.Y., Sohn, T.S., Bae, J.M., Choi, M.G., Lim, D.H., Min, B.H., Lee, J.H., Rhee, P.L., Kim, J.J., Choi, D.I., Tan, I.B., Das, K., Tan, P., Jung, S.H., Kang, W.K., Kim, S., 2014. Nanostring-Based Multigene Assay to Predict Recurrence for Gastric Cancer Patients after Surgery. *PLOS ONE* 9, e90133. <https://doi.org/10.1371/journal.pone.0090133>
- Lee, K.-C., Ou, Y.-C., Hu, W.-H., Liu, C.-C., Chen, H.-H., 2016. Meta-analysis of outcomes of patients with stage IV colorectal cancer managed with

- chemotherapy/radiochemotherapy with and without primary tumor resection. *OncoTargets Ther.* 9, 7059–7069. <https://doi.org/10.2147/OTT.S112965>
- Levine, Morgan E., Suarez, J.A., Brandhorst, S., Balasubramanian, P., Cheng, C.-W., Madaia, F., Fontana, L., Mirisola, M.G., Guevara-Aguirre, J., Wan, J., Passarino, G., Kennedy, B.K., Wei, M., Cohen, P., Crimmins, E.M., Longo, V.D., 2014. Low protein intake is associated with a major reduction in IGF-1, cancer, and overall mortality in the 65 and younger but not older population. *Cell Metab.* 19, 407–417. <https://doi.org/10.1016/j.cmet.2014.02.006>
- Levine, Morgan E., Suarez, J.A., Brandhorst, S., Balasubramanian, P., Cheng, C.-W., Madaia, F., Fontana, L., Mirisola, M.G., Guevara-Aguirre, J., Wan, J., Passarino, G., Kennedy, B.K., Wei, M., Cohen, P., Crimmins, E.M., Longo, V.D., 2014. Low Protein Intake Is Associated with a Major Reduction in IGF-1, Cancer, and Overall Mortality in the 65 and Younger but Not Older Population. *Cell Metab.* 19, 407–417. <https://doi.org/10.1016/j.cmet.2014.02.006>
- Li, Z., Henning, S.M., Lee, R.-P., Lu, Q.-Y., Summanen, P.H., Thames, G., Corbett, K., Downes, J., Tseng, C.-H., Finegold, S.M., Heber, D., 2015. Pomegranate extract induces ellagitannin metabolite formation and changes stool microbiota in healthy volunteers. *Food Funct.* 6, 2487–2495. <https://doi.org/10.1039/c5fo00669d>
- Liao, C.-Y., Rikke, B.A., Johnson, T.E., Diaz, V., Nelson, J.F., 2010. Genetic variation in the murine lifespan response to dietary restriction: from life extension to life shortening. *Aging Cell* 9, 92–95. <https://doi.org/10.1111/j.1474-9726.2009.00533.x>
- Liao, H., Bai, Y., Qiu, S., Zheng, L., Huang, L., Liu, T., Wang, X., Liu, Y., Xu, N., Yan, X., Guo, H., 2015. MiR-203 downregulation is responsible for chemoresistance in human glioblastoma by promoting epithelial-mesenchymal transition via SNAI2. *Oncotarget* 6, 8914–8928.
- Liberal, J., Carmo, A., Gomes, C., Cruz, M.T., Batista, M.T., 2017. Urolithins impair cell proliferation, arrest the cell cycle and induce apoptosis in UMUC3 bladder cancer cells. *Invest. New Drugs* 35, 671–681. <https://doi.org/10.1007/s10637-017-0483-7>
- Lin, S.-Y., Xia, W., Wang, J.C., Kwong, K.Y., Spohn, B., Wen, Y., Pestell, R.G., Hung, M.-C., 2000. β -catenin, a novel prognostic marker for breast cancer: its roles in cyclin D1 expression and cancer progression. *Proc. Natl. Acad. Sci.* 97, 4262–4266.
- Lipper, C.H., Karmi, O., Sohn, Y.S., Darash-Yahana, M., Lammert, H., Song, L., Liu, A., Mittler, R., Nechushtai, R., Onuchic, J.N., Jennings, P.A., 2018. Structure of the human monomeric NEET protein MiNT and its role in regulating iron and reactive oxygen species in cancer cells. *Proc. Natl. Acad. Sci. U. S. A.* 115, 272–277. <https://doi.org/10.1073/pnas.1715842115>
- Liu, F., Kohlmeier, S., Wang, C.-Y., 2008. Wnt signaling and skeletal development. *Cell. Signal.* 20, 999–1009.
- Liu, P., Rudick, M., Anderson, R.G.W., 2002. Multiple Functions of Caveolin-1. *J. Biol. Chem.* 277, 41295–41298. <https://doi.org/10.1074/jbc.R200020200>
- Liu, Y., Wang, P., Chen, F., Yuan, Y., Zhu, Y., Yan, H., Hu, X., 2015. Role of plant polyphenols in acrylamide formation and elimination. *Food Chem., ISPMF 2015: International Symposium on Phytochemicals in Medicine and Food (Shanghai,*

- China, June 26th –29th, 2015) 186, 46–53.
<https://doi.org/10.1016/j.foodchem.2015.03.122>
- Lochs, H., Allison, S.P., Meier, R., Pirlich, M., Kondrup, J., van den Berghe, G., Pichard, C., 2006. Introductory to the ESPEN guidelines on enteral nutrition: terminology, definitions and general topics. *Clin. Nutr.* 25, 180–186.
- Longchamp, A., Mirabella, T., Arduini, A., MacArthur, M.R., Das, A., Treviño-Villarreal, J.H., Hine, C., Ben-Sahra, I., Knudsen, N.H., Brace, L.E., Reynolds, J., Mejia, P., Tao, M., Sharma, G., Wang, R., Corpataux, J.-M., Haefliger, J.-A., Ahn, K.H., Lee, C.-H., Manning, B.D., Sinclair, D.A., Chen, C.S., Ozaki, C.K., Mitchell, J.R., 2018. Amino acid restriction triggers angiogenesis via GCN2/ATF4 regulation of VEGF and H2S production. *Cell* 173, 117–129.e14. <https://doi.org/10.1016/j.cell.2018.03.001>
- Lopez-Guadamillas, E., Fernandez-Marcos, P.J., Pantoja, C., Muñoz-Martin, M., Martínez, D., Gómez-López, G., Campos-Olivas, R., Valverde, A.M., Serrano, M., 2016a. p21 Cip1 plays a critical role in the physiological adaptation to fasting through activation of PPAR α . *Sci. Rep.* 6, 34542.
- Lopez-Guadamillas, E., Fernandez-Marcos, P.J., Pantoja, C., Muñoz-Martin, M., Martínez, D., Gómez-López, G., Campos-Olivas, R., Valverde, A.M., Serrano, M., 2016b. p21 Cip1 plays a critical role in the physiological adaptation to fasting through activation of PPAR α . *Sci. Rep.* 6, 34542.
- Losso, J.N., Bansode, R.R., Trappey, A., Bawadi, H.A., Truax, R., 2004. In vitro anti-proliferative activities of ellagic acid. *J. Nutr. Biochem.* 15, 672–678.
<https://doi.org/10.1016/j.jnutbio.2004.06.004>
- Lu, Y., Tao, F., Zhou, M.-T., Tang, K.-F., 2019. The signaling pathways that mediate the anti-cancer effects of caloric restriction. *Pharmacol. Res.* 141, 512–520.
<https://doi.org/10.1016/j.phrs.2019.01.021>
- Ma, C.X., 2015. The PI3K Pathway as a Therapeutic Target in Breast Cancer. *Am. J. Hematol. Oncol.* 11.
- Ma, D., Chen, X., Zhang, P.-Y., Zhang, H., Wei, L.-J., Hu, S., Tang, J.-Z., Zhou, M.-T., Xie, C., Ou, R., Xu, Y., Tang, K.-F., 2018. Upregulation of the ALDOA/DNA-PK/p53 pathway by dietary restriction suppresses tumor growth. *Oncogene* 37, 1041–1048. <https://doi.org/10.1038/onc.2017.398>
- Ma, S.S., 2009. Integrative analysis of cancer genomic data.
- Maasberg, S., Knappe-Drzikova, B., Vonderbeck, D., Jann, H., Weylandt, K.H., Grieser, C., Pascher, A., Schefold, J.C., Pavel, M., Wiedenmann, B., 2017. Malnutrition predicts clinical outcome in patients with neuroendocrine neoplasia. *Neuroendocrinology* 104, 11–25.
- MacConaill, L.E., Garraway, L.A., 2010. Clinical Implications of the Cancer Genome. *J. Clin. Oncol.* 28, 5219–5228. <https://doi.org/10.1200/JCO.2009.27.4944>
- Machon, C., Thezenas, S., Dupuy, A.-M., Assenat, E., Michel, F., Mas, E., Senesse, P., Cristol, J.-P., 2012. Immunonutrition before and during radiochemotherapy: improvement of inflammatory parameters in head and neck cancer patients. *Support. Care Cancer* 20, 3129–3135.
- Madeo, F., Carmona-Gutierrez, D., Hofer, S.J., Kroemer, G., 2019. Caloric Restriction Mimetics against Age-Associated Disease: Targets, Mechanisms, and Therapeutic Potential. *Cell Metab.* 29, 592–610. <https://doi.org/10.1016/j.cmet.2019.01.018>

- Magnon, C., Hall, S.J., Lin, J., Xue, X., Gerber, L., Freedland, S.J., Frenette, P.S., 2013. Autonomic Nerve Development Contributes to Prostate Cancer Progression. *Science* 341, 1236361. <https://doi.org/10.1126/science.1236361>
- Malinauskas, T., Jones, E.Y., 2014. Extracellular modulators of Wnt signalling. *Curr. Opin. Struct. Biol.* 29, 77–84. <https://doi.org/10.1016/j.sbi.2014.10.003>
- Malvezzi, M., Carioli, G., Bertuccio, P., Boffetta, P., Levi, F., La Vecchia, C., Negri, E., 2018. European cancer mortality predictions for the year 2018 with focus on colorectal cancer. *Ann. Oncol.* 29, 1016–1022. <https://doi.org/10.1093/annonc/mdy033>
- Mann, E.A., Steinbrecher, K.A., Stroup, C., Witte, D.P., Cohen, M.B., Giannella, R.A., 2005. Lack of guanylyl cyclase C, the receptor for Escherichia coli heat-stable enterotoxin, results in reduced polyp formation and increased apoptosis in the multiple intestinal neoplasia (Min) mouse model. *Int. J. Cancer* 116, 500–505. <https://doi.org/10.1002/ijc.21119>
- Marchetti, P., Guerreschi, P., Mortier, L., Kluza, J., 2015. Integration of Mitochondrial Targeting for Molecular Cancer Therapeutics [WWW Document]. *Int. J. Cell Biol.* <https://doi.org/10.1155/2015/283145>
- Marcus, J.N., Watson, P., Page, D.L., Narod, S.A., Lenoir, G.M., Tonin, P., Linder-Stephenson, L., Salerno, G., Conway, T.A., Lynch, H.T., 1996. Hereditary breast cancer: pathobiology, prognosis, and BRCA1 and BRCA2 gene linkage. *Cancer* 77, 697–709.
- Marisa, L., de Reyniès, A., Duval, A., Selves, J., Gaub, M.P., Vescovo, L., Etienne-Grimaldi, M.-C., Schiappa, R., Guenot, D., Ayadi, M., Kirzin, S., Chazal, M., Fléjou, J.-F., Benchimol, D., Berger, A., Lagarde, A., Pencreach, E., Piard, F., Elias, D., Parc, Y., Olschwang, S., Milano, G., Laurent-Puig, P., Boige, V., 2013. Gene expression classification of colon cancer into molecular subtypes: characterization, validation, and prognostic value. *PLoS Med.* 10, e1001453. <https://doi.org/10.1371/journal.pmed.1001453>
- Markowitz, S.D., 2007. Aspirin and colon cancer--targeting prevention? *N. Engl. J. Med.* 356, 2195–2198. <https://doi.org/10.1056/NEJMe078044>
- Markowitz, S.D., Bertagnolli, M.M., 2009. Molecular Origins of Cancer. *N. Engl. J. Med.* 361, 2449–2460. <https://doi.org/10.1056/NEJMra0804588>
- Martí, M., Martínez, V., Lis, M.J., Valldeperas, J., de la Maza, A., Parra, J.L., Coderch, L., 2014. Gallic Acid vehiculized through liposomes or mixed micelles in biofunctional textiles. *J. Text. Inst.* 105, 175–186.
- Martinez-Romero, J., Bueno-Fortes, S., Martín-Merino, M., Ramirez de Molina, A., De Las Rivas, J., 2018. Survival marker genes of colorectal cancer derived from consistent transcriptomic profiling. *BMC Genomics* 19, 857. <https://doi.org/10.1186/s12864-018-5193-9>
- Martín-Montalvo, A., Villalba, J.M., Navas, P., de Cabo, R., 2011. NRF2, cancer and calorie restriction. *Oncogene* 30, 505–520. <https://doi.org/10.1038/onc.2010.492>
- Mashima, T., Seimiya, H., Tsuruo, T., 2009. De novo fatty-acid synthesis and related pathways as molecular targets for cancer therapy. *Br. J. Cancer* 100, 1369.
- Masin, M., Vazquez, J., Rossi, S., Groeneveld, S., Samson, N., Schwalie, P.C., Deplancke, B., Frawley, L.E., Gouttenoire, J., Moradpour, D., 2014. GLUT3 is induced during epithelial-mesenchymal transition and promotes tumor cell proliferation in non-small cell lung cancer. *Cancer Metab.* 2, 11.

- Mattson, M.P., 2005. ENERGY INTAKE, MEAL FREQUENCY, AND HEALTH: A Neurobiological Perspective. *Annu. Rev. Nutr.* 25, 237–260. <https://doi.org/10.1146/annurev.nutr.25.050304.092526>
- Mattson, M.P., Longo, V.D., Harvie, M., 2017. Impact of intermittent fasting on health and disease processes. *Ageing Res. Rev.* 39, 46–58. <https://doi.org/10.1016/j.arr.2016.10.005>
- Mattson, M.P., Wan, R., 2005. Beneficial effects of intermittent fasting and caloric restriction on the cardiovascular and cerebrovascular systems. *J. Nutr. Biochem.* 16, 129–137. <https://doi.org/10.1016/j.jnutbio.2004.12.007>
- McCall, M.N., Bolstad, B.M., Irizarry, R.A., 2010. Frozen robust multiarray analysis (fRMA). *Biostat. Oxf. Engl.* 11, 242–253. <https://doi.org/10.1093/biostatistics/kxp059>
- Medina, R.A., Owen, G.I., 2002. Glucose transporters: expression, regulation and cancer. *Biol. Res.* 35, 9–26. <https://doi.org/10.4067/S0716-97602002000100004>
- Menegon, S., Columbano, A., Giordano, S., 2016. The Dual Roles of NRF2 in Cancer. *Trends Mol. Med.* 22, 578–593. <https://doi.org/10.1016/j.molmed.2016.05.002>
- Mertens-Talcott, S.U., Lee, J.-H., Percival, S.S., Talcott, S.T., 2006. Induction of cell death in Caco-2 human colon carcinoma cells by ellagic acid rich fractions from muscadine grapes (*Vitis rotundifolia*). *J. Agric. Food Chem.* 54, 5336–5343. <https://doi.org/10.1021/jf060563f>
- Meyerhardt, J.A., Kroenke, C.H., Prado, C.M., Kwan, M.L., Castillo, A., Weltzien, E., Cespedes, E.M., Xiao, J., Caan, B.J., 2017. Association of Weight Change after Colorectal Cancer Diagnosis and Outcomes in the Kaiser Permanente Northern California Population. *Cancer Epidemiol. Prev. Biomark.* <https://doi.org/10.1158/1055-9965.EPI-16-0145>
- Meynet, O., Ricci, J.-E., 2014. Caloric restriction and cancer: molecular mechanisms and clinical implications. *Trends Mol. Med.* 20, 419–427. <https://doi.org/10.1016/j.molmed.2014.05.001>
- Michael J Crawley, 2013. *The R book*, Imperial College London at Silwood Park. ed. John Wiley & Sons, Ltd, UK.
- Michelakis, E.D., Webster, L., Mackey, J.R., 2008. Dichloroacetate (DCA) as a potential metabolic-targeting therapy for cancer. *Br. J. Cancer* 99, 989–994. <https://doi.org/10.1038/sj.bjc.6604554>
- Mihaylova, M.M., Shaw, R.J., 2011. The AMPK signalling pathway coordinates cell growth, autophagy and metabolism. *Nat. Cell Biol.* 13, 1016–1023. <https://doi.org/10.1038/ncb2329>
- Mizushima, N., Levine, B., Cuervo, A.M., Klionsky, D.J., 2008. Autophagy fights disease through cellular self-digestion. *Nature* 451, 1069–1075. <https://doi.org/10.1038/nature06639>
- Molina, S., Moran-Valero, M.I., Martin, D., Vázquez, L., Vargas, T., Torres, C.F., De Molina, A.R., Reglero, G., 2013. Antiproliferative effect of alkylglycerols as vehicles of butyric acid on colon cancer cells. *Chem. Phys. Lipids* 175, 50–56.
- Moo, T.-A., Sanford, R., Dang, C., Morrow, M., 2018. Overview of Breast Cancer Therapy. *PET Clin.* 13, 339–354. <https://doi.org/10.1016/j.cpet.2018.02.006>
- Moon, R.T., Kohn, A.D., De Ferrari, G.V., Kaykas, A., 2004. WNT and β -catenin signalling: diseases and therapies. *Nat. Rev. Genet.* 5, 691.

- Moreno-Bueno, G., Peinado, H., Molina, P., Olmeda, D., Cubillo, E., Santos, V., Palacios, J., Portillo, F., Cano, A., 2009. The morphological and molecular features of the epithelial-to-mesenchymal transition. *Nat. Protoc.* 4, 1591.
- Moreschi, 1909. Beziehungen zwischen Ernährung und Tumorwachstum. *Z Immunitätsforsch Orig* 651–675.
- Moustakas, A., Heldin, C.-H., 2007. Signaling networks guiding epithelial–mesenchymal transitions during embryogenesis and cancer progression. *Cancer Sci.* 98, 1512–1520. <https://doi.org/10.1111/j.1349-7006.2007.00550.x>
- Muaddi, H., Majumder, M., Peidis, P., Papadakis, A.I., Holcik, M., Scheuner, D., Kaufman, R.J., Hatzoglou, M., Koromilas, A.E., 2010. Phosphorylation of eIF2 α at Serine 51 Is an Important Determinant of Cell Survival and Adaptation to Glucose Deficiency. *Mol. Biol. Cell* 21, 3220–3231. <https://doi.org/10.1091/mbc.e10-01-0023>
- Mueckler, M., Thorens, B., 2013. The SLC2 (GLUT) Family of Membrane Transporters. *Mol. Aspects Med.* 34, 121–138. <https://doi.org/10.1016/j.mam.2012.07.001>
- Mukherjee, P., El-Abadi, M.M., Kasperzyk, J.L., Raney, M.K., Seyfried, T.N., 2002. Dietary restriction reduces angiogenesis and growth in an orthotopic mouse brain tumour model. *Br. J. Cancer* 86, 1615–1621. <https://doi.org/10.1038/sj.bjc.6600298>
- Muku, G.E., Murray, I.A., Espín, J.C., Perdew, G.H., 2018. Urolithin A Is a Dietary Microbiota-Derived Human Aryl Hydrocarbon Receptor Antagonist. *Metabolites* 8. <https://doi.org/10.3390/metabo8040086>
- Murphy, L.L.S., Hughes, C.C.W., 2002. Endothelial Cells Stimulate T Cell NFAT Nuclear Translocation in the Presence of Cyclosporin A: Involvement of the wnt/Glycogen Synthase Kinase-3 β Pathway. *J. Immunol.* 169, 3717–3725. <https://doi.org/10.4049/jimmunol.169.7.3717>
- Muscaritoli, M., Lucia, S., Farcomeni, A., Lorusso, V., Saracino, V., Barone, C., Plastino, F., Gori, S., Magarotto, R., Carteni, G., Chiurazzi, B., Pavese, I., Marchetti, L., Zagonel, V., Bergo, E., Tonini, G., Imperatori, M., Iacono, C., Maiorana, L., Pinto, C., Rubino, D., Cavanna, L., Di Cicilia, R., Gamucci, T., Quadrini, S., Palazzo, S., Minardi, S., Merlano, M., Colucci, G., Marchetti, P., 2017. Prevalence of malnutrition in patients at first medical oncology visit: the PreMiO study. *Oncotarget* 8, 79884–79896. <https://doi.org/10.18632/oncotarget.20168>
- Nagelkerke, A., Bussink, J., Mujcic, H., Wouters, B.G., Lehmann, S., Sweep, F.C., Span, P.N., 2013. Hypoxia stimulates migration of breast cancer cells via the PERK/ATF4/LAMP3-arm of the unfolded protein response. *Breast Cancer Res.* 15, R2.
- Nagy, J.A., Chang, S.-H., Dvorak, A.M., Dvorak, H.F., 2009. Why are tumour blood vessels abnormal and why is it important to know? *Br. J. Cancer* 100, 865–869. <https://doi.org/10.1038/sj.bjc.6604929>
- Narayanan, B.A., Re, G.G., 2001. IGF-II down regulation associated cell cycle arrest in colon cancer cells exposed to phenolic antioxidant ellagic acid. *Anticancer Res.* 21, 359–364.
- Narod, S.A., 1994. Genetics of breast and ovarian cancer. *Br. Med. Bull.* 50, 656–676.
- NCBI-GEO, 2017. Home - GEO - NCBI [WWW Document]. URL <https://www.ncbi.nlm.nih.gov/geo/> (accessed 5.7.19).

- Ng, T.L., Leprivier, G., Robertson, M.D., Chow, C., Martin, M.J., Laderoute, K.R., Davicioni, E., Triche, T.J., Sorensen, P.H.B., 2012. The AMPK stress response pathway mediates anoikis resistance through inhibition of mTOR and suppression of protein synthesis. *Cell Death Differ.* 19, 501–510. <https://doi.org/10.1038/cdd.2011.119>
- Nickens, K.P., Wikstrom, J.D., Shirihai, O.S., Patierno, S.R., Ceryak, S., 2013. A bioenergetic profile of non-transformed fibroblasts uncovers a link between death-resistance and enhanced spare respiratory capacity. *Mitochondrion* 13, 662–667. <https://doi.org/10.1016/j.mito.2013.09.005>
- Niraula, S., Ocana, A., Ennis, M., Goodwin, P.J., 2012. Body size and breast cancer prognosis in relation to hormone receptor and menopausal status: a meta-analysis. *Breast Cancer Res. Treat.* 134, 769–781.
- Nkondjock, A., Ghadirian, P., 2004. Epidemiology of breast cancer among BRCA mutation carriers: an overview. *Cancer Lett.* 205, 1–8.
- Núñez-Sánchez, M.A., García-Villalba, R., Monedero-Saiz, T., García-Talavera, N.V., Gómez-Sánchez, M.B., Sánchez-Álvarez, C., García-Albert, A.M., Rodríguez-Gil, F.J., Ruiz-Marín, M., Pastor-Quirante, F.A., Martínez-Díaz, F., Yáñez-Gascón, M.J., González-Sarrías, A., Tomás-Barberán, F.A., Espín, J.C., 2014. Targeted metabolic profiling of pomegranate polyphenols and urolithins in plasma, urine and colon tissues from colorectal cancer patients. *Mol. Nutr. Food Res.* 58, 1199–1211. <https://doi.org/10.1002/mnfr.201300931>
- Núñez-Sánchez, M.Á., Karmokar, A., González-Sarrías, A., García-Villalba, R., Tomás-Barberán, F.A., García-Conesa, M.T., Brown, K., Espín, J.C., 2016. In vivo relevant mixed urolithins and ellagic acid inhibit phenotypic and molecular colon cancer stem cell features: A new potentiality for ellagitannin metabolites against cancer. *Food Chem. Toxicol. Int. J. Publ. Br. Ind. Biol. Res. Assoc.* 92, 8–16. <https://doi.org/10.1016/j.fct.2016.03.011>
- Nusse, R., 2005. Wnt signaling in disease and in development. *Cell Res.* 15, 28–32. <https://doi.org/10.1038/sj.cr.7290260>
- Nutrition in Cancer Care (PDQ®), 2019. Nutrition in Cancer Care (PDQ®)—Health Professional Version - National Cancer Institute [WWW Document]. URL <https://www.cancer.gov/about-cancer/treatment/side-effects/appetite-loss/nutrition-hp-pdq/> (accessed 1.17.18).
- Oba, S.M., Wang, Y.-J., Song, J.-P., Li, Z.-Y., Kobayashi, K., Tsugane, S., Hamada, G.S., Tanaka, M., Sugimura, H., 2001. Genomic structure and loss of heterozygosity of EPHB2 in colorectal cancer. *Cancer Lett.* 164, 97–104. [https://doi.org/10.1016/S0304-3835\(00\)00716-3](https://doi.org/10.1016/S0304-3835(00)00716-3)
- O’Flanagan, C.H., Smith, L.A., McDonnell, S.B., Hursting, S.D., 2017a. When less may be more: calorie restriction and response to cancer therapy. *BMC Med.* 15, 106. <https://doi.org/10.1186/s12916-017-0873-x>
- O’Flanagan, C.H., Smith, L.A., McDonnell, S.B., Hursting, S.D., 2017b. When less may be more: calorie restriction and response to cancer therapy. *BMC Med.* 15, 106. <https://doi.org/10.1186/s12916-017-0873-x>
- Omar, H.A., Berman-Booty, L., Kulp, S.K., Chen, C.-S., 2010. Energy restriction as an antitumor target. *Future Oncol.* 6, 1675–1679. <https://doi.org/10.2217/fon.10.130>

- Overby, K.J., Litt, I.F., 1988. Mediastinal Emphysema in an Adolescent With Anorexia Nervosa and Self-Induced Emesis. *Pediatrics* 81, 134–136.
- Pagnotta, S.M., Laudanna, C., Pancione, M., Sabatino, L., Votino, C., Remo, A., Cerulo, L., Zoppoli, P., Manfrin, E., Colantuoni, V., Ceccarelli, M., 2013. Ensemble of gene signatures identifies novel biomarkers in colorectal cancer activated through PPAR γ and TNF α signaling. *PLoS One* 8, e72638. <https://doi.org/10.1371/journal.pone.0072638>
- Paik, S., Shak, S., Tang, G., Kim, C., Baker, J., Cronin, M., Baehner, F.L., Walker, M.G., Watson, D., Park, T., Hiller, W., Fisher, E.R., Wickerham, D.L., Bryant, J., Wolmark, N., 2004. A multigene assay to predict recurrence of tamoxifen-treated, node-negative breast cancer. *N. Engl. J. Med.* 351, 2817–2826. <https://doi.org/10.1056/NEJMoa041588>
- Palmer, N.D., Goodarzi, M.O., Langefeld, C.D., Wang, N., Guo, X., Taylor, K.D., Fingerlin, T.E., Norris, J.M., Buchanan, T.A., Xiang, A.H., Haritunians, T., Ziegler, J.T., Williams, A.H., Stefanovski, D., Cui, J., Mackay, A.W., Henkin, L.F., Bergman, R.N., Gao, X., Gauderman, J., Varma, R., Hanis, C.L., Cox, N.J., Highland, H.M., Below, J.E., Williams, A.L., Burt, N.P., Aguilar-Salinas, C.A., Huerta-Chagoya, A., Gonzalez-Villalpando, C., Orozco, L., Haiman, C.A., Tsai, M.Y., Johnson, W.C., Yao, J., Rasmussen-Torvik, L., Pankow, J., Snively, B., Jackson, R.D., Liu, S., Nadler, J.L., Kandeel, F., Chen, Y.-D.I., Bowden, D.W., Rich, S.S., Raffel, L.J., Rotter, J.I., Watanabe, R.M., Wagenknecht, L.E., 2015. Genetic Variants Associated With Quantitative Glucose Homeostasis Traits Translate to Type 2 Diabetes in Mexican Americans: The GUARDIAN (Genetics Underlying Diabetes in Hispanics) Consortium. *Diabetes* 64, 1853–1866. <https://doi.org/10.2337/db14-0732>
- Pan, M., Reid, M.A., Lowman, X.H., Kulkarni, R.P., Tran, T.Q., Liu, X., Yang, Y., Hernandez-Davies, J.E., Rosales, K.K., Li, H., 2016. Regional glutamine deficiency in tumours promotes dedifferentiation through inhibition of histone demethylation. *Nat. Cell Biol.* 18, 1090.
- Pelicano, H., Martin, D.S., Xu, R.-H., Huang, P., 2006. Glycolysis inhibition for anticancer treatment. *Oncogene* 25, 4633. <https://doi.org/10.1038/sj.onc.1209597>
- Pereira, M.A., Khoury, M.D., 1991. Prevention by chemopreventive agents of azoxymethane-induced foci of aberrant crypts in rat colon. *Cancer Lett.* 61, 27–33.
- Perou, C.M., Sørlie, T., Eisen, M.B., van de Rijn, M., Jeffrey, S.S., Rees, C.A., Pollack, J.R., Ross, D.T., Johnsen, H., Akslen, L.A., Fluge, O., Pergamenschikov, A., Williams, C., Zhu, S.X., Lønning, P.E., Børresen-Dale, A.L., Brown, P.O., Botstein, D., 2000. Molecular portraits of human breast tumours. *Nature* 406, 747–752. <https://doi.org/10.1038/35021093>
- Pillai, R.S., Bhattacharyya, S.N., Filipowicz, W., 2007. Repression of protein synthesis by miRNAs: how many mechanisms? *Trends Cell Biol.* 17, 118–126. <https://doi.org/10.1016/j.tcb.2006.12.007>
- Pino, M.S., Chung, D.C., 2010. The Chromosomal Instability Pathway in Colon Cancer. *Gastroenterology, Colon Cancer: An Update and Future Directions* 138, 2059–2072. <https://doi.org/10.1053/j.gastro.2009.12.065>
- Piowowski, J.P., Granica, S., Stefańska, J., Kiss, A.K., 2016. Differences in Metabolism of Ellagitannins by Human Gut Microbiota ex Vivo Cultures. *J. Nat. Prod.* 79, 3022–3030. <https://doi.org/10.1021/acs.jnatprod.6b00602>

- Platten, M., Wick, W., Van den Eynde, B.J., 2012. Tryptophan catabolism in cancer: beyond IDO and tryptophan depletion. *Cancer Res.* 72, 5435–5440.
- Podszycalowa-Bartnicka, P., Cmoch, A., Wolczyk, M., Bugajski, L., Tkaczyk, M., Dadlez, M., Nieborowska-Skorska, M., Koromilas, A.E., Skorski, T., Piwocka, K., 2016. Increased phosphorylation of eIF2 α in chronic myeloid leukemia cells stimulates secretion of matrix modifying enzymes. *Oncotarget* 7, 79706.
- Polakis, P., 2000. Wnt signaling and cancer. *Genes Dev.* 14, 1837–1851. <https://doi.org/10.1101/gad.14.15.1837>
- Potthast, R., Ehler, E., Scheving, L.A., Sindic, A., Schlatter, E., Kuhn, M., 2001. High Salt Intake Increases Uroguanylin Expression in Mouse Kidney. *Endocrinology* 142, 3087–3097. <https://doi.org/10.1210/endo.142.7.8274>
- Prado, C.M., Cushen, S.J., Orsso, C.E., Ryan, A.M., 2016. Sarcopenia and cachexia in the era of obesity: clinical and nutritional impact. *Proc. Nutr. Soc.* 75, 188–198.
- Pressoir, M., Desné, S., Berchery, D., Rossignol, G., Poiree, B., Meslier, M., Traversier, S., Vittot, M., Simon, M., Gekiere, J.P., 2010. Prevalence, risk factors and clinical implications of malnutrition in French Comprehensive Cancer Centres. *Br. J. Cancer* 102, 966.
- Pulaski, B.A., Ostrand-Rosenberg, S., 1998. Reduction of established spontaneous mammary carcinoma metastases following immunotherapy with major histocompatibility complex class II and B7.1 cell-based tumor vaccines. *Cancer Res.* 58, 1486–1493.
- Pundavela, J., Roselli, S., Faulkner, S., Attia, J., Scott, R.J., Thorne, R.F., Forbes, J.F., Bradshaw, R.A., Walker, M.M., Jobling, P., Hondermarck, H., 2015. Nerve fibers infiltrate the tumor microenvironment and are associated with nerve growth factor production and lymph node invasion in breast cancer. *Mol. Oncol.* 9, 1626–1635. <https://doi.org/10.1016/j.molonc.2015.05.001>
- Puupponen-Pimiä, R., Seppänen-Laakso, T., Kankainen, M., Maukonen, J., Törrönen, R., Kolehmainen, M., Leppänen, T., Moilanen, E., Nohynek, L., Aura, A.-M., Poutanen, K., Tomás-Barberán, F.A., Espín, J.C., Oksman-Caldentey, K.-M., 2013. Effects of ellagitannin-rich berries on blood lipids, gut microbiota, and urolithin production in human subjects with symptoms of metabolic syndrome. *Mol. Nutr. Food Res.* 57, 2258–2263. <https://doi.org/10.1002/mnfr.201300280>
- Qiu, Z., Zhou, B., Jin, L., Yu, H., Liu, L., Liu, Y., Qin, C., Xie, S., Zhu, F., 2013. In vitro antioxidant and antiproliferative effects of ellagic acid and its colonic metabolite, urolithins, on human bladder cancer T24 cells. *Food Chem. Toxicol. Int. J. Publ. Br. Ind. Biol. Res. Assoc.* 59, 428–437. <https://doi.org/10.1016/j.fct.2013.06.025>
- Qiu, Z., Zhou, J., Zhang, C., Cheng, Y., Hu, J., Zheng, G., 2018. Antiproliferative effect of urolithin A, the ellagic acid-derived colonic metabolite, on hepatocellular carcinoma HepG2.2.15 cells by targeting Lin28a/let-7a axis. *Braz. J. Med. Biol. Res.* 51. <https://doi.org/10.1590/1414-431X20187220>
- R Core Team, 2017. R: A language and environment for statistical computing. R Foundation for Statistical Computing, Vienna, Austria.
- Raffaghello, L., Lee, C., Safdie, F.M., Wei, M., Madia, F., Bianchi, G., Longo, V.D., 2008. Starvation-dependent differential stress resistance protects normal but not cancer cells against high-dose chemotherapy. *Proc. Natl. Acad. Sci.* 105, 8215–8220. <https://doi.org/10.1073/pnas.0708100105>

- Ramírez de Molina, A., Vargas, T., Molina, S., Sánchez, J., Martínez-Romero, J., González-Vallinas, M., Martín-Hernández, R., Sánchez-Martínez, R., Gómez de Cedrón, M., Dávalos, A., Calani, L., Del Rio, D., González-Sarrías, A., Espín, J.C., Tomás-Barberán, F.A., Reglero, G., 2015. The ellagic acid derivative 4,4'-di-O-methylellagic acid efficiently inhibits colon cancer cell growth through a mechanism involving WNT16. *J. Pharmacol. Exp. Ther.* 353, 433–444.
<https://doi.org/10.1124/jpet.114.221796>
- Ramirez de Molina, A., Vargas, T., Molina, S., Sanchez, J., Martinez-Romero, J., Gonzalez-Vallinas, M., Martin-Hernandez, R., Sanchez-Martinez, R., Gomez de Cedron, M., Davalos, A., Calani, L., Del Rio, D., Gonzalez-Sarrias, A., Espin, J.C., Tomas-Barberan, F.A., Reglero, G., 2015. The Ellagic Acid Derivative 4,4'-Di-O-Methylellagic Acid Efficiently Inhibits Colon Cancer Cell Growth through a Mechanism Involving WNT16. *J. Pharmacol. Exp. Ther.* 353, 433–444.
<https://doi.org/10.1124/jpet.114.221796>
- Rangan, P., Choi, I., Wei, M., Navarrete, G., Guen, E., Brandhorst, S., Enyati, N., Pasia, G., Maesincee, D., Ocon, V., Abdulridha, M., Longo, V.D., 2019. Fasting-Mimicking Diet Modulates Microbiota and Promotes Intestinal Regeneration to Reduce Inflammatory Bowel Disease Pathology. *Cell Rep.* 26, 2704-2719.e6.
<https://doi.org/10.1016/j.celrep.2019.02.019>
- Reddy, K.B., 2015. MicroRNA (miRNA) in cancer. *Cancer Cell Int.* 15, 38.
<https://doi.org/10.1186/s12935-015-0185-1>
- Reya, T., Clevers, H., 2005. Wnt signalling in stem cells and cancer. *Nature* 434, 843.
- Rhodes, D.R., Chinnaiyan, A.M., 2005. Integrative analysis of the cancer transcriptome. *Nat. Genet.* 37, S31.
- Rifaï, K., Judes, G., Idrissou, M., Daures, M., Bignon, Y.-J., Penault-Llorca, F., Bernard-Gallon, D., 2017. Dual SIRT1 expression patterns strongly suggests its bivalent role in human breast cancer. *Oncotarget* 8, 110922–110930.
<https://doi.org/10.18632/oncotarget.23006>
- Riley, D.J., Thakker-Varia, S., 1995. Effect of Diet on Lung Structure, Connective Tissue Metabolism and Gene Expression. *J. Nutr.* 125, 1657S-1660S.
https://doi.org/10.1093/jn/125.suppl_6.1657S
- Ritchie, M.E., Phipson, B., Wu, D., Hu, Y., Law, C.W., Shi, W., Smyth, G.K., 2015. limma powers differential expression analyses for RNA-sequencing and microarray studies. *Nucleic Acids Res.* 43, e47–e47. <https://doi.org/10.1093/nar/gkv007>
- Romo-Vaquero, M., García-Villalba, R., González-Sarrías, A., Beltrán, D., Tomás-Barberán, F.A., Espín, J.C., Selma, M.V., 2015. Interindividual variability in the human metabolism of ellagic acid: Contribution of *Gordonibacter* to urolithin production. *J. Funct. Foods* 17, 785–791.
<https://doi.org/10.1016/j.jff.2015.06.040>
- Ruvinsky, I., Sharon, N., Lerer, T., Cohen, H., Stolovich-Rain, M., Nir, T., Dor, Y., Zisman, P., Meyuhas, O., 2005. Ribosomal protein S6 phosphorylation is a determinant of cell size and glucose homeostasis. *Genes Dev.* 19, 2199–2211.
<https://doi.org/10.1101/gad.351605>
- Ryo, A., Nakamura, M., Wulf, G., Liou, Y.-C., Lu, K.P., 2001. Pin1 regulates turnover and subcellular localization of β -catenin by inhibiting its interaction with APC. *Nat. Cell Biol.* 3, 793.

- Sadanandam, A., Lyssiottis, C.A., Homicsko, K., Collisson, E.A., Gibb, W.J., Wullschleger, S., Ostos, L.C.G., Lannon, W.A., Grotzinger, C., Del Rio, M., Lhermitte, B., Olshen, A.B., Wiedenmann, B., Cantley, L.C., Gray, J.W., Hanahan, D., 2013. A colorectal cancer classification system that associates cellular phenotype and responses to therapy. *Nat. Med.* 19, 619–625. <https://doi.org/10.1038/nm.3175>
- Sadik, N.A.H., Shaker, O.G., 2013. Inhibitory Effect of a Standardized Pomegranate Fruit Extract on Wnt Signalling in 1, 2-Dimethylhydrazine Induced Rat Colon Carcinogenesis. *Dig. Dis. Sci.* 58, 2507–2517. <https://doi.org/10.1007/s10620-013-2704-z>
- Sancak, Y., Peterson, T.R., Shaul, Y.D., Lindquist, R.A., Thoreen, C.C., Bar-Peled, L., Sabatini, D.M., 2008. The Rag GTPases bind raptor and mediate amino acid signaling to mTORC1. *Science* 320, 1496–1501.
- Sánchez-González, C., Ciudad, C.J., Izquierdo-Pulido, M., Noé, V., 2016. Urolithin A causes p21 up-regulation in prostate cancer cells. *Eur. J. Nutr.* 55, 1099–1112. <https://doi.org/10.1007/s00394-015-0924-z>
- Sánchez-González, C., Ciudad, C.J., Noé, V., Izquierdo-Pulido, M., 2014. Walnut polyphenol metabolites, urolithins A and B, inhibit the expression of the prostate-specific antigen and the androgen receptor in prostate cancer cells. *Food Funct.* 5, 2922–2930. <https://doi.org/10.1039/c4fo00542b>
- Sánchez-Lara, K., Turcott, J.G., Juárez-Hernández, E., Nuñez-Valencia, C., Villanueva, G., Guevara, P., De la Torre-Vallejo, M., Mohar, A., Arrieta, O., 2014. Effects of an oral nutritional supplement containing eicosapentaenoic acid on nutritional and clinical outcomes in patients with advanced non-small cell lung cancer: randomised trial. *Clin. Nutr.* 33, 1017–1023.
- Saneyoshi, T., Kume, S., Amasaki, Y., Mikoshiba, K., 2002. The Wnt/calcium pathway activates NF-AT and promotes ventral cell fate in *Xenopus* embryos. *Nature* 417, 295.
- Sarver, A.L., French, A.J., Borralho, P.M., Thayanithy, V., Oberg, A.L., Silverstein, K.A., Morlan, B.W., Riska, S.M., Boardman, L.A., Cunningham, J.M., Subramanian, S., Wang, L., Smyrk, T.C., Rodrigues, C.M., Thibodeau, S.N., Steer, C.J., 2009. Human colon cancer profiles show differential microRNA expression depending on mismatch repair status and are characteristic of undifferentiated proliferative states. *BMC Cancer* 9, 401. <https://doi.org/10.1186/1471-2407-9-401>
- Saxton, R.A., Sabatini, D.M., 2017. mTOR signaling in growth, metabolism, and disease. *Cell* 168, 960–976.
- Scheuner, D., Song, B., McEwen, E., Liu, C., Laybutt, R., Gillespie, P., Saunders, T., Bonner-Weir, S., Kaufman, R.J., 2001. Translational control is required for the unfolded protein response and in vivo glucose homeostasis. *Mol. Cell* 7, 1165–1176.
- Schreinemachers, D.M., Everson, R.B., 1994. Aspirin Use and Lung, Colon, and Breast Cancer Incidence in a Prospective Study. *Epidemiology* 5, 138–146.
- Selesniemi, K., Lee, H.-J., Tilly, J.L., 2008. Moderate caloric restriction initiated in rodents during adulthood sustains function of the female reproductive axis into advanced chronological age. *Aging Cell* 7, 622–629. <https://doi.org/10.1111/j.1474-9726.2008.00409.x>
- Selma, M.V., Beltrán, D., García-Villalba, R., Espín, J.C., Tomás-Barberán, F.A., 2014a. Description of urolithin production capacity from ellagic acid of two human

- intestinal *Gordonibacter* species. *Food Funct.* 5, 1779–1784.
<https://doi.org/10.1039/c4fo00092g>
- Selma, M.V., Beltrán, D., Luna, M.C., Romo-Vaquero, M., García-Villalba, R., Mira, A., Espín, J.C., Tomás-Barberán, F.A., 2017. Isolation of Human Intestinal Bacteria Capable of Producing the Bioactive Metabolite Isourolithin A from Ellagic Acid. *Front. Microbiol.* 8, 1521. <https://doi.org/10.3389/fmicb.2017.01521>
- Selma, M.V., Tomás-Barberán, F.A., Beltrán, D., García-Villalba, R., Espín, J.C., 2014b. *Gordonibacter urolithinifaciens* sp. nov., a urolithin-producing bacterium isolated from the human gut. *Int. J. Syst. Evol. Microbiol.* 64, 2346–2352.
<https://doi.org/10.1099/ij.s.0.055095-0>
- SEOM, 2018. Las cifras del cancer en España.
- Sethi, J.K., Vidal-Puig, A.J., 2008. Wnt signalling at the crossroads of nutritional regulation. *Biochem. J.* 416, e11–e13.
- Seyfried, T.N., Kiebish, M., Mukherjee, P., Marsh, J., 2008. Targeting energy metabolism in brain cancer with calorically restricted ketogenic diets. *Epilepsia* 49, 114–116.
<https://doi.org/10.1111/j.1528-1167.2008.01853.x>
- Sharma, M., Li, L., Cerver, J., Killian, C., Koor, A., Seeram, N.P., 2010a. Effects of fruit ellagitannin extracts, ellagic acid, and their colonic metabolite, urolithin A, on Wnt signaling. *J. Agric. Food Chem.* 58, 3965–3969.
<https://doi.org/10.1021/jf902857v>
- Sharma, M., Li, L., Cerver, J., Killian, C., Koor, A., Seeram, N.P., 2010b. Effects of fruit ellagitannin extracts, ellagic acid, and their colonic metabolite, urolithin A, on Wnt signaling. *J. Agric. Food Chem.* 58, 3965–3969.
<https://doi.org/10.1021/jf902857v>
- Siegel, R.L., Miller, K.D., Fedewa, S.A., Ahnen, D.J., Meester, R.G.S., Barzi, A., Jemal, A., 2017. Colorectal cancer statistics, 2017. *CA. Cancer J. Clin.* 67, 177–193.
<https://doi.org/10.3322/caac.21395>
- Simmons, R.A., 2017. 43 - Cell Glucose Transport and Glucose Handling During Fetal and Neonatal Development, in: Polin, R.A., Abman, S.H., Rowitch, D.H., Benitz, W.E., Fox, W.W. (Eds.), *Fetal and Neonatal Physiology (Fifth Edition)*. Elsevier, pp. 428-435.e3. <https://doi.org/10.1016/B978-0-323-35214-7.00043-3>
- Simon, N., Friedman, J., Hastie, T., Tibshirani, R., 2011. Regularization paths for Cox's proportional hazards model via coordinate descent. *J. Stat. Softw.* 39, 1.
- Simone, B.A., Dan, T., Palagani, A., Jin, L., Han, S.Y., Wright, C., Savage, J.E., Gitman, R., Lim, M.K., Palazzo, J., Mehta, M.P., Simone, N.L., 2016. Caloric restriction coupled with radiation decreases metastatic burden in triple negative breast cancer. *Cell Cycle* 15, 2265–2274. <https://doi.org/10.1080/15384101.2016.1160982>
- Simpson, I.A., Dwyer, D., Malide, D., Moley, K.H., Travis, A., Vannucci, S.J., 2008. The facilitative glucose transporter GLUT3: 20 years of distinction. *Am. J. Physiol. - Endocrinol. Metab.* 295, E242–E253.
<https://doi.org/10.1152/ajpendo.90388.2008>
- Simpson, S.J., Le Couteur, D.G., Raubenheimer, D., Solon-Biet, S.M., Cooney, G.J., Cogger, V.C., Fontana, L., 2017. Dietary protein, aging and nutritional geometry. *Ageing Res. Rev.* 39, 78–86. <https://doi.org/10.1016/j.arr.2017.03.001>
- Smart, R.C., Huang, M.T., Chang, R.L., Sayer, J.M., Jerina, D.M., Conney, A.H., 1986. Disposition of the naturally occurring antimutagenic plant phenol, ellagic acid,

- and its synthetic derivatives, 3-O-decylellagic acid and 3,3'-di-O-methylellagic acid in mice. *Carcinogenesis* 7, 1663–1667.
- Snover, D.C., 2011. Update on the serrated pathway to colorectal carcinoma. *Hum. Pathol.* 42, 1–10. <https://doi.org/10.1016/j.humpath.2010.06.002>
- Sriskanthadevan, S., Jeyaraju, D.V., Chung, T.E., Prabha, S., Xu, W., Skrtic, M., Jhas, B., Hurren, R., Gronda, M., Wang, X., Jitkova, Y., Sukhai, M.A., Lin, F.-H., Maclean, N., Laister, R., Goard, C.A., Mullen, P.J., Xie, S., Penn, L.Z., Rogers, I.M., Dick, J.E., Minden, M.D., Schimmer, A.D., 2015. AML cells have low spare reserve capacity in their respiratory chain that renders them susceptible to oxidative metabolic stress. *Blood* 125, 2120–2130. <https://doi.org/10.1182/blood-2014-08-594408>
- Staal, F.J., Luis, T.C., Tiemessen, M.M., 2008. WNT signalling in the immune system: WNT is spreading its wings. *Nat. Rev. Immunol.* 8, 581.
- Stacker, S.A., Williams, S.P., Karnezis, T., Shayan, R., Fox, S.B., Achen, M.G., 2014. Lymphangiogenesis and lymphatic vessel remodelling in cancer. *Nat. Rev. Cancer* 14, 159–172. <https://doi.org/10.1038/nrc3677>
- Stanley H, Lauri A, S.H., 2000. WHO Pathology and Genetics of Tumours of the Digestive System. International Agency for Research on Cancer (IARC) Press, Lyon.
- Steelman, L.S., Martelli, A.M., Cocco, L., Libra, M., Nicoletti, F., Abrams, S.L., McCubrey, J.A., 2016. The therapeutic potential of mTOR inhibitors in breast cancer. *Br. J. Clin. Pharmacol.* 1189–1212. [https://doi.org/10.1111/bcp.12958@10.1111/\(ISSN\)1365-2125.NorthAmericaVirtualIssueNov2016](https://doi.org/10.1111/bcp.12958@10.1111/(ISSN)1365-2125.NorthAmericaVirtualIssueNov2016)
- Stratton, M.R., Campbell, P.J., Futreal, P.A., 2009. The cancer genome. *Nature* 458, 719. <https://doi.org/10.1038/nature07943>
- Sullivan, L.B., Luengo, A., Danaï, L.V., Bush, L.N., Diehl, F.F., Hosios, A.M., Lau, A.N., Elmiligy, S., Malstrom, S., Lewis, C.A., 2018. Aspartate is an endogenous metabolic limitation for tumour growth. *Nat. Cell Biol.* 20, 782.
- Sun, Y., Campisi, J., Higano, C., Beer, T.M., Porter, P., Coleman, I., True, L., Nelson, P.S., 2012. Treatment-induced damage to the tumor microenvironment promotes prostate cancer therapy resistance through WNT16B. *Nat. Med.* 18, 1359–1368. <https://doi.org/10.1038/nm.2890>
- Sunpaweravong, S., Puttawibul, P., Ruangsing, S., Laohawiriyakamol, S., Sunpaweravong, P., Sangthawan, D., Pradutkanchana, J., Raungkhajorn, P., Geater, A., 2014. Randomized study of antiinflammatory and immune-modulatory effects of enteral immunonutrition during concurrent chemoradiotherapy for esophageal cancer. *Nutr. Cancer* 66, 1–5.
- Sutendra, G., Michelakis, E.D., 2013. Pyruvate dehydrogenase kinase as a novel therapeutic target in oncology. *Front. Oncol.* 3. <https://doi.org/10.3389/fonc.2013.00038>
- Suzuki, K., Hayashi, R., Ichikawa, T., Imanishi, S., Yamada, T., Inomata, M., Miwa, T., Matsui, S., Usui, I., Urakaze, M., Matsuya, Y., Ogawa, H., Sakurai, H., Saiki, I., Tobe, K., 2012. SRT1720, a SIRT1 activator, promotes tumor cell migration, and lung metastasis of breast cancer in mice. *Oncol. Rep.* 27, 1726–1732. <https://doi.org/10.3892/or.2012.1750>
- Suzuki, R., Orsini, N., Saji, S., Key, T.J., Wolk, A., 2009. Body weight and incidence of breast cancer defined by estrogen and progesterone receptor status—a meta-analysis. *Int. J. Cancer* 124, 698–712.

- Szczuka, I., Gamian, A., Terlecki, G., 2017. 3-Bromopyruvate as a potential pharmaceutical in the light of experimental data. *Postepy Hig. Med. Doswiadczalnej Online* 71, 988–996. <https://doi.org/10.5604/01.3001.0010.6666>
- Sztupinski, Z., Gyórfy, B., 2016. Colon cancer subtypes: concordance, effect on survival and selection of the most representative preclinical models. *Sci. Rep.* 6, 37169. <https://doi.org/10.1038/srep37169>
- Tabara, H., Sarkissian, M., Kelly, W.G., Fleenor, J., Grishok, A., Timmons, L., Fire, A., Mello, C.C., 1999. The rde-1 Gene, RNA Interference, and Transposon Silencing in *C. elegans*. *Cell* 99, 123–132. [https://doi.org/10.1016/S0092-8674\(00\)81644-X](https://doi.org/10.1016/S0092-8674(00)81644-X)
- Talvas, J., Garrait, G., Goncalves-Mendes, N., Rouanet, J., Vergnaud-Gauduchon, J., Kwiatkowski, F., Bachmann, P., Bouteloup, C., Bienvenu, J., Vasson, M.-P., 2015. Immunonutrition stimulates immune functions and antioxidant defense capacities of leukocytes in radiochemotherapy-treated head & neck and esophageal cancer patients: a double-blind randomized clinical trial. *Clin. Nutr.* 34, 810–817.
- Taminau, J., Taminau, M.J., Meganck, S., BiocGenerics, S., 2013. Package 'inSilicoMerging.' Citeseer.
- Tannenbaum A, 1940. The initiation and growth of tumors. Introduction I. Effects of underfeeding. *Am J Cancer* 335–350.
- Taube, J.H., Malouf, G.G., Lu, E., Sphyris, N., Vijay, V., Ramachandran, P.P., Ueno, K.R., Gaur, S., Nicoloso, M.S., Rossi, S., Herschkowitz, J.I., Rosen, J.M., Issa, J.-P.J., Calin, G.A., Chang, J.T., Mani, S.A., 2013. Epigenetic silencing of microRNA-203 is required for EMT and cancer stem cell properties. *Sci. Rep.* 3, 2687.
- Teel, R.W., 1986. Ellagic acid binding to DNA as a possible mechanism for its antimutagenic and anticarcinogenic action. *Cancer Lett.* 30, 329–336.
- Therneau, T.M., Grambsch, P.M., 2013. Modeling survival data: extending the Cox model. Springer Science & Business Media.
- Tian, W., Wang, Y., Xu, Y., Guo, X., Wang, B., Sun, L., Liu, L., Cui, F., Zhuang, Q., Bao, X., 2014. The hypoxia-inducible factor renders cancer cells more sensitive to vitamin C-induced toxicity. *J. Biol. Chem.* 289, 3339–3351.
- Tilly, J.L., Sinclair, D.A., 2013. Germline Energetics, Aging, and Female Infertility. *Cell Metab.* 17, 838–850. <https://doi.org/10.1016/j.cmet.2013.05.007>
- Timosenko, E., Ghadbane, H., Silk, J.D., Shepherd, D., Gileadi, U., Howson, L.J., Laynes, R., Zhao, Q., Strausberg, R.L., Olsen, L.R., 2016. Nutritional stress induced by tryptophan-degrading enzymes results in ATF4-dependent reprogramming of the amino acid transporter profile in tumor cells. *Cancer Res.* 76, 6193–6204.
- Toker, A., Marmiroli, S., 2014. Signaling specificity in the Akt pathway in biology and disease. *Adv. Biol. Regul.* 55, 28–38. <https://doi.org/10.1016/j.jbior.2014.04.001>
- Toledo, E., Salas-Salvadó, J., Donat-Vargas, C., Buil-Cosiales, P., Estruch, R., Ros, E., Corella, D., Fitó, M., Hu, F.B., Arós, F., Gómez-Gracia, E., Romaguera, D., Ortega-Calvo, M., Serra-Majem, L., Pintó, X., Schröder, H., Basora, J., Sorlí, J.V., Bulló, M., Serra-Mir, M., Martínez-González, M.A., 2015. Mediterranean Diet and Invasive Breast Cancer Risk Among Women at High Cardiovascular Risk in the PREDIMED Trial: A Randomized Clinical Trial. *JAMA Intern. Med.* 175, 1752–1760. <https://doi.org/10.1001/jamainternmed.2015.4838>
- Tomás-Barberan, F.A., Espín, J.C., García-Conesa, M.T., 2009. Bioavailability and Metabolism of Ellagic Acid and Ellagitannins, in: *Chemistry and Biology of*

- Ellagitannins. *WORLD SCIENTIFIC*, pp. 273–297.
https://doi.org/10.1142/9789812797414_0007
- Tomás-Barberán, F.A., García-Villalba, R., González-Sarrías, A., Selma, M.V., Espín, J.C., 2014. Ellagic acid metabolism by human gut microbiota: consistent observation of three urolithin phenotypes in intervention trials, independent of food source, age, and health status. *J. Agric. Food Chem.* 62, 6535–6538.
<https://doi.org/10.1021/jf5024615>
- Tomás-Barberán, F.A., González-Sarrías, A., García-Villalba, R., Núñez-Sánchez, M.A., Selma, M.V., García-Conesa, M.T., Espín, J.C., 2017. Urolithins, the rescue of “old” metabolites to understand a “new” concept: Metabotypes as a nexus among phenolic metabolism, microbiota dysbiosis, and host health status. *Mol. Nutr. Food Res.* 61. <https://doi.org/10.1002/mnfr.201500901>
- Tomasetti, C., Li, L., Vogelstein, B., 2017. Stem cell divisions, somatic mutations, cancer etiology, and cancer prevention. *Science* 355, 1330–1334.
<https://doi.org/10.1126/science.aaf9011>
- Torregrosa, D., Bolufer, P., Lluch, A., López, J.A., Barragán, E., Ruiz, A., Guillem, V., Munárriz, B., García Conde, J., 1997. Prognostic significance of c-erbB-2/neu amplification and epidermal growth factor receptor (EGFR) in primary breast cancer and their relation to estradiol receptor (ER) status. *Clin. Chim. Acta Int. J. Clin. Chem.* 262, 99–119.
- Truchado, P., Larrosa, M., García-Conesa, M.T., Cerdá, B., Vidal-Guevara, M.L., Tomás-Barberán, F.A., Espín, J.C., 2012. Strawberry processing does not affect the production and urinary excretion of urolithins, ellagic acid metabolites, in humans. *J. Agric. Food Chem.* 60, 5749–5754. <https://doi.org/10.1021/jf203641r>
- Tsugane, S., Sawada, N., 2014. The JPHC Study: Design and Some Findings on the Typical Japanese Diet. *Jpn. J. Clin. Oncol.* 44, 777–782.
<https://doi.org/10.1093/jjco/hyu096>
- Tucci, P., 2012. Caloric restriction: is mammalian life extension linked to p53? *Aging* 4, 525–534.
- Umesalma, S., Nagendraprabhu, P., Sudhandiran, G., 2015. Ellagic acid inhibits proliferation and induced apoptosis via the Akt signaling pathway in HCT-15 colon adenocarcinoma cells. *Mol. Cell. Biochem.* 399, 303–313.
<https://doi.org/10.1007/s11010-014-2257-2>
- Umesalma, S., Nagendraprabhu, P., Sudhandiran, G., 2014. Antiproliferative and apoptotic-inducing potential of ellagic acid against 1,2-dimethyl hydrazine-induced colon tumorigenesis in Wistar rats. *Mol. Cell. Biochem.* 388, 157–172.
<https://doi.org/10.1007/s11010-013-1907-0>
- Umesalma, S., Sudhandiran, G., 2011. Ellagic acid prevents rat colon carcinogenesis induced by 1, 2 dimethyl hydrazine through inhibition of AKT-phosphoinositide-3 kinase pathway. *Eur. J. Pharmacol.* 660, 249–258.
<https://doi.org/10.1016/j.ejphar.2011.03.036>
- Umesalma, S., Sudhandiran, G., 2010. Differential inhibitory effects of the polyphenol ellagic acid on inflammatory mediators NF-kappaB, iNOS, COX-2, TNF-alpha, and IL-6 in 1,2-dimethylhydrazine-induced rat colon carcinogenesis. *Basic Clin. Pharmacol. Toxicol.* 107, 650–655. <https://doi.org/10.1111/j.1742-7843.2010.00565.x>

- Vamecq, J., Colet, J.-M., Vanden Eynde, J.J., Briand, G., Porchet, N., Rocchi, S., 2012. PPARs: Interference with Warburg' Effect and Clinical Anticancer Trials [WWW Document]. PPAR Res. <https://doi.org/10.1155/2012/304760>
- Van der Meij, B.S., Langius, J.A., Spreeuwenberg, M.D., Slootmaker, S.M., Paul, M.A., Smit, E.F., van Leeuwen, P.A., 2012. Oral nutritional supplements containing n-3 polyunsaturated fatty acids affect quality of life and functional status in lung cancer patients during multimodality treatment: an RCT. *Eur. J. Clin. Nutr.* 66, 399.
- van Lieshout, E.M., Bedaf, M.M., Pieter, M., Ekkel, C., Nijhoff, W.A., Peters, W.H., 1998. Effects of dietary anticarcinogens on rat gastrointestinal glutathione S-transferase theta 1-1 levels. *Carcinogenesis* 19, 2055–2057.
- Vasson, M.-P., Talvas, J., Perche, O., Dillies, A.-F., Bachmann, P., Pezet, D., Achim, A.-C., Pommier, P., Racadot, S., Weber, A., 2014. Immunonutrition improves functional capacities in head and neck and esophageal cancer patients undergoing radiochemotherapy: a randomized clinical trial. *Clin. Nutr.* 33, 204–210.
- Vecchia, C.L., 2004. Mediterranean diet and cancer. *Public Health Nutr.* 7, 965–968. <https://doi.org/10.1079/PHN2004562>
- Veeman, M.T., Axelrod, J.D., Moon, R.T., 2003. A Second Canon: Functions and Mechanisms of β -Catenin-Independent Wnt Signaling. *Dev. Cell* 5, 367–377. [https://doi.org/10.1016/S1534-5807\(03\)00266-1](https://doi.org/10.1016/S1534-5807(03)00266-1)
- Veer, L.J. van 't, Dai, H., Vijver, M.J. van de, He, Y.D., Hart, A.A.M., Mao, M., Peterse, H.L., Kooy, K. van der, Marton, M.J., Witteveen, A.T., Schreiber, G.J., Kerkhoven, R.M., Roberts, C., Linsley, P.S., Bernards, R., Friend, S.H., 2002. Gene expression profiling predicts clinical outcome of breast cancer. *Nature* 415, 530. <https://doi.org/10.1038/415530a>
- Veronesi, U., Viale, G., Rotmensz, N., Goldhirsch, A., 2006. Rethinking TNM: breast cancer TNM classification for treatment decision-making and research. *Breast Edinb. Scotl.* 15, 3–8. <https://doi.org/10.1016/j.breast.2005.11.011>
- Vicinanza, R., Zhang, Y., Henning, S.M., Heber, D., 2013. Pomegranate Juice Metabolites, Ellagic Acid and Urolithin A, Synergistically Inhibit Androgen-Independent Prostate Cancer Cell Growth via Distinct Effects on Cell Cycle Control and Apoptosis. *Evid.-Based Complement. Altern. Med. ECAM* 2013, 247504. <https://doi.org/10.1155/2013/247504>
- Vidali, S., Aminzadeh, S., Lambert, B., Rutherford, T., Sperl, W., Kofler, B., Feichtinger, R.G., 2015. Mitochondria: The ketogenic diet--A metabolism-based therapy. *Int. J. Biochem. Cell Biol.* 63, 55–59. <https://doi.org/10.1016/j.biocel.2015.01.022>
- Vogelstein, B., Kinzler, K.W., 2004. Cancer genes and the pathways they control. *Nat. Med.* 10, 789. <https://doi.org/10.1038/nm1087>
- Volinia, S., Calin, G.A., Liu, C.-G., Ambs, S., Cimmino, A., Petrocca, F., Visone, R., Iorio, M., Roldo, C., Ferracin, M., Prueitt, R.L., Yanaihara, N., Lanza, G., Scarpa, A., Vecchione, A., Negrini, M., Harris, C.C., Croce, C.M., 2006. A microRNA expression signature of human solid tumors defines cancer gene targets. *Proc. Natl. Acad. Sci.* 103, 2257–2261. <https://doi.org/10.1073/pnas.0510565103>
- Wahnefried, W., Rimer, B.K., Winer, E.P., 1997. Weight Gain in Women Diagnosed with Breast Cancer. *J. Am. Diet. Assoc.* 97, 519–529. [https://doi.org/10.1016/S0002-8223\(97\)00133-8](https://doi.org/10.1016/S0002-8223(97)00133-8)

- Wang, L., Xiao, X., Li, D., Chi, Y., Wei, P., Wang, Y., Ni, S., Tan, C., Zhou, X., Du, X., 2012. Abnormal expression of GADD45B in human colorectal carcinoma. *J. Transl. Med.* 10, 215. <https://doi.org/10.1186/1479-5876-10-215>
- Wang, Y., Qiu, Z., Zhou, B., Liu, C., Ruan, J., Yan, Q., Liao, J., Zhu, F., 2015. In vitro antiproliferative and antioxidant effects of urolithin A, the colonic metabolite of ellagic acid, on hepatocellular carcinomas HepG2 cells. *Toxicol. Vitro Int. J. Publ. Assoc. BIBRA* 29, 1107–1115. <https://doi.org/10.1016/j.tiv.2015.04.008>
- Wang, Z., Liu, P., Chen, Q., Deng, S., Liu, X., Situ, H., Zhong, S., Hann, S., Lin, Y., 2016. Targeting AMPK Signaling Pathway to Overcome Drug Resistance for Cancer Therapy [WWW Document]. URL <https://www.ingentaconnect.com/contentone/ben/cdt/2016/00000017/00000008/art00004> (accessed 5.6.19).
- Warburg, O., 1956. On the Origin of Cancer Cells. *Science* 123, 309–314.
- Watanabe, M., Naraba, H., Sakyo, T., Kitagawa, T., 2010. DNA damage-induced modulation of GLUT3 expression is mediated through p53-independent extracellular signal-regulated kinase signaling in HeLa cells. *Mol. Cancer Res. MCR* 8, 1547–1557. <https://doi.org/10.1158/1541-7786.MCR-10-0011>
- Waterman, P.G., Mole, S., 1994. *Analysis of Phenolic Plant Metabolites*. Wiley.
- WCRF, 2018. Breast cancer statistics [WWW Document]. *World Cancer Res. Fund.* URL <https://www.wcrf.org/dietandcancer/cancer-trends/breast-cancer-statistics> (accessed 5.2.19).
- Weigelt, B., Mackay, A., A'hern, R., Natrajan, R., Tan, D.S.P., Dowsett, M., Ashworth, A., Reis-Filho, J.S., 2010. Breast cancer molecular profiling with single sample predictors: a retrospective analysis. *Lancet Oncol.* 11, 339–349. [https://doi.org/10.1016/S1470-2045\(10\)70008-5](https://doi.org/10.1016/S1470-2045(10)70008-5)
- Weindruch, R., Walford, R.L., 1982. Dietary restriction in mice beginning at 1 year of age: effect on life-span and spontaneous cancer incidence. *Science* 215, 1415–1418.
- WHO, 2019. WHO. Cancer facts.
- Widschwendter, P., Friedl, T.W., Schwentner, L., DeGregorio, N., Jaeger, B., Schramm, A., Bekes, I., Deniz, M., Lato, K., Weissenbacher, T., 2015. The influence of obesity on survival in early, high-risk breast cancer: results from the randomized SUCCESS A trial. *Breast Cancer Res.* 17, 129.
- Wilkins, M.R., Redondo, J., Brown, L.A., 1997. The natriuretic-peptide family. *Lancet Lond. Engl.* 349, 1307–1310. [https://doi.org/10.1016/S0140-6736\(96\)07424-7](https://doi.org/10.1016/S0140-6736(96)07424-7)
- Wilson, D.O., Rogers, R.M., Hoffman, R.M., 1985. Nutrition and chronic lung disease. *Am. Rev. Respir. Dis.* 132, 1347–1365.
- Winer, L.S.P., Wu, M., 2014. Rapid Analysis of Glycolytic and Oxidative Substrate Flux of Cancer Cells in a Microplate. *PLOS ONE* 9, e109916. <https://doi.org/10.1371/journal.pone.0109916>
- Wu, M., Wang, Q., McKinstry, W.J., Ren, B., 2015. Characterization of a tannin acyl hydrolase from *Streptomyces sviveus* with substrate preference for digalloyl ester bonds. *Appl. Microbiol. Biotechnol.* 99, 2663–2672. <https://doi.org/10.1007/s00253-014-6085-9>
- Wu, W.-S., 2006. The signaling mechanism of ROS in tumor progression. *Cancer Metastasis Rev.* 25, 695–705.
- Xu, X.M., Qian, J.C., Deng, Z.L., Cai, Z., Tang, T., Wang, P., Zhang, K.H., Cai, J.-P., 2012. Expression of miR-21, miR-31, miR-96 and miR-135b is correlated with the clinical

- parameters of colorectal cancer. *Oncol. Lett.* 4, 339–345.
<https://doi.org/10.3892/ol.2012.714>
- Yamamoto-Ibusuki, M., Arnedos, M., André, F., 2015. Targeted therapies for ER+/HER2-metastatic breast cancer. *BMC Med.* 13, 137. <https://doi.org/10.1186/s12916-015-0369-5>
- Yang, W., Ma, Y., Smith-Warner, S., Song, M., Wu, K., Wang, M., Chan, A.T., Ogino, S., Fuchs, C.S., Poylin, V., Ng, K., Meyerhardt, J.A., Giovannucci, E.L., Zhang, X., 2019. Calcium Intake and Survival after Colorectal Cancer Diagnosis. *Clin. Cancer Res.* 25, 1980–1988. <https://doi.org/10.1158/1078-0432.CCR-18-2965>
- Yee, D., 2018. 40 YEARS OF IGF1: Anti-insulin-like growth factor therapy in breast cancer. *J. Mol. Endocrinol.* 61, T61–T68. <https://doi.org/10.1530/JME-17-0261>
- Yousef, A.I., El-Masry, O.S., Abdel Mohsen, M.A., 2016. Impact of Cellular Genetic Make-up on Colorectal Cancer Cell Lines Response to Ellagic Acid: Implications of Small Interfering RNA. *Asian Pac. J. Cancer Prev. APJCP* 17, 743–748.
- Zamore, P.D., 2006. RNA Interference: Big Applause for Silencing in Stockholm. *Cell* 127, 1083–1086. <https://doi.org/10.1016/j.cell.2006.12.001>
- Zhan, T., Rindtorff, N., Boutros, M., 2017. Wnt signaling in cancer. *Oncogene* 36, 1461.
- Zhang, K., Kaufman, R.J., 2006. The unfolded protein response: a stress signaling pathway critical for health and disease. *Neurology* 66, S102-109.
<https://doi.org/10.1212/01.wnl.0000192306.98198.ec>
- Zhao, W., Shi, F., Guo, Z., Zhao, J., Song, X., Yang, H., 2018. Metabolite of ellagitannins, urolithin A induces autophagy and inhibits metastasis in human sw620 colorectal cancer cells. *Mol. Carcinog.* 57, 193–200. <https://doi.org/10.1002/mc.22746>
- Zheng, Y., Wang, C., Zhang, H., Shao, C., Gao, L.-H., Li, S.-S., Yu, W.-J., He, J.-W., Fu, W.-Z., Hu, Y.-Q., 2016. Polymorphisms in Wnt signaling pathway genes are associated with peak bone mineral density, lean mass, and fat mass in Chinese male nuclear families. *Osteoporos. Int.* 27, 1805–1815.
- Zhuang, Y., Chan, D.K., Haugrud, A.B., Miskimins, W.K., 2014. Mechanisms by Which Low Glucose Enhances the Cytotoxicity of Metformin to Cancer Cells Both In Vitro and In Vivo. *PLOS ONE* 9, e108444. <https://doi.org/10.1371/journal.pone.0108444>

10. Publications and posters

Parts of this dissertation appeared in the following publications:

10.1. Paper 1: BMC Genomics: “Gene markers of colorectal cancer survival derived from consistent transcriptomic profiling”

Jorge Martinez-Romero, Santiago Bueno-Fortes, Manuel Martín-Merino, Ana Ramirez de Molina & Javier De Las Rivas.

<https://bmcbgenomics.biomedcentral.com/articles/10.1186/s12864-018-5193-9>

Abstract

Background

Identification of biomarkers associated with the prognosis of different cancer subtypes is critical to achieve better therapeutic assistance. In colorectal cancer (CRC) the discovery of stable and consistent survival markers remains a challenge due to the high heterogeneity of this class of tumors. In this work, we identified a new set of gene markers for CRC associated to prognosis and risk using a large unified cohort of patients with transcriptomic profiles and survival information.

Results

We built an integrated dataset with 1273 human colorectal samples, which provides a homogeneous robust framework to analyze genome-wide expression and survival data. Using this dataset, we identified two sets of genes that are candidate prognostic markers for CRC in stages III and IV, showing either up-regulation correlated with poor prognosis or up-regulation correlated with good prognosis. The top 10 up-regulated genes found as survival markers of poor prognosis (i.e. low survival) were: DCBLD2, PTPN14, LAMP5, TM4SF1, NPR3, LEMD1, LCA5, CSGALNACT2, SLC2A3 and GADD45B. The stability and robustness of the gene survival markers was assessed by cross-validation, and the best-ranked genes were also validated with two external independent cohorts: one of microarrays with 482 samples; another of RNA-seq with 269 samples. Up-regulation of the top genes was also proved in a comparison with normal colorectal tissue samples. Finally, the set of top 100 genes that showed overexpression correlated with low survival was used to build a CRC risk predictor applying a multivariate Cox proportional hazards regression analysis. This risk predictor yielded an optimal separation of the individual patients of the cohort according to their survival, with a p-value of $8.25e-14$ and Hazard Ratio 2.14 (95% CI: 1.75–2.61).

Conclusions

The results presented in this work provide a solid rationale for the prognostic utility of a new set of genes in CRC, demonstrating their potential to predict colorectal tumor progression and evolution towards poor survival stages. Our study does not provide a fixed gene signature for prognosis and risk prediction, but instead proposes a robust set of genes ranked according to their predictive power that can be selected for additional tests with other CRC clinical cohorts.

10.2. Paper 2: Journal of Pharmacology: “The Ellagic Acid Derivative 4,4’-Di-O-Methylellagic Acid Efficiently Inhibits Colon Cancer Cell Growth through a Mechanism involving Wnt16”

Ana Ramírez de Molina, Teodoro Vargas, Susana Molina, Jenifer Sánchez, Jorge Martínez-Romero, Margarita González-Vallinas, Roberto Martín-Hernández, Ruth Sánchez-Martínez, Marta Gómez de Cedrón, Alberto Dávalos, Luca Calani, Daniele Del Rio, Antonio González-Sarrias, Juan Carlos Espín, Francisco A. Tomás-Barberán and Guillermo Reglero.

Journal of Pharmacology and Experimental Therapeutics May 2015, 353 (2) 433-444; DOI: <https://doi.org/10.1124/jpet.114.221796>

<http://jpet.aspetjournals.org/content/353/2/433>

Abstract

Ellagic acid (EA) and some derivatives have been reported to inhibit cancer cell proliferation, induce cell cycle arrest, and modulate some important cellular processes related to cancer. This study aimed to identify possible structure-activity relationships of EA and some in vivo derivatives in their antiproliferative effect on both human colon cancer and normal cells, and to compare this activity with that of other polyphenols. Our results showed that 4,4’-di-O-methylellagic acid (4,4’-DiOMEA) was the most effective compound in the inhibition of colon cancer cell proliferation. 4,4’-DiOMEA was 13-fold more effective than other compounds of the same family. In addition, 4,4’-DiOMEA was very active against colon cancer cells resistant to the chemotherapeutic agent 5-fluoracil, whereas no effect was observed in nonmalignant colon cells. Moreover, no correlation between antiproliferative and antioxidant activities was found, further supporting that structure differences might result in dissimilar molecular targets involved in their differential effects. Finally, microarray analysis revealed that 4,4’-DiOMEA modulated Wnt signaling, which might be involved in the potential antitumor action of this compound. Our results suggest that structural-activity differences between EA and 4,4’-DiOMEA might constitute the basis for a new strategy in anticancer drug discovery based on these chemical modifications.

10.3. Poster at NIA-NIH: "Cancer Protection by the fasting mimicking diet; composition, calories or fasting time?"

Nelson Castillo-Rivera, Alberto Diaz-Ruiz, Jorge Martinez-Romero, Tyler Rhinesmith, Monica Bodogai, Margaux Ehrlich, Jacqueline Moats, Michael Leone, Arya Biragyn, Isabel Beerman, Michel Bernier, Rafael de Cabo

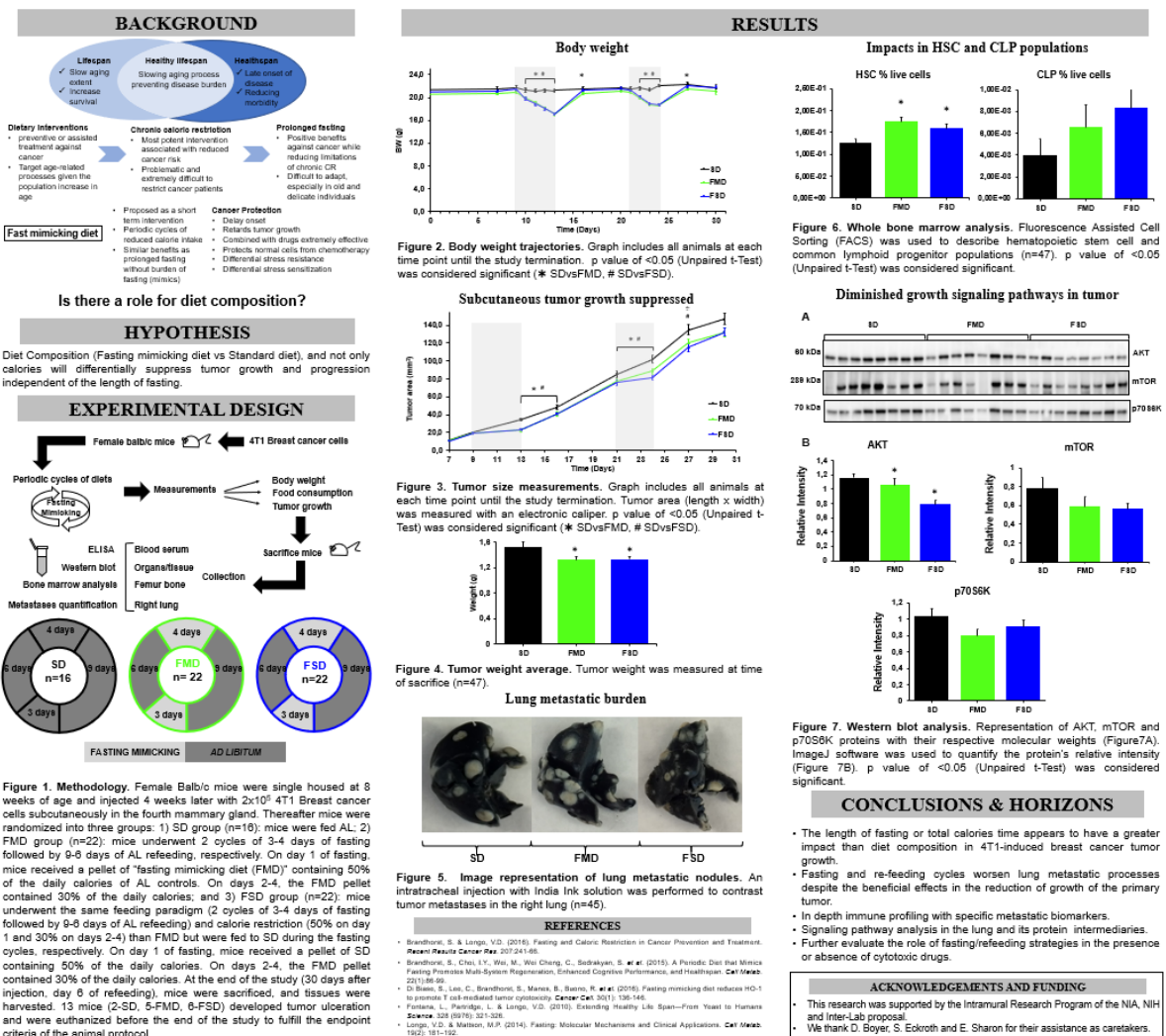
Translational Gerontology Branch, National Institute on Aging, National Institutes of Health, 251 Bayview Boulevard, Suite 100, Baltimore, MD 21224, USA. 2018



Cancer protection by the fasting mimicking diet; Composition, Calories or Fasting Time?

Nelson Castillo-Rivera, Alberto Diaz Ruiz, Jorge Martinez Romero, Tyler Rhinesmith, Monica Bodogai, Margaux Ehrlich, Jacqueline Moats, Michael Leone, Arya Biragyn, Isabel Beerman, Michel Bernier, Rafael de Cabo

Translational Gerontology Branch, National Institute on Aging, National Institutes of Health, 251 Bayview Boulevard, Suite 100, Baltimore, MD 21224, USA



CONCLUSIONS & HORIZONS

- The length of fasting or total calories time appears to have a greater impact than diet composition in 4T1-induced breast cancer tumor growth.
- Fasting and re-feeding cycles worsen lung metastatic processes despite the beneficial effects in the reduction of growth of the primary tumor.
- In depth immune profiling with specific metastatic biomarkers.
- Signaling pathway analysis in the lung and its protein intermediaries.
- Further evaluate the role of fasting/refeeding strategies in the presence or absence of cytotoxic drugs.

ACKNOWLEDGEMENTS AND FUNDING

- This research was supported by the Intramural Research Program of the NIA, NIH and Inter-Lab proposal.
- We thank D. Boyer, S. Ekroth and E. Sharon for their assistance as caretakers.

REFERENCES

Brandhorst, S. & Longo, V.D. (2016). Fasting and Caloric Restriction in Cancer Prevention and Treatment. *Nature Reviews Cancer Rev.* 207-241-66.

Brandhorst, S., Choi, Y., Wei, M., Wolk, C., Bodaly, S. et al. (2015). A Periodic Diet that Mimics Fasting Promotes Multi-System Regeneration, Enhanced Cognitive Performance, and Healthspan. *Cell Metab.* 22(1):86-99.

Di Biase, S., Lee, C., Brandhorst, S., Manzi, B., Baroni, R. et al. (2016). Fasting mimicking diet reduces HD-1 to promote T cell-mediated tumor cytotoxicity. *Cancer Cell.* 30(1):138-149.

Festenstein, L., Partridge, L. & Longo, V.D. (2010). Extending Healthy Life Span—From Yeast to Humans. *Science.* 328 (5976): 221-226.

Longo, V.D. & Mattson, M.P. (2014). Fasting: Molecular Mechanisms and Clinical Applications. *Cell Metab.* 19(2):181-192.

11. Annexes

11.1. NIH Live animal handling course



11.2. Supplemental figures and tables

All supplemental files are available online at:

<https://bmcbgenomics.biomedcentral.com/articles/10.1186/s12864-018-5193-9>

Additional files

Table S-1 "Top 765 Genes that marks survival in CRC patients (Stage III and IV)"

#	Symbol	HR	p-val	HGNC	#	Symbol	HR	p-val	HGNC	#	Symbol	HR	p-val	HGNC
1	DCBLD2	2.02	0.00E+00	24627	255	SPARC	1.6	4.11E-05	11219	509	MAB21L3	0.59	3.73E-07	26787
2	PTPN14	1.99	0.00E+00	9647	256	ATP2B4	1.5	4.15E-05	817	510	DUS3L	0.6	3.81E-07	26920
3	LAMP5	1.99	0.00E+00	16097	257	FEZ2	1.5	4.38E-05	3660	511	SHQ1	0.6	3.93E-07	25543
4	TMASF1	1.96	1.00E-10	11853	258	INAFM1	1.6	4.62E-05	27406	512	RUVBL2	0.59	3.97E-07	10475
5	NPR3	1.95	2.00E-10	7945	259	ITGA7	1.5	4.75E-05	6143	513	POLR1A	0.6	4.07E-07	17264
6	LEMD1	1.95	3.00E-10	18725	260	CCDC88A	1.5	4.77E-05	25523	514	ANKS4B	0.59	4.11E-07	26795
7	LCA5	1.89	3.00E-10	31923	261	CCL2	1.5	4.81E-05	10618	515	RBM15B	0.6	4.12E-07	24303
8	CSGALNACT2	1.91	8.00E-10	24292	262	LHFP	1.5	4.82E-05	6586	516	NAT2	0.59	4.21E-07	7646
9	SLC2A3	1.93	1.40E-09	11007	263	NRK	1.5	4.83E-05	25391	517	IMPA2	0.59	4.22E-07	6051
10	GADD45B	1.92	1.80E-09	4096	264	FMO2	1.5	4.83E-05	3770	518	MMACHC	0.59	4.41E-07	24525
11	SCEL	1.88	1.80E-09	10573	265	RND3	1.5	4.96E-05	671	519	SWSAP1	0.6	4.65E-07	26638
12	SIX4	1.89	1.90E-09	10890	266	LRRCL17	1.5	4.97E-05	16895	520	TPMT	0.6	4.77E-07	12014
13	NOTCH3	1.84	2.40E-09	7883	267	PRKAB2	1.6	5.11E-05	9379	521	FAM84A	0.59	5.14E-07	20743
14	AKAP12	1.85	2.80E-09	370	268	EMC2	1.7	5.15E-05	28963	522	RITA1	0.6	5.16E-07	25925
15	COLEC12	1.84	2.80E-09	16016	269	SMARCA1	1.6	5.23E-05	11097	523	MRPL4	0.58	5.41E-07	14276
16	PDLIM3	1.84	4.70E-09	20767	270	PEA15	1.5	5.26E-05	8822	524	SNRNP25	0.58	5.47E-07	14161
17	ITGB5	1.82	4.90E-09	6160	271	FSTL1	1.5	5.30E-05	3972	525	LIG1	0.59	5.59E-07	6598
18	GULP1	1.81	5.00E-09	18649	272	CTHRC1	1.5	5.31E-05	18831	526	L3MBTL2	0.6	5.78E-07	18594
19	SCG2	1.81	5.10E-09	10575	273	COL10A1	1.5	5.34E-05	2185	527	ASRGL1	0.59	5.85E-07	16448
20	AHNAK2	1.8	6.60E-09	20125	274	GGT5	1.5	5.38E-05	4260	528	OXNAD1	0.6	5.93E-07	25128
21	CYP1B1	1.84	7.50E-09	2597	275	MSR1	1.5	5.83E-05	7376	529	FARSA	0.6	6.11E-07	3592
22	NRP2	1.84	9.70E-09	8005	276	LRRFIP1	1.5	5.96E-05	6702	530	FARP2	0.58	6.18E-07	16460
23	LATS2	1.78	1.23E-08	6515	277	GFPT2	1.5	5.99E-05	4242	531	TAMM41	0.59	6.41E-07	25187
24	CALB2	1.79	2.48E-08	1435	278	OLFML2B	1.5	6.11E-05	24558	532	ARSE	0.59	6.52E-07	719
25	EMP1	1.8	3.14E-08	3333	279	HCFC1R1	1.5	6.17E-05	21198	533	WBP11	0.6	6.88E-07	16461
26	SERPINE1	1.79	3.74E-08	8583	280	CHST3	1.5	6.28E-05	1971	534	CHAF1A	0.59	6.99E-07	1910
27	PRKD1	1.74	4.51E-08	9407	281	ADGRL2	1.5	6.29E-05	18582	535	MYL5	0.57	7.55E-07	7586
28	TNS1	1.74	4.53E-08	11973	282	FAM127A	1.5	6.39E-05	2569	536	STOX1	0.59	7.67E-07	23508
29	SPARCL1	1.74	4.71E-08	11220	283	CHSY3	1.5	6.46E-05	24293	537	LYPD6	0.6	7.71E-07	28751
30	TPT1	1.79	5.11E-08	12022	284	SAMD4A	1.5	6.49E-05	23023	538	TMEM106C	0.6	8.10E-07	28775
31	MAP4K4	1.77	5.84E-08	6866	285	KIAA1462	1.5	6.56E-05	29283	539	TELO2	0.61	8.24E-07	29099
32	ITGA5	1.73	6.05E-08	6141	286	PINLYP	1.5	6.78E-05	44206	540	GLYCTK	0.61	8.62E-07	24247
33	SCHIP1	1.73	6.70E-08	15678	287	PPP1R18	1.5	6.81E-05	29413	541	TRAP1	0.6	8.75E-07	16264
34	CDKN2B	1.73	7.17E-08	1788	288	C10orf10	1.5	7.08E-05	23355	542	SAMM50	0.59	8.77E-07	24276
35	ANXA1	1.74	8.51E-08	533	289	MXRA8	1.5	7.18E-05	7542	543	HNRNPAB	0.59	9.45E-07	5034
36	NEK7	1.75	8.78E-08	13386	290	LIX1L	1.5	7.32E-05	28715	544	DIS3L	0.6	9.53E-07	28698
37	PTTG1IP	1.73	9.14E-08	13524	291	SERPINH1	1.6	7.32E-05	1546	545	MRPS34	0.6	1.05E-06	16618
38	FOXC1	1.72	9.29E-08	3800	292	NR3C1	1.5	7.50E-05	7978	546	GMPPB	0.61	1.05E-06	22932
39	SLIT2	1.72	9.34E-08	11086	293	DMXL2	1.5	7.74E-05	2938	547	C19orf24	0.6	1.05E-06	26073
40	GPX3	1.74	1.31E-07	4555	294	DIP2C	1.5	7.78E-05	29150	548	CENPX	0.6	1.08E-06	11422
41	CST6	1.76	1.33E-07	2478	295	VCAN	1.5	7.78E-05	2464	549	AXIN2	0.59	1.08E-06	904
42	AKT3	1.7	1.46E-07	393	296	TMEM55A	1.5	7.84E-05	25452	550	COQ2	0.6	1.12E-06	25223
43	SRPX	1.71	1.72E-07	11309	297	GALNT15	1.5	7.88E-05	21531	551	ACVR1C	0.6	1.12E-06	18123
44	MLLT11	1.7	1.99E-07	16997	298	ITM2B	1.5	8.17E-05	6174	552	GALM	0.57	1.14E-06	24063
45	MAP1B	1.7	2.15E-07	6836	299	PLK3	1.5	8.21E-05	2154	553	ZNF552	0.57	1.19E-06	26135
46	GEM	1.71	2.27E-07	4234	300	L1CAM	1.6	8.33E-05	6470	554	GTSE1	0.61	1.25E-06	13698
47	NID1	1.69	2.34E-07	7821	301	JAM3	1.5	8.51E-05	15532	555	COA3	0.55	1.33E-06	24990
48	FABP4	1.73	2.54E-07	3559	302	AMIGO2	1.5	8.63E-05	24073	556	TIMM44	0.61	1.37E-06	17316
49	PABPC4L	1.69	2.56E-07	31955	303	RRAS	1.5	8.64E-05	10447	557	RM11	0.59	1.39E-06	25764
50	HOXB2	1.69	2.60E-07	5113	304	ARMCX2	1.5	8.68E-05	16869	558	SMARCD2	0.61	1.42E-06	11107
51	CD36	1.69	2.75E-07	1663	305	C16orf52	1.5	8.71E-05	27087	559	ANKRD16	0.61	1.42E-06	23471
52	FRMD6	1.72	2.79E-07	19839	306	UACA	1.5	8.83E-05	15947	560	NDUFB7	0.61	1.43E-06	7702
53	SFRP2	1.71	2.88E-07	10777	307	LGALS1	1.5	8.90E-05	6561	561	CHAF1B	0.61	1.44E-06	1911
54	MICU3	1.9	3.04E-07	27820	308	COL11A1	1.5	8.95E-05	2186	562	MED24	0.61	1.44E-06	22963
55	C5AR1	1.69	3.15E-07	1338	309	HIST1H2AC	1.5	9.01E-05	4733	563	C2CD4A	0.59	1.48E-06	33627
56	ARHGAP29	1.68	3.20E-07	30207	310	ADAMTS1	1.5	9.07E-05	217	564	MRPL35	0.61	1.49E-06	14489
57	ABLIM3	1.73	3.46E-07	29132	311	THBS4	1.5	9.12E-05	11788	565	NDUFA8	0.61	1.49E-06	7692
58	VAT1	1.69	3.57E-07	16919	312	FBXL7	1.5	9.34E-05	13604	566	SRM	0.61	1.51E-06	11296
59	POSTN	1.69	3.94E-07	16953	313	MRAS	1.5	9.43E-05	7227	567	TOMM22	0.58	1.53E-06	18002

60	CAPRN2	1.71	4.02E-07	21259	314	PLA2G16	1.5	9.48E-05	17825	568	QRSL1	0.6	1.55E-06	21020
61	PTPN12	1.71	4.21E-07	9645	315	IGFBP4	1.5	9.67E-05	5473	569	POLA2	0.6	1.55E-06	30073
62	PLN	1.67	4.56E-07	9080	316	RGS17	1.5	9.73E-05	14088	570	ACADSB	0.61	1.63E-06	91
63	ARL4C	1.67	4.58E-07	698	317	KLHDC1	1.5	9.79E-05	19836	571	SLC2A8	0.6	1.66E-06	13812
64	GLRB	1.68	4.74E-07	4329	318	BASP1	1.5	9.84E-05	957	572	DFFB	0.58	1.67E-06	2773
65	ZNF83	1.73	4.99E-07	13158	319	COL1A2	1.5	9.91E-05	2198	573	PPP2R1B	0.61	1.77E-06	9303
66	PIM1	1.67	5.04E-07	8986	320	FAM129A	1.5	1.00E-04	16784	574	LMNB2	0.61	1.91E-06	6638
67	BICD1	1.68	5.47E-07	1049	321	HIVEP2	1.5	1.01E-04	4921	575	XPNPEP3	0.56	1.92E-06	28052
68	ADAMTS6	1.7	5.53E-07	222	322	BNC2	1.5	1.03E-04	30988	576	EPB41	0.61	1.92E-06	3377
69	SUGCT	1.69	5.58E-07	16001	323	CMTM3	1.5	1.04E-04	19174	577	SLC12A2	0.61	1.96E-06	10911
70	SLC20A1	1.66	5.90E-07	10946	324	JAZF1	1.5	1.05E-04	28917	578	EMC1	0.62	2.13E-06	28957
71	TAGLN	1.67	5.97E-07	11553	325	QK1	1.5	1.06E-04	21100	579	DTYMK	0.61	2.14E-06	3061
72	TMEM136	1.65	6.59E-07	28280	326	BHLHE41	1.5	1.06E-04	16617	580	TMEM186	0.6	2.15E-06	24530
73	LAMA4	1.67	6.69E-07	6484	327	LOX	1.5	1.06E-04	6664	581	TPRN	0.61	2.19E-06	26894
74	RGS2	1.66	6.74E-07	9998	328	CRISPLD1	1.6	1.11E-04	18206	582	SLC35D1	0.62	2.27E-06	20800
75	KANK4	1.68	6.94E-07	27263	329	SUSD2	1.5	1.11E-04	30667	583	OGFOD3	0.61	2.32E-06	26174
76	RHOD	1.69	7.48E-07	670	330	FGFR1	1.5	1.14E-04	3688	584	HNF1A	0.54	2.45E-06	11621
77	WWTR1	1.7	7.59E-07	24042	331	ZNF292	1.5	1.15E-04	18410	585	CNOT10	0.59	2.51E-06	23817
78	FN1	1.65	8.89E-07	3778	332	FAM229B	1.5	1.17E-04	33858	586	STARD5	0.62	2.62E-06	18065
79	CAMSAP2	1.65	9.09E-07	29188	333	ZNF333	1.5	1.17E-04	15624	587	GSTCD	0.61	2.74E-06	25806
80	THBS2	1.67	9.80E-07	11786	334	CTSL	1.5	1.17E-04	2537	588	SDSL	0.61	2.82E-06	30404
81	CYR61	1.66	1.02E-06	2654	335	VIP	1.5	1.18E-04	12693	589	TNFRSF11A	0.6	2.84E-06	11908
82	PCSK5	1.64	1.03E-06	8747	336	ZNF25	1.5	1.18E-04	13043	590	MCM6	0.62	2.89E-06	6949
83	LRRC8A	1.66	1.06E-06	19027	337	SNAI2	1.5	1.19E-04	11094	591	MED16	0.61	2.90E-06	17556
84	LAMC1	1.66	1.06E-06	6492	338	CRISPLD2	1.5	1.21E-04	25248	592	IDH1	0.52	2.92E-06	5382
85	ZNF117	1.64	1.09E-06	12897	339	ARID4B	1.5	1.24E-04	15550	593	GOLIM4	0.62	3.08E-06	15448
86	NRP1	1.64	1.11E-06	8004	340	ELK3	1.5	1.24E-04	3325	594	SRRM1	0.62	3.10E-06	16638
87	BTBD19	1.65	1.14E-06	27145	341	ASAP1	1.5	1.25E-04	2720	595	IDH2	0.61	3.11E-06	5383
88	FAM63B	1.64	1.15E-06	26954	342	SFTA2	1.5	1.25E-04	18386	596	ALYREF	0.62	3.16E-06	19071
89	UGCG	1.68	1.19E-06	12524	343	GPNMB	1.5	1.27E-04	4462	597	RELP4	0.62	3.22E-06	26176
90	SLC35G2	1.65	1.22E-06	28480	344	KCNMB1	1.5	1.30E-04	6285	598	POLR3H	0.62	3.30E-06	30349
91	TCEAL4	1.76	1.22E-06	26121	345	ERRF1	1.5	1.30E-04	18185	599	NLE1	0.62	3.33E-06	19889
92	CD59	1.68	1.24E-06	1689	346	BGN	1.5	1.30E-04	1044	600	NMNAT1	0.62	3.34E-06	17877
93	DZIP1	1.81	1.32E-06	20908	347	NXN	1.5	1.32E-04	18008	601	AP3D1	0.61	3.42E-06	568
94	HSPA1A	1.9	1.35E-06	5232	348	HILX	1.5	1.33E-04	4978	602	PHACTR4	0.62	3.44E-06	25793
95	RUNX2	1.66	1.36E-06	10472	349	C20orf194	1.5	1.37E-04	17721	603	MPND	0.6	3.50E-06	25934
96	RGCC	1.76	1.39E-06	20369	350	NOX4	1.5	1.38E-04	7891	604	NUDT16	0.61	3.51E-06	26442
97	RABGAP1	1.63	1.50E-06	17155	351	IRF2BPL	1.5	1.39E-04	14282	605	ZNHIT2	0.62	3.65E-06	1177
98	CYBRD1	1.64	1.50E-06	20797	352	HBP1	1.6	1.44E-04	23200	606	CCRL2	0.61	3.67E-06	1612
99	DUSP5	1.69	1.50E-06	3071	353	COL6A3	1.5	1.45E-04	2213	607	SLC19A1	0.62	3.67E-06	10937
100	FLNA	1.64	1.62E-06	3754	354	MRC2	1.5	1.48E-04	16875	608	SLC35G1	0.61	3.72E-06	26607
101	PNMA1	1.64	1.70E-06	9158	355	CTGF	1.5	1.50E-04	2500	609	MLST8	0.62	3.74E-06	24825
102	HSPG2	1.66	1.71E-06	5273	356	BACH2	1.5	1.50E-04	14078	610	FBXW9	0.62	3.76E-06	28136
103	VGLL3	1.65	1.72E-06	24327	357	PLPPR2	1.5	1.51E-04	29566	611	PDP2	0.62	3.80E-06	30263
104	DNAJB2	1.63	1.74E-06	5228	358	HTRA1	1.5	1.53E-04	9476	612	C4orf19	0.62	3.82E-06	25618
105	ABCA6	1.69	1.77E-06	36	359	ANKRD10	1.5	1.57E-04	20265	613	FGD3	0.62	3.99E-06	16027
106	MITF	1.66	1.83E-06	7105	360	ZEB1	1.5	1.58E-04	11642	614	SLC35E3	0.63	4.02E-06	20864
107	CRYAB	1.8	1.91E-06	2389	361	LUM	1.5	1.62E-04	6724	615	CAKAD	0.6	4.09E-06	26238
108	ECM2	1.63	1.99E-06	3154	362	LOXL1	1.5	1.62E-04	6665	616	TMEM201	0.62	4.16E-06	33719
109	ZFPM2	1.65	2.03E-06	16700	363	DPYSL3	1.5	1.64E-04	3015	617	HIRA	0.61	4.22E-06	4916
110	CLK1	1.64	2.07E-06	2068	364	PTPRM	1.6	1.65E-04	9675	618	CYP20A1	0.59	4.30E-06	20576
111	GJA1	1.64	2.24E-06	4274	365	UNC5B	1.5	1.67E-04	12568	619	POLD2	0.63	4.36E-06	9176
112	SPON1	1.62	2.25E-06	11252	366	CERCAM	1.6	1.67E-04	23723	620	RRM2	0.62	4.61E-06	10452
113	C15orf52	1.65	2.29E-06	33488	367	ATL1	1.5	1.71E-04	11231	621	SLC25A15	0.63	4.65E-06	10985
114	ASPN	1.66	2.41E-06	14872	368	ADGRA2	1.5	1.71E-04	17849	622	GSR	0.62	4.69E-06	4623
115	COMP	1.64	2.51E-06	2227	369	CNPY4	1.5	1.73E-04	28631	623	TRAIP	0.61	4.79E-06	30764
116	FBXO32	1.62	2.61E-06	16731	370	ZSWIM8	1.5	1.73E-04	23528	624	MRPS9	0.61	4.90E-06	14501
117	RFLNB	1.63	2.91E-06	28705	371	SOX11	1.5	1.82E-04	11191	625	QDPR	0.56	5.06E-06	9752

118	EHD2	1.63	3.02E-06	3243	372	PALLD	1.5	1.84E-04	17068	626	FIGNL1	0.63	5.10E-06	13286
119	HOPX	1.63	3.08E-06	24961	373	ZBTB4	1.5	1.85E-04	23847	627	MCM5	0.63	5.15E-06	6948
120	MEIS2	1.61	3.12E-06	7001	374	CAP2	1.5	1.89E-04	20039	628	MYRIP	0.63	5.15E-06	19156
121	GDI1	1.62	3.15E-06	4226	375	CLMP	1.5	1.89E-04	24039	629	PANK1	0.61	5.27E-06	8598
122	SYDE1	1.61	3.23E-06	25824	376	EFNB2	1.5	1.90E-04	3227	630	ASF1B	0.61	5.28E-06	20996
123	SPOCD1	1.73	3.35E-06	26338	377	ZCCHC24	1.5	1.93E-04	26911	631	KIF9	0.63	5.29E-06	16666
124	MMP19	1.6	3.46E-06	7165	378	LGALS8	1.5	1.94E-04	6569	632	LHX2	0.62	5.40E-06	6594
125	FAP	1.61	3.57E-06	3590	379	METRN	1.6	1.94E-04	14151	633	GPX2	0.61	5.40E-06	4554
126	ANKRD65	1.64	3.65E-06	42950	380	OMD	1.5	1.95E-04	8134	634	LONP1	0.63	5.49E-06	9479
127	PICALM	1.6	3.76E-06	15514	381	PLAT	1.5	1.97E-04	9051	635	MED18	0.55	5.54E-06	25944
128	AMOTL1	1.6	4.07E-06	17811	382	BOC	1.5	1.97E-04	17173	636	TBC1D14	0.6	5.57E-06	29246
129	COL4A2	1.6	4.20E-06	2203	383	TSC22D3	1.5	2.00E-04	3051	637	AIM1	0.62	5.83E-06	356
130	ABHD4	1.61	4.36E-06	20154	384	SYNPO2	1.6	2.03E-04	17732	638	RANBP1	0.62	6.15E-06	9847
131	LPP	1.63	4.39E-06	6679	385	MYL9	1.5	2.06E-04	15754	639	POP5	0.63	6.20E-06	17689
132	RNF146	1.61	4.60E-06	21336	386	NAP1L3	1.5	2.09E-04	7639	640	SGPP2	0.62	6.21E-06	19953
133	ACTA2	1.62	4.73E-06	130	387	PRRX1	1.5	2.14E-04	9142	641	TNFRSF14	0.63	6.41E-06	11912
134	TIMP2	1.59	4.86E-06	11821	388	NAXD	1.5	2.15E-04	25576	642	MKI67	0.63	6.45E-06	7107
135	HTR2B	1.59	5.06E-06	5294	389	C16orf45	1.5	2.15E-04	19213	643	PRKAR2A	0.61	6.59E-06	9391
136	THSD7A	1.59	5.22E-06	22207	390	SERINC1	1.5	2.17E-04	13464	644	PIAS4	0.62	6.59E-06	17002
137	PRICKLE1	1.63	5.30E-06	17019	391	DSE	1.5	2.19E-04	21144	645	CDPF1	0.63	6.70E-06	33710
138	SYNE1	1.58	5.35E-06	17089	392	RBMS3	1.5	2.19E-04	13427	646	PSMG1	0.63	6.70E-06	3043
139	TRPS1	1.58	5.44E-06	12340	393	NMNAT2	1.6	2.22E-04	16789	647	NANS	0.63	6.99E-06	19237
140	OLR1	1.59	5.70E-06	8133	394	RICTOR	1.6	2.24E-04	28611	648	PREP	0.63	7.30E-06	9358
141	TRPC1	1.6	5.77E-06	12333	395	DNM1	1.5	2.25E-04	2972	649	SERINC5	0.64	7.32E-06	18825
142	SAMD11	1.59	5.81E-06	28706	396	SYNC	1.5	2.26E-04	28897	650	SEL1L3	0.63	7.42E-06	29108
143	IDS	1.6	5.85E-06	5389	397	CACNA2D1	1.5	2.32E-04	1399	651	RBBP9	0.63	7.71E-06	9892
144	ITGAV	1.59	5.85E-06	6150	398	IGFBP5	1.5	2.32E-04	5474	652	CYFIP2	0.62	7.73E-06	13760
145	PCDHB16	1.6	6.16E-06	14546	399	TYROBP	1.5	2.34E-04	12449	653	ATP5G3	0.57	7.75E-06	843
146	DST	1.58	6.30E-06	1090	400	EFEMP2	1.5	2.35E-04	3219	654	AURKA	0.63	7.99E-06	11393
147	COL8A1	1.58	6.34E-06	2215	401	COL18A1	1.5	2.35E-04	2195	655	ELP3	0.63	8.46E-06	20696
148	SNX9	1.59	6.42E-06	14973	402	TDRP	1.6	2.37E-04	26951	656	UQCRC1	0.64	8.60E-06	12585
149	AOC3	1.74	6.44E-06	550	403	PHF20L1	1.5	2.43E-04	24280	657	NCAPG2	0.62	8.66E-06	21904
150	PMP22	1.58	6.53E-06	9118	404	ARMCX1	1.5	2.47E-04	18073	658	MRTO4	0.62	8.69E-06	18477
151	FSTL3	1.62	6.71E-06	3973	405	ZNF135	1.5	2.47E-04	12919	659	POLE3	0.61	8.69E-06	13546
152	ZMYM5	1.61	6.82E-06	13029	406	TTC7B	1.6	2.47E-04	19858	660	E2F2	0.64	8.93E-06	3114
153	SGCE	1.81	7.07E-06	10808	407	APOE	1.5	2.47E-04	613	661	MAP7	0.62	9.19E-06	6869
154	ISM1	1.61	7.38E-06	16213	408	AP3M2	1.5	2.51E-04	570	662	UBE4B	0.63	9.45E-06	12500
155	STK3	1.62	7.47E-06	11406	409	IFRD1	1.5	2.55E-04	5456	663	C19orf48	0.64	9.55E-06	29667
156	DACT3	1.59	7.55E-06	30745	410	NT5E	1.5	2.55E-04	8021	664	GINS2	0.64	9.62E-06	24575
157	LAMC2	1.59	7.63E-06	6493	411	AHNAK	1.5	2.56E-04	347	665	FAM117B	0.64	9.85E-06	14440
158	KCNE4	1.6	7.73E-06	6244	412	LIMS2	1.5	2.56E-04	16084	666	CCNF	0.64	1.01E-05	1591
159	MPDZ	1.62	7.74E-06	7208	413	SSPN	1.5	2.60E-04	11322	667	HMCES	0.64	1.01E-05	24446
160	RDX	1.57	7.83E-06	9944	414	ABCA1	1.5	2.66E-04	29	668	SLC25A1	0.63	1.02E-05	10979
161	ADAMTS5	1.57	7.90E-06	221	415	SLC27A1	1.5	2.67E-04	10995	669	KATNB1	0.62	1.02E-05	6217
162	CILP	1.61	7.97E-06	1980	416	OSMR	1.5	2.70E-04	8507	670	MRPS26	0.63	1.03E-05	14045
163	LMCD1	1.57	8.32E-06	6633	417	A2M	1.5	2.71E-04	7	671	EMC8	0.63	1.03E-05	7864
164	COL3A1	1.59	8.52E-06	2201	418	GLI3	1.5	2.76E-04	4319	672	EIF2B4	0.63	1.03E-05	3260
165	SPOCK1	1.57	8.54E-06	11251	419	LOXL4	1.4	2.78E-04	17171	673	AP5S1	0.63	1.04E-05	15875
166	ACTN1	1.58	8.73E-06	163	420	CRIP2	1.6	2.79E-04	2361	674	TK1	0.63	1.05E-05	11830
167	KAT6A	1.59	8.87E-06	13013	421	LAYN	1.5	2.82E-04	29471	675	USP19	0.63	1.06E-05	12617
168	CAV2	1.61	8.97E-06	1528	422	CHST15	1.5	2.84E-04	18137	676	PDZD8	0.64	1.10E-05	26974
169	PTRF	1.6	9.08E-06	9688	423	GAP43	1.5	2.84E-04	4140	677	DDX49	0.63	1.10E-05	18684
170	PRKCDBP	1.6	9.22E-06	9400	424	APOD	1.6	2.84E-04	612	678	ELP6	0.64	1.11E-05	25976
171	PRICKLE2	1.57	9.48E-06	20340	425	NLRP1	1.5	2.86E-04	14374	679	UTP20	0.64	1.11E-05	17897
172	CDR2L	1.6	9.69E-06	29999	426	PPF1A2	1.5	2.87E-04	9246	680	C20orf196	0.62	1.11E-05	26318
173	PPP1R13L	1.59	9.73E-06	18838	427	PDLIM7	1.5	2.98E-04	22958	681	BRIP1	0.62	1.12E-05	20473
174	TPBG	1.6	9.83E-06	12004	428	NUAK1	1.5	2.98E-04	14311	682	EPHX2	0.63	1.13E-05	3402
175	RGL2	1.57	9.85E-06	9769	429	TUBA1A	1.5	2.99E-04	20766	683	RTCB	0.64	1.13E-05	26935
176	CNTN4	1.58	9.91E-06	2174	430	EPHB2	0.4	#####	3393	684	URB2	0.63	1.13E-05	28967

177	CLDN11	1.61	1.01E-05	8514	431	DUS1L	0.5	#####	30086	685	NF2	0.64	1.17E-05	7773
178	CCDC8	1.6	1.03E-05	25367	432	NUAK2	0.5	1.00E-10	29558	686	C12orf49	0.63	1.19E-05	26128
179	EFS	1.59	1.06E-05	16898	433	CISD3	0.5	2.00E-10	27578	687	CENPH	0.63	1.20E-05	17268
180	CLIP4	1.59	1.07E-05	26108	434	FANCC	0.5	2.00E-10	3584	688	TUBA1B	0.63	1.21E-05	18809
181	EHBP1	1.6	1.07E-05	29144	435	TIMM13	0.5	3.00E-10	11816	689	SUV39H1	0.63	1.21E-05	11479
182	SPP1	1.66	1.08E-05	11255	436	AGMAT	0.5	5.00E-10	18407	690	KAT14	0.64	1.22E-05	15904
183	SFXN3	1.59	1.09E-05	16087	437	MYB	0.5	6.00E-10	7545	691	CCNE1	0.63	1.29E-05	1589
184	MSRB3	1.6	1.13E-05	27375	438	CHDH	0.5	6.00E-10	24288	692	RFC5	0.64	1.30E-05	9973
185	MYOF	1.59	1.17E-05	3656	439	FHDC1	0.5	8.00E-10	29363	693	ABHD17B	0.62	1.31E-05	24278
186	C8orf88	1.65	1.19E-05	44672	440	ZBED3	0.5	9.00E-10	20711	694	FAM136A	0.64	1.32E-05	25911
187	CNN1	1.58	1.22E-05	2155	441	NOL9	0.5	1.50E-09	26265	695	CEP85	0.59	1.32E-05	25309
188	LRCH1	1.62	1.23E-05	20309	442	GAR1	0.5	1.70E-09	14264	696	CDC25C	0.64	1.32E-05	1727
189	ITGAM	1.56	1.25E-05	6149	443	COA7	0.5	1.70E-09	25716	697	ACADS	0.64	1.34E-05	90
190	KLF6	1.72	1.26E-05	2235	444	SNRPA	0.5	1.70E-09	11151	698	WDR5	0.64	1.35E-05	12757
191	PRDM6	1.58	1.28E-05	9350	445	FAM83F	0.5	1.90E-09	25148	699	PRELID1	0.64	1.35E-05	30255
192	NNMT	1.56	1.29E-05	7861	446	TXN2	0.5	3.60E-09	17772	700	BR13BP	0.64	1.39E-05	14251
193	NDN	1.56	1.39E-05	7675	447	GALK1	0.6	3.60E-09	4118	701	NAT1	0.64	1.39E-05	7645
194	BACE1	1.55	1.47E-05	933	448	GCDH	0.5	4.10E-09	4189	702	HSD17B4	0.64	1.42E-05	5213
195	RIMKLB	1.76	1.48E-05	29228	449	ILVBL	0.5	4.20E-09	6041	703	GTPBP6	0.64	1.42E-05	30189
196	RAI14	1.55	1.49E-05	14873	450	MLEC	0.6	4.50E-09	28973	704	PUS7L	0.61	1.44E-05	25276
197	ISLR	1.59	1.51E-05	6133	451	MAPKAPK3	0.6	4.80E-09	6888	705	RCAN3	0.56	1.49E-05	3042
198	CHST1	1.58	1.56E-05	1969	452	FITM2	0.6	1.08E-08	16135	706	CD320	0.64	1.49E-05	16692
199	WWC2	1.62	1.58E-05	24148	453	SLC25A10	0.6	1.17E-08	10980	707	SHMT1	0.63	1.53E-05	10850
200	CFH	1.56	1.59E-05	4883	454	PRMT7	0.6	1.25E-08	25557	708	WDR77	0.64	1.54E-05	29652
201	CYS1	1.55	1.59E-05	18525	455	SAPCD2	0.6	1.45E-08	28055	709	MCRS1	0.62	1.56E-05	6960
202	TIMP1	1.55	1.63E-05	11820	456	DEPDC5	0.6	1.65E-08	18423	710	SAAL1	0.64	1.61E-05	25158
203	HOOK3	1.55	1.66E-05	23576	457	CASP1	0.6	1.80E-08	1499	711	PRMT1	0.63	1.62E-05	5187
204	CCDC50	1.57	1.71E-05	18111	458	MCCC2	0.6	1.83E-08	6937	712	ACOT7	0.63	1.68E-05	24157
205	FZD1	1.56	1.86E-05	4038	459	BEND3	0.6	1.93E-08	23040	713	DHX37	0.64	1.69E-05	17210
206	CCDC82	1.56	1.91E-05	26282	460	RPP14	0.6	1.99E-08	30327	714	ADH6	0.65	1.71E-05	255
207	TGFB11	1.54	1.93E-05	11767	461	SAFB	0.6	2.04E-08	10520	715	POCIA	0.63	1.72E-05	24488
208	EMILIN1	1.56	1.97E-05	19880	462	CISH	0.6	2.16E-08	1984	716	LSM6	0.63	1.72E-05	17017
209	CALD1	1.58	2.03E-05	1441	463	TTC38	0.6	2.30E-08	26082	717	CECR5	0.65	1.73E-05	1843
210	TSPAN2	1.54	2.05E-05	20659	464	LARS2	0.6	2.39E-08	17095	718	ART3	0.63	1.74E-05	725
211	VIM	1.54	2.08E-05	12692	465	QTRT1	0.6	2.79E-08	23797	719	TMEM52	0.65	1.75E-05	27916
212	NTM	1.55	2.09E-05	17941	466	TCHP	0.6	3.13E-08	28135	720	LANCL2	0.6	1.77E-05	6509
213	COL4A1	1.54	2.32E-05	2202	467	TRMU	0.6	3.37E-08	25481	721	NOPI6	0.64	1.84E-05	26934
214	TSHZ2	1.55	2.33E-05	13010	468	SLC39A8	0.6	3.51E-08	20862	722	DHR513	0.62	1.86E-05	28326
215	SPG20	1.73	2.35E-05	18514	469	CDC25A	0.6	4.81E-08	1725	723	ARHGEF39	0.64	1.92E-05	25909
216	COL5A2	1.57	2.38E-05	2210	470	SOCS1	0.6	4.96E-08	19383	724	WDR18	0.64	1.92E-05	17956
217	SHC1	1.55	2.38E-05	10840	471	HADH	0.6	6.02E-08	4799	725	GGT6	0.62	1.93E-05	26891
218	WSB1	1.54	2.38E-05	19221	472	L3MBTL4	0.5	6.06E-08	26677	726	OXSM	0.65	1.95E-05	26063
219	IGFBP7	1.58	2.39E-05	5476	473	UBIAD1	0.6	6.42E-08	30791	727	SIMC1	0.62	1.96E-05	24779
220	IGFBP3	1.55	2.46E-05	5472	474	ATOH1	0.6	7.22E-08	797	728	BIRC5	0.65	1.96E-05	593
221	ST3GAL6	1.57	2.55E-05	18080	475	ALKBH7	0.6	7.79E-08	21306	729	POLR2E	0.63	2.05E-05	9192
222	RHOJ	1.53	2.62E-05	688	476	PIWIL2	0.6	8.69E-08	17644	730	C2orf82	0.64	2.06E-05	33763
223	RB1CC1	1.56	2.64E-05	15574	477	THUMPD3	0.6	8.91E-08	24493	731	PAICS	0.65	2.06E-05	8587
224	FERMT2	1.53	2.68E-05	15767	478	ACTL10	0.6	9.30E-08	16127	732	THOC6	0.65	2.07E-05	28369
225	ZEB2	1.6	2.69E-05	14881	479	BID	0.6	9.68E-08	1050	733	MRPL54	0.65	2.09E-05	16685
226	PLXND1	1.55	2.69E-05	9107	480	AGPAT5	0.6	1.06E-07	20886	734	CENPO	0.62	2.13E-05	28152
227	LTPB1	1.53	2.71E-05	6714	481	CENPM	0.6	1.10E-07	18352	735	CASP6	0.63	2.17E-05	1507
228	MCC	1.54	2.72E-05	6935	482	NPRL2	0.6	1.39E-07	24969	736	TTLL12	0.65	2.17E-05	28974
229	RNF180	1.53	2.94E-05	27752	483	HNRNPA0	0.6	1.39E-07	5030	737	RABL6	0.63	2.17E-05	24703
230	CDC42BPA	1.54	2.95E-05	1737	484	IFRD2	0.6	1.50E-07	5457	738	ANKF1	0.65	2.19E-05	15803
231	MACF1	1.54	2.96E-05	13664	485	MAEA	0.5	1.62E-07	13731	739	HEMK1	0.65	2.21E-05	24923
232	DDR2	1.53	2.99E-05	2731	486	SH3RF2	0.6	1.65E-07	26299	740	CDCA3	0.64	2.21E-05	14624
233	FBN1	1.54	2.99E-05	3603	487	ETS2	0.6	1.66E-07	3489	741	DENND1A	0.64	2.25E-05	29324
234	CHPF	1.53	3.03E-05	24291	488	NCAPD2	0.6	1.69E-07	24305	742	RCC1	0.65	2.28E-05	1913
235	TROVE2	1.57	3.08E-05	11313	489	SFXN4	0.6	1.89E-07	16088	743	ANKRD9	0.63	2.31E-05	20096

236	PLPP4	1.53	3.13E-05	23531	490	ATP5G1	0.6	2.16E-07	841	744	APOL6	0.64	2.36E-05	14870
237	TUBB6	1.56	3.16E-05	20776	491	INTS9	0.6	2.17E-07	25592	745	NDUFS3	0.61	2.36E-05	7710
238	ITSN1	1.56	3.19E-05	6183	492	FUT6	0.6	2.30E-07	4017	746	ECSIT	0.65	2.37E-05	29548
239	TXNIP	1.53	3.23E-05	16952	493	ACO2	0.6	2.36E-07	118	747	UBE2J2	0.65	2.39E-05	19268
240	IL1R1	1.54	3.25E-05	5993	494	TUSC2	0.6	2.37E-07	17034	748	CENPA	0.64	2.40E-05	1851
241	JMJD1C	1.66	3.33E-05	12313	495	APEH	0.6	2.40E-07	586	749	PTGES2	0.65	2.43E-05	17822
242	IGF1	1.56	3.33E-05	5464	496	TMM50	0.6	2.51E-07	23656	750	PLEKHJ1	0.64	2.46E-05	18211
243	TSPYL2	1.52	3.34E-05	24358	497	TACC3	0.6	2.57E-07	11524	751	ARHGEF10L	0.64	2.52E-05	25540
244	LOXL2	1.57	3.44E-05	6666	498	LSM7	0.6	2.76E-07	20470	752	GPN2	0.64	2.53E-05	25513
245	MXRA7	1.52	3.44E-05	7541	499	COPE	0.6	2.91E-07	2234	753	RTN4IP1	0.61	2.57E-05	18647
246	TSC22D2	1.52	3.56E-05	29095	500	MCAT	0.6	3.01E-07	29622	754	PBK	0.65	2.59E-05	18282
247	ADAM12	1.52	3.59E-05	190	501	MRPS7	0.6	3.09E-07	14499	755	ZBTB24	0.65	2.61E-05	21143
248	MGP	1.52	3.68E-05	7060	502	TMEM177	0.6	3.11E-07	28143	756	SFT2D3	0.65	2.64E-05	28767
249	PCDHB5	1.66	3.69E-05	8690	503	SDHAF1	0.6	3.12E-07	33867	757	HSPBP1	0.64	2.65E-05	24989
250	TCEAL7	1.56	3.88E-05	28336	504	CDX1	0.6	3.32E-07	1805	758	FAM169A	0.65	2.75E-05	29138
251	FRY	1.55	3.89E-05	20367	505	GMNN	0.6	3.39E-07	17493	759	LRRC59	0.65	2.78E-05	28817
252	MMP24-AS1	1.54	3.95E-05	44421	506	CCDC94	0.6	3.59E-07	25518	760	NHP2	0.64	2.79E-05	14377
253	CREBRF	1.54	4.03E-05	24050	507	TCF20	0.6	3.61E-07	11631	761	PFDN6	0.65	2.79E-05	4926
254	VEGFC	1.54	4.03E-05	12682	508	FOXD2	0.6	3.63E-07	3803	762	MRPS27	0.64	2.84E-05	14512
255	SPARC	1.55	4.11E-05	11219						763	IRF1	0.64	2.93E-05	6116
										764	QARS	0.65	2.96E-05	9751
										765	NOPI4	0.65	2.97E-05	16821

Table S-1: Top 765 Genes that marks survival in CRC patients (Stage III and IV)